Investigating the role of EphA/ ephrin-A signalling during trigeminal ganglion axon guidance

A thesis submitted for the degree of Doctor of Philosophy

Molecular and Biomedical Science (Discipline of Genetics),
University of Adelaide

By

Chathurani S. Jayasena, B.Sc. (Hons.)

December 2004

Table of Contents

List of Figures and Tables

Declaration

I declare that this thesis contains no material which has been accepted for the award of any other degree or diploma in any university or other tertiary institution. To the best of my knowledge and belief, this thesis contains no material previously published or written by another person, except where due reference has been made in the text.

I consent to this copy of my thesis, when deposited in the University of Adelaide library, being made available for photocopying and loan if accepted for the award of Doctor of Philosophy.

I declare that 95% of the material presented in this thesis is my work, except for the Real-Time PCR results in Chapter 4, which were kindly generated by Dr. Warren D. Flood.

Chathurani Jayasena,

December 2004

Abstract

The ophthalmic, maxillary and mandibular axon branches of the trigeminal ganglion (TG) provide cutaneous sensory innervation to the vertebrate face, and multiple families of guidance cues amalgamate to direct the navigation of these branches. However, target tissue specific guidance cues that discriminately guide the three TG axon branches are unknown. Prior work demonstrated that EphAs and ephrin-As could discriminately direct dorsal versus ventral motor axon projections into the hindlimb. Similarly, do EphA tyrosine kinases and ephrin-A ligands discriminately guide trigeminal ganglion ophthalmic (TGop) lobe versus maxillomandibular (TGmm) axon projections into the chick embryo face? The aims of this work were two-fold: (1) to identify candidate EphA and ephrin-A molecules during TG axon guidance, and (2) to determine the functional significance of TG axon EphA and ephrin-A signalling in *vitro*.

This study identified EphA3, EphA4, *ephrin-A2* and *ephrin-A5* at stages 13, 15 and 20, as putative guidance cues to TG axons. TG-EphA3 and *-ephrin-A5* were identified as putative receptors to guidance cues expressed in the target fields. EphA3 receptor was differentially expressed, with the TGop lobe expressing higher levels compared to the TGmm lobe. However, *ephrin-A5* transcript was not differentially expressed between the two ganglion lobes.

In a substratum choice *in vitro* assay, ephrin-A5-Fc was found to repel approximately 50 % of axons growing from stage 20 whole TG explants. This population of axons was identified to be from the TGop lobe. The *in vitro* data supports the contention that during facial development there may be trigeminal ganglion lobe specific guidance of TGop in comparison to TGmm peripheral sensory axonal projections to target fields coordinated through EphA3 and ephrin-A2/A5 repulsive interactions.

In vitro, EphA4-Fc caused morphological changes to TG growth cones, which is likely mediated through TG ephrin-A5 reverse signaling. Furthermore, this study provided *in vitro* evidence that trigeminal ganglion axons were not responsive to EphA4-Fc, possibly implying that EphAs expressed in the target fields were not repulsive to ganglionic axons during pathfinding.

The data suggests that EphA/ ephrin-A interactions may specifically guide TGop projections into the ophthalmic process similar to lateral motor axon guidance into the hindlimb. For the first time, a model of how EphA/ ephrin-A interactions and other families of guidance cues may act in concert to guide trigeminal ganglion axons is suggested.

Acknowledgements

I would like to firstly thank my supervisor Dr. Simon Koblar, for having confidence in my scientific abilities, especially at times when I was in doubt.

I would also like to take this opportunity to say a huge thank you to my co-supervisors: Dr. Kemal Turker and Dr. Kirk Jensen, for providing me with support during my PhD. Especially Dr. Jensen, who provided me with valuable feedback regarding my thesis.

Thank you to the past and present Koblar lab members, especially: Dr. Paul Tosch (Toschie), Edwina Ashby (Ed), Agnes Stokowski (Aggyneshka), Amanda West, Dr. Warren Flood (Wazza), Dr. Robert Moyer, Dr. Martin Lewis, and Colleen Bindloss. It has truly been a great pleasure to work with these lovely people. Without their support, friendship, and scientific guidance/ help I could not have done this. I wish all of you well in your life endeavours.

Thank you to the past and present Saint lab members, especially: Dr. Tetyana Shandala (Tenushka), Dr. Hazel Dalton, Jane Sibbons, and Dr. Stephen Gregory. Thanks especially to Drs. Shandala and Dalton for their friendship and support, and for including me in their discussions about science and everything else in the universe, I truly appreciate it.

Thanks also go to members of the genetics discipline, especially Dr. Joan Kelly, for supporting me through the hard times and providing me with advice. Also a huge thanks to: Velta Vingelis (the legend for friendship/ support), Dr. Christine Heppele (for friendship/ support) and Helli Meinecke (Helga) (for friendship/ support).

I have been fortunate to have a great family, especially my parents: Dr. Jayasena and Mrs. Jayasena. They have been with me every step of the way. Also, I am fortunate to have a great little sister (Warunika) and also my brother (Kassun). Without your love, support and strength, this would not have been possible. So thank you!

Personal bibliography

Chathurani S. Jayasena[1], Warren D. Flood[1, 2] and Simon A. Koblar[1] (2004). *In vitro* EphA-ephrin-A interactions during lobe specific guidance of trigeminal ganglion axons. (Submitted to Journal of Neurobiology).

[1]ARC Centre for Molecular Genetics of Development (CMGD), School of Molecular and Biomedical Science, The University of Adelaide, South Australia, 5005, Australia.
[2] Centre for Medical Genetics, Department of Laboratory Genetics, Women's and Children's Hospital, South Australia, 5006, Australia.

Chapter 1: Introduction

"This coffee falls into your stomach, and straightway there is a general commotion. Ideas begin to move like the battalions of the Grand Army of the battlefield, and the battle takes place. Things remembered arrive at full gallop, ensuing to the wind. The light cavalry of comparisons deliver a magnificent deploying charge, the artillery of logic hurry up with their train and ammunition, the shafts of with start up like sharpshooters. Similes arise, the paper is covered with ink; for the struggle commences and is concluded with torrents of black water, just as a battle with powder".

--Honore de Balzac, "The Pleasures and Pains of Coffee"

Chapter 1: Introduction

The setting up of the neural network (both central and peripheral) is a complicated event that begins in the embryo and may continue on into and during adulthood. Most adult vertebrates do not have the capacity to repair damaged neural circuits following severe injury. If however, one can understand the molecular blueprint that establishes the neural circuitry during embryogenesis, one may also begin to understand how to repair damaged neural connections in the adult (reviewed by Koeberle and Bahr, 2004). The fundamental assumption often made is that the re-establishment of damaged neural connections is a recapitulation of events that occur during early development, and was postulated first by Sperry in 1951.

Roger Sperry's work into the visual system and nerve regeneration, led him to make four major assumptions that now form the basis of developmental neurobiology. He proposed that: (1) neurons had differential molecules (receptors), and (2) these corresponded to the molecules (ligands or guidance cues) being expressed by their target tissues, (3) those proteins were a by-product of cellular differentiation, and (4) the establishment of neural connections (axon guidance) relied on receptor-ligand interactions (Sperry, 1951; Sperry, 1963).

Since Sperry put forward his assumptions, evidence has accumulated for the existence of molecular guidance cues. It is becoming apparent that there are a limited number of guidance cues that belong to four broad classes and that the molecules utilised in the central and peripheral nervous systems roughly are the same. The specificity of neural connections in different regions of the body is not due to the use of a particular guidance cue in one system and another cue in another system. Rather, specificity is achieved through the combinatorial use of a limited set of guidance cues in the organism that are controlled in a spatiotemporal manner (reviewed by Tessier-Lavigne and Goodman, 1996).

What is axon guidance? What are the four classes of guidance cues? How do guidance cues navigate the trajectory of axons and influence cytoskeletal reorganisation? These topics will be overviewed in the following section.

1.1 Axon guidance

In the embryo, each neuron sends out an axon, which extends in the vicinity of its appropriate target regions in a stereotypical and directed manner, making very few navigational errors (reviewed by (Tessier-Lavigne and Goodman, 1996). This occurs through interactions

between receptors on the axons and ligands/ guidance cues in the cellular environment. Typically, the first neurons to be born will extend axons (pathfind) through an axon free environment when the embryo is relatively small (Bastiani *et al.,* 1984; Bate, 1976). These extending axons will interact with microenvironments en route to the target tissue. In the case where axons have to travel long distances in order to reach the target tissue, axons make decisions at a number of choice points (intermediate targets) made up of specialized cells. At such choice points, axons decipher messages conveyed by guidance cues, thereby reducing the complicated task of navigating a distant target into manageable shorter segments (reviewed by Isbister and O'Connor, 2000; Silver, 1993). Later developing axons however will face an ever-expanding environment as the embryo grows, and consequently may travel along pre-existing axons tracts laid down by pioneer axons. These late born axons are also less likely to sample the environmental terrain between the place of birth and the target tissue field. This selective adhesion between axons is referred to as axon-fasciculation (Bak and Fraser, 2003; Bastiani *et al.,* 1984; Lopresti *et al.,* 1973).

1.1.1 Types of guidance cues

Four broad characteristics of guidance molecules ensure correct navigation of axons to the correct target zone. Firstly, guidance molecules may be attractive and/or repulsive. The ability of an axon to interpret a particular guidance cue as either being attractive or repulsive is dependent on a number of factors. This can include the intracellular state of the growth cone, differential expression of receptor complexes and cross talk between intracellular signalling cascades (reviewed by Huber *et al.,* 2003). Secondly, guidance cues can be either cell membrane attached or secreted. Molecules attached to the cell membrane exert contact-mediated attraction or repulsion. Additionally, secreted signals from distant cells mediate either chemoattraction or chemorepulsion (reviewed by Tessier-Lavigne and Goodman, 1996) (Figure 1.1).

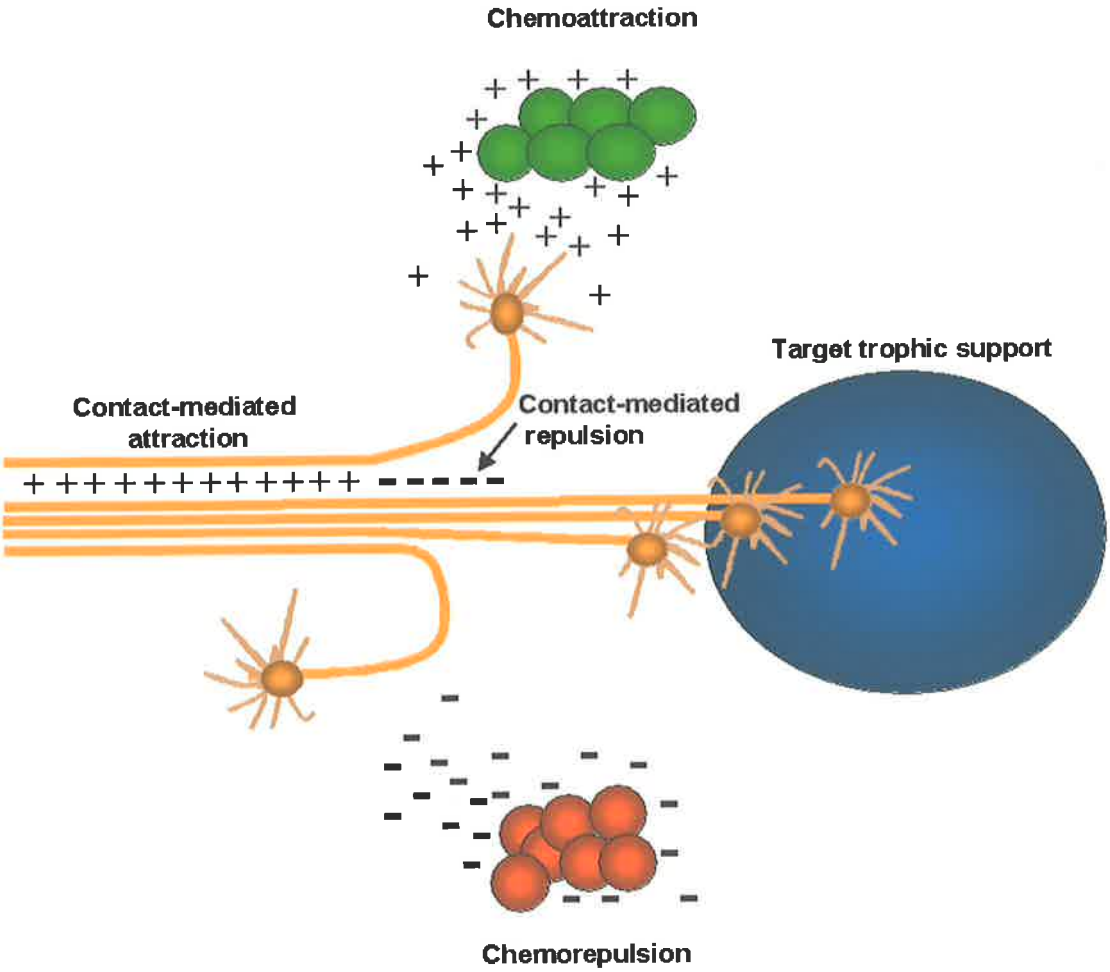

Figure 1.1 Growing axons respond to multiple molecular cues in the environment.
Contact mediated attraction and repulsion for example between axons relies on interactions between cell-membrane bound receptors and ligands. Also, short-range signalling can be exerted through interactions between axons and the cellular microenvironment. Molecules that are secreted by distant cells mediate chemorepulsion and chemoattraction. When axons reach the target tissue, trophic factors such as neurotrophins help maintain these projections.

1.1.2 Growth cone machinery and dynamics

1.1.2.1 Structure of the growth cone

The growth cone is a highly dynamic structure at the end of the axon that responds to molecular cues in the surrounding environment. The growth cone has two main domains, the peripheral domain and the central domain (Figure 1.2).

The peripheral domain is composed predominantly of filopodia (narrow cylindrical cellular extensions) and lamellipodia (flattened veil like cellular extensions). Filopodia are capable of extending tens of microns from the periphery of the growth cone and are involved in sensing the surrounding environment. Lamellipodia on the other hand expand between the filopodia in the forward movement of the growth cone. The motility of filopodia and lamellipodia is based on the changing dynamics of the underlying F-actin cytoskeleton. In filopodia, F-actin fibres are arranged in a parallel bundled form. Furthermore, to enable rapid exploration of the environment, there is a concentration of fast growing F-actin barbed ends (where F-actin polymerisation occurs), oriented towards the leading edge of each filopodial tip. In contrast, lamellipodia are filled with a crosslinked F-actin meshwork, thereby facilitating growth cone-substrate adhesion during movement (reviewed by Dent and Gertler, 2003; Huber *et al.*, 2003)) (Figure 1.3).

The central growth cone domain has organelles and vesicles, and is composed mainly of microtubules, the motile cytoskeletal component of the growth cone. The peripheral F-actin structures influence central microtubule advancement into the peripheral domain by affecting microtubule assembly and translocation (reviewed by Dent and Gertler, 2003; Huber *et al.*, 2003)) (Figure 1.3).

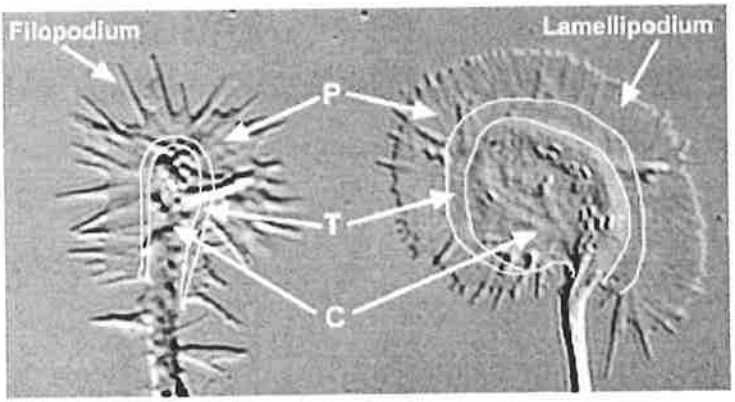

Figure 1.2. The structure of the growth cone.
An example of a filopodial (left) and a lamellapodial (right) growth cone are shown. C, central domain; P, peripheral domain; T, transition domain (the interface between C and P domains). Image from Dent and Gertler (2003).

1.1.2.2 Guidance cues and the growth cone cytoskeleton

The integration of attractive and repulsive signals received from the environment is crucial to axon guidance and this occurs in the growth cone. Guidance cues affect the trajectory of an axon by regulating F-actin polymerisation in the distal regions and depolymerisation of F-actin in the proximal regions of the growth cone. In addition, guidance cues affect F-actin retrograde flow rates (the continuous rearward Myosin-motor driven movement of F-actin) within filopodia. By having an effect on F-actin polymerisation/ depolymerisation, and retrograde flow rates, guidance cues can control growth cone advancement and retraction. Attractive cues appear to promote F-actin polymerisation and/or slow retrograde F-actin flow. Repulsive cues on the other hand, promote F-actin depolymerisation and/or retrograde F-actin flow (reviewed by Dent and Gertler, 2003; Huber et al., 2003) (Figure 1.3).

1.1.2.3 Rho GTPases and axon guidance

Axon guidance cues regulate cytoskeletal dynamics of growth cones through the Rho family of small GTP binding proteins. The best-characterised Rho GTPases are Cdc42, Rac and RhoA, and evidence suggests that they are involved in controlling lamellapodial and fillopodial dynamics. The Rho GTPases cycle between active and inactive forms by binding guanine nucleotides; GTP-bound Rho GTPases are active, while GDP-bound proteins are inactive. The guanine nucleotide exchange factors (GEFs) and GTPase activating proteins (GAPs) mediate the cycling of Rho GTPases between active and inactive states. Axon guidance cues may directly or indirectly influence GEFs and GAPs, thereby directly influencing the activity of Rho GTPases. Specificity of guidance cue signalling is likely to be mediated through tissue specific and temporal specific expression of GEFs and GAPs (reviewed by Giniger, 2002; Huber *et al.,* 2003)).

1.1.2.4 Overview

To summarise, growth cones respond to multiple molecular cues in the environment. These cues affect the cycling of Rho GTPases from active to inactive state thereby changing F-acting and microtubule cytoskeletal dynamics in the growth cone and affecting the trajectory of an axon.

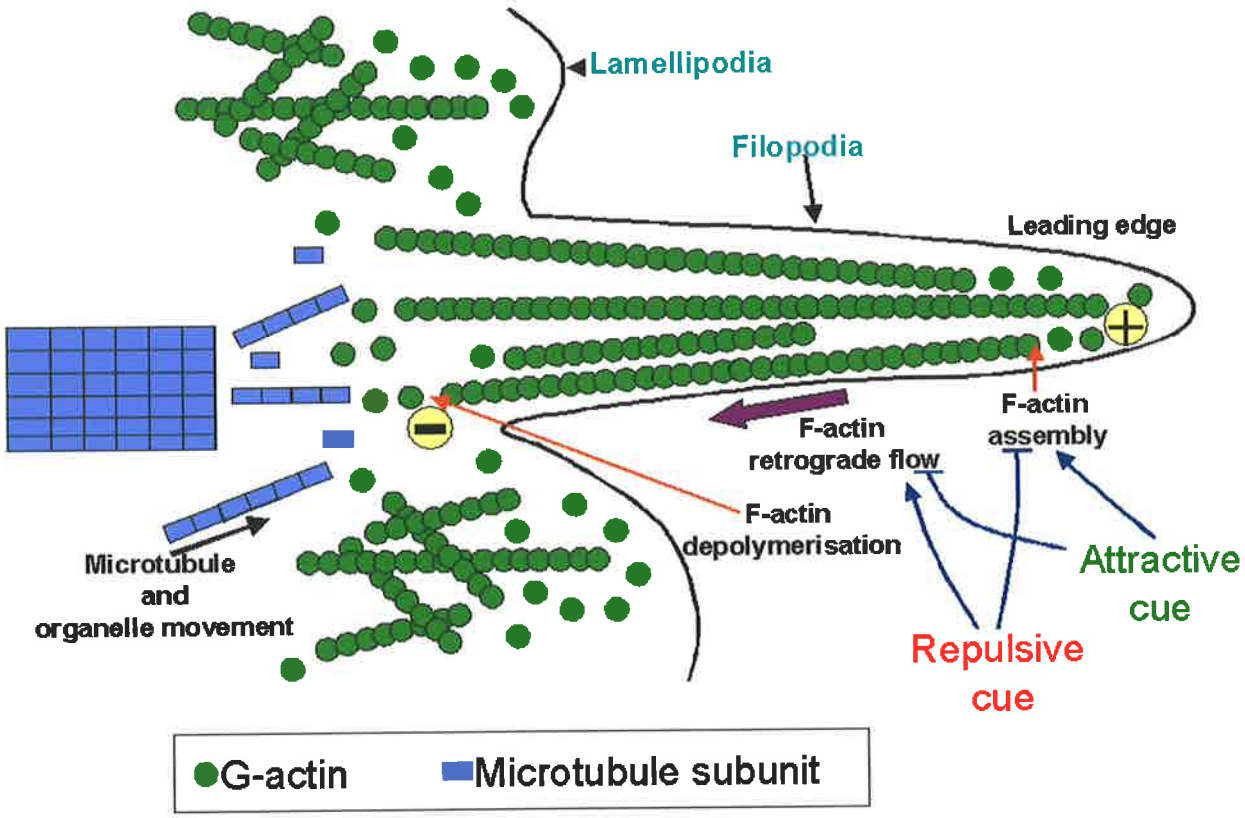

Figure 1.3 Effects of repulsive and attractive guidance cues on F-actin polymerisation.

G-actin (actin-monomers) are used to polymerise F-actin. In lamellipodia, F-actin exists as a meshwork. In filopodia, F-actin is in a parallel bundled form. Polymerisation of F-actin occurs at the plus (+ or barbed) end in the filopodia and become de-polymerised at the minus end (-). Filopodial extension and retraction is dependent on the rate of F-actin assembly, F-actin polymerisation and F-actin retrograde flow (purple arrow). Repulsive guidance cues promote F-actin retrograde flow and inhibit F-actin assembly at the + end. Attractive cues in contrast promote F-actin assembly at the leading edge and inhibit F-actin retrograde flow. As the filopodia protrude forward, microtubules invade the filopodia, bringing organelles and membranous vesicles.

Adapted from Huber et. al., (2003).

1.2 The trigeminal ganglion- a model system?

Our understanding of axon guidance has come from studying the central nervous system and the trunk peripheral nervous system. However, little effort has been devoted to studying the patterning of the cranial sensory peripheral nervous system.

The trigeminal ganglion, one of the first sensory ganglia to develop, has the most densely innervated receptive fields in the periphery, and offers a wonderful system to study axon guidance in the cranial peripheral nervous system (Davies, 1988). The ganglion has three stereotypical branches of axon projections into the face and multiple families of guidance cues appear to amalgamate to direct the navigation of these branches (discussed in detail in sections 1.2.1 and 1.3.2). Therefore, some insight may be gained into how different guidance cues are integrated to pattern neural projections of not only the trigeminal ganglion, but also those in the central and trunk peripheral nervous systems. Additionally, the ganglion is unique in that it has three target fields, and it remains to be determined if there are target tissue specific guidance cues (O'Connor and Tessier-Lavigne, 1999).

This chapter will provide an overview of the morphology and development of the trigeminal ganglion, particularly focused on information derived from the chick embryo. Furthermore, specific guidance cues identified so far to play a role during patterning of ganglionic axon scaffold will be introduced and this review will endeavour to integrate experimental evidence from both mouse and chick models. Finally, the family of Eph receptors and ephrins are introduced, and why they are excellent candidate guidance cues for trigeminal ganglion axons, particularly during trigeminal branch specific guidance.

1.2.1 Morphology of the trigeminal ganglion

Sensory ganglia in the trunk and cranial regions of the vertebrates are involved in conveying sensory information to the central nervous system. Somatosensory cutaneous innervation (pain, touch, temperature, proprioception) to the vertebrate face is provided by sensory neurons of the trigeminal ganglion. The bilobed avian ganglion (Figure 1.4) consists of the ophthalmic and the maxillomandibular lobes. This is in contrast to mammals, which have trilobed ganglia that consist of ophthalmic, maxillary and mandibular lobes (reviewed by Davies, 1988).

The ophthalmic, maxillary and mandibular processes are the three mesenchymal target fields for emerging trigeminal ganglion axons during early vertebrate embryogenesis (Figure 1.4). Later in development, axons from each of the three branches, having travelled through mesenchyme project to their respective target epithelia (reviewed by (Davies, 1988).

1.2.2 Dual embryonic origin of the trigeminal ganglion

Classic embryological transplant, cell tracing and extirpation (extermination) studies in the past 100 years have established the embryological origins of sensory cranial ganglia. Like all the other cranial sensory ganglia, neurons of the avian (D'Amico-Martel and Noden, 1980; Hamburger, 1961) and mammalian (Chan and Tam, 1988; Verwoerd and van Oostrom, 1979) trigeminal ganglion are derived from two embryonic sources: the cranial neural crest and epidermal neurogenic placodes (Figure 1.5A).

1.2.2.1 Neural crest

During gangliogenesis, neural crest cells migrate from the midbrain (mesencephalon), rhombomeres 1 and 2 (metencephalon), and condense to form the trigeminal ganglion around stages 9.5 to 13 in the chick embryo near rhombomere 2 (reviewed by Baker *et al.,* 1997; Le Douarin and Kalcheim, 1999) (Figure 1.5A). These cells contribute to the generation of ganglionic support cells (glia and satellite cells), and small neurons in the proximal region of the ganglion (D'Amico-Martel and Noden, 1980; D'Amico-Martel and Noden, 1983) (Figure 1.5B).

1.2.2.2 Epidermal neurogenic placode

The neurogenic placodes are transient specialised focal regions of ectoderm in vertebrate embryos that generate sensory neurons. During development, precursor sensory cells within such placodes delaminate and migrate to form the sensory ganglion (reviewed by Baker and Bronner-Fraser, 2001; Graham and Begbie, 2000) (Figure 1.5A). The ophthalmic and maxillomandibular trigeminal placodes located near the midbrain-hindbrain junction contribute to the ophthalmic and the maxillomandibular lobes respectively. Trigeminal neurons derived from the two placodes have been shown to give rise to large neurons in the distal regions of the ganglion and do not produce any ganglionic support cells (D'Amico-Martel and Noden, 1980; Hamburger, 1961) (Figure 1.5B).

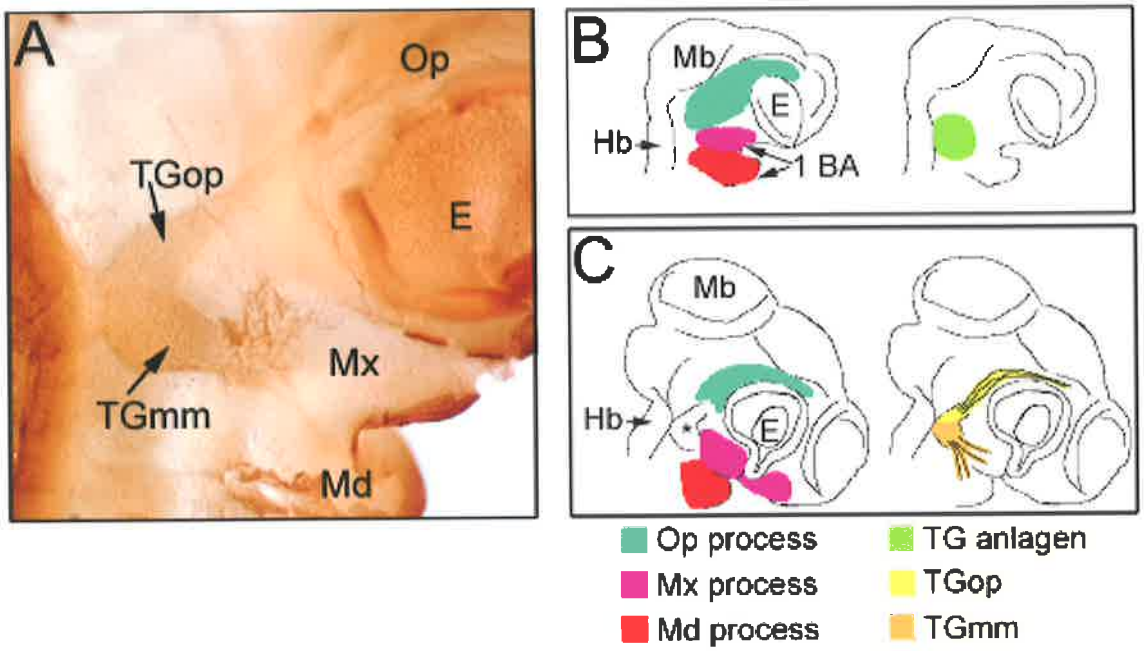

Figure 1.4 The bilobed chick trigeminal ganglion (TG) has three target fields.

(A) Lateral view of an approximately 3 day old chick embryo (stage 20; staging according to Hamburger and Hamilton, 1951) showing the morphology of the maturing trigeminal ganglion, which has been stained with a neuronal marker. The ophthalmic lobe (TGop) innervates the ophthalmic process (Op) around the eye (future cornea, and eyelids). The maxillomandibular lobe (TGmm) innervates the maxillary process (Mx) and the mandibular process (Md), the future upper and lower jaw regions respectively. E, eye.

(B-C) Schematic showing the relationship between target fields and the developing trigeminal ganglion (TG) at stage 13 (2-days old; Hamburger and Hamilton, 1951) (B), and at stage 20 (C) during chick embryogenesis.

(B) At stage 13, the two lobes of ganglion are not discernable. The target regions to which early TG axons innervate are shown on the left hand schematic. Only the Md process (red) is evident at this stage, while the Mx process (pink) does not become fully discernable till around stage 18. Right hand schematic: Neural crest and placode cells (lime green) begin aggregating to form the ganglion (refer to section 1.2.2 and see figure 1.5). This

(C) Left hand schematic: all three target fields are discernable (including the Mx process; pink), as shown in (A). Right hand schematic: the two lobes of the TG (yellow and orange) are clearly visible. Asterisk, TG.

1 BA, first branchial arch (maxillary and mandibular processes); Hb, hindbrain; Mb, midbrain.

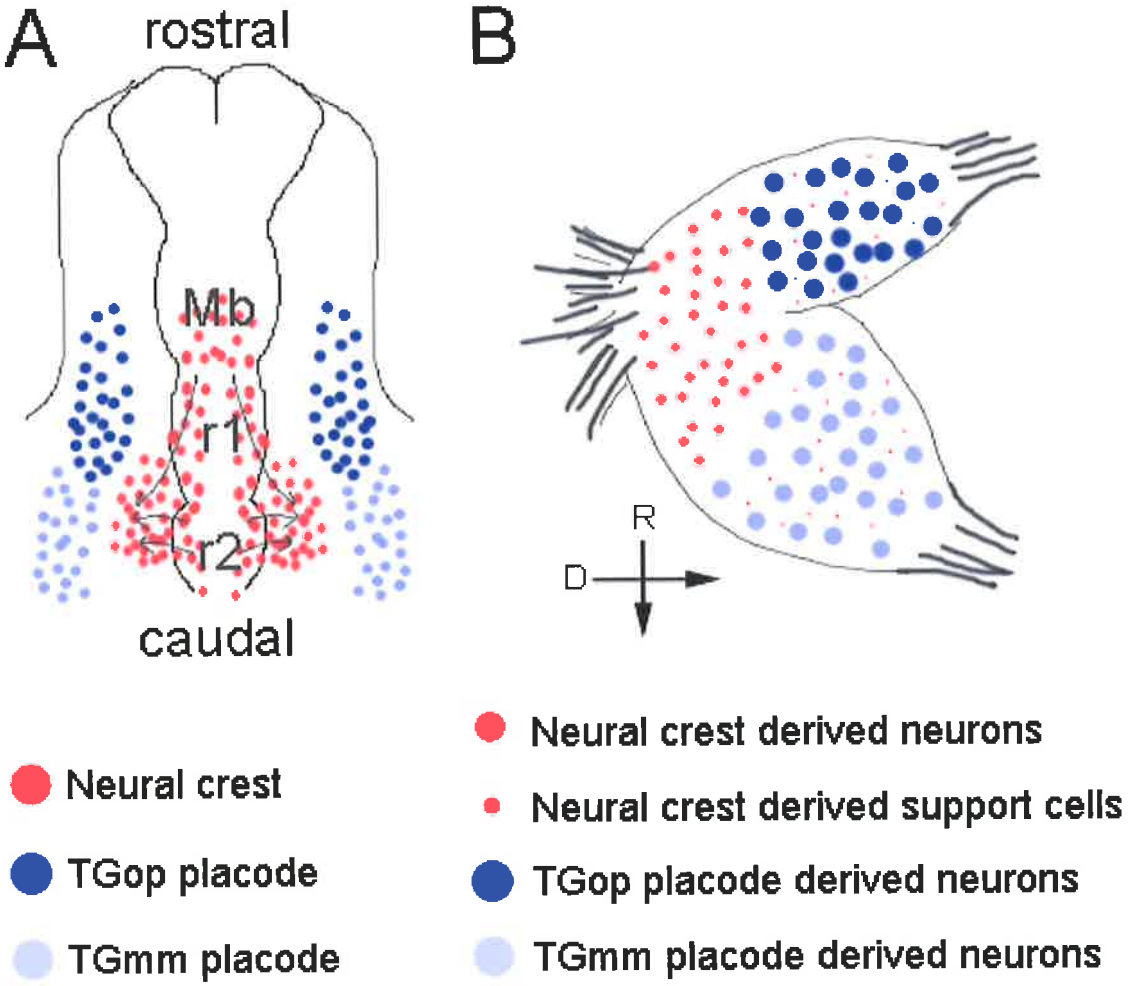

Figure 1.5. The dual embryonic origin of the trigeminal ganglion.

(A) Schematic of a stage 9.5-10 chick (Hamburger and Hamilton, 1951) embryo viewed dorsally. Neural crest cells (red) migrate laterally (arrows) from the midbrain (Mb), and rhombomeres 1-2 (r1 and r2) to contribute to the ganglion in the periphery. Two epidermal placodes, the trigeminal ganglion ophthalmic (TGop; dark blue) placode and the trigeminal ganglion maxillomandibular (TGmm; light blue) placode located adjacent to the neural tube also contribute to the ganglion.

(B) Lateral schematic view of a maturing trigeminal ganglion (~ 4-5 day old embryo) showing the relationship between neural crest and placode derived cells in the ganglion. The proximal region of the ganglion is composed of neural crest derived neurons (red). Throughout the distal lobes, neural crest support cells can be found (red) and placode derived neurons (blue). TGop, ophthalmic lobe; TGmm, maxillomandibular lobe. Arrows indicate orientation. D, dorsal and R, rostral.

Adapted from D'Amico-Martel and Noden (1989).

1.2.2.3 Requirement for both neural crest and placode components

1.2.2.3.1 Ablation studies

Ablating (removing) either the placode or neural crest components have highlighted the requirement and certain degree of mutual dependence for both cells types during various aspects of trigeminal ganglion development (Hamburger, 1961; Lwigale, 2001; Stark *et al.,* 1997). Ablation of the neural crest indicates that this component is not required for placode formation (Stark *et al.,* 1997) or gangliogenesis by placode derived cells (Hamburger, 1961). In neural crest ablated embryos, two-separate ganglia are formed, but are dispersed more than in the presence of neural crest (Hamburger, 1961). Recently it was also noted that ganglia do not form in the correct place following neural crest ablation, although the formation of two separate ganglia was not observed (Lwigale, 2001). This evidence suggests that the neural crest cells act as an aggregation centre for the placode component. Ablating both placodes at stage 12 in the chick embryo causes the complete loss of the ophthalmic lobe, and the slight reduction of the maxillomandibular lobe (Hamburger, 1961; Lwigale, 2001), demonstrating that the placode component is absolutely necessary for the formation of the ophthalmic lobe. However, in the absence of placode, the maxillomandibular lobe has been suggested to form due to the presence of the trigeminal motor nerve (Lwigale, 2001).

1.2.2.3.2 Genetic evidence

The requirement for ophthalmic placode in forming the ophthalmic lobe projections of the trigeminal ganglion is also clearly supported by genetic evidence from *Splotch* mice (Tremblay *et al.,* 1995). In such mice, *Splotch* encodes for a defective allele of the *Pax3* gene (Epstein *et al.,* 1991). Despite the transcription factor Pax3 being important for neural crest cell development, migration of neural crest cells in *Splotch* mice at the level of the trigeminal ganglion was not affected (Serbedzija and McMahon, 1997). Nevertheless, in *Splotch* mice, ophthalmic lobe projections were severely reduced (Tremblay *et al.,* 1995). These observations and the reported expression of *Pax3* in the mouse ophthalmic placode (Stark *et al.,* 1997) implied that the ophthalmic defect in *Splotch* mice (Tremblay *et al.,* 1995) was due to the loss of placodal Pax3 function.

Indeed, the function of Pax3 in the placode appears to be conserved between species. In chick, the ophthalmic placode expresses high levels of *Pax3* transcript starting from about the 4 somite stage (Stark *et al.,* 1997), and high Pax3 protein expression is also localised to

ophthalmic placode derived neurons in the ganglion (Baker *et al.,* 2002). Pax3 expression in the chick ophthalmic placode and invaginated placode cells was demonstrated to correlate with the induction, specification and commitment of these cells to an ophthalmic neuronal fate (Baker and Bronner-Fraser, 2000; Baker *et al.,* 2002; Baker *et al.,* 1999; Stark *et al.,* 1997).

1.3 The trigeminal ganglion and axon guidance

1.3.1 The placode and axon pathfinding

The trigeminal ganglion is one of the earliest cranial sensory ganglia to develop, and project axons to establish connections in the embryo. Interactions between neural crest and placode-derived components are not just necessary for gangliogenesis but are also necessary for setting up the peripheral axon scaffold (Hamburger, 1961; Lwigale, 2001; Noden, 1978; Stark *et al.,* 1997).

One of the major functions for placode-derived cells was highlighted by the impediment of neural crest derived neurons to project peripheral axons when the placode component was removed in the chick embryo. However, when neural crest was ablated, peripheral axon projections by placode derived neurons into the target fields was normal (Hamburger, 1961), although there is very little or complete lack of corneal innervation when neural crest cells are ablated around stages 8-9 (Lwigale, 2001). Indeed, quail-chick chimera experiments revealed that corneal innervation is derived entirely from neural crest neurons. Interestingly, neural crest derived corneal innervation is completely lost when placode cells are ablated around stage 12, perhaps suggesting a pathfinding role for ophthalmic placode derived nerves, even though ophthalmic placode derived neurons do not innervate the cornea *per se* (Lwigale, 2001).

Initial contacts with target fields are made by trigeminal ganglion pioneer axons (Hamburger, 1961; Moody *et al.,* 1989a; Stainier and Gilbert, 1990). The placode component of the trigeminal ganglion is the first to generate neurons in mouse and chick embryos (Begbie *et al.,* 2002; D'Amico-Martel and Noden, 1980; Ma *et al.,* 1998; Moody *et al.,* 1989a; Stark *et al.,* 1997), while neurons from the neural crest component are not produced till at least stage 15 in the chick embryo (Moody *et al.,* 1989a) (Table 1.1). At present, as to whether axons first observed at E8.5-9 in the murine trigeminal ganglion correspond to placode derived neurons is speculative (Easter *et al.,* 1993; Stainier and Gilbert, 1990; Stainier and Gilbert,

1991); although the expression pattern of early pan-neuronal cytoskeletal marker β-tubulin (Easter *et al.,* 1993) corresponded well with the expression of neuronal specific transcription factor *neurogenin-1* in the E8.5 trigeminal placode (Ma *et al.,* 1998). The early generation of neurons by the trigeminal placode, particularly in the ophthalmic placode could therefore denote a role for these cells in establishing the initial peripheral axon scaffold. In agreement with this, labelling with the enzyme horse radish-peroxidase of the ophthalmic placode has demonstrated the presence of conspicuous placode-derived neurons near the midbrain and the optic vesicle during stages 13 to 20 in the chick embryo, suggesting that these neurons differentiate near the site of origin and later shift into the trigeminal ganglion (Covell and Noden, 1989).

1.3.2 Trigeminal ganglion guidance cues

The focus in the past 20-30 years has been to identify molecular cues that generate the patterning of cranial sensory axon projections, particularly those of the trigeminal ganglion in embryogenesis. Early findings of chemotropism came from co-culture explant studies that demonstrated targets of the trigeminal ganglion secreted an attractive cue (Lumsden and Davies, 1983; Lumsden and Davies, 1986) called Maxillary factor (Lumsden, 1988). In such explant co-culture studies trigeminal ganglion explants from E10-11 embryos always showed directed axon outgrowth towards maxillary process tissue and never towards control tissue such as limb bud (Lumsden and Davies, 1983; Lumsden and Davies, 1986). Subsequently, the two components of Maxillary factor were identified as being relatives of Nerve Growth factor, Brain Derived Growth Factor (BDNF) and Neurotrophin-3 (NT-3). However, mice deficient for either one or both molecules did not reveal any obvious guidance defects suggesting that these molecules acted perhaps as permissive cues to growing trigeminal ganglion axons (O'Connor and Tessier-Lavigne, 1999).

On the other hand, there has been much success on the front of identifying guidance cues that restrict trigeminal ganglion axon projections during target field innervation. The chemorepellant semaphorin-3A (Sema3A) (Kobayashi *et al.,* 1997; Taniguchi *et al.,* 1997; Ulupinar *et al.,* 1999), and its cognate receptor, neuropilin-1 (Kitsukawa *et al.,* 1997) are two such molecules. Studies have demonstrated that Sema3A (Taniguchi *et al.,* 1997; Ulupinar *et al.,* 1999), and neuropilin-1 (Kitsukawa *et al.,* 1997) mutant mice have disorganised axon tracts emerging from the trigeminal ganglion, however these projections correctly innervate the target tissue fields (Taniguchi *et al.,* 1997; Ulupinar *et al.,* 1999). Furthermore, neuropilin-

2 deficiencies result in a weak axon defasciculation of the ophthalmic and maxillary axon branches of the trigeminal ganglion (Chen *et al.,* 2000; Giger *et al.,* 2000), and once again axons correctly innervate target tissues.

Other axon guidance molecules likely to contribute to trigeminal ganglion axon guidance are netrin-3 (Seaman and Cooper, 2001) and DCC (Deleted in Colorectal Cancer) (Seaman *et al.,* 2001) interactions as these two molecules are localised to the trigeminal ganglion axonal tracts and target tissues. The extracellular matrix molecule, laminin is also found to localise to trigeminal ganglion peripheral sensory pathways and may provide permissive cues to axons (Moody *et al.,* 1989b). Conditional deletion of neural crest β1-integrin from E8 during mouse embryogenesis however, did not show a trigeminal ganglion axon guidance phenotype at E10, due to incomplete loss of β1-integrin (Pietri *et al.,* 2004).

1.3.3 Trigeminal ganglion lobe specific guidance cues?

Most guidance cues identified to play a role during trigeminal ganglion axon guidance thus far have been non-discriminatory, and do not appear to differentiate between specific trigeminal ganglion lobe projections. Interestingly, recent expression analysis of Sema3 ligands and neuropilin receptors (Chilton and Guthrie, 2003) in the chick at stage 19 (Hamburger and Hamilton, 1951) insinuate that the trigeminal ganglion lobes differentially express these molecules. Therefore, Sema3 ligands and neuropilins may play a role in differential branch specific guidance of trigeminal ganglion axons. This hypothesis is supported by the observation that defects in neuropilin-2 weakly affect only two of the three trigeminal ganglion axon branches (Chen *et al.,* 2000; Giger *et al.,* 2000). Furthermore, mice deficient for Plexin-A3, a receptor for both Sema3F and Sema3A exhibit only a defasciculation defect in the ophthalmic branch at E10.5 onwards (Cheng *et al.,* 2001), once again suggesting a likely role for this family during lobe specific guidance. A suggested schematic of chick trigeminal ganglion axon guidance is shown in Figure 1.6.

Table 1. 1. Timeline of trigeminal ganglion formation, neurogenesis and axon pathfinding in the chick embryo.

Neural crest component	Placode component
St. 9.5 Neural crest emigrate from the posterior mesencephalon and metencephalon to form the ganglion near rhombomere 2.[a]	**St. 10** Neurogenesis in the TGop placode.[b]
	St 11 Pax3 cells enter the mesenchyme from the TGop placode[c]
	St. 12 Neurogenesis in the TGmm placode.[b]
	St. 13 Post-mitotic TGop placode cells invaginate to form the ganglion.[b]
	St. 13-14 TGop neurons undergo axon pathfinding.[d, e]
St. 15 Subset of neural crest cells become neurons. Majority remain undifferentiated.[d, f]	
St. 15 Two lobes converge to form the primitive ganglion.[d]	
St. 15-16 Axons from TGmm lobe are pathfinding into the first branchial arch.[d]	
St. 17-18 Appearence of the separate maxillary and mandibular axon branches observed.[d]	
	St. 21 Cessation of placode invagination to form the ganglion.[f]
St. 23-31 Post-mitotic neurons generated in the proximal region of the ganglion.[f]	

Abbreviations: TGop, trigeminal ganglion ophthalmic placode; TGmm, trigeminal ganglion maxillomandibular.
[a] D'Amico-Martel and Noden (1983); [b] Begbie et. al., (2002); [c] Stark et. al., (1997); [d] Moody et. al., (1989); [e] Covell and Noden (1989); [f] D'Amico-Martel and Noden (1980).

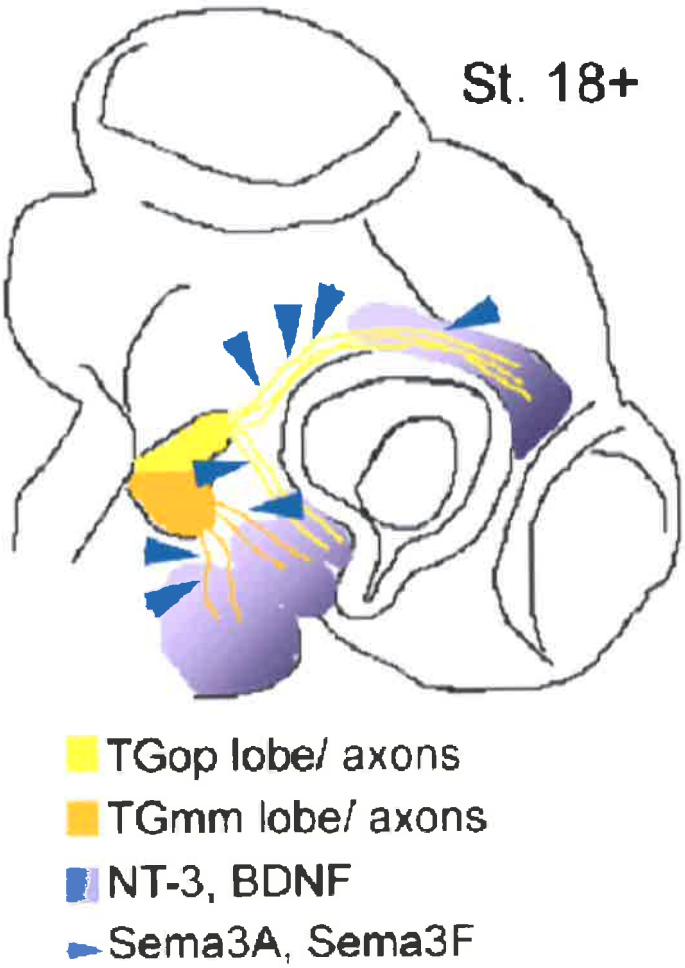

Figure 1.6. A schematic model of trigeminal ganglion sensory axon guidance during chick facial development.

At about stage 18+, it is suggested that the graded expression of neurotrophins (BDNF, NT-3) in a high to low levels (dark blue to light blue tone) act as permissive cues to growing TG axons (O'Connor and Tessier-Lavigne, 1999). Semaphorin-3/ neuropilin interactions (indicated as arrowheads) (Chen et al., 1997; Chilton and Guthrie, 2003; Giger et al., 2000; Kitsukawa et al., 1997; Kobayashi et al., 1997; Taniguchi et al., 1997) may play a role in maintaining TG axon projections by causing axon fasciculation.

BDNF, brain derived neurotrophic factor; NT-3, neurtrophin-3; Sema3A, semaphorin-3A; Sema3F, semaphorin-3F; TGop, trigeminal ganglion ophthalmic lobe/axons; TGmm, trigeminal ganglion maxillomandibular lobe/ axons.

However, Sema3, neuropilins, and neutropohins (Chen *et al.,* 2000; Giger *et al.,* 2000; Kitsukawa *et al.,* 1997; Kobayashi *et al.,* 1997; O'Connor and Tessier-Lavigne, 1999; Taniguchi *et al.,* 1997) are all expressed late during trigeminal ganglion axon guidance (around embryonic day (E) 10 onwards in the mouse; or stage 18 in the chick). Therefore, the expression of these guidance cues does not coincide with the early specification of ophthalmic versus maxillomandibular lobe projections. Initial axons are seen at stage 13 in the chick ophthalmic process (Moody *et al.,* 1989a) and at E9 in the mouse (Stainier and Gilbert, 1990); although in the chick embryo, neurofilament positive cells are observed as early as 13- to 14-somite stage in the ophthalmic placode ectoderm (Baker and Bronner-Fraser, 2000). Since establishment of the initial lobe specific peripheral axon projections appear to involve pioneering axons (Lwigale, 2001; Moody *et al.,* 1989a; Stainier and Gilbert, 1990), the cues responsible for discriminating trigeminal lobe specific axon projections are predicted to be expressed early during development when axons are pathfinding. These molecular cues, such as the Ephs and ephrins, are likely to be differentially laid down en route to the cutaneous target fields.

1.4 Ephs and ephrins as candidates

Ephs and ephrins are excellent candidates for providing branch-specific directions to ophthalmic versus maxillomandibular lobe axons during trigeminal ganglion development. The membrane-bound Eph receptors belong to one of the largest family of tyrosine kinases and have been implicated in a number of developmental processes, including patterning of the nervous system (reviewed by Drescher, 1997; Kullander and Klein, 2002) by providing repulsive as well as attractive cues. There are nine EphA receptors and five EphB receptors in mammals (Figure 1.7). In contrast, there are five A-class and four identified B-class receptors in chicken. The division of Eph receptors into A and B subclasses is based on their structural similarities and also their binding affinities to either glycosylphosphatidylinositol (GPI)-linked or transmembrane ligands (Gale *et al.,* 1996). EphA receptors bind ephrin-A ligands, which are GPI-linked, and EphB receptors bind ephrin-B transmembrane ligands (Figure 1.7-1.8). Within each subclass, there is high degree of binding promiscuity between Eph receptors and ephrin ligands, and the degree of binding affinity a particular receptor has for different ligands varies (Gale *et al.,* 1996). Until now, it was believed that there was very little cross talk between the A and B subclasses, with the exception being EphA4 which can bind both classes of ligands (Gale *et al.,* 1996; Mellitzer *et al.,* 1999). However, it has recently been

shown that EphB2 can also bind ephrin-A5 in addition to its interactions with ephrin-B ligands (Himanen *et al.*, 2004) (Figure 1.7).

1.4.1 Eph receptor structure

The extracellular domain of Eph receptors includes a ligand binding globular domain, a cystein rich region and two fibronectin type III repeats. The intracellular domain consists of the juxtamembrane domain (which has two conserved tyrosine sites), the kinase domain, the sterile α-motif (SAM) domain and the PDZ-binding motif. The SAM domain is involved in receptor dimerisation and oligomerisation, while the PDZ-binding motif is involved in protein-protein interactions (reviewed by (Kullander and Klein, 2002)) (Figure 1.8).

1.4.2 Signalling mechanisms

Both Eph receptors and ephrins can signal intracellularly and thus complicate analysis of their function during developmental processes. The conventional activation of Eph receptors by ephrin ligands is referred to as "forward signalling" (Drescher *et al.*, 1995; Krull *et al.*, 1997; Wang and Anderson, 1997). However, the ligand-bearing cell, upon interaction with its cognate receptor may also transduce a signal, and this is referred to as "reverse signalling" (Birgbauer *et al.*, 2000; Birgbauer *et al.*, 2001; Cutforth *et al.*, 2003; Davy *et al.*, 1999; Davy and Robbins, 2000; Knoll *et al.*, 2001). In addition, depending on the developmental and cellular context, there can be either unidirectional signalling, either through the receptor or the ligand, or bi-directional signalling into both receptor and ligand bearing cells (Mellitzer *et al.*, 1999), and reviewed by Cowan and Henkemeyer, 2002; Holmberg and Frisen, 2002; Klein, 1999; Kullander and Klein, 2002) (Figure 1.8).

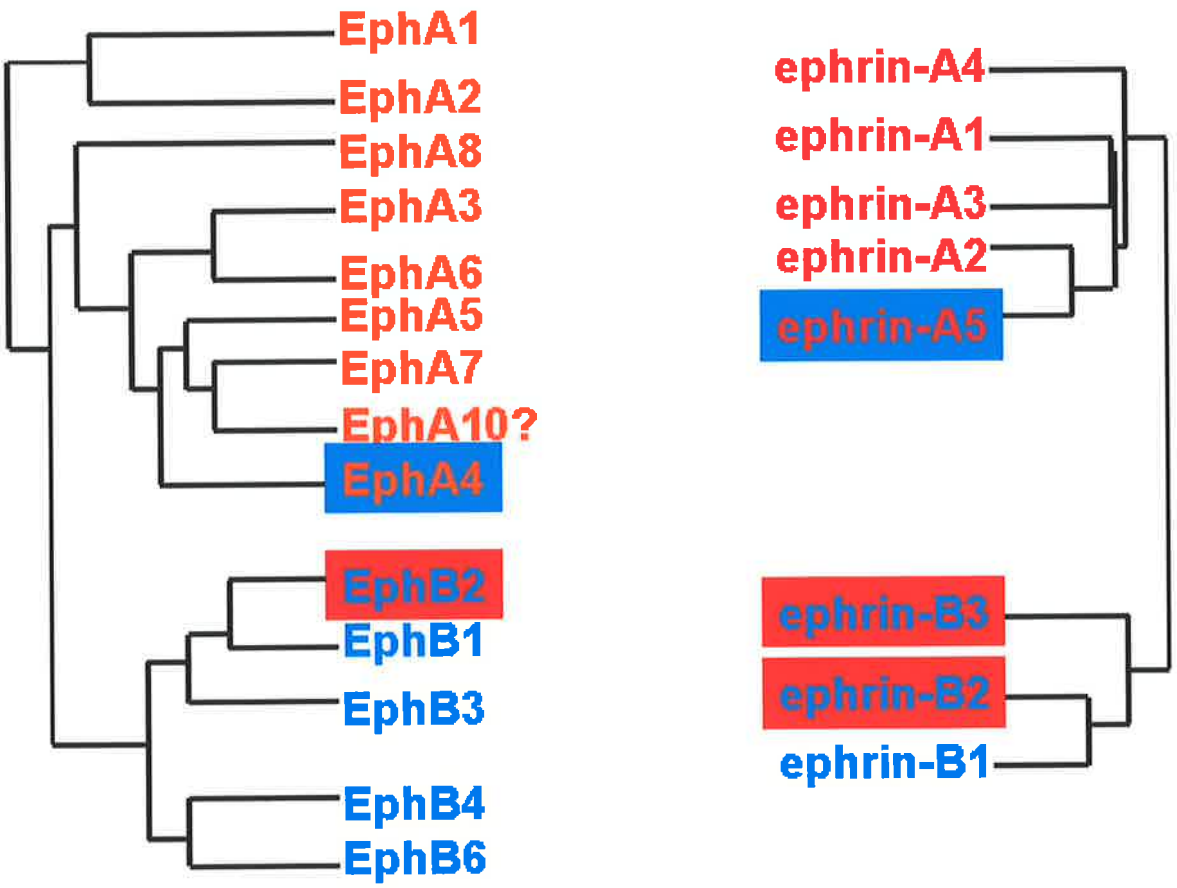

Figure 1.7 Eph receptors and ephrin ligands are divided into A and B subclasses.

The phylogenic relationships between human EphA and EphB and also between ephrin-A and ephrin-B are shown respectively. The ligands that interact with EphA10 have not been identified. Generally there is promiscuous binding between the receptors and ligands within the A (red) and B (blue) subclasses respectively, with little inter-subclass interactions. Ephs and ephrins that participate in inter-subclass low affinity interactions are highlighted either in blue or red. EphA4 (highlighted in blue) has low affinity interactions with ephrin-B2 and ephrin-B3 (highlighted in red). EphB2 (highlighted in red) has low affinity interaction with ephrin-A5 (highlighted in blue).

Image adapted from Pasquale (2004).

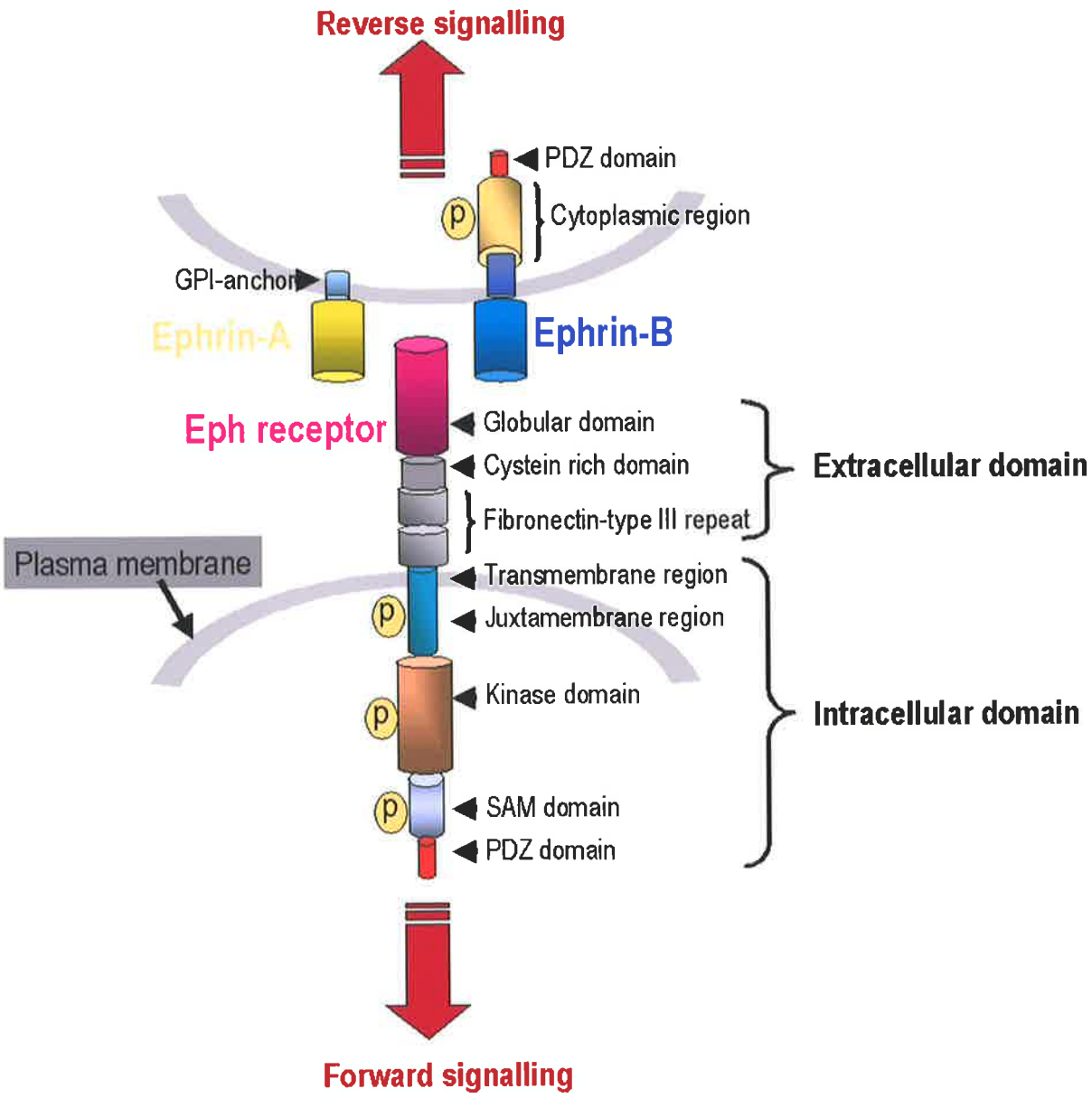

Figure 1.8 Structure of Eph receptors and ephrin ligands.

Schematic shows one cell expressing a generic Eph receptor and another expressing the ephrin ligands. The globular domain of the Eph receptor (pink) is involved in interactions with the ligands (indicated in yellow for ephrin-A and blue for ephrin-B). The globular region is involved in forming receptor-ligand dimers and oligomers. The PDZ domains are involved in protein-protein interactions.

GPI, glycosylphosphatidylinositol; SAM, sterile α-motif.

Adapted from (Kullander and Klein, 2002).

1.4.2.1 Eph kinase "forward" signalling

Since both Eph receptors and ephrins are membrane bound *in vivo*, Eph activation requires cell-cell contact. Another pre-requisite for Eph signalling activation are interactions with dimeric and/or oligomeric (clustered) ligand forms (Davis *et al.,* 1994). However, it has been shown that soluble chimeric-Fc fusion ligands (containing the extracellular ephrin domain fused to Fc-portion of immunoglobulin protein) can be artificially clustered with an anti-Fc antibody to activate Eph receptors (Davis *et al.,* 1994) and can exert biological effects (Wang and Anderson, 1997). Furthermore, there is evidence to suggest that EphB receptors are able to distinguish between ligand dimers and oligomers, influencing the recruitment of different signalling complexes to the receptor (Stein *et al.,* 1998). Following ligand engagement, receptor auto-phosphorylation of the juxtamembrane tyrosine residues unmasks the catalytic domain and fully activates the receptor (Wybenga-Groot *et al.,* 2001).

Interactions between activated receptors and a number of adaptor proteins through the SH2 domain (reviewed by Kullander and Klein, 2002)), can lead to cytoskeletal rearrangement through the Rho-GTPases (Shamah *et al.,* 2001) and the mitogen activated protein kinase (MAPK) pathway (Elowe *et al.,* 2001), as well as changes to β1-integrin mediated cell-substrate adhesion (Becker *et al.,* 2000; Miao *et al.,* 2000; Zou *et al.,* 1999). The biological consequences of activating Eph receptors appear to cause growth cone collapse and neurite retraction, as well as reducing β1-integrin mediated cell-substrate adhesion (Becker *et al.,* 2000; Elowe *et al.,* 2001; Miao *et al.,* 2000; Shamah *et al.,* 2001; Zou *et al.,* 1999) (Figure 1.9).

1.4.2.2 ephrin "reverse" / Eph-kinase independent signalling

The first line of genetic evidence from mice indicated that EphB receptors have a kinase independent function during commissural axon pathfinding in the central nervous system. In absence of functional EphB2 kinase activity, the commissural axon tract was found to be normal, suggesting that axon tract formation was not EphB2 kinase dependent (Henkemeyer *et al.,* 1996). Since then, other studies demonstrated that ephrin-B ligands can mediate reverse signalling in the presence of kinase-inactive EphA4 and EphB receptors and this signalling is sufficient for axon guidance (Birgbauer *et al.,* 2000; Kullander *et al.,* 2001). Upon interactions with cognate receptors, ephrin-B ligands have been demonstrated to mediate phosphorylation dependent and independent signalling (reviewed by Kullander and Klein, 2002).

Unlike ephrin-B transmembrane ligands, it was not clear whether GPI-anchored ephrins participated in Eph kinase independent signalling. Nonetheless, genetic evidence to suggest GPI-anchored ephrin ligand capacity to signal came from analysis of *vab-1 (Eph)* mutants (George *et al.,* 1998), as well as from close inspection of *efn* (*ephrin*) ligands 1-3 *C. elegans* mutants (Chin-Sang *et al.,* 1999; Wang *et al.,* 1999). It was shown that VAB-1 functioned non cell autonomously in the nervous system during normal epidermal development. Unlike the *vab-1* null mutants, which exhibited severe disruption to the coordinated movement of neuroblasts during epidermal morphogenesis, the kinase inactive VAB-1 mutants did not exhibit a complete loss of function. This implied kinase dependent and independent roles for VAB-1 in the nervous system (George *et al.,* 1998). Subsequently, GPI-anchored ephrins as the ligands for VAB-1 was discovered (Chin-Sang *et al.,* 1999; Wang *et al.,* 1999). Since, mutations in *C. elegans* ephrins synergistically enhance the VAB-1 kinase domain mutant phenotype, EFN ligands might partly function in a kinase-independent VAB-1 pathway by mediating reverse signalling (Chin-Sang *et al.,* 1999; Wang *et al.,* 1999).

Further evidence for EphA receptor kinase independent function comes from genetic analysis of ephrin-A5 mutant mice during establishment of the vomeronasal projections (Knoll *et al.,* 2001). In wildtype mice, ephrin-A5 expressing vomeronasal axons project to high EphA6 expressing regions in the accessory olfactory bulb during development. Also *in vitro*, vomeronasal axons showed a preference for growing on lanes containing high concentrations of EphA receptor. However, *in vivo* topographic targeting of vomeronasal axons to the accessory olfactory bulb is disrupted in ephrin-A5 mutants, suggesting that ephrin-A5 in this case may have been acting as a "receptor" (Knoll *et al.,* 2001). Also, ephrin-A5 was shown *in vitro* to induce a signalling response in ephrin-A expressing cells when bound to substratum bound Eph extracellular domains (Davy *et al.,* 1999; Davy and Robbins, 2000). The downstream consequence of ephrin-A signalling was the modulation of integrins, which resulted in changes to cell adhesion and morphology (Davy *et al.,* 1999; Davy and Robbins, 2000; Huai and Drescher, 2001).

How might ephrin-A ligands convey signals intracellularly given their GPI-mode of attachment to the cell membrane? One way in which ephrin-A ligands could mediate reverse signalling is through engagement with a transmembrane co-receptor localised to lipid rafts in the cell membrane. Lipid rafts are dynamic regions of the plasma membrane that are enriched

with cholesterol and glycosphingolipids (Brown and London, 1998; Simons and Toomre, 2000). Additionally, these rafts are enriched with proteins such as caveolins, Src family non-receptor tyrosine kinases and GPI-anchored proteins (Brown and London, 1998; Friedrichson and Kurzchalia, 1998; Shenoy-Scaria *et al.,* 1994; Simons and Toomre, 2000; Varma and Mayor, 1998). Based on the observation that many intracellular proteins are enriched in them, lipid rafts may serve to integrate many different signalling cascades (Simons and Toomre, 2000). Indeed, ephrin-A5 (Davy *et al.,* 1999) and ephrin-A2 (Huai and Drescher, 2001) were demonstrated to localise to caveolin protein fractions, suggesting that ephrin-A ligands are sequestered into lipid rafts. Furthermore, transmembrane B-class ligands, which have the capacity to signal, have also been demonstrated to localise to lipid rafts (Bruckner *et al.,* 1999). Downstream of ephrin-A activation, Fyn, a member of the Src family tyrosine kinase family that is enriched to lipid rafts was identified (Davy *et al.,* 1999; Huai and Drescher, 2001). This also indicated that ephrin-As localises to lipid rafts, and either direct or indirect interactions with Fyn facilitated transduction of ephrin-A signals intracellularly (Figure 1.10).

Figures 1.9 Eph receptor signal transduction.

The schematic shows some of the adaptor proteins interact with Eph kinases that lead to effects in cell proliferation, cytoskeletal changes and integrin-mediated adhesion. Activation of Eph leads to suppression of mitogen-activated protein kinase (MAPK) pathway, causing growth cone collapse and retraction. Cell proliferation may also be inhibited as a result of MAPK signalling inhibition. Ephexin interactions with the Eph receptor kinase domain can lead to changes in cytoskeleton because it differentially affects Rho-GTPases (Rho, Rac, Cdc42). As to whether Eph activation leads to cell adhesion or suppression of adhesion is thought to depend on the cellular context.

Abl, Abelson; Arg, Abl-related gene; GAP, GTPase activating protein; PI3K, phosphatidylinositol 3-kinase; FAK, focal adhesion kinase; LMW-PTP, light molecular weight protein tyrosine phosphatase; NcK, SH2-SH3 adaptor protein.

Adapted from Kullander and Klein (2002).

Figure 1.10 Ephrin ligand signal transduction.

Ephrin-A signalling (left hand-side schematic): upon engagement with an Eph receptor, ephrin-A initiate a signal cascade that requires the Src-family tyrosine kinases. This leads to the activation of MAPK pathway and also causes integrin-mediated adhesion (through inside out signalling).

Ephrin-B signalling (right hand-side schematic): tyrosine phosphorylation of the ephrin-B cytoplasmic tail occurs via the activity of Src-family tyrosine kinases following engagement with the Eph receptor. SH2 adaptors such as Grb4 bind to the tyrosine phosphorylated site, and activate the PAK pathway. Phosphorylation state independent activation of the JNK pathway can also occur following engagement of ephrin-B with Eph receptors. A number of PDZ binding proteins can also interact with ephrin-B and activate signalling. The JNK, PAK and PDZ dependent signalling pathways result in cytoskeletal changes, and modulate integrin-mediated adhesion.
It has been suggested that ephrin-A and ephrin-B may be sequestered to different membrane lipid raft environments (grey versus brown membrane).
JNK, c-Jun N-terminal kinases; PAK, p21-activated kinases.

Adapted from Gauthier and Robbins (2003).

Figure 1.9 Eph receptor signal transduction.

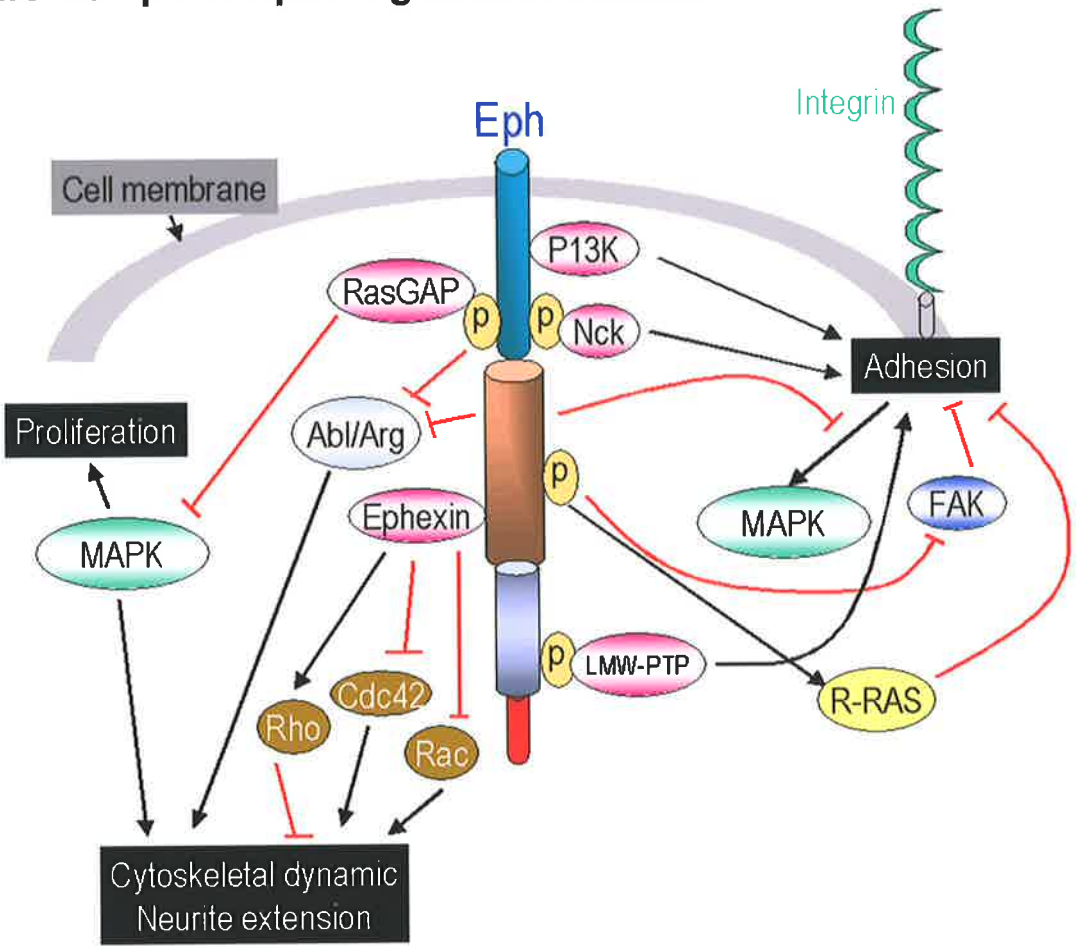

Figure 1.10 Ephrin signal transduction.

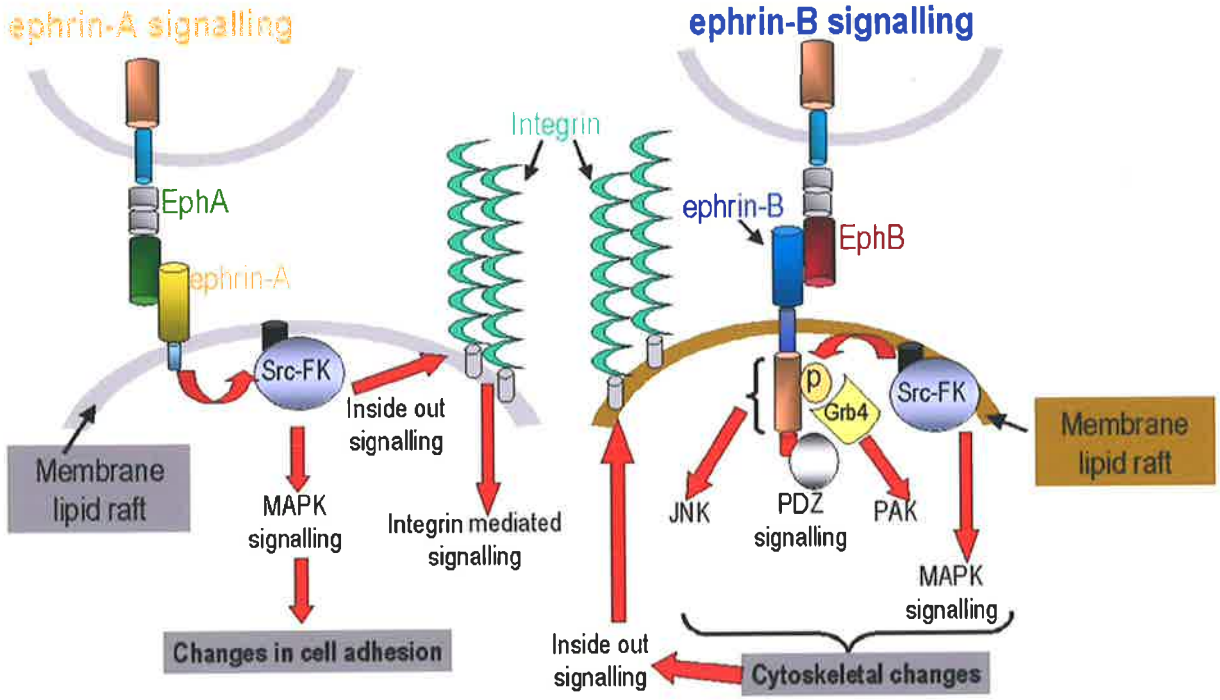

1.4.2.3 Adhesive/ attractive and repulsive Eph/ ephrin interactions

The interaction of Eph receptors with ephrins occurs with high affinity (Gale *et al.,* 1996) and this presents a paradox. How are high affinity interactions between cells converted to repulsion in which cells disengage and move apart? How is this repulsion terminated? There are several mechanisms that have been identified and these are described below (Figure 1.11-1.12).

1.4.2.3.1 Proteolytic cleavage

One mechanism for terminating EphA-ephrin-A mediated contact is through the activation of ADAM10/ Kuzbanian (a metalloprotease), which has been shown to cleave the juxtamembrane domain of ephrin-A (Hattori *et al.,* 2000) (Figure 1.11A, B).

1.4.2.3.2 Transcytosis

An alternative possibility was suggested for terminating EphB-ephrin-B signalling since proteolytic cleavage was found to be not very efficient (Mann *et al.,* 2003; Marston *et al.,* 2003; Zimmer *et al.,* 2003). It has been discovered that following EphB receptor interactions with ephrin-B ligands, membrane patches containing full-length EphB-ephrin-B complexes become engulfed or transcytosed from one cell into the neighbouring cell (Marston *et al.,* 2003; Zimmer *et al.,* 2003) (Figure 1.11A, C). As for EphB-ephrin-B, transcytosis may also serve to remove EphA-ephrin-A receptor complexes from the cell surface (Davy and Robbins, 2000; Jurney *et al.,* 2002; Wimmer-Kleikamp *et al.,* 2004), although this has not been investigated in depth. It is believed that initiation of intracellular signalling may also drive cell repulsion. Evidently, cells expressing truncated forms of EphB or ephrin-B lacked the capacity to transcytose (Zimmer *et al.,* 2003). Nevertheless, neighbouring cells that express the full-length cognate binding partner can transcytose the truncated EphB or ephrin-B, signifying that the cytoplasmic domain is required for internalisation (Zimmer *et al.,* 2003) (Figure 1.11D).

1.4.2.3.3 Truncated receptors

The view that intracellular signalling might lead to repulsion is further substantiated by the examination of EphA7 splice forms (Holmberg *et al.,* 2000). Mouse embryos that lack EphA7 or ephrin-A5 fail to undergo neural tube closure because both molecules are important for adhesion. Holmberg *et al.,* (2000) demonstrated that cells expressing the truncated splice form of EphA7 do not become repelled by ephrin-A5 unlike those that expressed full length EphA7. Therefore, Eph repulsive signalling was concluded to dependent on the

phosphorylation of the receptor kinase domain. The authors also showed that the repulsive interactions between full length EphA7 and ephrin-A5 could be converted to adhesion merely by co-expressing truncated EphA7s with full-length EphA7 receptors. In fact during development, the splice form and full-length EphA7 receptors are expressed in the closing neural tube in addition to ephrin-A5. Based on these results, the authors proposed that the splice form of EphA7 was able to reduce or modulate full length EphA7 repulsive signalling in response to stimulation with ephrin-A5 (Holmberg *et al.,* 2000) (Figure 1.11E). These results concurred with an observation that truncated EphA3 could act as a dominant negative of EphA3 full length function *in vivo* (Lackmann *et al.,* 1998). Holmberg *et al.,* (2000) however, did not discuss the added possibility that there might be ephrin-A5 reverse or EphA7 kinase independent signalling in the ephrin-A5 bearing cell, which leads to increased β1-integrin signalling and adhesion (Davy and Robbins, 2000; Huai and Drescher, 2001). Therefore, the reduction or lack of signalling via EphAs in the receptor bearing cell, in addition to signalling through ephrin-A bearing cell may collectively lead to adhesion.

1.4.2.3.4 Strength of Eph signalling

Eph activation is proposed to involve two steps: ligand binding and ligand-independent receptor-receptor oligomerisation (clustering) events (Lackmann *et al.,* 1998). Therefore, the strength of Eph signalling within a cell could be modulated at either or both steps. As alluded to before (Holmberg *et al.,* 2000), the resulting strength of Eph signalling may be correlated with adhesive or repulsive cellular responses.

The view that the level of ligand abundance is proportional to the level of ligand induced Eph clustering and thus signalling, was substantiated by recent examination of retinal topographic mapping (discussed in section 1.4.3.3) *in vitro*, which revealed that EphA-ephrin-A adhesion could be converted to repulsion (Hansen *et al.,* 2004). Low concentrations of ephrin-A2 substrate were found to promote growth of EphA expressing retinal axons, and conversely, high concentrations of ephrin-A2 substrate were found to inhibit axon growth. The authors proposed that the increasing concentration of ephrin-A2 was proportionately related to the recruitment of EphA receptors into higher order signalling clusters. Although there is a linear increase in adhesion as the concentration of ephrin-A increases, there is increasing repulsion because of exponential EphA receptor recruitment into higher order EphA-ephrin-A complexes. Consequently, inhibitory signalling would predominate over adhesive receptor-ligand interactions (Figure 1.12) (Hansen *et al.,* 2004). In support of this notion, it has been

demonstrated that ephrin mediated signalling is highly dependent on ephrin density and oligomerisation: ephrin monomers do not activate Eph signalling, dimers activate weak signalling and higher-order receptor-ligand clusters result in strong receptor activation (Davis *et al.,* 1994; Huynh-Do *et al.,* 1999; Stein *et al.,* 1998).

As previously mentioned, the degree of ligand-independent Eph clustering may also dynamically modulate a cellular response (Lackmann *et al.,* 1998). When stimulated with ephrin-A5, EphA3 assembles into large signalling clusters that exceed the size of the interacting ephrin surface severalfold. This expansion of receptor clustering and phosphorylation was apparently due to the recruitment of new receptors, as demonstrated with Green Fluorescent Protein tagged EphA3 using confocal time-lapse and fluorescent resonance energy transfer microscopy. Evidence suggested that this propagation of receptor clustering following ligand contact did not require direct ephrin contact, since EphA3 mutants with compromised ephrin-binding activity were incapable of cluster formation and phosphorylation. However, these mutants can be effectively recruited into clusters and phosphorylated when co-expressed with functional receptors. Thus, this may provide a mechanism for recruiting kinase impaired and ephrin-binding compromised receptors into the same signalling complexes (Wimmer-Kleikamp *et al.,* 2004). As a result, ephrin-independent Eph clustering could modulate a cellular response depending on the overall composition and abundance of receptor variants within a cell (Holmberg *et al.,* 2000; Wimmer-Kleikamp *et al.,* 2004).

Figure 1.11 (Part A) Mechanisms of Eph and ephrin repulsion.

(A) Following contact between receptor and ligand, there are phosphorylation events (P), and intracellular signalling (maroon arrows) leading to repulsion.

(B) In the case of EphA and ephrin-A, there is proteolytic cleavage of the ligand by a metalloprotease (red). Ephrin-As that are not engaged are spared by the metalloprotease.

(C) In the case of EphB and ephrin-B, there is transcytosis of full length proteins into cells (red arrows).

Adapted from Noren and Pasquale (2004).

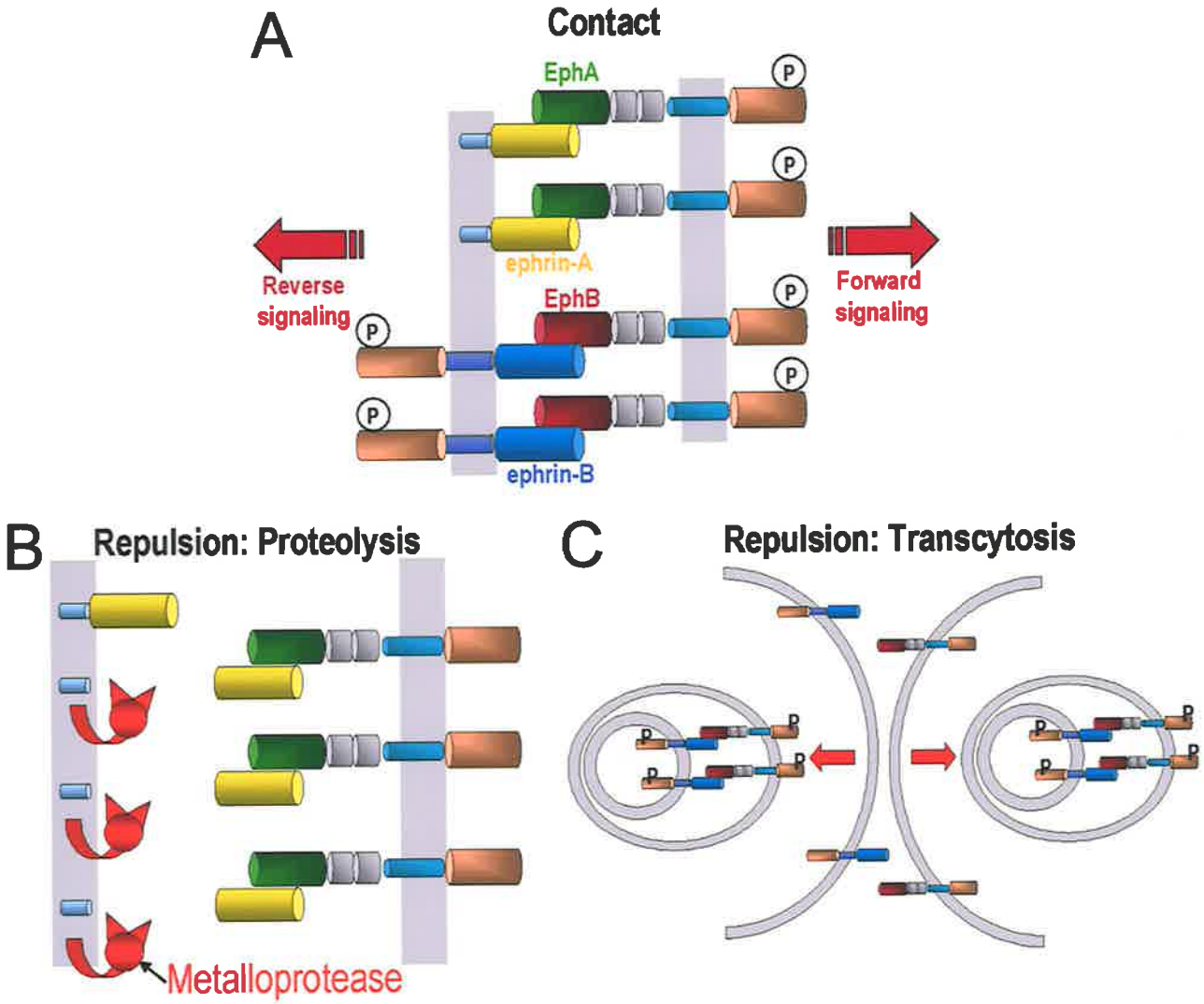

Figure continued on the next page.

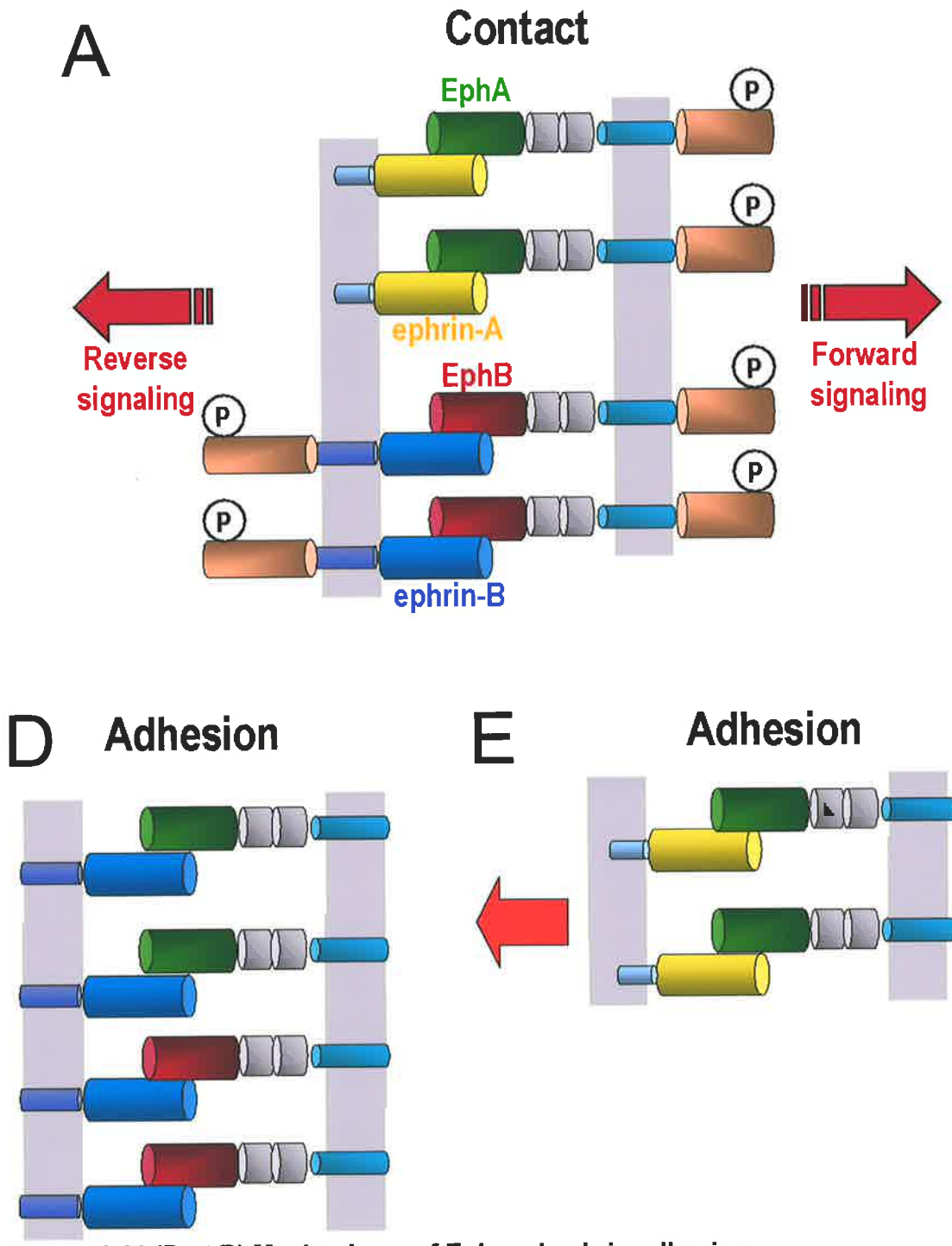

Figure 1.11 (Part B) Mechanisms of Eph and ephrin adhesion.
(A) Following contact between receptor and ligand, there are phosphorylation events (P), and intracellular signalling (maroon arrows) leading to repulsion.
(D) A cell expressing truncated versions of Eph receptors and ephrin-B. Due to lack of intracellular signalling, there is no repulsion.
(E) Modulation of full length EphA activity by a co-expressed truncated EphA can also lead to adhesion following ephrin-A interactions. There may also be reverse signalling through ephrin-A (red arrow).

Adapted from Noren and Pasquale (2004).

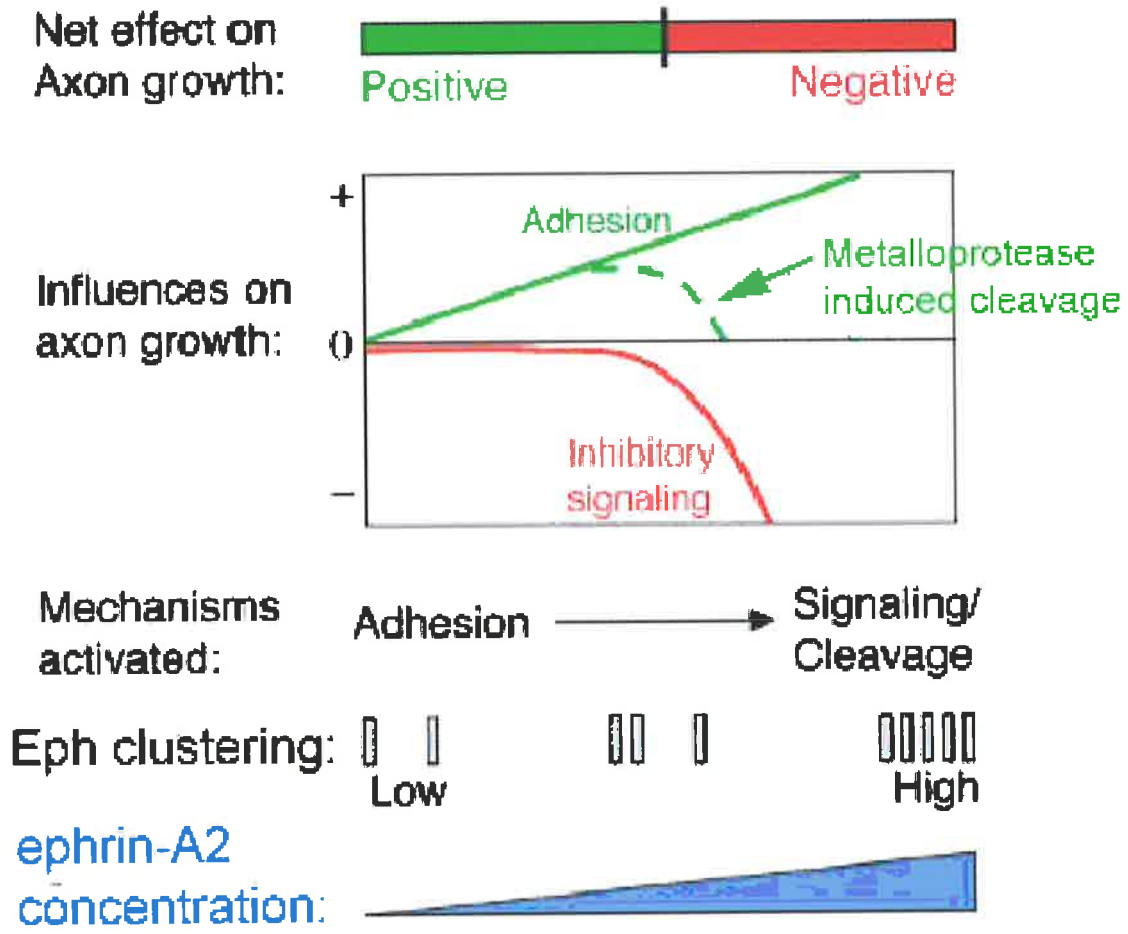

Figure 1.12 Ephrin-A2 positive and negative effects on retinal axon growth are concentration dependent.

As the concentration of ephrin-A2 increases (blue triangle at the bottom) in the target, it is proposed that there is increased clustering and activation of axonal EphA receptors. It is proposed that low activation of EphA receptors promotes growth of axons due to adhesion. However, higher clustering of EphA receptors leads to an exponential increase in EphA receptor transduction, and causes axon repulsion. The authors also propose that higher order receptor-ligand complexes induce metalloprotease cleavage of ephrin-A2 from the cell membrane and thereby further promoting repulsion (inhibitory signalling).

Image adapted from Hansen et. al., (2004).

1.4.2.4 Modulation of Eph signalling by co-expressed ephrins

During development, Eph receptors and ephrin ligands can be expressed on the same cell (Blanco *et al.*, 2002; Connor *et al.*, 1998; Eberhart *et al.*, 2000; Marcus *et al.*, 1996). This presents another added layer of complexity to Eph-ephrin interactions in that receptors may interact with not only target ephrins but also with co-expressed ephrins. Hornberger et. al., (1999) have demonstrated that EphA signalling in retinal ganglion axons can be modified by co-expressed ephrin-A ligands during guidance into the tectum (discussed in section 1.4.3.3). In this system, the level of receptor activation may be dependent on the level of ephrin co-expression. The observation that the level of co-expressed ephrin-A is inversely correlated with the level of EphA phosphorylation suggested two possibilities. One possibility was that the binding of ligand to receptor on the same (*cis*) or adjacent (*trans*) axons resulted in a pool of "silenced" receptors, and a complementary pool of "free" receptors that could be activated by external (*trans*) ephrin-As. The other thought was that sustained phosphorylation of EphA by co-expressed ephrin-A might render the axons/ growth cones insensitive to external cues. It was however unclear whether such a modulation of EphA receptor function by co-expressed ephrin-A was cell-autonomous (Hornberger *et al.*, 1999).

A later study demonstrated that EphA function could be modulated by co-expressed ephrin-As in a cell autonomous manner *in vitro* (Yin *et al.*, 2004). This was shown using three different methods. Firstly, it was found that the binding of functional blocking monoclonal antibodies to ephrin-A2 was reduced when ephrin-A2 and EphA4 were co-expressed. Secondly, patches of EphA3 were found to co-localise with co-expressed ephrin-A2, and not with ephrin-B2. Thirdly, the group showed that *trans*-activation of EphA4 was inhibited when ephrin-A2 ligands are co-expressed. It was proposed that during *cis*-interactions, EphA and ephrin-A interact through their functional extracellular binding domains, and that these occupied receptors were unable to transduce a signal inside the cell. Therefore, the ability of *cis*-interactions to inhibit *trans*-interactions will be dependent on the levels of EphA and ephrin-A in *trans* (Yin *et al.*, 2004) (Figure 1.13).

In summary, co-expression of ligands and receptors *in vivo* have the capacity to modulate Eph signalling capacity by reducing the pool of receptors that are capable of interacting in *trans*.

1.4.3 Examples of Eph/ ephrin interactions during development of the nervous system

As mentioned previously, Ephs and ephrins play an important role during patterning of the nervous system axon pathfinding and axon fasciculation.

1.4.3.1 Axon pathfinding- roles during optic nerve formation and during commissural axon tract formation

1.4.3.1.1 Optic nerve formation

During establishment of the visual system, retinal ganglion cell (RGC) axons within the retina project through to the optic disc, and subsequently into the optic stalk to form the optic nerve. This event is followed by the formation of a topographic map onto the superior colliculus in mammals (discussed in section 1.4.3.3). It has been demonstrated that RGC layer expressed EphB receptors uniformly or in a high ventral to low dorsal pattern, while ephrin-B ligands are either expressed uniformly or in an opposite high dorsal to low ventral manner. Analysis of *EphB2; EphB3* null mice revealed an increased incidence of RGC axon pathfinding errors to the optic disc. More specifically, removing both receptors affected only axon pathfinding of dorsal RGC axons, and this phenotype was synergistically enhanced by loss of both receptors. A role for EphB kinase independent function was also demonstrated because mutants lacking EphB2 kinase activity in an *EphB3* null background had milder axon pathfinding errors compared to the *EphB2; EphB3* null mice. These results led to the conclusion that some aspects of retinal axon pathfinding required EphB kinase independent function and possibly involved ephrin-B reverse signalling (Birgbauer *et al.*, 2000).

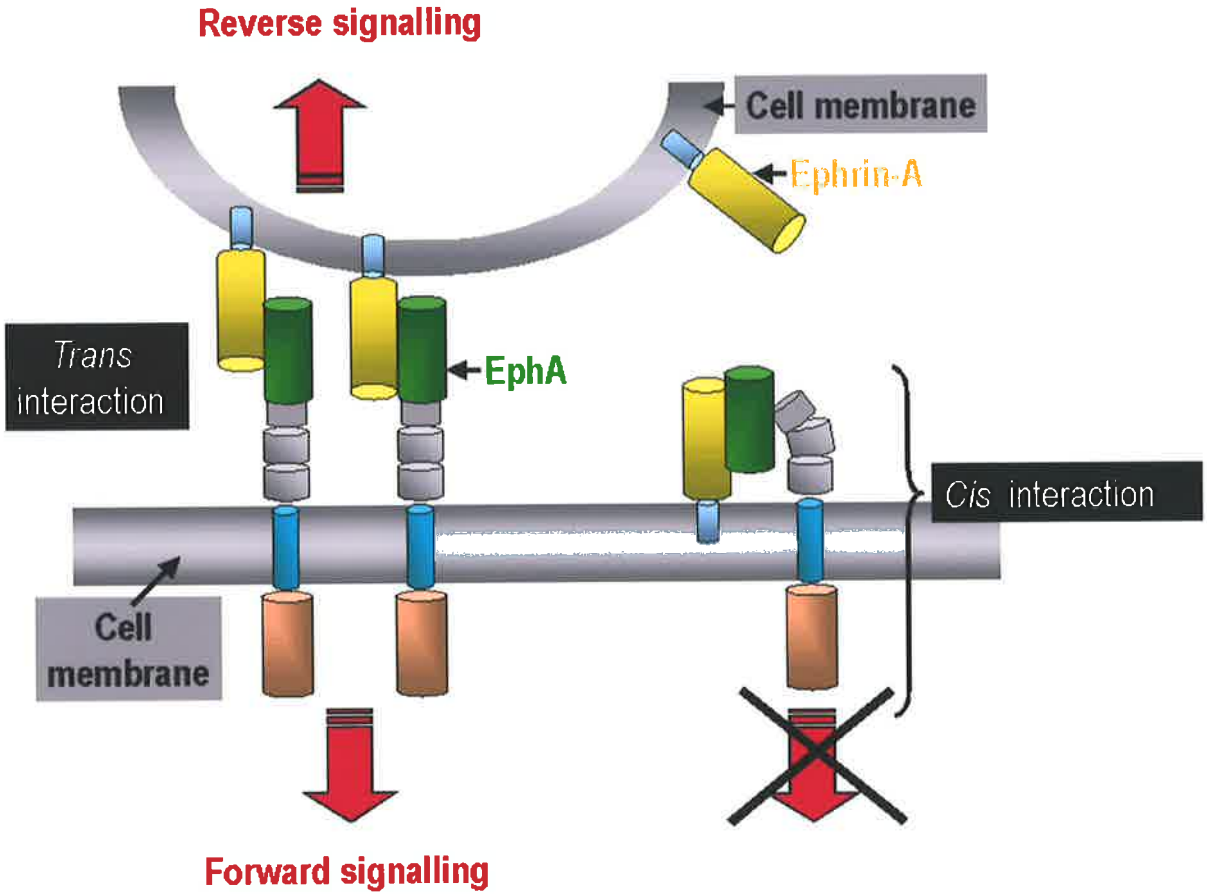

Figure 1.13 A Schematic model showing how co-expressed ephrin-A can modulate EphA activity.

When an EphA (green) expressing cell contacts an ephrin-A (yellow) expressing cell (*trans* interaction), there is forward and/or reverse signal transduction (marron arrows into both cells). However, if the EphA expressing cell also co-expresses ephrin-A ligands, the receptors can be participate in *cis* which involves the extracellular domain of the Eph and ephrin. *Cis*-interactions has two proposed consequences: (1) it may reduce the number of receptors involved in *trans*-activation, as shown by the unbound ephrin-A remaining on the opposing cell, and (2) prevent receptor forward signal transduction.

Adapted from Yin et. al., (2004).

1.4.3.1.2 Commissural axon tract formation

Another example that displayed the requirement for Eph/ephrin interactions in axon pathfinding is during commissural axon tract formation. In the central nervous system, axon tracts from each hemisphere cross the midline and connect with the other side. In murine *EphB2* null mutants, one of the cortical axon tracts that form the posterior tract of the anterior commissure (pAC) become misrouted and cause a functional defect in communication between the two lobes of the temporal cortex (Henkemeyer *et al.,* 1996). The misrouting occurs in *EphB2* null mice because in wildtype mice, EphB2 is expressed predominantly in cells that is normally avoided by ephrin-B2 positive pAC axons (Cowan *et al.,* 2004; Henkemeyer *et al.,* 1996; Orioli *et al.,* 1996), In the presence of truncated EphB2, which lacks the kinase domain, pAC tract defect was not observed suggesting EphB2 kinase independent signalling was required (Henkemeyer *et al.,* 1996). Therefore, the experiments of Henkemeyer et. al., (1996) had two interpretations and these were: that another EphB receptor was functioning redundantly during pAC formation or there was ephrin-B2 reverse signalling. The issue of redundancy was addressed and it was shown that EphB3 cooperated with EphB2, although EphB2 alone was found to be sufficient for pAC pathfinding (Orioli *et al.,* 1996). To address the possibility of ephrin-B2 reverse signalling, the kinase function of ephrin-B2 was interrogated by removing the kinase domain. When ephrin-B2 kinase deficient mice were analysed, it was noted that the pathfinding of commissure axons were compromised at the midline. Thus, EphB2 kinase independent signalling together with ephrin-B2 reverse signalling was concluded to be important during the formation of this tract (Cowan *et al.,* 2004).

Another member of the Eph family, EphA4 was also found to be important for the formation of the pAC in a kinase independent manner. Unlike *EphA4* knockout mice, which showed agenesis of the anterior commissure tracts, *EphA4* kinase domain mutants showed a complete rescue of the knockout phenotype (Kullander *et al.,* 2001). These *EphA4* results, together with the *EphB2* and *ephrin-B2* mutant analysis indicated that non cell autonomous Eph function played a crucial role during pAC axon pathfinding (Cowan *et al.,* 2004; Henkemeyer *et al.,* 1996; Kullander *et al.,* 2001; Orioli *et al.,* 1996).

1.4.3.2 Axon fasciculation

Axon tract/ bundle formation is essential during axon guidance to prevent growing axons from wandering into non-target regions. A role for Ephs and ephrins during axon

fasciculation has been described *in vitro* and *in vivo* (Birgbauer *et al.,* 2000; Eberhart *et al.,* 2000; Eberhart *et al.,* 2002; Winslow *et al.,* 1995) (Figure 1.14).

Co-culturing cortical neurons on astrocytes *in vitro* is analogous to advanced stages of late brain development when neural pathways and axon fiber tracts are laid down. In such a system, the formation of large axon bundles (fascicles) is observed. It is reported that adding a soluble EphA5-IgG or ephrin-A5-IgG (antagonist) completely blocks fascicle formation, although neurite outgrowth is unaffected, suggesting that EphA5 and ephrin-A5 function during axon fasciculation. In adding the agonists, the normal interaction between neuronal-EphA5 and astrocyte-ephrin-A5 is prevented (Winslow *et al.,* 1995). The requirement for direct interaction between EphA5 and ephrin-A5 to form axon bundles was supported by the evidence that separation of the two cell types with a permeable filter also prevents axon fasciculation. Further to this, EphA5 was only phosphorylated when neurons and astrocytes were co-cultured. This suggests that EphA5 might regulate axonal adhesion molecules such as L1/NgCAM, which are thought to mediate axon fasciculation (Caras, 1997). In support of this, it has been shown *in vivo*, that chicken L1 is tyrosine phosphorylated, and *in vitro* is a target for phosphorylation by EphB2 (Zisch *et al.,* 1997). It is also worth noting that mice deficient for both *EphB2* and *EphB3* exhibit fasciculation defects in brain structures in which L1 is highly expressed (Henkemeyer *et al.,* 1996; Orioli *et al.,* 1996). Therefore, there appears to be a link between axonal adhesion molecules such as L1 that participate during axon fasciculation and the Eph and ephrins.

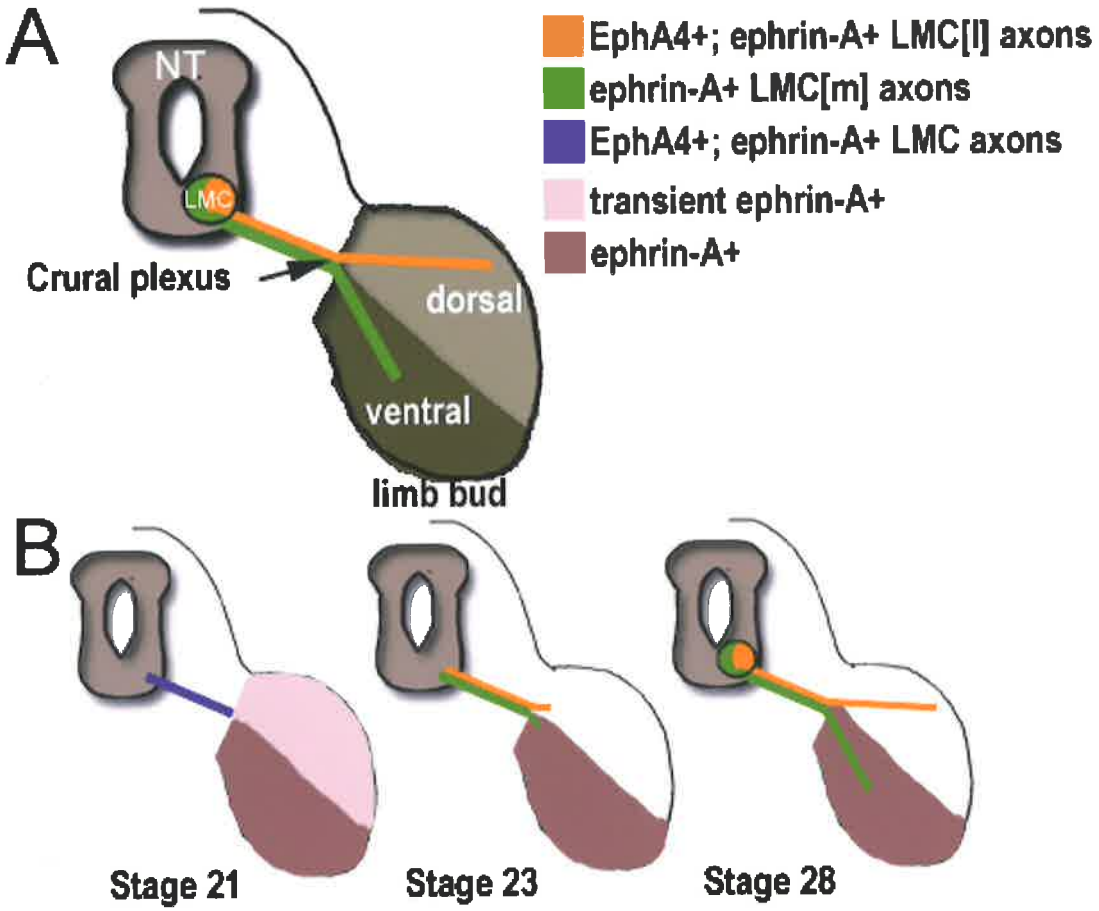

Figure 1.14 EphA4 is a switch that controls dorsoventral motor axon trajectories in the hind limb.

(A) Schematic shows lateral motor column (LMC) in the ventral neural tube (NT) projecting axons into the limb bud. Lateral LMC (LMC[l]) axons (shown in orange) project into the dorsal limb bud (light grey), and the medial LMC (LMC[m]) axons (shown in green) project into the ventral limb bud (dark grey).

(B) During initial stages of chick development (stage 21; Hamburger and Hamilton, 1951) All LMC axons express EphA4, ephrin-A2 and ephrin-A5 (shown in blue). The entire limb bud expresses ephrin-A (pink/maroon), thereby preventing the premature entry of motor axons into the limb bud. Note that the dorsal limb bud mesenchyme only transiently expresses ephrin-As (pink; stage 21). Around stage 23, EphA4 is progressively restricted to the LMC[l], as axons sort at the crural plexus. The dorsal limb bud at this stage does not express ephrin-A. At stage 28, EphA4+ LMC[l] axons invade the ephrin-A2 negative dorsal limb bud and EphA4 negative LMC[m] axons invade the ventral limb bud.

Image adapted from Eberhart et. al., (2004).

In vivo evidence for Eph signalling during axon fasciculation comes from examination of motor axon guidance into the developing limb bud (Eberhart *et al.,* 2000; Eberhart *et al.,* 2002) (Figure 1.14). In the ventral neural tube (NT) of the embryo, spinal motor neurons extend axons along stereotypic trajectories to innervate target muscles in the limb. These neurons are present in the lateral motor column (LMC) (Figure 1.14). At the entry of the limb, LMC axons sort into two distinct axon tracts that innervate the dorsal and ventral musculature respectively. There is a direct relationship between the location of motor neuron cell bodies in the spinal cord and their preferences to project in either the dorsal or ventral nerve trunk. In the limb, neurons in the medial LMC (LMC[m]) innervate ventral muscles, while those in the lateral LMC (LMC[l]) innervate the dorsal musculature (Landmesser, 1978; Tosney and Landmesser, 1985). During early development, LMC[m] and LMC[l] axons fasciculate together and all express EphA4, ephrin-A2 and ephrin-A5 (Eberhart *et al.,* 2000) (Figure 1.14). However prior to limb innervation, sorting into the ventral and dorsal axon trajectories at the crural plexus coincides with EphA4 becoming restricted to lateral axons (Figure 1.14) The restricted expression of EphA4 by LMC[l] axons and the continued expression of ephrin-As by all axons was suggested to influence axon fasciculation and sorting into dorsal and ventral axon trajectories (Eberhart *et al.,* 2000). Concurring with this belief, ectopic expression of EphA4 in LMC[m] neurons, caused the redirection of LMC[m] axons dorsally (Eberhart *et al.,* 2002). On the contrary, loss of EphA4 function in certain mouse genetic backgrounds divert projection of LMC[l] axons into the ventral limb (Helmbacher *et al.,* 2000). These results provide strong evidence that EphA4 functions as a switch to promote the segregation of dorsal from ventral motor axons prior to innervation of the hindlimb (Eberhart *et al.,* 2002) (Figure 1.14).

1.4.3.3 Roles during anterior-posterior retinotectal topographic mapping

During topographic mapping, an array of neurons project onto a target field, so that spatial arrangement of the neurons is maintained in the spatial order of their projections. The retinotectal system serves as an excellent model system for understanding topographic projections, which can be found in central and peripheral nervous systems. Retinal ganglion cell (RGC) axons from the retina course through the optic nerve and optic tract and enter the anterior tectum (or the superior colliculus (SC) in mammalian brains). Nasal axons project to the posterior tectum and temporal axons terminate to the anterior tectum (reviewed by Flanagan and Vanderhaeghen, 1998). Sperry (1963) hypothesised that

topographic mapping could be accomplished by complementary labels of gradients across the projecting and target regions.

Initial evidence that Ephs and ephrins were involved in establishing appropriate anteroposterior neural connections in the retinotectal system came from the observation that EphAs and ephrin-As were expressed in a graded manner (Figure 1.15). In both the chick and mouse, ephrin-A2 and ephrin-A5 were expressed in an overlapping posterior to anterior gradients across the midbrain (Cheng and Flanagan, 1994; Cheng *et al.,* 1995; Drescher *et al.,* 1995). In the chick, EphA3 was expressed in a temporal to nasal gradient, while EphA4 is expressed uniformly across the retina (Cheng *et al.,* 2001; Connor *et al.,* 1998) (Figure 1.15). In comparison to the chick however, the graded expression of EphA3 is replaced with the expression of EphA5 and EphA6 in a temporal to nasal RGC gradient in mice (Brown *et al.,* 2000; Feldheim *et al.,* 1998). Therefore, the expression suggested that ephrin-A2 and -A5 act in retinotectal/ retinocollicular mapping as repellents.

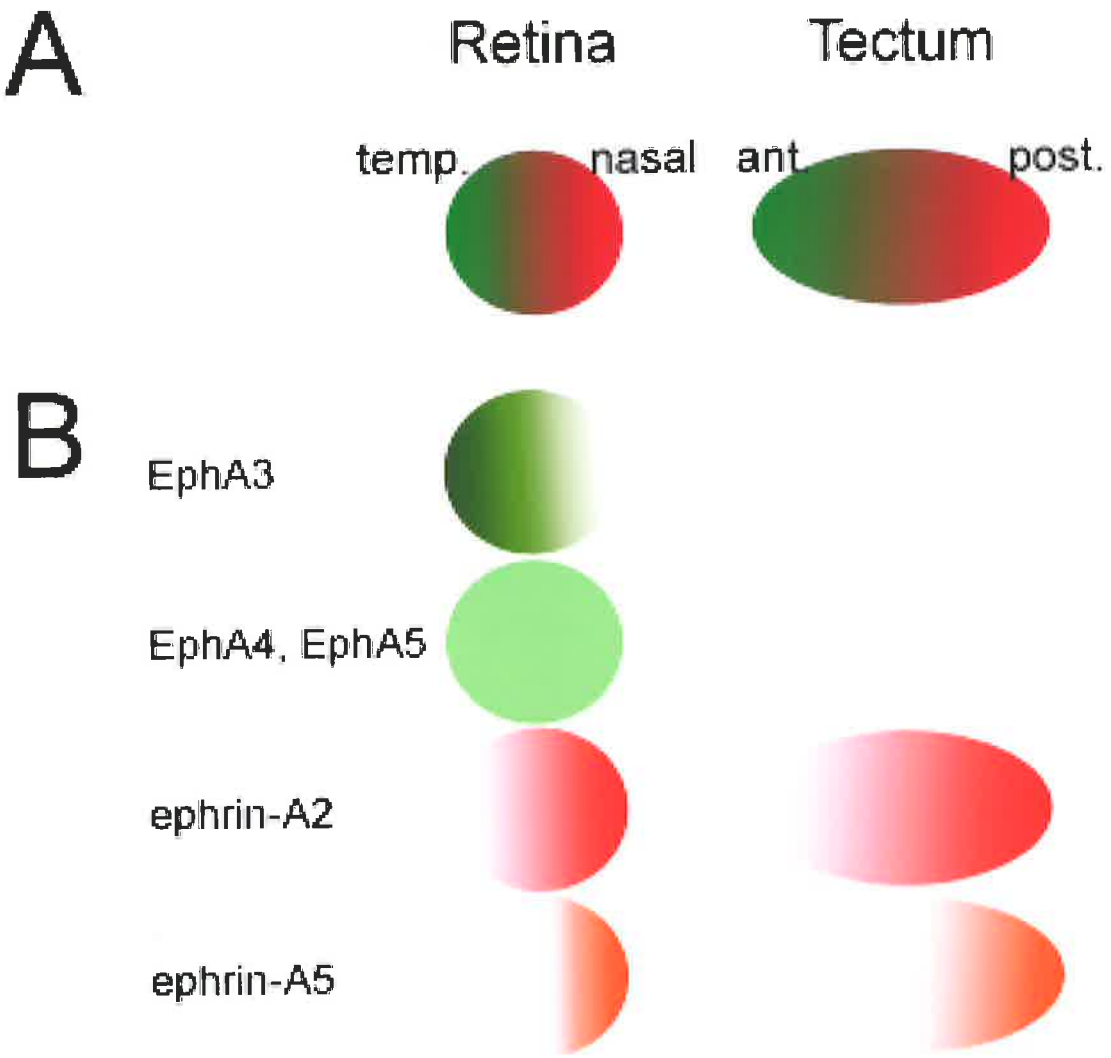

Figure 1.15 EphA and ephrin-A expression during anteroposterior retinal topographic mapping in the chick embryo.
(A) The temporal (temp.) retina and anterior (ant.) tectum is depicted in green, while the nasal retina and posterior tectum shown in red. During topographic mapping, temporal retinal ganglion cell axons project to anterior regions of the tectum, while nasal retinal ganglion cell axons map to the posterior tectum. (B) There are gradients of EphA and ephrin-A expression in the retina and the tectum. Dark tones of colour illustrate high expression while lighter tones depict low expression of EphA or ephrin-A. EphA expression is shown in green and ephrin-A expression in red. Note that EphA4 and/or EphA5 are not expressed in a gradient in the retina. Within the retina, there is a counter-gradient of EphA and ephrin-A expression; the temporal retina expresses high levels of EphA and low levels of ephrin-A. Conversely, the nasal retina expresses low EphA and high ephrin-A. The posterior tectum expresses high levels of ephrin-A, compared to the anterior region. Image adapted from Hornberger et al., (1999).

This hypothesis was confirmed by *in vitro* assays and *in vivo* gain of function experiments which showed topographic specific repulsion of temporal RGC axons by ephrin-A2 and ephrin-A5 being expressed in the posterior tectum (Brown *et al.*, 2000; Feldheim *et al.*, 1998; Monschau *et al.*, 1997; Nakamoto *et al.*, 1996). Examination of corresponding mouse mutants has provided a valuable insight into the role of ephrin-A expression in the SC (Feldheim *et al.*, 2000; Frisen *et al.*, 1998). In comparison to wild type mice, temporal axons are found to project into inappropriate posterior regions in *ephrin-A2*$^{-/-}$, *ephrin-A5*$^{-/-}$, *ephrin-A2*$^{+/-}$; *ephrin-A5*$^{+/-}$ and in *ephrin-A2*$^{-/-}$; *ephrin-A5*$^{-/-}$ (Feldheim *et al.*, 2000; Frisen *et al.*, 1998) (Figure 1.16). This is certainly consistent with a lack of repellent activity in the posterior SC. Further to this, Feldheim *et al.*, (2000) showed that double homozygous mutants exhibited a synergistic phenotype more severe than either the single mutant, therefore demonstrating that ephrin-A2 and ephrin-A5 were partially redundant in topographic mapping. The redundant function for ephrin-As was also confirmed by similar temporal axon projection defects observed in *ephrin-A2*$^{-/-}$, *ephrin-A5*$^{-/-}$ and *ephrin-A2*$^{+/-}$; *ephrin-A5*$^{+/-}$ mutants (Feldheim *et al.*, 2000). Analysis of *ephrin-A2*$^{-/-}$ mice revealed that nasal axons project normally (Feldheim *et al.*, 2000), while analysis of *ephrin-A5*$^{-/-}$ mutants showed an anterior shift of these axons (Feldheim *et al.*, 2000; Frisen *et al.*, 1998). The *ephrin-A5*$^{-/-}$ mutant phenotype therefore suggested that ephrin-A5 had a dominant function in the posterior SC, as confirmed by its steeper posterior gradient and also its high affinity for EphA receptors (Drescher, 1997; Flanagan and Vanderhaeghen, 1998) (Figure 1.16).

According to the chemoaffinity model predicted by Sperry (1963), the generation of a continuous map was dependent on the graded responsiveness across different retinal position. As a consequence, mapping was believed to involve counter gradients of attractants and repellents or a graded molecule that could be both positive and negative (reviewed by Hansen *et al.*, 2004). To test this hypothesis, an *in vitro* assay in which the RGC position and ephrin concentration was varied systematically revealed that RGC axon responses varied continuously with RGC position (Hansen *et al.*, 2004). Ephrin-A2 was found to inhibit axon growth at high concentrations, and promote axon growth at lower concentrations. Additionally, the concentration that produced a transition from growth to inhibition (the neutral position) was found to vary in position within the retina; this was demonstrated to occur at higher ephrin-A concentrations for nasal axons, and lower

concentrations for temporal axons. Thus these results could explain the generation of a smooth topographic map (Hansen *et al.,* 2004) (Figure 1.17).

However, retinal topographic axon guidance was further complicated by the discovery that the retina also expressed ephrin-A in a nasal to temporal gradient (Connor *et al.,* 1998; Hornberger *et al.,* 1999; Marcus *et al.,* 1996) (Figure 1.15). Nasal axons were found to be insensitive to ephrin-A2 *in vitro* and *in vivo* (Monschau *et al.,* 1997; Nakamoto *et al.,* 1996), despite nasal axons expressing EphA4 (Hornberger *et al.,* 1999). This paradox was resolved because nasal axons were found to co-express ephrin-A and EphA4, and removing ephrin-A chemically rendered these axons sensitive to ephrin-A. Conversely, ectopically expressing ephrin-A on temporal axons made them insensitive to ephrin-A (Hornberger *et al.,* 1999) (Figure 1.15). Therefore, in addition to expressing EphA receptors in a temporal to nasal gradient, retinal axons co-expressed ephrin-A ligands in an opposing gradient (Brown *et al.,* 2000; Cheng *et al.,* 1995; Connor *et al.,* 1998; Feldheim *et al.,* 1998; Hornberger *et al.,* 1999; Marcus *et al.,* 1996). As discussed previously (section 1.4.2.4), receptor function on axons may be modulated by co-expressed ligands (Yin *et al.,* 2004) and therefore in this case, explain nasal RGC axon insensitivity to high concentrations of target ephrin-As (Hornberger *et al.,* 1999; Monschau *et al.,* 1997; Nakamoto *et al.,* 1996)

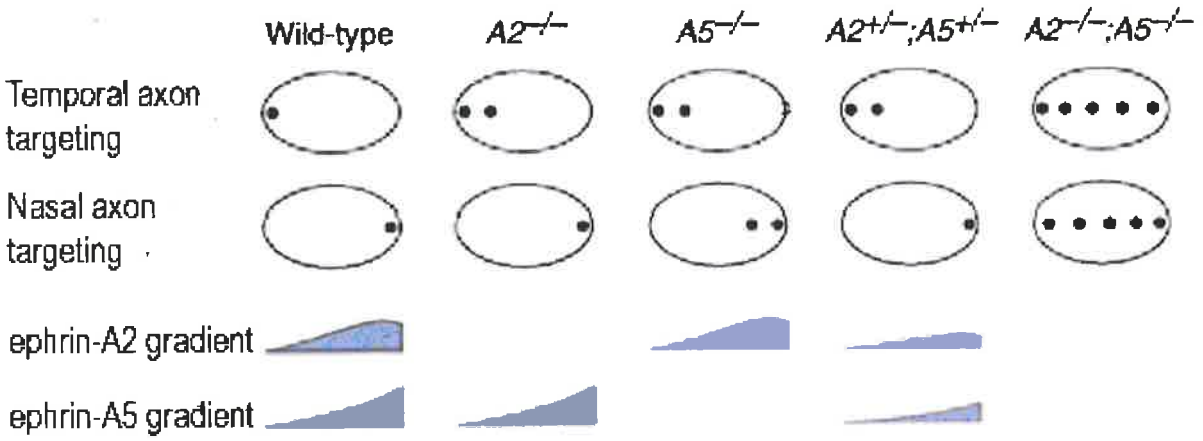

Figure 1.16 The role of ephrin-A2 and ephrin-A5 during anteroposterior retinal topographic mapping.

The schematic shows temporal and nasal retinal axon projections (closed circles) in the superior colliculus (SC) (indicated as an oval; anterior to the left) for wild type, *ephrin-A2* homozygote ($A2^{-/-}$); *ephrin-A5* homozygote ($A5^{-/-}$), *ephrin-A2; ephrin-A5* double heterozygote ($A2^{+/-}$; $A5^{+/-}$) and *ephrin-A2; ephrin-A5* homozygotes ($A2^{-/-}$; $A5^{-/-}$).

The corresponding ephrin-A2 and ephrin-A5 expressions in the SC in different genotype are also shown. $A2^{-/-}$, $A5^{-/-}$, and $A2^{+/-}$; $A5^{+/-}$ genotypes show a movement of temporal axon projections towards the posterior SC, and nasal axon projections are not affected; the similar temporal axon phenotype observed indicates that ephrin-A2 and ephrin-A5 function is partially redundant. Ephrin-A2 cannot compensate for the loss of ephrin-A5 function, and as a result there is an anterior shift of nasal axon projections, providing evidence that ephrin-A5 has a dominant role in the posterior SC. Loss of ephrin-A ligands causes a loss of retinal topographic mapping and axons terminate at various SC locations regardless of their position in the retina.

Image adapted from Feldheim et. al., (2000).

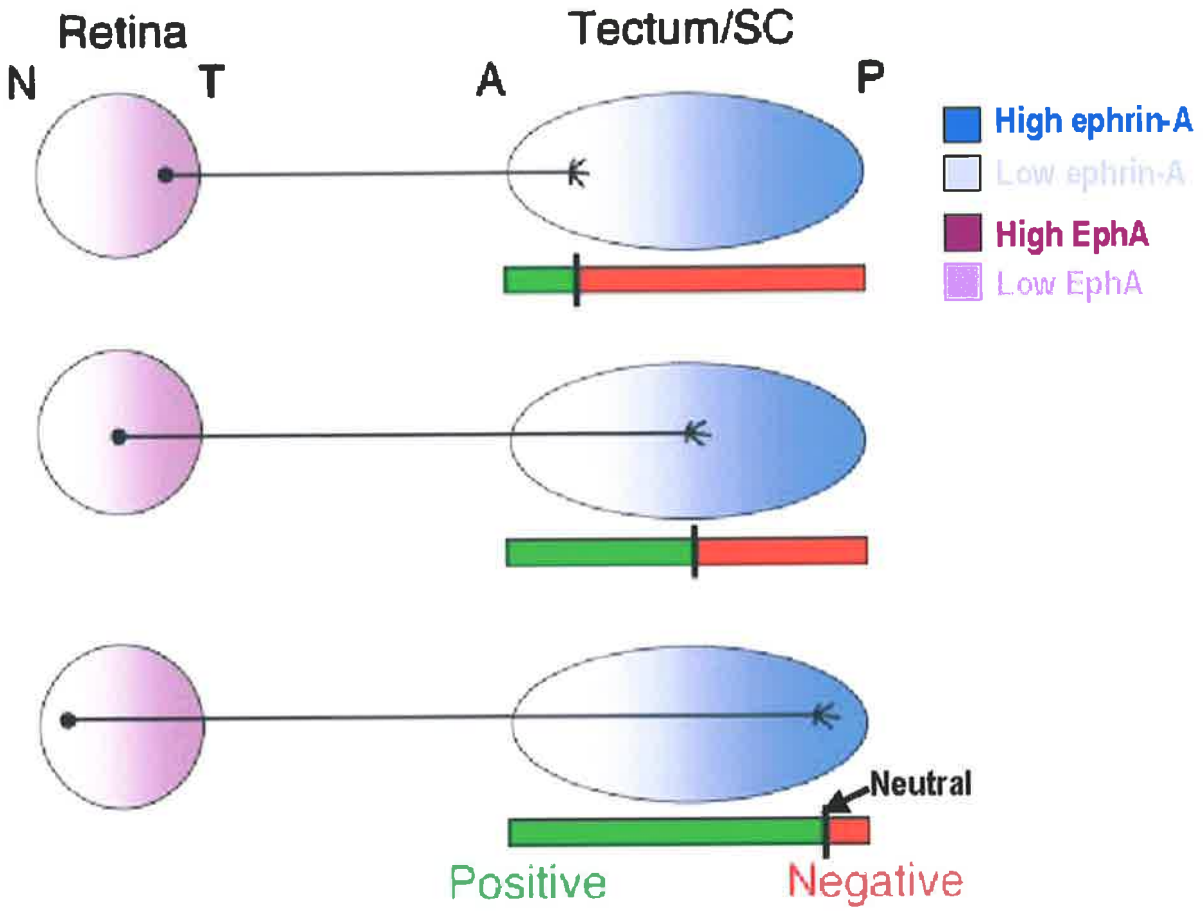

Figure 1.17 A model for generating a smooth anteroposterior retinal topographic map during development.

Graded expression of ephrin-A2 in the superior colliculus (SC) is shown in blue (low expression- white at the anterior SC and high expression- dark blue at the posterior SC

Low concentrations of ephrin-A2 promote growth of retinal ganglion cell (RGC) axons. High concentrations of ephrin-A2 inhibit growth of RGC axons. Axons terminate at a neutral position between these positive and negative ephrin-A2 effects (represented by the black mark on the green-red bar). However, since there is graded expression of EphA in the retina (as indicated by shades of purple; high expression indicated by dark purple), RGC axons originating from different positions of the retina will have a different neutral position. Also refer to figure 1.12.

A, anterior; P, posterior; N, nasal; T, temporal.

Image reproduced from Hansen et. al., (2004).

1.5 Summary: EphAs and ephrinAs- possible candidates for lobe specific trigeminal ganglion axon guidance?

Thus, Ephs and ephrins play diverse roles in patterning not only the central nervous system but also the peripheral one during embryogenesis. A prime example can be found in the in the peripheral trunk nervous system, where EphA/ephrin-A interactions direct dorsal versus ventral trajectories of LMC axons in the developing limb bud (Figure 1.14B). Following sorting into dorsal and ventral trajectories prior to entering the hindlimb (stage 23), EphA4 positive lateral motor axons originating from the LMC then encounter limb mesenchyme that differentially expresses ephrin-A ligands (stage 28). Consequently, these EphA4 positive LMC[l] motor axons become repelled from ephrin-A expressing dorsal limb bud (Eberhart *et al.,* 2004; Eberhart *et al.,* 2000; Eberhart *et al.,* 2002). However unlike the guidance of LMC[l] axons into the hindlimb, the guidance mechanism of LMC[m] into the ephrin-A positive ventral hindlimb is not well understood and is believed to be EphA/ ephrin-A independent (Helmbacher *et al.,* 2000; Kania and Jessell, 2003).

The guidance of LMC[l] axons into the dorsal hindlimb (Figure 1.14B; stage 28) may be somewhat developmentally analogous to the guidance of trigeminal ophthalmic lobe axon projections into the ophthalmic process. Ephrin-A ligands do not localise to the dorsal hindlimb (Eberhart *et al.,* 2000; Kania and Jessell, 2003), and similarly ephrin-A ligands do not appear to localise to the ophthalmic process during ophthalmic lobe axon guidance in the mouse at E9-10.5 (Flenniken *et al.,* 1996; Gale *et al.,* 1996). Potentially, both LMC[l] axons and ophthalmic lobe axons may rely on the same EphA/ ephrin-A repulsive interactions during guidance into their respective target fields. Akin to LMC[l] axons that are repelled from ephrin-A expressing ventral-mesenchyme in the limb (Eberhart *et al.,* 2004; Eberhart *et al.,* 2000; Eberhart *et al.,* 2002; Helmbacher *et al.,* 2000; Kania and Jessell, 2003), ophthalmic lobe axons are hypothesised to be repelled from ephrin-A positive first branchial arch mesenchyme in the chick embryo. If this prediction holds true, just like LMC[l] axons express EphA4 receptor which enables these axons to respond to ephrin-As in the non-target ventral hindlimb (Eberhart *et al.,* 2004; Eberhart *et al.,* 2000; Eberhart *et al.,* 2002; Helmbacher *et al.,* 2000), ophthalmic lobe axons may express a EphA receptor making these axons sensitive to ephrin-A ligands in the first branchial arch non-target field.

This notion of possible EphA/ ephrin-A interactions during trigeminal ganglion guidance is supported by prior studies in both chick and mouse, which have reported expression of EphAs and ephrin-As in the developing head (Araujo and Nieto, 1997; Baker and Antin, 2003; Flenniken *et al.,* 1996; Gale *et al.,* 1996; Kury *et al.,* 2000; Santiago and Erickson, 2002). Although, a comprehensive expression analysis of EphAs and ephrin-As specifically during stages 13-20 of chick embryogenesis when trigeminal ganglion axons are pathfinding has not been conducted.

Why study lobe specific guidance in the chick embryo? The bilobed nature and large size of the trigeminal ganglion in the chick embryo offered a unique opportunity to study ophthalmic versus maxillomandibular lobe projection specification. This cannot be done readily in mice since the ophthalmic lobe is smaller at equivalent stages of chick trigeminal ganglion development and therefore cannot be easily microdissected. Furthermore, the chick embryo is highly accessible and easily manipulated genetically using the method of *in ovo* electroporation (Momose *et al.,* 1999).

1.5.1 Project Aims

The aim of the study therefore was to investigate the role of EphAs and ephrin-As during trigeminal ganglion axon guidance in the chick embryo. In order to do this, it was necessary to:

(1) characterise the spatiotemporal expression of EphA and ephrin-A in the trigeminal ganglion target fields and within the ganglion itself, so that candidates important during axon guidance could be identified, and
(2) characterise EphA/ephrin-A functional interactions.

To validate that ephrin-As were indeed restricted to the first branchial arch (maxillary and mandibular processes) of chick embryos in a manner observed in the mouse (Flenniken *et al.,* 1996; Gale *et al.,* 1996), the expression patterns of ephrin-As were examined. The assumption being made here was that the guidance of ophthalmic lobe axons would be conserved between species (chapter 3), validating the chick as an appropriate model organism to study trigeminal ganglion lobe specific guidance. Consistent with guidance of LMC[l] axons through repulsive interactions with ventral mesenchyme hindlimb ephrin-A

ligands (Eberhart *et al.*, 2004; Eberhart *et al.*, 2000; Eberhart *et al.*, 2002), the candidate ephrin-As expressed in the first branchial arch needed to also be restricted to the mesenchyme of the maxillary and mandibular processes. Therefore, whole embryos stained for ephrin-A transcripts were sectioned to reveal the tissues that expressed these ligands. Additionally, where antibodies to certain ephrin-As were available, the RNA *in situ* hybridisation results was confirmed with immunofluorescent staining on vibratome sections (chapter 3).

To determine whether EphA receptors localise to the trigeminal ganglion, particularly to the ophthalmic lobe neurons, RNA *in situ* hybridisation and antibody staining was performed (Chapter 3 and 4). Antibodies to molecular markers aided the localisation of EphA receptors to various populations of ganglionic cells. The presence of EphA receptor(s) localisation to the ophthalmic lobe neurons was speculated to mediate cognate repulsive interactions with candidate ephrin-As being expressed in the mesenchyme of the first branchial arch (maxillary and mandibular processes).

In order to test for repulsive interactions between trigeminal ganglion EphAs, more specifically those localised to the ophthalmic lobe, and ephrin-As in the target, the substratum choice *in vitro* assay was utilised (Chapter 5). Axon response from 24 hour cultured whole trigeminal ganglion or trigeminal ganglion lobe explants to a substrate of ephrin-A was assessed. If interactions were repulsive, a sub-population of axons from whole ganglionic explants, and the majority of axons from ophthalmic lobe explants were predicted to be responsive to substrate ephrin-A. The significance of this finding would be that ophthalmic lobe axons and LMC[l] axons share similar EphA/ ephrin-A guidance mechanisms.

In the LMC-hindlimb system, EphA4 receptor has been demonstrated to localise to the dorsal hindlimb mesenchyme, which is innervated by LMC[l] axons (Eberhart *et al.*, 2000; Helmbacher *et al.*, 2000; Kania and Jessell, 2003). In a similar manner, complementary to the expression of ephrin-As in the first branchial arch, EphAs were predicted to be expressed in the ophthalmic process, further substantiating the notion that the LMC-hindlimb system was analogous to trigeminal ganglion system. Additionally EphA receptors appeared to localise to the ophthalmic process in mice during trigeminal ganglion

axon guidance (Flenniken *et al.,* 1996), further providing evidence for the presence of EphA receptors in the ophthalmic process. Therefore, the expression of individual EphA receptors in the target fields of trigeminal ganglion was analysed using RNA *in situ* hybridisation and immunofluorescent antibody staining (Chapter 3). To validate that EphAs were localised to the mesenchyme, possibly consistent with a guidance role, transcript and/ or protein expression was inspected in cryostat/ vibratome sections.

The speculated localisation of EphA receptors to the mesenchyme of trigeminal ganglion target fields, also predicted the presence of cognate interacting ephrin-A(s) on ganglionic axons. To assess if this was the case, RNA *in situ* hybridisation and antibody staining was performed (Chapter 4). The expression of ephrin-A(s) in the trigeminal ganglion would be further consistent with what is observed in the LMC-hindlimb system, since all LMC axons express ephrin-As (Eberhart *et al.,* 2000; Kania and Jessell, 2003) (Figure 1.14).

The potential significance of ephrin-A localisation to the trigeminal ganglion, and target expression of EphA receptors was analysed using the *in vitro* substratum choice assay (Chapter 6). Ephrin-A positive axons from whole trigeminal ganglion axons were predicted to be non-responsive to a substrate of EphA, suggesting that EphAs were not repulsive *in vivo*. Since ephrin-As have the capacity to signal into the ephrin-A bearing cell causing an increase in adhesion and neurite extension (Davy *et al.,* 1999; Davy and Robbins, 2000; Huai and Drescher, 2001), it was conceivable that ephrin-As expressed in the ganglion may promote neurite growth and mediate adhesion to EphA expressing mesenchyme *in vivo*. To test this potential, a uniform EphA substrate *in vitro* assay was performed with 24 hour trigeminal ganglion lobe explants (Chapter 6).

Collectively, data generated in this study had the potential to provide:

(1) insights into repulsive and/ or adhesive EphA/ ephrin-A interactions that may exist during trigeminal ganglion axon guidance, more specifically during ophthalmic lobe axon guidance,

(2) insights into the similarities and differences in EphA/ ephrin-A interactions that exist between the LMC-hindlimb system and that of the trigeminal ganglion sensory system, and

(3) an understanding of where EphA/ ephrin-A interactions may fit in the global developmental scheme of early trigeminal ganglion axon guidance with respect to other trigeminal ganglion guidance cues (refer to section 1.3.2),

(4) insights into how EphA/ ephrin-A interactions and other families of guidance cues act in concert to guide trigeminal ganglion axons.

Chapter 2: Materials and methods

"Over second and third cups flow matters of high finance, high state, common gossip and low comedy. [Coffee] is a social binder, a warmer of tongues, a soberer of minds, a stimulant of wit, a foiler of sleep if you want it so. From roadside mugs to the classic demi-tasse, it is the perfect democrat".--Unknown

"Behind every successful woman... is a substantial amount of coffee".
--Stephanie Piro

Chapter 2: Materials and methods

2.1 Abbreviations

bp	Base pairs
BSA	Bovine serum albumin
BCIP	5-bromo-4-chloro-3-indolyl-phosphate disodium salt
cDNA	Complementary DNA
DEPC-dH_2O	Diethylpyrocarbonate treated water
DIG	Digoxigenin
DTT	DL-Dithiothreitol
EDTA	Disodium Salt
IPTG	Isopropyl-β-D-thiogalactopyranoside
kb	Kilobases
LB	Luria broth
M	Molar
MQ-H_2O	Milli-Q water
NaAc	Sodium acetate
NaOH	Sodium hydroxide
NBT	4-Nitroblue tetrazolium chloride
OD	Optical density
PBS	Phosphate buffered saline
PBST	Phosphate buffered saline with 0.1% Tween-20
PCR	Polymerase chain reaction
PFA	Paraformaldehyde
rpm	Rotations per minute
SDS	Sodium Dodecyl Sulphate
X-gal	5-bromo-4-chloro-3-indolyl-β-D-galactopyranoside

2.2 Materials

2.1.1 Chemicals

All chemicals used were of analytical grade or other grade suitable for use in molecular biological techniques. Suppliers of reagents or kits are referred to as necessary in the description of the particular method.

2.1.2 Enzymes

Suppliers of restriction endonucleases and nucleic acid modifying enzymes are referred to as required.

2.1.3 DNA plasmids

All vectors used in this study are as follows: pGEM T-Easy (Promega); pBluescript (pBS) -SK+ (Stratagene); pBluescript (pBS) -KS+ (Stratagene); PCR.II (Invitrogen); pMES (Swartz *et al.*, 2001).

2.1.3 RNA in situ hybridisation probes

RNA riboprobes used for whole-mount *in situ* hybridisation are described in Table 2.3.

2.1.4 Antibodies/ Fc-fusion chimeras

A comprehensive list of antibodies/ Fc-fusion chimera proteins used in this study is shown in Table 2.1.

Table 2.1 List of antibodies and Fc-fusion proteins

Antibody/ Fc-fusion chimera	Source	Origin	Dilution	Procedure
Anti-DIG-alkaline phosphatase	Roche		1/ 2000	Whole-mount *In situ* hybridisation
Anti-human ephrin-B2	Santa Cruz	Rabbit	1/ 200	Explant staining
Anti-HNK-1	Dr. Don Newgreen	Monoclonal	1/20	Immunofluorescent staining
Anti-mouse EphA3	R & D systems (AF640)	Goat	1/ 20	Immunofluorescent staining/ explant staining
Anti-mouse EphA4	Dr. David Wilkinson	Rabbit	1/ 5000	Immunofluorescent staining
Anti-ephrin-A5	R & D systems (AF3743)	Goat	1/20	Immunofluorescent staining
Anti-rat Neurofilament-M (Clone # RMO-270)	Zymed	Monoclonal	1/ 200 to 1/ 400	Immunofluorescent staining/ explant staining
Anti-quail Pax3	Dr. Charles Ordahl	Monoclonal	1/ 500 to 1/ 2000	Immunofluorescent staining

Table 2.1 continued.

Antibody/ Fc-fusion chimera	Source	Origin	Dilution	Procedure
Anti-TuJ1	Dr. Edwin Rubel	Monoclonal	1/ 1000	Immunofluorescent staining/ explant staining
Human-Fc fragment	Rockland (009-0103)		1/ 500 to 1/ 2500	In vitro assays, Whole-mount Fc-fusion staining
Human EphA3-Fc	Dr. Douglas Cerreti		1/1000 to 1/200	Whole-mount Fc-fusion staining
Human ephrin-A5-Fc	R & D Systems (#374-EA)		1/ 40 to 1/ 200	In vitro assays, Whole-mount and explant Fc-fusion staining
Mouse EphA4-Fc	R & D Systems (#641-A4)		1/ 40 to 1/ 200	In vitro assays, Whole-mount and explant Fc-fusion staining
Mouse EphB2-Fc	R & D Systems (#467-B2)		1/ 200	Whole-mount Fc-fusion staining
Cy2-anti-human Fcγ-specific IgG	Jackson ImmunoResearch (#109-225-008)	Goat	1/ 50	Explant Fc-fusion staining
Cy3-anti-mouse IgG	Jackson ImmunoResearch	Donkey	1/ 200 to 1/ 500	Immunofluorescent staining/ explant staining
Anti-goat biotinylated IgG	Jackson ImmunoResearch	Rabbit	1/ 500	Immunofluorescent staining/ explant staining
Anti-human Fcγ-specific IgG	Jackson ImmunoResearch (#109-005-008)	Goat	1/ 40	In vitro assays
Anti-mouse biotinylated IgG	Jackson ImmunoResearch	Donkey	1/ 500	Whole-mount immunohistochemistry
Anti-rabbit biotinylated IgG	Jackson ImmunoResearch	Donkey	1/ 500	Immunofluorescent staining/ explant staining

2.1.6 Chick embryos

Fertilized eggs for use in this work were supplied by Hi-Chick breeding company (South Australia).

2.3 Methods

2.3.1 Chick embryos

White-Leghorn eggs were grown in a humidified incubator at 37-39°C, and embryos were staged as described previously (Hamburger and Hamilton, 1951). All experiments involving embryos conformed to standards set by the University of Adelaide Ethics Committee.

2.3.2 Bacteriological techniques

2.3.2.1 Bacterial culture

Bacteria were cultured in LB or on 1.5% LB and agar plates. For long-term storage, 0.5ml of the overnight liquid culture was mixed with 0.5ml sterile 80% glycerol and stored at -80°C.

2.3.2.2 Bacterial stains

DH5α strain of *Escherichia coli* was used.

2.3.2.3 Preparation of electrocompetent DH5α cells

From an overnight culture, 1/100 volume was used to inoculate a 500mL LB culture and cells were grown at 37°C for ~ 3 hours with vigorous shaking. The OD cells were checked regularly, and once an OD of about 0.5-1.0 was reached, the cells were harvested. Cells were spun down in prechilled tubes at 4°C (4500 rpm using a Beckman JA14 rotor), 15-30 mins. Cells were maintained at 4°C and supernatant resulting from the spins was discarded for the rest of the protocol unless otherwise stated. Cells were resuspended in 0.5L prechilled MQ-H_2O, and centrifuged at 4000 rpm for 15 mins. Following this, the pellet was resuspended in 250ml cold MQ-H_2O, and centrifuged for a further 15 mins at 4500 rpm. The resulting pellet was resuspended in 10ml cold 10% glycerol and centrifuged at 5000 rpm for 15 mins using a Beckman JA20 rotor. The cells were resuspended in 1ml cold 10% glycerol and aliquoted (~ 45μl) into eppendorf tubes. The aliquoted cells were frozen in an ethanol slurry (consisting of dry ice and 100% ethanol) and stored at -80°C for up to 6 months.

2.3.2.4 Transformation of DH5α cells

About 45 µl of electrocompetent cells were thawed on ice before plasmid (1-10 ng) being added to the cells. The plasmid-bacteria mixture was transferred to a pre-chilled cuvette and electroporated at 2500 volts. About 975 µl of SOC plus glucose (200 µl 20% glucose/ 10ml SOC) solution was immediately added to the cells and transferred to an eppendorf. The tube was incubated at 37°C for 45-60 mins before being plated onto LB agar plates with the appropriate antibiotic concentration and being grown overnight at 37°C.
For blue/ white selection of recombinant clones in the plasmid pBS (SK+), LB agar plates were supplemented with X-gal (50 µg/ml; Promega) and IPTG (20 µg/ml; Promega). White colonies were selected the following day and grown overnight at 37°C in 10 ml LB, supplemented with appropriate antibiotics.

2.3.2.5 Plasmid screening for transformed recombinant clones- cracking

Cracking solution

0.4M NaOH	125 µl
10% SDS	50 µl
0.5M EDTA	10 µl
80% Glycerol	125 µl
MQ H20	715 µl
	1 ml

A small quantity (~ 20 µl) of Bromophenol blue power (Sigma) was added to the mix until it turned a deep blue, for visualisation during electrophoresis.

The SDS cracking solution was aliquoted at 20 µl/ 1.5 ml eppendorf tube, depending on the number of clones that were going to be screened (i.e. one colony/ eppendorf). Under sterile conditions, each colony from the master agar plate was sampled with a fresh yellow P200 tip, touched to a new LB agar plate with the appropriate antibiotic resistance (replica plate) and placed into an eppendorf tube containing the cracking mix. The replica plate was immediately placed at 37°C and allowed to grow overnight. The tubes were transferred to 65°C for 15 min during which time, the yellow tips were thoroughly mixed with the cracking solution to lyse the bacterial cells and release genetic material. The samples were dry loaded onto an agarose gel (refer to section 2.3.3.2), filled with enough 1x TAE buffer to produce a current and run at 40 volts for 10 min. Once samples had progressed into the gel, 1x TAE buffer was used to cover the remainder of the gel, and the samples were further electrophoresed at 80-90 volts until the loading front had progressed approximately

¾ down the gel. The agarose gel was then analysed under UV light and the positive colonies identified.

2.3.2.6 Plasmid screening for transformed recombinant clones- alkaline lysis

Solution I

20% glucose	450 µl
0.5M EDTA	200 µl
1M Tris (pH 8)	250 µl
MQ H_2O	9.1 ml
Total	10 ml

Solution II

5M NaOH	400 µl
10% SDS	1 ml
MQ H_2O	9.1 ml
Total	10 ml

Note: solution I and II were made fresh when required.

Overnight 10 ml cultures from selected white transformants were aliquoted into 1.5 ml eppendorf tubes. The bacterial cells were spun down in eppendorf tubes at 8000 rpm for 1 min. The pellets were resuspended in 100 µl solution I. 200 µl of solution II was added and the tubes were vortexed thoroughly. To the mixture, 150 µl 3M NaAc (pH 4.6) was added and mixed by inversion. Following a 10 min spin at 14000 rpm, the supernatant was harvested and 1ml of absolute ethanol added. Following a further 10 min spin at 14000 rpm, the supernatant was discarded and to the pellet 100 µl of a solution containing 0.1M NaAc (pH 4.6) and 0.05M Tris (pH 8) was added. The pellet was resuspended and 200 µl of absolute ethanol added. After a 10 min spin at 14000 rpm, the supernatant was discarded and the pellets were air dried, and resuspended in 50 µl MQ H_2O. To remove RNA, 0.5 µl of RNase A (10 mg/ml stock) was added and incubated at 37°C. The plasmid preparations were digested with appropriate restriction endonucleases and analysed on agarose gel. The selected clones were also sequenced to confirm identity of the DNA insert.

2.3.3 DNA techniques

2.3.3.1 Plasmid preparations

For small-scale preparations of high purity plasmid DNA, 2-5 ml of an overnight culture was processed using Qiagen plasmid mini kit (Qiagen) according to the manufacturer's instructions. For large-scale preparations of high purity plasmid DNA, 250-500 ml overnight culture was processed using Qiagen plasmid midi kit (Qiagen) according to the manufacturer's protocol.

2.3.3.2 Electrophoretic separation of DNA

DNA was routinely run in 1-2% agarose supplemented with 10 mg/ml ethidium bromide in 1x TAE. The DNA molecular marker used was 1 kb Plus Ladder (Life Technologies).

2.3.3.3 DNA modifying enzyme reactions

Restriction endonuclease digestion of DNA was performed in 20-50 µl volumes in 1x buffer supplied by the manufacturer. Reactions were incubated at 37°C for 1-3 hours.
Ligation of compatible DNA fragments was performed using T4 DNA ligase in 1x quick ligation buffer (New England Biolabs) according to manufacturer's instructions. The ligation was allowed to proceed for 5 mins at room temperature prior to being chilled on ice.

2.3.3.4 Preparation of DNA for ligations

Digested DNA was separated electrophoretically from other DNA species on an agarose gel. The bands were visualised with a 254 nm UV light source and the band of interest was excised with a sterile scalpel blade. The QIAquick PCR purification kit (Qiagen) was used to purify the DNA from the excised band.

2.3.3.5 Cleanup of ligation products for transformation into DH5α cells

Ligation products were precipitated for use in transformation using the phenol-chloroform method. Ligation reactions were made up to 100 µl with MQ H_2O and an equal volume of 1:1 phenol: chloroform added. Following vortexing, the solution was centrifuged for 5 mins at 14000 rpm. The aqueous layer was carefully extracted and transferred to a new eppendorf tube. To precipitate DNA, 10 µl 3M NaAc (pH 4.6) and 300 µl cold absolute ethanol was added, and mixed. Following incubation at -20°C overnight or -80°C for 30-40

mins, the tube was centrifuged at 14000 rpm for 15 mins at room temperature. The supernatant was discarded by aspirating carefully with a P200 pipette and the pellet was washed with 70% pre-chilled ethanol, after which the tube was further centrifuged for 5 mins at room temperature. The alcohol was aspirated with a P200 pipette and the pellet allowed to air dry. The DNA was resuspended in 20 µl MQ-H_2O at room temperature and the entire volume was used for transformation.

2.3.3.6 Cleanup of cDNA for real-time PCR

cDNA synthesised from total RNA for use in real-time PCR was purified using the QIAquick PCR purification kit (Qiagen) according to manufacturer's protocol.

2.3.3.7 Real-time PCR

Real-time PCR reactions were performed using SYBR green master mix on an ADI SDS 7000 light cycler driven by ABI prism SDS v1.1 (Applied Biosystems). Chick specific primers were designed using Primer Express v2.0 (Applied Biosystems) and synthesised locally (Table 2.2; GeneWorks). Primers were used at a final concentration of 300 nM, and reactions were performed 4-6 times for each primer set and each lobe. *18srRNA* was treated as the internal reference to control for loading and facilitate relative quantification using the ddCt approach (see below). The primers assayed were similar in reaction efficiency to the *18srRNA* internal reference primers.

Table 2.2 Real-time PCR primers used in this study.

Gene	Accession ID	Forward Primer	Reverse Primer
EphA3	M68514	TCCACACCCGTGAAAATGC	GCAGCAAGGCCATCAAATCT
ephrin-A5	NM205184	GATGATACCGTGCGTGAGTCA	GCATTGCCAGGAGGAACAA
18srRNA	AF173612	GCCGCTAGAGGTGAAATTCTTG	CATTCTTGGCAAATGCTTTCG

Quantification of fold-changes:

Firstly, the change in cycle threshold (ΔC_T) was calculated:

$\Delta C_T = C_T$ (TGop or TGmm) - C_T (*18srRNA*$_{(TGop)}$ or *18srRNA* $_{(TGmm)}$),

where C_T was the cycle threshold (mean ± standard deviation of the mean (SD)), TGop, ophthalmic lobe and TGmm, maxillomandibular lobe.

The comparative $\Delta\Delta C_T$ calculation was used to determine any differences between the ophthalmic and maxillomandibular lobes. The formula is as follows:

$$\Delta\Delta C_T = \Delta C_{T\,(TGop)} - \Delta C_{T\,(TGmm)}$$

To formula used to transform the $\Delta\Delta C_T$ to an absolute value was:

$$\text{Comparative expression level} = 2^{\Delta\Delta CT}$$

Any fold-changes below two-fold were not considered as being differentially expressed, a criterion used for microarray analysis. Any obvious outliers were excluded from further analysis.

2.3.3.8 Automated DNA sequencing

DNA sequencing was performed using the big-dye III terminator automated sequencing kit (Applied Biosystems) and T7 forward primer (Promega) was used. The thermal cycler conditions used were: 96°C for 2 min followed by 25 cycles of 96°C for 30 sec, 50°C for 15 sec, 60°C for 4 min, followed by a final 10 min extension at 72°C. Sequences were analysed by the sequencing facility at the Institute of Medical and Veterinary Science (South Australia).

2.3.4 RNA techniques

2.3.4.1 Total RNA extraction from trigeminal ganglion lobes

A combination of the TRIzol method (Gibco/BRL) and RNeasy mini kit (Qiagen) was used to extract RNA from trigeminal ganglion lobes. Dissected lobes (section 2.3.5.1), which were collected in eppendorfs under RNase free conditions were removed from -80°C and spun down for a few seconds. Most of the medium was removed with a P20 or P200 pipette so as not to disturb the tissue. About 200 µl of TRIzol reagent was added to the tissue and homogenised thoroughly using a Kontes pellet pestle (# K-749521-1500;

Adelab Scientific). After the volume was made to 1 ml with TRIzol, the homogenate was further passed through a 6 x 21G needle followed by a 3 x 30G needle attached to a 1ml syringe. To remove cellular debris, the tubes were centrifuged at 13000 rpm for 10 min at 4°C. The liquid was decanted into a 2mL eppendorf tube and an additional 0.5 ml TRIzol was added and incubated at 15 min, room temperature. To the tube, 0.3 ml chloroform was added, vortexed for 1 min and centrifuged for 15 min at 13000 rpm. The aqueous layer was collected using a P1000 pipette and transferred to a new 2 ml eppendorf tube. An equal volume of absolute ethanol was added and vortexed. 0.7 ml of the mixture was loaded onto an RNeasy column and centrifuged at 13000 rpm for 30 sec. The elute was discarded and loadings were repeated until the entire sample had been passed through the column. Following a wash with 0.7 ml RW1 buffer, the columns were centrifuged for 13000 rpm for 30 sec. The column was transferred to a fresh collection tube and washed with 0.5 ml RPE buffer. The wash with RPE buffer was repeated and the elute was discarded each time. The column was further centrifuged for 1 min at 13000 rpm to remove any traces of the buffer and transferred to an RNase free 1.5 ml eppendorf. To rehydrate the column, 30 µl DEPC-dH_2O was added directly to the membrane and allowed to stand for 1 min at room temperature, then centrifuged for 1 min at 13000 rpm to elute the RNA. The RNA samples were concentrated under reduced pressure (speed vac) to ~10 µl on medium heat setting. The quality of RNA was analysed on an agarose gel and RNA samples were stored at -20-80°C until required.

2.3.4.2 Reverse transcription

RNA samples stored at -20-80°C were allowed to thaw by incubating at 37°C for 2 min. A maximum of 12 µl of total RNA was added to an RNase free 0.5 ml eppendorf for each sample. A mixture of 4 µl Random Hexamers (500 ng/µl; Promega) and 2 µl oligo-d(T) (500 ng/µl; Promega) was added to each sample, volume adjusted to 18 µl with DEPC-dH_2O and incubated at 70°C for 10 min in a thermal cycler with heated lid. Following this, the samples were chilled on ice for 5 min. The master mix was prepared and 12 µl and added to each sample.

Master mix for reverse transcription

	1x reaction	2x reaction
5x Superscript III Buffer (Invitrogen)	6 µl	12µl
0.1M DTT (Invitrogen)	2 µl	4 µl
Superscript III (Invitrogen)	2 µl	4 µl
dNTP mix (10mM) (Promega)	1 µl	2 µl
RNaseIN (# N2111; Promega)	1 µl	2 µl

Following incubation at 50°C for 2.5 hrs, 10 µl of 0.25M NaOH and 10 µl of 0.5M EDTA were added to the samples, vortexed and incubated at 65°C for 15 min to degrade the RNA. To neutralize the reaction 15 µl of 0.2M acetic acid was added and mixed. cDNA generated was quantitated and used in real-time PCR.

2.3.4.3 Transcription of RNA probes for *in situ* hybridisation

DNA plasmid template was linearised with restriction endonucleases as described in section 2.2.3.3. After 2 hrs at 37°C, the progress of digestion was analysed by running a small sample of the reaction (1/20th) on an agarose gel; in the case of incomplete digestion the reactions were allowed to proceed for a further 1-2 hrs. Following ethanol precipitation, the linearised plasmid was quantitated using a spectrophotometer (Eppendorf).

Transcription reaction

Linearised plasmid template (1ug)	X µl
DEPC-dH2O	upto 20 µl
10x transcription buffer (Roche)	2 µl
10x DIG nucleotide mix (pH 8) (Roche)	2 µl
0.1M DTT (Invitrogen)	2 µl
RNaseIN (# N2111; Promega)	1.5 µl
RNA polymerase (T7, SP6 or T3; 20 U/ul) (Roche)	2 µl

The reactions were mixed thoroughly and incubated for 2 hrs at 37°C. The quality of riboprobe synthesised was analysed by running 1 µl on an agarose gel. To remove the DNA template, 2 µl of RQ1 DNase (Promega) was added and the reaction was further incubated at 37°C for 15 min. Probes were cleaned using RNeasy mini columns (Qiagen) and quantitated using spectrophotometer (Eppendorf).

2.3.5 Embryo/ Trigeminal ganglion harvesting

2.3.5.2 Chick embryos

Eggs were wiped with 70% ethanol and a window opened with a pair of scissors. Stage 20 chick embryos were harvested and dissected in either cold Dulbecco's modified Eagle medium (DMEM) with 20mM HEPES: nutrient mixture F-12 (Ham) in a 1:1 combination (GIBCO BRL, Life Technologies) with antibiotics or cold sterile-PBS under a dissection microscope. For RNase free applications, all dissecting instruments were treated with RNase Away (Molecular Bioproducts) following sterilisation in 70% ethanol. For whole-mount *in situ* hybridisation/ antibody staining, embryos were dissected in sterile cold-PBS. For real-time PCR or tissue culture, embryos were dissected in cold DMEM/F-12 medium.

2.3.5.1 Trigeminal ganglia and trigeminal ganglion lobes

Following harvesting, embryos were decapitated at the level of the mandibular process with dissecting forceps, and each head was positioned perpendicular to the dish such that the tectum/ forebrain regions were lying ventrally in contact with the dish surface and the hindbrain was oriented dorsally. To separate the face into two-halves, an incision was made with a microsurgical ophthalmic scalpel (FEATHER, Japan, #500) along the dorsal midline of the head, transecting the tectum, the frontonasal process and the first branchial arch. However, the hindbrain was left intact such that each head now resembled an open book, with both sides of the face laying flat on the dish surface. The developing eyes were dissected away using a pair of forceps and the microsurgical scalpel and the remaining head tissue transferred to a new 35-mm dish (BD Biosciences) containing new cold DMEM/F-12 medium.

To dissect out the trigeminal ganglion, each half of the head was now separated by making an incision along the hindbrain using the scalpel and an electrolytically sharpened fine tungsten hook with an ~ 90° attached to a loop holder. To expose the trigeminal ganglion, the overlying epithelium was removed in a filleting manner using the tungsten hook, while the face held in place with the scalpel. The surrounding mesenchyme was also gradually teased away from the ganglion in a similar manner.

For trigeminal ganglion lobe cultures or real-time PCR, ganglia were micro-dissected into ophthalmic and maxillomandibular lobes. Care was taken to prevent tissue cross contamination. For real-time PCR, dissected lobes (~60-80 lobes) were transferred

immediately to RNase free 1.5 ml eppendorfs and frozen on dry ice prior to being stored at -80°C. For trigeminal ganglion lobe cultures, tissue was transferred to 1.5 ml eppendorfs and kept on ice; dissections were also limited to 2 hr periods.

At any given time, only ganglia from 5-6 embryos were dissected to minimise tissue degradation. Furthermore, dissecting instruments were sterilized frequently with 70% ethanol.

2.3.6 Tissue sectioning

2.3.6.1 Vibratome sections

Embryos fixed in 4% PFA were rinsed in PBST, transferred to cryomoulds (TissueTek) and embedded in 7% Ultra-low gelling temperature agarose (A-2576; Sigma) in PBS. The embryos were quickly oriented, and placed on ice. A Leica vibratome machine was used to cut 100 μm sections.

2.3.6.2 Cryostat sections

For cryostat sectioning, embryos were fixed in 4% PFA, followed by incubation in 30% sucrose in PBS. Embryos were placed in cryomoulds (TissueTek) and embedded in OCT (TissueTek), oriented in the desired position, and frozen on dry ice. Sections (12-16 μm) were cut at -20°C using a Leica Cryostat machine, air dried and stored at -20°C until required.

2.3.7 Whole-mount RNA in situ hybridisation

Whole-mount *in situ* hybridisation was performed as described previously using 1 μg/ml DIG-labelled riboprobes (Henrique *et al.*, 1995) using the riboprobes described in Table 2.3. Collected embryos were fixed overnight at 4°C or at room temperature 4-5 hrs in 4% PFA. Prior to hybridisation, embryos were bleached in 6% hydrogen peroxide plus PBST for 30-60 min at room temperature to make them translucent. The embryos were digested with 10 μg/ml proteinase-K at room temperature for 30 min regardless of age of the embryos. De-ionised formamide was used to make the hybridisation solution. Sense controls did not show any specific staining. Following staining with NBT/ BCIP (Roche) solution, embryos were cleared in 80% glycerol and visualised under the dissection microscope (Olympus SZH10) mounted with a Polaroid digital camera or on a Zeiss Axiophot microscope using

Fujix HC-1000 3CCD image capturing camera driven by Fujix Photograb software (Fuji-film).

The EphA4 riboprobe described in Table 2.3 was generated as follows. Approximately the first 800bp from the EphA4 full length insert in the pMES vector (generated by Edwina Ashby) was excised with XbaI (Gibco) and HindIII (Gibco) restriction endonuclease enzymes and ligated into the XbaI/ HindIII site in the pBS-KS+ vector. To determine if the cloning was successful and confirm orientation of the insert, EphA4-pBS-KS+ was sequenced.

Table 2.3 List of chick specific riboprobes used in whole-mount RNA *in situ* hybridisation.

Gene	Accession ID/ reference	Vector backbone	Nucleotide region (bp)	Restriction enzyme/ RNA polymerase used for transcription	Source
ephrin-A2	L40932	pGEM T-Easy	91-531	SacII/ SP6 (AS) PstI/ T7 (S)	Edwina Ashby
ephrin-A5	X90377	pGEM T-Easy	**105-653**	NcoI/ SP6 (AS) PstI/ T7 (S)	Edwina Ashby
EphA3	(Baker and Antin, 2003)	pBS-SK+	2012-3241	EcoRI/ T7 (AS) XhoI/ T3 (S)	Robert Baker
EphA4	D38174	pBS-KS+	1-800	XbaI/ T3 (AS) XhoI/ T7 (S)	Chathurani Jayasena
EphA5	(Iwamasa *et al.*, 1999)	PCR.II	2371-3132	XbaI/ SP6 (AS) BamHI/ T7 (S)	Hideaki Tanaka
EphA7	(Marin *et al.*, 2001)	pBS-KS+	-47-1375	XbaI/ T3 (AS) PstI/ T7 (S)	Angela Nieto
EphA9	(Baker and Antin, 2003)	pBS-SK+	2084-3919	EcoRI/ T7 (AS) XhoI/ T3 (S)	Robert Baker

AS, anti-sense riboprobe; S, sense riboprobes. All restriction endonuclease enzymes were supplied by the following suppliers: BamHI (NEB); EcoRI, PstI, NcoI, XbaI, XhoI, (Gibco); SacII (Promega).

2.3.8 Antibody/ Fc-Fusion techniques

2.3.8.1 Antibody staining

Sections/ explants/ half-mount embryos were blocked with 2% BSA in PBST and then endogenous avidin-biotin blocked (unlabeled avidin/biotin kit; Vector Laboratories).

Sections were incubated overnight with primary antibodies in 2% BSA and PBST. Secondary antibodies were diluted in 1% BSA plus PBST and incubated 1 hr at room temperature or overnight at 4°C. Signals from polyclonal antibodies were amplified using 1:500 strepavidin-Alexa-488 (Molecular Probes) and incubations were for 1-2 hrs at room temperature. For all post-antibody washes, PBST was used.

For visualisation of trigeminal ganglia whole-mount in older embryos (stages 15 and 20), following 4% PFA fixation, embryos were bleached with 5% hydrogen peroxide in PBST, for 1 hr at room temperature. Endogenous avidin/biotin was blocked, and embryos incubated overnight with anti-neurofilament (1:400) diluted with 2% BSA in PBST at 4°C. Embryos were incubated with secondary anti-mouse biotinylated (diluted in 1% BSA/ PBST) overnight at 4°C, and colour developed with diaminobenzidine tetrahydro-chloride (DAB; Sigma).

2.3.8.2 Eph and ephrin-Fc staining

Eph/ephrin-Fc whole-mount staining was performed essentially as previously described (Gale *et al.,* 1996), with the following modifications. Embryos were blocked in 4% BSA, 0.02% sodium azide in PBS for 1-4 hrs at 4°C. Following incubation Fc-fusion chimeras (1-5 μg/ml), and extensive washes in cold PBS, embryos were fixed for 1 hr with 4% PFA. Embryos were permeablised with 0.1% PBST, and incubated with goat anti-human-alkaline phosphatase in 2% BSA/ PBST overnight at 4°C. Post-antibody washes were performed in TBS (pH 7.5) with 0.1% Tween-20. Colour developed embryos with NBT/BCIP (Roche) were mounted in 80% glycerol for imaging.

Trigeminal ganglion explants grown for 24 hrs were blocked in 2% BSA plus DMEM/ F12 medium for 30 mins at 37°C. Cultures were incubated with 4 μg/ml Fc-chimera protein diluted in DMEM/ F12 medium for 60 mins at 37°C. Following cold PBS washes, explants were fixed in 4% PFA for 30 mins at room temperature, washed with PBST and incubated overnight with mouse anti-neurofilament in 2% BSA/ PBST. Secondary antibodies were incubated for 2 hrs in PBST.

2.3.8.3 Microscopy

Fluorescently stained specimens were mounted onto slides with anti-fade mounting medium (DAKO) and imaged by confocal microscopy (BioRad Radiance 2100). Images were processed using Confocal Assistant v.4.02 or an Olympus AX70 microscope fitted with a cooled CCD camera, and V++ v.4 software. Bright-field images were acquired

using Nomarski optics. Confocal z-images were analysed using Confocal Assistant v.4.02. All digital images were processed using Adobe Photoshop 6 and only brightness and/or contrast altered.

2.3.8.4 Whole-mount EphA3 trigeminal ganglion intensity readings

Whole dissected ganglia attached to hindbrain from at least 3 embryos were stained with anti-EphA3 and anti-neurofilament as indicated above. Three stained ganglia were imaged using an Olympus AX70 microscope. Whole fluorescence was measured using V++ v.4 software. Intensity measurements from the two lobes for each ganglion were acquired using the flag option, and the mean intensity was calculated as follows:

Mean intensity = the intensity readout/ number of pixels measured.

Since the readout for each lobe differed from one ganglion to the next, the mean intensity was expressed as a ratio of ophthalmic lobe: maxillomandibular lobe.

2.3.8.5 EphA3 growth cone intensity readings

Ophthalmic and maxillomandibular explants stained for EphA3 were viewed with an Olympus AX70 microscope fitted with a cooled CCD camera, and driven with V++ v.4 software. Growth cones were viewed under 100x objective and imaged under identical exposure conditions. The mean intensity for each growth cone central domain and peripheral, including filopodia, was measured using the selection and the histogram tools in Scion Image Software (Scion). The mean intensity calculations were as follows:

Mean EphA3 intensity/ area (μm^2) = [mean intensity/ area of growth cone analysed (μm^2)] – [mean background intensity/ area of background analysed (μm^2)].

By normalising the mean intensity against the area of growth cone analysed, comparisons could be made between ophthalmic and maxillomandibular growth cones. Data was generated from two pooled experiments and 15 growth cones were analysed. A Mann-Whitney U test was used to determine statistical significance. Data was expressed as mean ± standard error of the mean (SEM).

2.3.9 Trigeminal ganglion culture

Explants were seeded onto either 35 mm tissue culture dishes (BD Biosciences) or 4-well plates (Nunc). Explants were grown on coverslips coated with poly-L-lysine (0.01% solution; Sigma) and laminin (5-7 µg/ml; Invitrogen). Cultures were maintained for 24 hr

in DMEM/ F12 medium containing penicillin and streptomycin, at 37°C, in a humidified tissue culture chamber with 5% CO_2.

2.3.9.1 Antibody/ Fc-fusion staining of cultures

Refer to section 2.2.7.

2.3.10 In vitro assays, analysis and statistics

2.3.10.1 Substratum choice assay and uniform substrate assay

The substratum choice assay was performed as previously described (Birgbauer *et al.*, 2001) except for the following modification; coverslips were placed in 35-mm tissue culture dishes (Becton Dickinson) and coated with 0.01% poly-L-lysine (Sigma). Fc-fusion protein (5 μg/ml) was pre-clustered at room temperature for 1 hr with goat anti-human Fcγ-specific IgG (50 μg/ml) in PBS, spotted onto coverslips and incubated as described previously (Birgbauer *et al.*, 2001). For visualisation of substratum-bound Fc-chimeric protein, 1:500 Cy3-conjugated anti-rabbit IgG was added to the pre-clustered mixture. In the case of uniform substratum, the entire poly-L-lysine coated surface was coated with the appropriate Fc-containing protein. Following incubation with Fc-fusion proteins, coverslips were coated with laminin (5-7 μg/ml) plus DMEM/ F12, and incubated for 2 hrs at 37°C. Trigeminal ganglion explants from stage 20 chick embryos were seeded onto the prepared dishes, allowed to settle and incubated at 37°C for 24 hrs. Axons were visualised anti-neurofilament in 2% BSA plus PBST as stated above for sections. Stained explant were visualised with an Olympus AX70 microscope as mentioned previously.

2.3.10.2 Analysis of neurite parameters

On uniform substrate, the 5 longest neurites from each explant were measured. Only explants that exhibited robust neurite growth were analysed for neurite length quantification. All measurements were performed using Scion Image Software (Scion Corporation).

2.3.10.3 Analysis of growth cone parameters

Growth cone morphology on uniform substrate was visualised with 1:2000 phalloidin-TRITC (Sigma). Growth cone staining was visualised with x60 or x100 objective lens. Digital images of phalloidin stained growth cones were erased in Photoshop such that only the cental and peripheral domains of the growth cones remained. The images were

subsequently imported into Scion Image Software (Scion Corporation), highlighted using the invert, threshold and binary options and then surface area measured.

Filopodial length measurements were made from phalloidin stained growth cones in Scion Image as stated for growth cone surface area measurements. Only the filopodial "stalks" were measured, and filopodial "branches" emanating from "stalks" were not considered. The tip of the filopodium to the edge of the central domain of the growth cone was measured for each condition. Results are from 3 independent experiments. Any filopodia ≤ 3 μm in length were excluded from analysis. If filopodial stalks had a length greater than the mean control-Fc filopodial stalk length, then they were categorised as being long. Since the mean filopodial lengths on control-Fc were different for the two TG lobes, filopodial stalks that were longer than > 20 μm (for ophthalmic growth cones) or > 16 μm (for maxillomandibular growth cones) were considered long.

2.3.10.4 Data processing and statistics

Blind-analysis of explants and quantification for the substratum choice assay was performed as previously described (Birgbauer *et al.*, 2001). Briefly, only axons that showed a leading growth cone were quantitated in the substratum choice assay. The assay therefore will not take into account axon fasciculation, and is an underestimate of the number of axons being quantitated. Axon behaviour was subclassed as being "responsive" to the substrate (i.e. stopping/ turning at the substratum border) or as being "non-responsive" to the substrate (i.e. growth into the substrate). About 240-740 axons were analysed from 14-35 explants.

Substratum choice assay calculations:

Total axon response (%) = Total number of axons responding / total number of axons quantified * 100

Mean axon response/ explant (%) = $\sum$ (% of axons responding for each explant analysed) / total number of explants analysed

Analysis of growth cone and neurite parameters was performed blindly, and data were from at least 3 independent experiments. A two-sample student t-test was performed to determine statistical significance, and a Mann-Whitney U-test was performed when the assumption of normality could not be made. All data were expressed as mean ± standard error of the mean (SEM).

Chapter 3: EphA and ephrin-A expression analysis in the trigeminal ganglion peripheral targets

"New ideas pass through three periods:
*It can't be done.
*It probably can be done, but it's not worth doing.
*I knew it was a good idea all along!"

--Arthur C. Clarke

Chapter 3: EphA and ephrin-A expression in the trigeminal peripheral target fields

3.1 Introduction

Analysing the spatiotemporal developmental pattern of gene expression can provide valuable insights in to the putative role of their gene products. In mice and chick, A- and B-class Ephs and ephrins are expressed at various stages of early development (Araujo and Nieto, 1997; Baker and Antin, 2003; Baker *et al.,* 2001; Flenniken *et al.,* 1996; Gale *et al.,* 1996; Henkemeyer *et al.,* 1994; Kury *et al.,* 2000; Santiago and Erickson, 2002). Majority of previous data have demonstrated EphB and ephrin-B expression in the target fields of the trigeminal ganglion in mouse embryonic day (E) 9-11 (Adams *et al.,* 2001; Henkemeyer *et al.,* 1996) and chick embryo stages 13-20 (Baker *et al.,* 2001; Santiago and Erickson, 2002), as well as EphB2 and EphB3 expression in the murine trigeminal ganglion at E9-10.5 (Adams *et al.,* 2001; Henkemeyer *et al.,* 1996) during trigeminal ganglion axon pathfinding.

For the A-subclass, previous data have revealed the expression of EphAs and ephrin-As in mouse trigeminal ganglion target fields during trigeminal ganglion axon pathfinding at E9-10.5, although a comprehensive analysis was not conducted (Flenniken *et al.,* 1996; Gale *et al.,* 1996). In the chick, EphAs and ephrin-As are expressed in the early embryonic face (stages 8-12) prior to trigeminal ganglion axon pathfinding (Baker and Antin, 2003). However, the expression of EphAs and ephrin-As during trigeminal ganglion axon pathfinding/ guidance at chick stages 13-20 has not been previously investigated, with EphA7 being the exception (Araujo and Nieto, 1997). Therefore, this study focused on the analysis of Eph/ ephrin-A subclass expression in the chick embryo at stages 13-20 to gain insights into the putative role of EphAs and ephrin-As during trigeminal ganglion axon guidance. Another reason for focusing on the EphA/ ephrin-A subclass was that it was speculated that lateral motor column lateral (LMC[l]) axon guidance into the hindlimb and trigeminal ophthalmic lobe axon guidance into the ophthalmic process would require EphA/ ephrin-A interactions in a similar manner (refer to section 1.5; Chapter1).

In the initial phase of this study, a preliminary analysis with EphA-Fc and ephrin-A-Fc proteins revealed that the A-subclass was expressed at appropriate stages 13-20 of

trigeminal ganglion axon pathfinding/ guidance. EphA-Fc and ephrin-A-Fc fusion proteins are useful tools since the promiscuous binding of Ephs and ephrins are exploited (Figure 3.1). As previously mentioned (Chapter 1; Figure 1.7), within each subclass each receptor or ligand can bind to a number cognate partners, although the affinity of cognate interactions can vary (Gale *et al.,* 1996; Himanen *et al.,* 2004). Whilst Fc-fusion proteins provided a global profile of EphA and ephrin-A expression, the identity and expression patterns of individual members remained largely unknown. Therefore, to identify EphA and ephrin-A candidates that may act as guidance cues to growing trigeminal ganglion axons, this study used RNA *in situ* hybridisation and immunofluorescent antibody staining methods. These two methods also enabled the verification of the Fc-fusion results. Accordingly, the characterisation of expression profiles for various members of the A-subclass is provided in this chapter.

In this study, the expression of EphAs and ephrin-As were analysed during three distinct stages of trigeminal ganglion axon guidance and development in the chick embryo. These stages were during: initial axon outgrowth (stage 13-13+; somite stage 19-21); primitive ganglion formation (stage 15), and axon pathfinding (stages 15-20). The previous work by Moody et. al., (1989) used TuJ1 antibody against the neuronal cytoskeletal marker β-tubulin to characterise the development of the trigeminal ganglion. An antibody against another neuronal cytoskeletal marker, neurofilament (Lee *et al.,* 1987), was used in this study, and found to substantiate the work of Moody et. al., (1989) (Figure 3.2).

Figure 3.1 Structure of Eph/ ephrin-A-Fc proteins and detecting expression of Eph/ ephrin-A.

(A) Left schematic: shows the structure of EphA (top left) and ephrin-A-Fc (bottom left) fusion proteins. The extracellular domain of the Eph/ ephrin-A (green/ yellow) is fused to the Fc portion of an immunoglobulin protein (red).
Right schematic: illustrates how Fc-fusion proteins allow the detection of endogenous Eph/ ephrin-A *in vivo*. When added to live tissue, the Fc-fusion protein binds (pink unidirectional arrows) to the EphA or ephrin-A being expressed on the cell membrane. Any given EphA-Fc can be used to detect numerous members belonging to the ephrin-A subclass due to promiscuous binding between receptors and ligands. Similarly, any given ephrin-A-Fc can be used to detect numerous members belonging to the A-subclass of receptors.

(B) When endogenous EphA and ephrin-A are involved in *cis*- (not shown) or *trans*-interactions (double headed maroon arrow), the binding of Eph/ ephrin-A-Fc protein to the cognate *in vivo* partner is blocked. This is referred to as the masking effect. Thus, Eph/ ephrin-A-Fc proteins compete with endogenous EphA/ ephrin-A for cognate binding partners. Only "free" ephrin-A or EphA, not involved in endogenous *cis*- or *trans*-interactions are revealed by Eph/ ephrin-A-Fc proteins binding (pink unidirectional arrows).

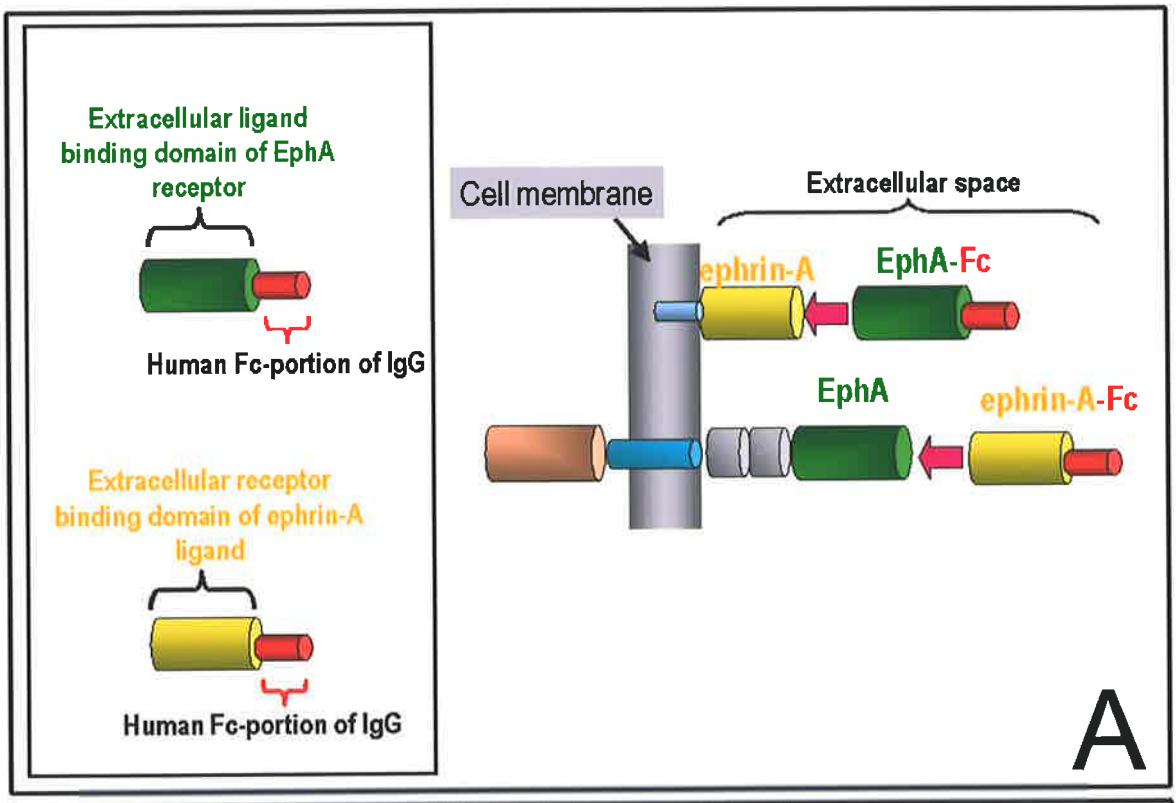
Extracellular ligand binding domain of EphA receptor
Human Fc-portion of IgG
Extracellular receptor binding domain of ephrin-A ligand
Human Fc-portion of IgG
Cell membrane
Extracellular space
ephrin-A
EphA-Fc
EphA
ephrin-A-Fc
A

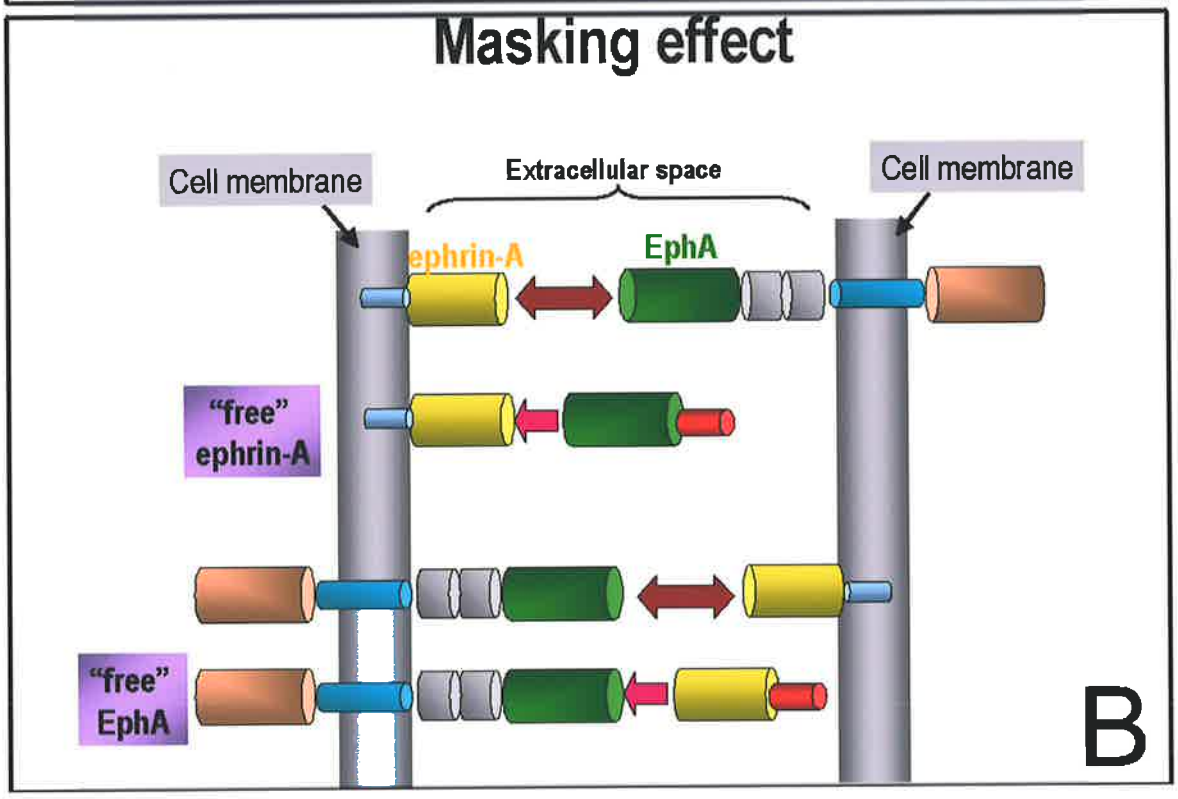
Masking effect
Cell membrane
Extracellular space
Cell membrane
ephrin-A
EphA
"free" ephrin-A
"free" EphA
B

Figure 3. 2 Development of the early trigeminal ganglion documented with anti-neurofilament (NFM) antibody.

(A) Half-mount confocal immunofluorescent image showing maturing NFM positive ophthalmic neurons (TGop) at stage 13 extending axons in the ophthalmic process.

(B) Whole-mount staining showing ophthalmic (TGop) and maxillomandibular (TGmm) lobes converging to form the primitive trigeminal ganglion at stage 15. The TGop lobe is developmentally advanced compared to the TGmm lobe. Numerous TGop axons can be observed in the ophthalmic (Op) process (red arrowheads).

(C) Whole-mount staining demonstrating the maturing trigeminal ganglion at stage 20. Both lobes have converged to form the ganglion, and pathfinding axons from the TGmm lobe are conspicuous (white arrowheads).

Abbreviations: E, eye; Fb, forebrain; Hb, hindbrain; Md, mandibular process; Mx, maxillary process. Scale: 50 μm (A); 200 μm (B-C).

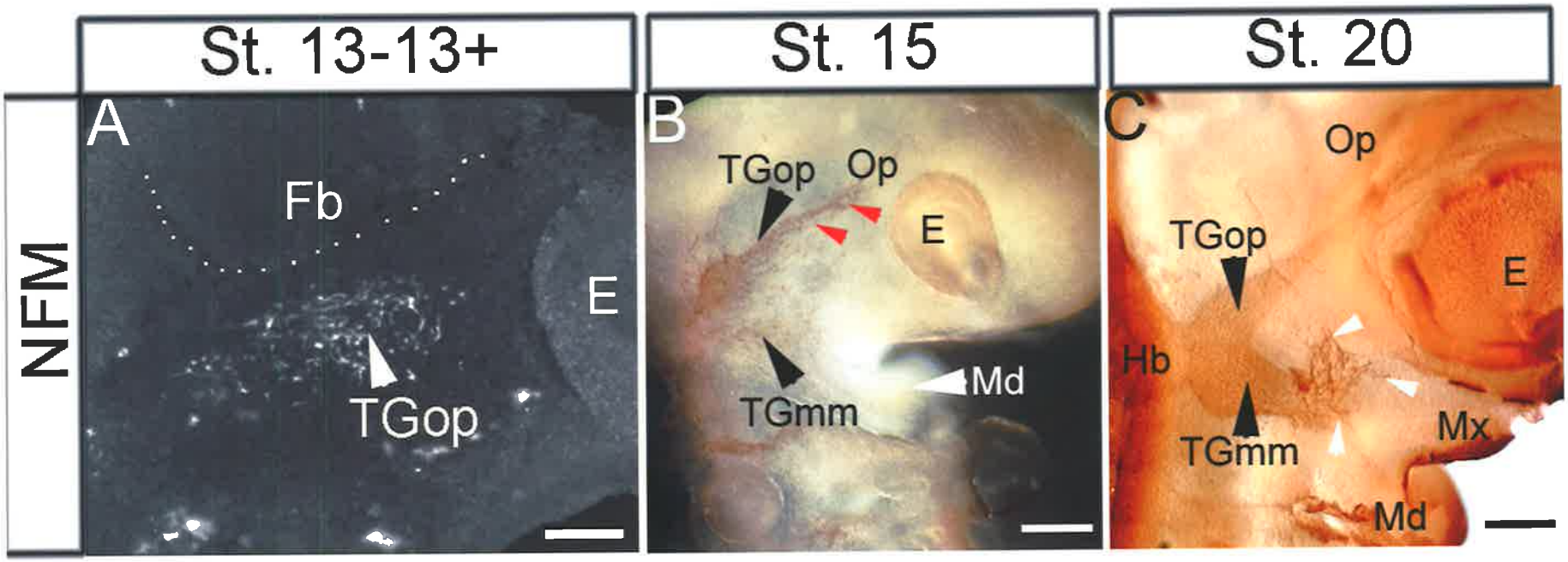
St. 13-13+
St. 15
St. 20
NFM
A
Fb
E
TGop
B
TGop
Op
E
TGmm
Md
C
Op
TGop
E
Hb
TGmm
Mx
Md

3.2 Results

3.2.1 EphA- and ephrin-A-Fc staining during trigeminal ganglion axon guidance

3.2.1.1 Complementary and overlapping EphA and ephrin-A expression in the trigeminal ganglion target fields

As previously described, the promiscuous binding of ephrin-A5-Fc and EphA3-Fc chimeric probes to a number of cognate partners was exploited to determine the global expression of EphA and ephrin-A respectively (Figure 3.3). The negative control, which was just the Fc portion of the human immunoglobulin protein (control-Fc), did not reveal any specific staining (Figure 3.3I).

The most obvious observation during stages 13 and 15 was the complementary expression of EphAs and ephrin-As in the target fields of the trigeminal ganglion. Notably, EphA receptors were expressed in the ophthalmic process (Figure 3.3A-B), while ephrin-A ligands were localised to the first branchial arch (future maxillary and mandibular processes) (Figure 3.3D-E). Other regions positive for EphAs during stages 13 and 15 were the forebrain, rhombomeres r3 and r5, and the otic placodes (Figure 3.3A-B). Ephrin-As were found to localise to the midbrain, the developing eye, and in the developing second branchial arch (Figure 3.3D-E). Furthermore, complementary domains of EphAs and ephrin-As were apparent in the central nervous system (compare expression of EphAs in the forebrain in Figure 3.3A-B with midbrain ephrin-A expression in Figure 3.3D-E). In addition, other regions of the embryo that was positive for EphAs (for example, the eye and otic placodes) appeared to show no ephrin-A expression (compare Figures 3.3A-B with 3.3D-E).

In comparison to stages 13 and 15, EphA (Figure 3.3C) and ephrin-A (Figure 3.3F) expression domains were found to be both complementary and overlapping at stage 20 in the target fields of the trigeminal ganglion. Whilst the ophthalmic process continued to express EphAs at stage 20, other areas that were now also positive for EphA receptors were the maxillary and mandibular processes (arrowheads: Figure 3.3C). Regions of EphA and ephrin-A overlapping expression were demonstrated in the mandibular process (Figure

3.3C, 3.3F). Most notably however, ephrin-A5-Fc and EphA3-Fc staining did not exhibit homogeneous staining of the mandibular process (Figure 3.3C and 3.3F).

To further verify the observed expression of ephrin-A ligands as revealed by EphA3-Fc staining, EphA4-Fc was used at stage 20 (Figure 3.3G). As with EphA3-Fc, a similar expression pattern was observed proximal to the trigeminal ganglion (asterisk) with EphA4-Fc (compare Figure 3.3F with 3.3G). In contrast to EphA3-Fc, EphA4-Fc was found to weakly localise to mandibular process and not to the maxillary process (arrowheads: Figure 3.3G). The differences in staining observed in the mandibular process are likely due to the varying affinities with which EphA3 and EphA4 binds to ephrin-A ligands that are not involved in cognate partner interactions (Figure 3.1B).

However, given that EphA4 binds to both ephrin-A and ephrin-B class ligands (Gale *et al.,* 1996), there was a possibility that EphA4-Fc was also revealing ephrin-B2 ligand expression. To exclude this possibility, EphB2-Fc fusion protein, a high affinity receptor for ephrin-B2 (Gale *et al.,* 1996) was used in this study (Figure 3.3H). The proximal region to the trigeminal ganglion (asterisk) did not appear to be stained (Figure 3.3H). This verified that the staining observed with EphA4-Fc was indeed that of ephrin-A ligands.

Overall, EphA and ephrin-As are expressed in complementary and overlapping domains during chick embryo face development, and these domains of expression are in keeping with studies described during equivalent stages of mouse embryogenesis (Flenniken *et al.,* 1996; Gale *et al.,* 1996).

3.2.1.2 Differential Eph/ ephrin-A expression in the trigeminal ganglion

In order to determine whether the maturing trigeminal ganglion was stained for EphA or ephrin-A, whole embryos stained with ephrin-A5-Fc and EphA3-Fc were examined more closely and subsequently sectioned to reveal tissues binding to Fc-fusion chimera proteins. To verify the position of the ganglion, sections from Fc-fusion chimera bound embryos were imaged using antibodies for the neuronal marker neurofilament (Figure 3.4). Weak binding of the ophthalmic lobe was revealed for ephrin-A5-Fc (asterisk, Figure 3.4A-B) when sectioned or viewed in whole-mount. Anti-neurofilament (Figure 3.4A') staining

confirmed localisation of ephrin-A5-Fc to the ophthalmic lobe, although the maxillomandibular lobe did not appear to be stained for EphA receptors (Figure 3.4A-A"). The intense EphA staining around the maxillomandibular lobe region did not correspond to the maxillomandibular lobe; this appeared to correspond to a domain of mesenchyme that is located behind the trigeminal ganglion (arrow; Figure 3.4A). EphA3-Fc binding revealed the expression of ephrin-As in the trigeminal ganglion (Figure 3.4C); the ophthalmic lobe was weakly stained (dotted outline) compared with maxillomandibular lobe (asterisk, Figure 3.4C-C").

Further evidence of ephrin-A(s) localisation to the maxillomandibular lobe of the trigeminal ganglion lobe was demonstrated with EphA4-Fc (asterisk; Figure 3.4D). The absence of EphB2-Fc binding further indicated that ephrin-B ligands did not appear to be expressed in the trigeminal ganglion (dotted outline; Figure 3.4E).

To summarise, regions within the area occupied by the trigeminal ganglion differentially expressed EphAs and ephrin-As. Therefore, these trigeminal ganglion expressed EphAs and ephrin-As are likely cognate binding partners for Eph/ ephrin-As expressed in the trigeminal ganglion target fields.

Figure 3. 3 EphA and ephrin-A global expression patterns during early trigeminal ganglion development.

(A-C) Whole-mount ephrin-A5-Fc binding to EphA receptors at stages 13-13+ (A), 15 (B), and 20 (C). (A) Dorsal view, (A') lateral view of same embryo. Dotted outline depicts the developing eye.

(D-F) Whole-mount EphA3-Fc binding to ephrin-A ligands at stages 13-13+ (D), 15 (E), and 20 (F).

(G) Whole-mount EphA4-Fc binding to ephrin-A ligands and ephrin-B2 at stage 20.

(H) Whole-mount EphB2-binding to ephrin-B ligands and ephrin-A5 staining at stage 20.

(I) Whole-mount human Fc portion binds non-specifically.

White asterisk: location of trigeminal ganglion.

Abbreviations: E, eye; Fb, Forebrain; Mb, midbrain; Md, mandibular process; Mx, maxillary process; Op, ophthalmic process; Ot, otic placode; r3, rhombomere 3; r5, rhombomere 5; 1 BA, first branchial arch; 2 BA, second branchial arch.

Scale: 200 μm (A-B), (D-E), (C, F), (G-I).

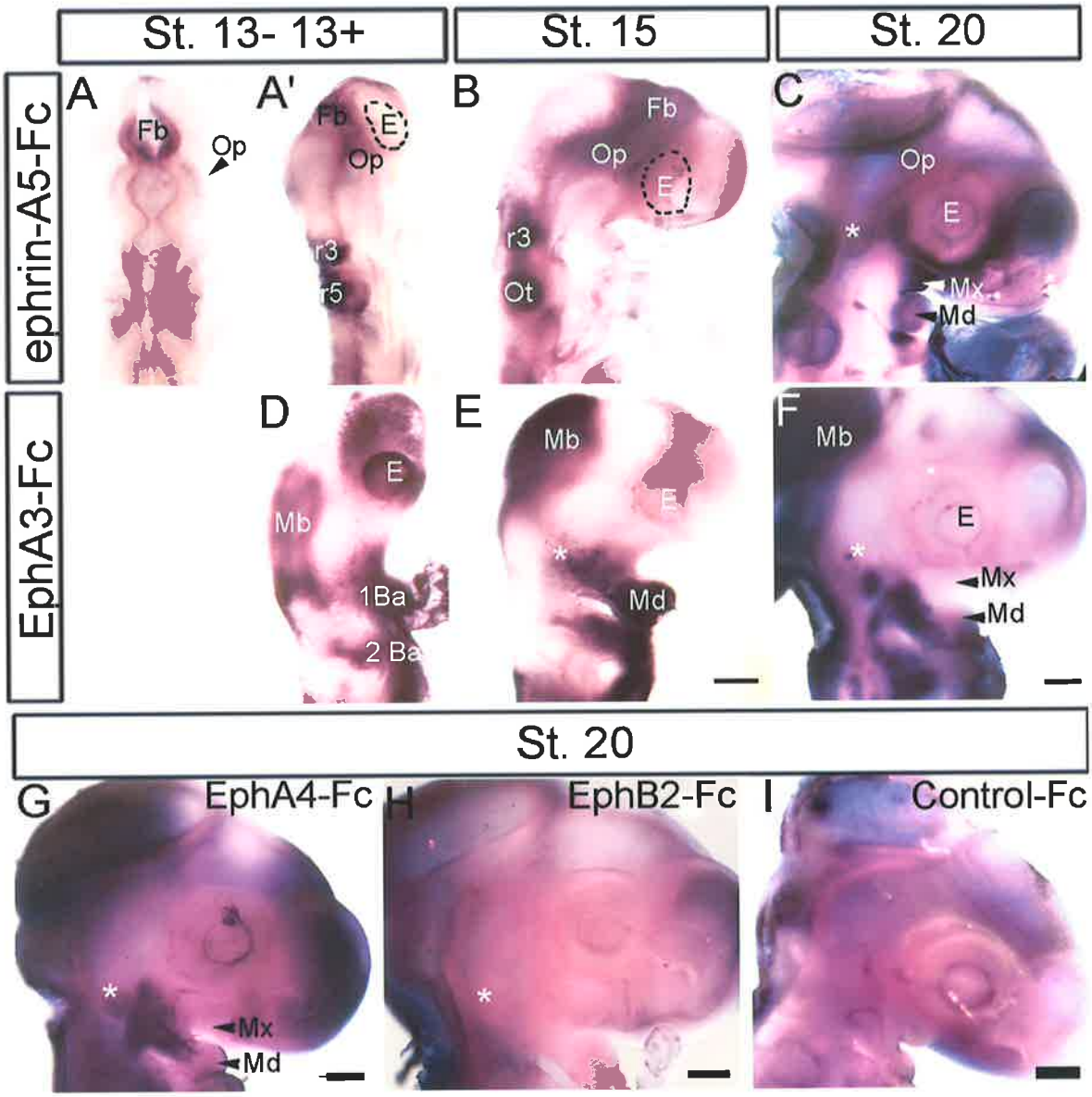
St. 13- 13+
St. 15
St. 20
ephrin-A5-Fc
EphA3-Fc
A
A'
B
C
D
E
F
Fb
Op
E
r3
r5
Ot
Mx
Md
Mb
1Ba
2 Ba
St. 20
G
EphA4-Fc
H
EphB2-Fc
I
Control-Fc

Figure 3. 4 EphA and ephrin-A expression in the maturing trigeminal ganglion at stage 20.

(A-A") Vibratome sagittal section of ephrin-A5-Fc bound embryo from Figure 3.2C showing ophthalmic (TGop) lobe staining (asterisk and dotted outline) for EphA. (A) Bright field ephrin-A5-Fc image. Arrow: possible mesenchymal EphA expression. (A') Co-stained with anti-neurofilament (NFM) antibody. (A") Merged image.

(B) Whole-mount view of the trigeminal ganglion (dotted outline) from another ephrin-A5-Fc bound embryo. Asterisk: weak ephrin-A5-Fc positive TGop lobe.

(C-C") Vibratome sagittal section of EphA3-Fc bound embryo revealing differential trigeminal ganglion lobe staining for ephrin-A. Asterisk denotes the TGmm lobe, and the dotted outline shows the TGop lobe. (C) Bright field EphA3-Fc image. (C') Co-stained with anti- NFM antibody. (C") Merged image.

(D) Whole-mount image of trigeminal ganglion bound with EphA4-Fc. The dotted outline indicates the ganglion. White asterisk: ephrin-A ligand localisation to the TGmm lobe.

(E) Whole-mount image of the trigeminal ganglion demonstrating no binding of EphB2-Fc. The dotted outline indicates the ganglion.

Scale: 200 μm (A, C, D, E); 250 μm (B).

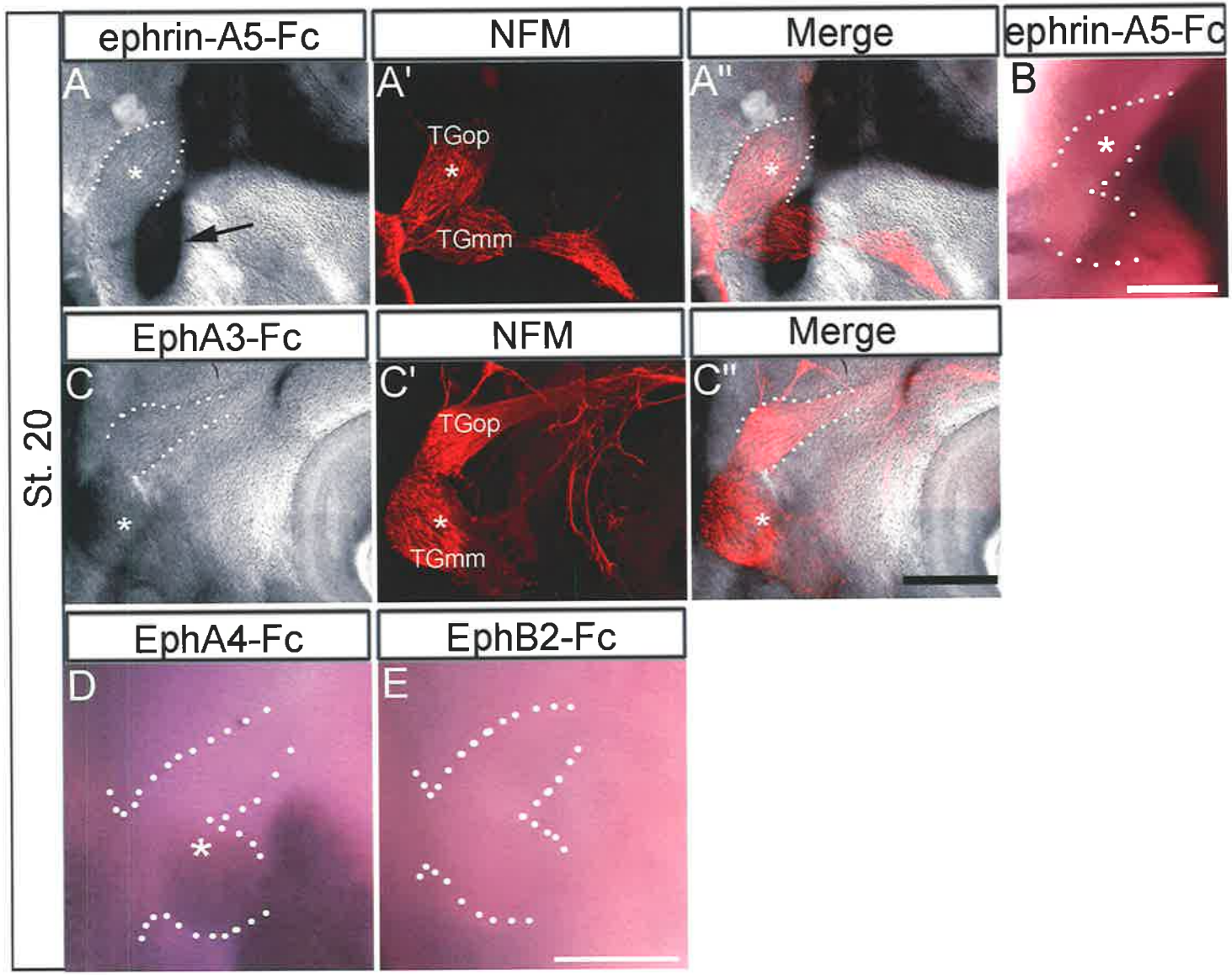
St. 20
ephrin-A5-Fc
NFM
Merge
ephrin-A5-Fc
A
A'
A''
B
TGop
TGmm
EphA3-Fc
NFM
Merge
C
C'
C''
TGop
TGmm
EphA4-Fc
EphB2-Fc
D
E

3.2.2 EphA expression in the trigeminal ganglion peripheral target fields

As mentioned previously, Fc-fusion proteins only allow the elucidation of global Eph/ ephrin-A expression patterns. Furthermore, Fc-fusion proteins only demonstrate the expression of Eph/ ephrins that are not involved in cognate partner interactions (Figure 3.1B). To overcome these limitations, RNA *in situ* hybridisation and immunofluorescent antibody staining assisted in: (1) the identification of individual Eph/ ephrin-A members, whose expression patterns correspond to the global Fc-fusion protein stains, and (2) the detection of individual Eph or ephrin mRNAs and presumably an accurate measure of protein levels that is independent of the Eph or ephrin cognate partner binding state.

The ephrin-A5-Fc binding revealed the presence of EphA receptors in the trigeminal ganglion target fields (Figure 3.3), and therefore the identity of possible candidate receptors was investigated. For this purpose, chick specific EphA receptors A3-A5, A7, and A9 were analysed. Receptors were excluded from further analysis if they were not expressed or were expressed but not in a pattern of expression consistent with a role for trigeminal ganglion axon guidance.

3.2.2.1 EphA3 is expressed in the ophthalmic process and is expressed in the trigeminal ganglion

Investigation of EphA receptors in the target regions of the trigeminal ganglion revealed EphA3 as a putative candidate guidance cue. RNA *in situ* hybridisation of whole-mount embryos demonstrated *EphA3* mRNA expression in the ophthalmic process at stages 13 (Figure 3.5A) and 15 (Figure 3.5B) consistent with ephrin-A5-Fc results (Figures 3.3A-B). Later at stage 20, the ophthalmic and mandibular processes were positive for *EphA3*, with the mandibular process exhibiting the strongest signal (arrowhead; Figure 3.5C). The maxillary process weakly expressed *EphA3* (Figure 3.5C). Target staining of *EphA3* was in agreement with ephrin-A5-Fc staining at stage 20 (Figure 3.3C). Negative control, which was the sense *EphA3* riboprobe, did not show any specific staining (Figure 3.5D).

Figure 3. 5 *EphA3* transcripts are localised to the ophthalmic process mesenchyme during trigeminal ganglion axon guidance.

(A-C) Whole-mount *in situ* hybridisation showing expression of *EphA3* at stages 13 (A), 15 (B) and 20 (C). (C) Asterisk: the trigeminal ganglion.

(D) An example of an embryo probed with *EphA3* sense (S) riboprobes illustrating non-specific staining.

(E-G') Cryostat sections showing expression of *EphA3* (E, F, G) and HNK-1 (E', G') at the level of the ophthalmic process (E-F) and mandibular process (G). Arrows: mesenchymal expression of EphA3. Arrowheads: epithelial expression (E-F) or lack of epithelial expression (G-G'). Dotted outline delineates epithelium from mesenchyme. (E-E'), (G-G') Arrows: lack of co-localisation with HNK-1 staining. (G-G') Asterisk: neural crest component of the trigeminal ganglion is weakly positive for *EphA3* transcripts. (G). Note: lack of expression in the mandibular process.

(H-I) Schematic images showing approximate plane of sections in (D-F).

Red lettering indicates orientation in (E) and applies to images (E-G). D, dorsal; V, Ventral.

Abbreviations: E, eye; Md, mandibular process; Mx, maxillary process; Op, ophthalmic process.

Scale: 200 μm (A-C); 100 μm (E-E'), (F), (G-G').

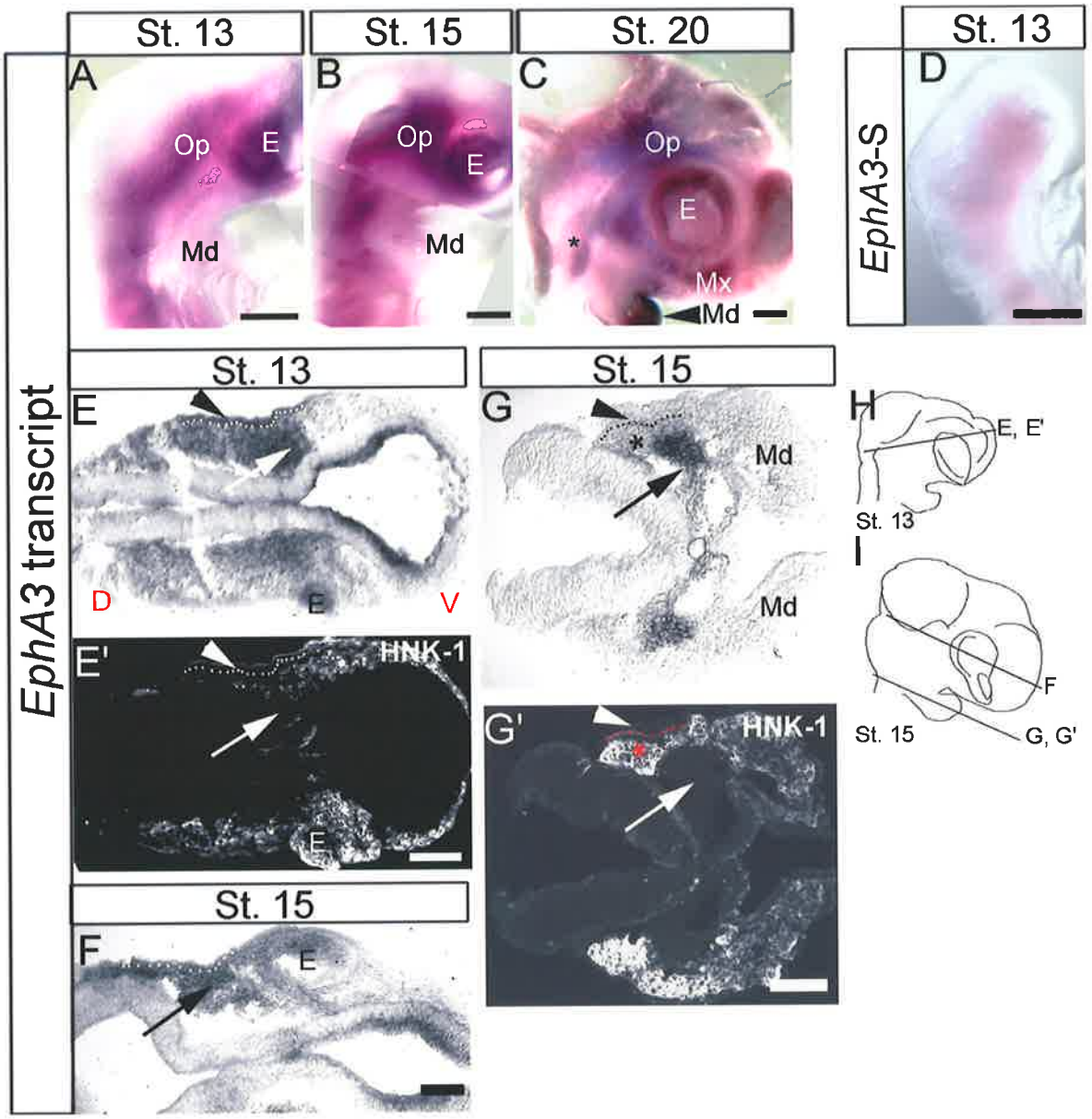
St. 13
St. 15
St. 20
St. 13
EphA3 transcript
EphA3-S
A
B
C
D
Op
E
Md
Mx
*
St. 13
St. 15
E
G
H
I
D
V
E'
G'
HNK-1
St. 15
F
E, E'
St. 13
F
G, G'
St. 15

To demonstrate that the expression observed for *EphA3* mRNA in whole-mount embryos was localised to the mesenchyme of the ophthalmic process, *EphA3* stained embryos were sectioned (Figures 3.5E-F). Cryostat sections through *EphA3* stained stage 13 and 15 embryos revealed localisation of transcript to the mesenchyme of the ophthalmic process (arrow; Figure 3.5E and 3.5F). Furthermore as noted from whole-mount embryos, sectioning did not show any apparent *EphA3* localisation to the mandibular process (Figure 3.5G). In summary, the ophthalmic process mesenchymal expression of *EphA3* is consistent with a role for the receptor during trigeminal ganglion axon guidance.

Since neural crest cells migrate from the neural tube into the periphery of the embryo and contribute to cranial structures, the patterns of localisation between neural crest marker HNK-1 and *EphA3* mRNA were analysed. At the level of the ophthalmic and mandibular processes, regions intensely stained for *EphA3* transcript did not appear to exhibit localisation for HNK-1 (arrow; Figure 3.5E-E', 3.5G-G'). Thus, *EphA3* mRNA does not appear to be expressed by neural crest cells that contribute to mesenchymal structures at least at stages 13 and 15.

To determine whether the ophthalmic mesenchyme continued to express *EphA3* mRNA at stage 20 (Figure 3.5C), sectioned *EphA3 in situ* hybridised embryos were analysed (Figure 3.6A). As observed at stages 13 and 15 (Figure 3.5), *EphA3* was expressed in the ophthalmic process mesenchyme (Figure 3.6A). At the level of the maxillary process, *EphA3* mesenchyme expression appeared to be weak (arrowheads; Figure 3.6B). In contrast to the maxillary process, strong *EphA3* localisation to the mandibular mesenchyme was exhibited (arrowhead: Figure 3.6C). As observed at stage 15 at level of the mandibular process (arrow; Figure 3.5G), a strong patch of *EphA3* positive tissue was visualised (arrow; Figure 3.6C). In summary at stage 20, in addition to be expressed in the ophthalmic process mesenchyme, *EphA3* mRNA localisation to the maxillary and mandibular process mesenchyme are further suggestive of a role for EphA3 as a trigeminal ganglion axon guidance cue.

In order to understand where trigeminal ganglion axons were with respect to EphA3 expressing mesenchyme, EphA3 mRNA/ protein stained sections were immuno-labelled with an antibody against the neuronal axon marker, neurofilament (Figure 3.6A'-C' and

Figure 3.6D'-F'). Immunofluorescence EphA3 protein staining during stage 20 (Figure 3.6D-F) was consistent with the results observed for *EphA3* transcripts (Figure 3.6A-C). Ophthalmic trigeminal ganglion axons appeared to course through *EphA3* positive mesenchyme (arrowheads; Figure 3.6A'). EphA3 antibody staining further showed that these ophthalmic axons coursed through a region of high (arrow; Figure 3.6D-D') to a region of low EphA3 expression (arrowheads; Figure 3.6D-D'). At the level of the maxillary process, trigeminal ganglion axons were found to grow in EphA3 protein positive regions (arrowheads; Figure 3.6E'). To summarise, trigeminal ganglion axons appeared to grow on and course through EphA3 positive mesenchyme in the target fields.

In addition to exhibiting localisation to the mesenchymal paths of growing trigeminal ganglion axons, the results for EphA3 mRNA and protein staining also revealed EphA3 expression in the trigeminal ganglion itself (asterisk; Figure 3.6B-B', 3.6E-E'). Also of note, the placode and neural crest components that contribute to the formation of the trigeminal ganglion appeared to be positive for *EphA3* transcript. The epidermal layer, which may correspond to the trigeminal ophthalmic placode, at the level of the ophthalmic process revealed strong *EphA3* localisation (arrowhead; Figure 3.5E, 3.5F), while the epidermal layer which may contribute to the trigeminal maxillomandibular placode did not exhibit such expression (dotted outline and arrowhead; Figure 3.5G-G'). Additionally, a weak *EphA3* mRNA signal was observed in the neural crest component of the ganglion at stage 15, as revealed by antibody staining against the neural crest marker HNK-1 (asterisk: Figure 3.5G-G').

In conclusion, EphA3 mRNA and protein expression patterns observed at stages 13, 15 and 20 (Figures 3.5-3.6) are consistent with the findings from ephrin-A5-Fc localisation in the trigeminal ganglion target fields (Figure 3.3).

Figure 3. 6 EphA3 mRNA and protein are expressed in all trigeminal ganglion target fields at stage 20.

(A-C') Bright field images of vibratome sections from *EphA3 in situ* hybridised embryo. *EphA3* appears as black staining at the level of the ophthalmic (A), maxillary (B) and mandibular (C) processes. (A'-C') Anti-neurofilament staining (red).

(A-A') Ophthalmic axons (arrowheads) are growing on *EphA3* mesenchyme.

(B-B') The maxillary process expresses low levels of *EphA3* (arrowheads). Asterisk: trigeminal ganglion staining.

(C-C') Arrow: mesenchymal staining. Arrowhead: high *EphA3* mRNA localisation to mandibular process mesenchyme staining.

(D-F') Immunofluorescent EphA3 antibody stains on vibratome sections at stage 20 (D-F), and merged with anti-NFM staining (red; D'-F') at the level of the ophthalmic (D-D'), maxillary (E-E'), and mandibular (F-F') processes. Images are confocal z-stacks.

(D-D') Axons course through high (arrow) to low EphA3 region (arrowheads).

(E-E') Arrowhead: axons grow on EphA3 positive mesenchyme. The trigeminal ganglion (asterisk) and growing trigeminal motor axons (arrow) are EphA3 positive. (G) Schematic showing approximate plane of sections in (A-F). Asterisk: highlights the position of the trigeminal ganglion. Orientation is highlighted in red lettering in (A) applies to all images (A-F'). D, dorsal; V, Ventral.

Abbreviations: Mx, maxillary process; Md, mandibular process; Op, ophthalmic process.

Scale: 200 μm (A-F).

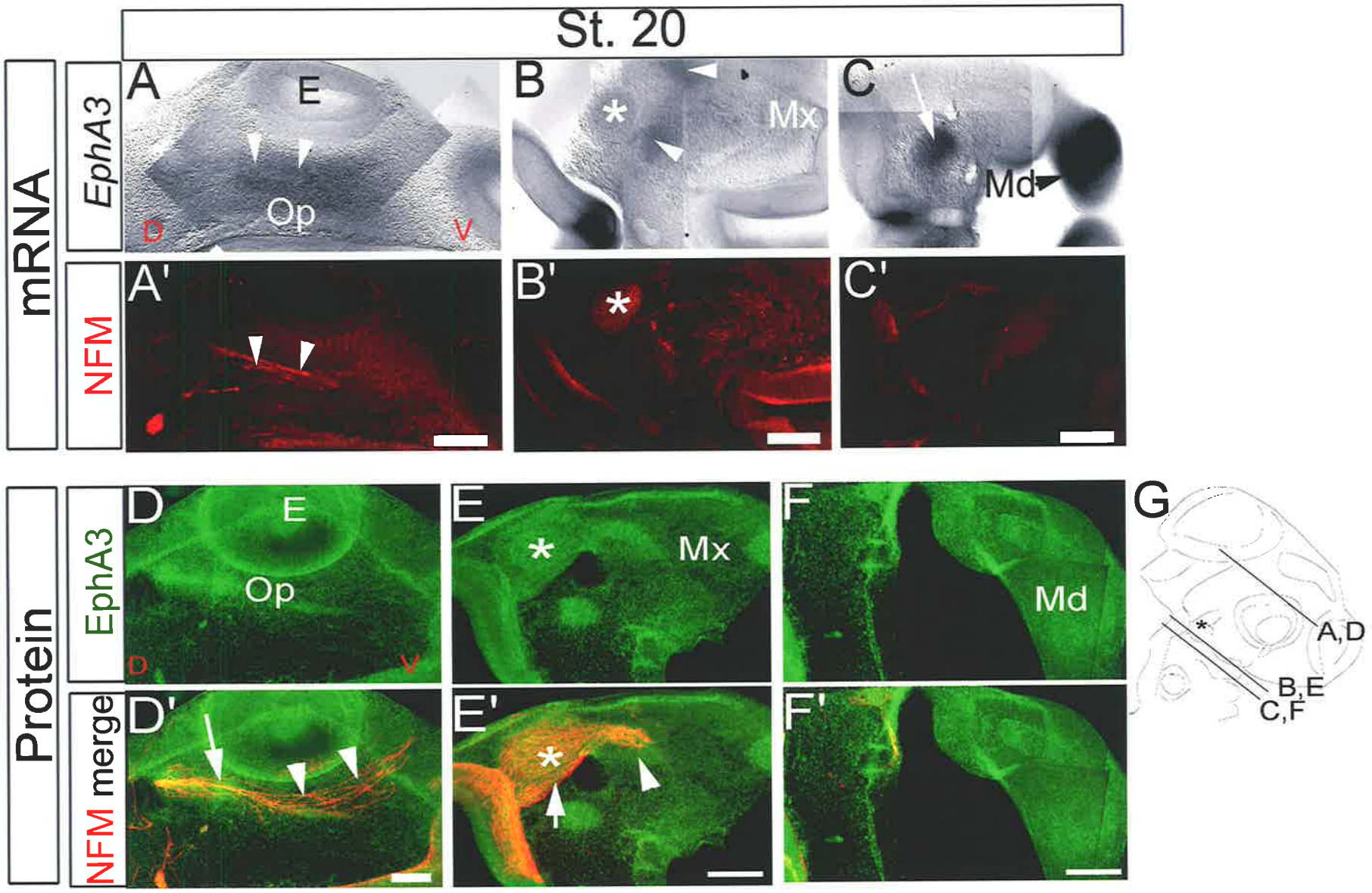
St. 20
mRNA
EphA3
NFM
A
E
Op
D
V
B
*
Mx
C
Md
A'
B'
C'
Protein
EphA3
NFM merge
D
E
Op
D
V
E
*
Mx
F
Md
D'
E'
F'
G
A,D
B,E
C,F
*

3.2.2.2 EphA4 is expressed in the ophthalmic process during ophthalmic trigeminal ganglion axon growth at stage 13

Another member of the EphA receptor family found to be a putative candidate guidance cue to growing trigeminal ganglion axons was EphA4. Therefore, the expression of EphA4 mRNA and protein is described herein.

As with EphA3 (Figures 3.5-3.6), expression of EphA4 transcript and protein was initially observed in the ophthalmic process at stage 13+ and then was found to localise to all target fields of the trigeminal ganglion at stage 20 (Figure 3.7-3.8). In the target fields at stage 20 (Figure 3.7A, 3.7E, 3.8A, 3.8C-D), EphA4 expression was similar to that observed with EphA3 (Figure 3.5C and 3.6). Further analysis of sections from *EphA4 in situ* hybridised embryos or those stained with anti-EphA4 revealed that EphA4 was localised to the mesenchyme at the level of the ophthalmic, maxillary and mandibular processes (Figure 3.7C-E' and 3.8A-C). It was also noted that EphA4 transcripts were restricted to the maxillary process epithelium (red outline and arrowhead; Figure 3.7C). In comparison to *EphA3* mRNA (Figure 3.5C), differential expression of *EphA4* mRNA in the mandibular process was observed (Figure 3.7A); the anterior mesenchymal region of the process was highly positive for *EphA4* compared with the weakly *EphA4* positive posterior region (Figure 3.7A). This was also evident in sections from EphA4 *in situ* hybridised embryos (Figure 3.7D) and following anti-EphA4 staining (arrow; Figure 3.7E, 3.8C-C'). Furthermore, when viewed in whole-mount and in sections, *EphA4* mRNA was expressed highly in the maxillary process (Figure 3.7A, C), unlike *EphA3* (Figure 3.5C). Inspection of sections at the level of the maxillary process revealed strong EphA4 receptor transcript and protein localisation to a distal region, and very little receptor was visualised proximal to the ganglion (asterisk; Figure 3.7C, 3.8B-B'). This distribution for EphA4 was in contrast to EphA3 mRNA and protein, which was distributed diffusely throughout the mesenchyme of the maxillary process, with rather strong expression proximal to the trigeminal ganglion (asterisk; Figure 3.6B-B', 3.6E-E'). No specific staining however was observed in the negative control experiments with the *EphA4* sense probe (Figure 3.7B).

Next it was determined whether EphA4 was expressed in a similar manner to EphA3 at stage 13. *EphA4* transcript expression in the stage 14 chick embryo has been previously

documented (Kury *et al.,* 2000; Santiago and Erickson, 2002), although protein expression was not investigated in the developing head. Therefore the expression of EphA4 was analysed using an anti-EphA4 antibody at stage 13. As observed for *EphA3* transcript, ophthalmic process mesenchyme was positive for EphA4 at stage 13+, (Figure 3.7B). Additionally, this EphA4 protein expression was consistent with previous *EphA4 in situ* hybridisation results (Kury *et al.,* 2000; Santiago and Erickson, 2002). Ophthalmic neurons appeared to extend on EphA4 positive ophthalmic mesenchyme at stage 13+ (arrowhead; Figure 3.7F'-F"), and this ophthalmic process EphA4 expression was maintained into stage 20 (Figure 3.7A, 3.7C, 3.7E-E', 3.8A). Therefore, the ophthalmic process mesenchyme expression pattern for EphA4 protein suggested that this receptor might also provide guidance cues to growing trigeminal ganglion axons at stage 13.

Figure 3. 7 EphA4 mRNA and protein expression at stages 13 and 20 in the trigeminal ganglion peripheral target fields.

(A) Whole-mount *EphA4 in situ* hybridised stage 20 embryo. (B) Embryo probed with EphA4 sense riboprobes demonstrates non-specific staining.
(C-D) Sagittal vibratome sections from *EphA4 in situ* hybridised embryo.
(C) Arrowheads: ophthalmic (Op) and maxillary (Mx) process mesenchymal staining. Dotted outline and asterisk: lack of *EphA4* expression in the trigeminal ganglion.
(D) Arrows: mesenchymal staining in the maxillary and mandibular (Md) processes. Red arrowhead and dotted outline: *EphA4* localisation to the epithelium of the Mx process.
(E-F) Confocal z-stacks at stage 20 (E-E') and 13+ (F-F"), demonstrating EphA4 (E-E', F, F") and neurofilament (NFM; E', F'-F") expression. Merged images shown in (E', F").
(E-E') Sagittal oblique vibratome section. Arrowheads: EphA4 positive mesenchyme. Arrow: anterior region of the Md process..
(F-F") Lateral view of a half-mount embryo head. Arrowhead: ophthalmic axons grow on EphA4 positive mesenchyme.
Orientation is indicated in red lettering in (F) applies to images (A-D). Orientation also shown in (E). D, dorsal; V, ventral.
Abbreviations. E, eye; *EA4, EphA4* transcript. Asterisk: the trigeminal ganglion.
Scale: 200 μm (A-D), (F-F"); 100 μm (E-E').

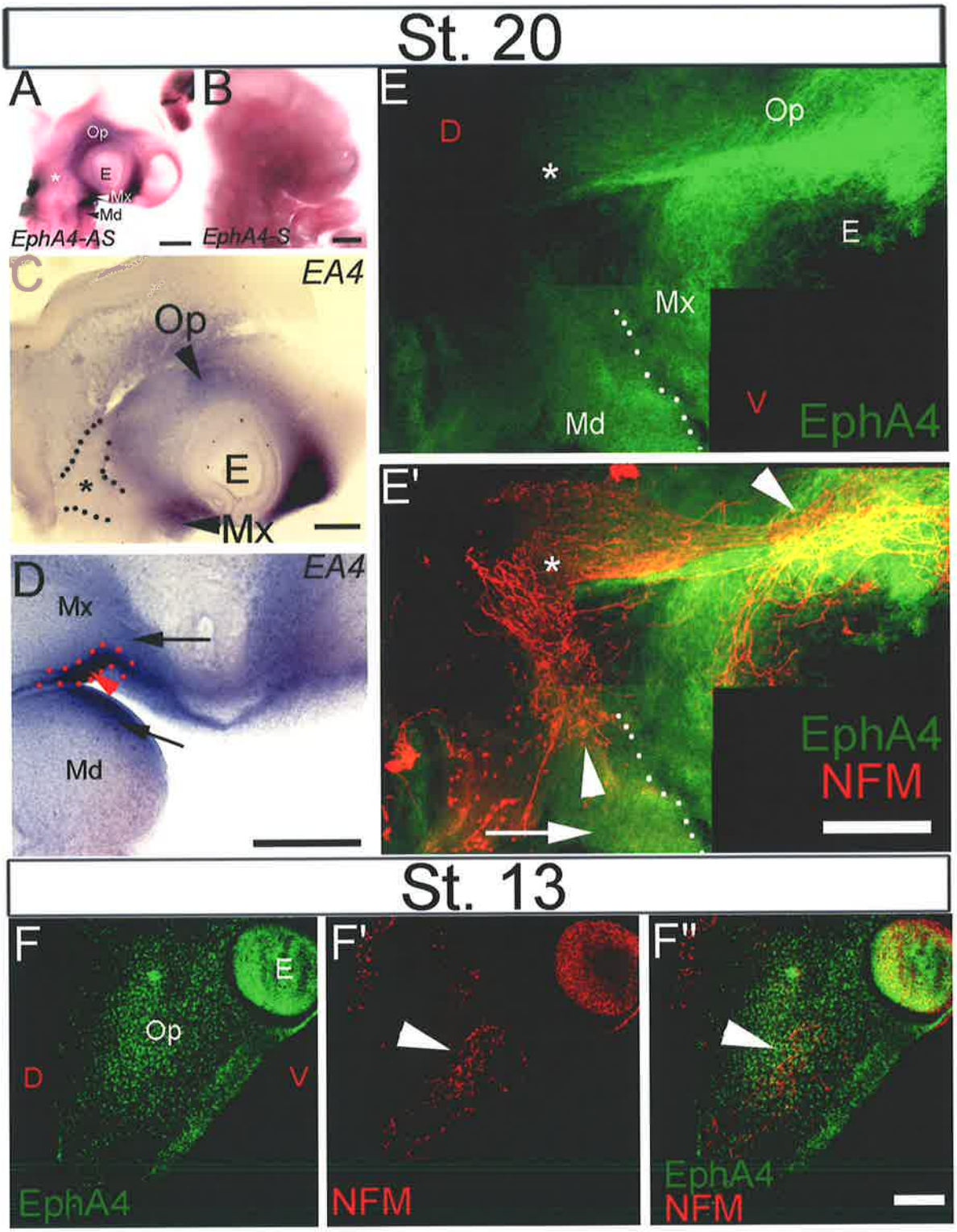
St. 20
A
Op
E
Mx
Md
EphA4-AS
B
EphA4-S
C
EA4
Op
E
Mx
D
EA4
Mx
Md
E
D
Op
E
Mx
Md
V
EphA4
E'
EphA4
NFM
St. 13
F
E
Op
D
V
EphA4
F'
NFM
F''
EphA4
NFM

To further examine the cellular relationships between trigeminal ganglion axons and EphA4 positive mesenchyme, EphA4 antibody stained sections were also stained for the neuronal axon marker neurofilament at stage 20 (Figure 3.8A-C). Trigeminal ganglion axons were found to be growing into, or through EphA4 positive mesenchyme at stage 20 (arrowheads; Figure 3.7E-E''), as observed for stage 13+ (Figure 3.7F"). As for EphA3 (Figure 3.5C and Figure 3.6D), EphA4 appeared to be expressed in a high to low, dorsal to ventral manner in the ophthalmic process during trigeminal ganglion axon growth (Figure 3.8A'). At the level of the maxillary process in sagittal view (Figure 3.7E-E') and transverse view (Figure 3.8B-B'), axons extending from the trigeminal ganglion demonstrated growth from a low to high region of EphA4. Similar to *in situ* hybridisation data (Figure 3.7A), the posterior region of the mandibular process weakly expressed EphA4 (arrowhead; Figure 3.8C-C'), although expression did not appear to be uniform. In summary, the expression of EphA4 is further consistent with a role for this receptor as a guidance cue to trigeminal ganglion axons.

Other regions that were noted to be positive for EphA4 were a group cells at the level of the maxillary process (dotted outline near asterisk; Figure 3.8B-B'). The identity of these cells is not known, and they are likely to be boundary cap cells located at the trigeminal motor axon exit point. Although EphA4 was not present in the trigeminal ganglion (asterisk; Figures 3.7A, C, E), an intense region of EphA4 mesenchyme was observed near the ganglion (blue arrowhead; Figure 3.8B). This region was reminiscent of the staining observed with EphA3 (arrow; Figure 3.5F, 3.6B-C).

Overall, the pattern of EphA4 localisation (Figure 3.7-3.8) was found to be similar to that of EphA3 at stages 13 and 20 (Figure 3.5-3.6). Given the similarity in expression observed for the two receptors, EphA3 and EphA4 are likely to perform overlapping or redundant functions during trigeminal ganglion axon guidance. Additionally, EphA4 expression pattern observed with RNA *in situ* hybridisation and immunofluorescent antibody staining was reminiscent of ephrin-A5-Fc localisation (Figure 3.3) in the trigeminal ganglion target fields.

3.2.2.3 EphA5, EphA7 and EphA9 are not candidate guidance cues for trigeminal ganglion axons

As mentioned previously, the expression of EphA5, A7 and A9 were also analysed using RNA *in situ* hybridisation. However, their patterns of expression were not consistent with a role for EphA5, A7 and A9 as guidance cues to trigeminal ganglion axons.

Analysis of *EphA5* mRNA expression at stage 20 indicated that the receptor was not expressed in the peripheral target fields of the trigeminal ganglion, or in the ganglion (asterisk; Figure 3.9A). Previous expression of *EphA5* in the hindbrain (arrow; Figure 3.9A) has been documented (Kury *et al.,* 2000). *EphA5* appeared to be expressed in the epibranchial placode regions (arrowheads; Figure 3.9A) and this was consistent with what is observed with ephrin-A5-Fc (Figure 3.3C). The sense negative control probe against *EphA5* did not show any specific staining (Figure 3.9B).

Previously, expression of *EphA7* at stages 12-18 was documented, and analysis at stages 12-14 did not reveal any expression outside the central nervous system (Araujo and Nieto, 1997). Analysis at stage 20 in this study revealed a similar expression pattern for *EphA7* (Figure 3.9C), to that previously observed at stage 18 (Araujo and Nieto, 1997). The negative control, which was the *EphA7* sense riboprobes, exhibited no specific staining. *EphA7* is expressed in rhombomeres r2 and r3 in the hindbrain, in the forebrain (blue arrows; Figure 3.9C), and there is restricted midline expression in the maxillary and mandibular processes (arrowheads; Figure 3.9C). The trigeminal ganglion did not show any apparent staining for EphA7 (asterisk; Figure 3.9C) and this was confirmed when stained embryos were sectioned (asterisk; Figure 3.9E). The ophthalmic process was not positive for EphA7 (Figure 3.9F). Further assessment of staining observed with whole-mount embryos revealed that EphA7 was restricted to the epithelial layer of the maxillary and mandibular processes (arrowheads; Figure 3.9G and Figure 3.9H). Furthermore, EphA7 was absent from the mesenchyme of the maxillary and mandibular processes, suggesting that this receptor did not play a role during trigeminal ganglion axon guidance. However, EphA7 localisation to the midline first branchial arch epithelium was suggestive of a role for this receptor during branchial arch morphogenesis.

Figure 3.8 EphA4 protein distribution in the trigeminal ganglion targets at stage 20.

(A-C) Confocal z-stacks at stage 20, demonstrating EphA4 (A-C) and neurofilament (red) (NFM; A'-C') expression. Merged images shown in (A'-C'). Sections are at the level of the ophthalmic (Op; A-A'), maxillary (Mx; B-B') and mandibular (Md; C-C') processes.

(A-A') High (arrow) and low EphA4 (arrowheads) regions.

(B-B') Arrow: trigeminal ganglion axons grow on EphA4 mesenchyme. Outside the trigeminal ganglion (asterisk), a group of cells are EphA4 positive (dotted region) (B'). Blue arrowhead: patch of strong EphA4 expressing mesenchyme.

(C-C') Arrow: Weak EphA4 expression at the level of posterior region of the mandibular process.

(D) Schematic showing approximate plane of sections in (A-C).

Orientation is highlighted in red lettering in (A) and applies to all images. D, dorsal; V, Ventral.

Abbreviations. E, eye. Asterisk: the trigeminal ganglion.

Scale: 200 μm (A-A'), (B-B'), (C-C').

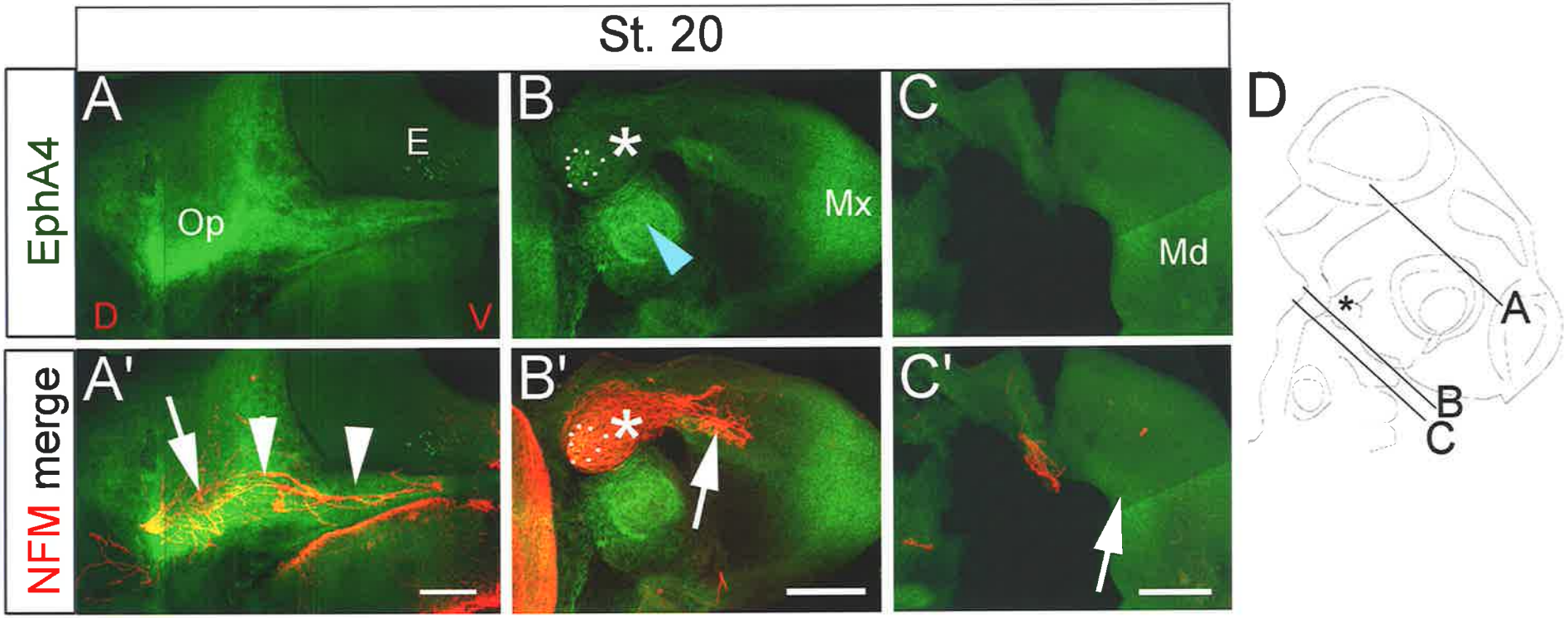
St. 20
EphA4
NFM merge
A
B
C
A'
B'
C'
E
Op
D
V
Mx
Md
*
D
A
B
C

Figure 3.9 Expression of *EphA5, EphA7* and *EphA9* transcripts at stage 20.

(A-D) Whole-mount *in situ* hybridised embryos stained with *EphA5* anti-sense (A), *EphA5* sense (B), *EphA7* anti-sense (C) and *EphA9* anti-sense riboprobes (D). Asterisk: trigeminal ganglion.

(A) *EphA5* expression in the hindbrain (arrow), and epibranchial placode regions (arrowheads).

(B) *EphA5* sense riboprobe only reveals background staining.

(C) *EphA7* localisation to maxillary (Mx) and mandibular (Md) process (arrowheads) to the forebrain (arrows). Rhombomere 2 (r2) and 3 (r3) staining in the hindbrain.

(D) Only background staining is observed with *EphA9* anti-sense probe.

(E-H) Detailed analysis of *EphA7* expression pattern at stage 20 in the trigeminal ganglion (E) and peripheral targets of the ganglion (F-H). All sections are vibratome sections, and approximate plane of sections are indicated in schematic (I).

(E, F) Sagittal view of the trigeminal ganglion (asterisk and dotted outline; F) and ophthalmic process (F). Unlike the staining in r2 and r3, *EphA7* does not restrict to the ganglion (E) and the ophthalmic process (F). E, eye.

(G-H) Transverse (G) and sagittal view (H) highlight *EphA7* positive epithelium of the Mx and Md processes (arrowheads) at the midline. There is no mesenchymal staining.

Orientation is indicated by red lettering in (F-H). D, dorsal; V, ventral.

Scale: 200 μm (A-D); (E-H).

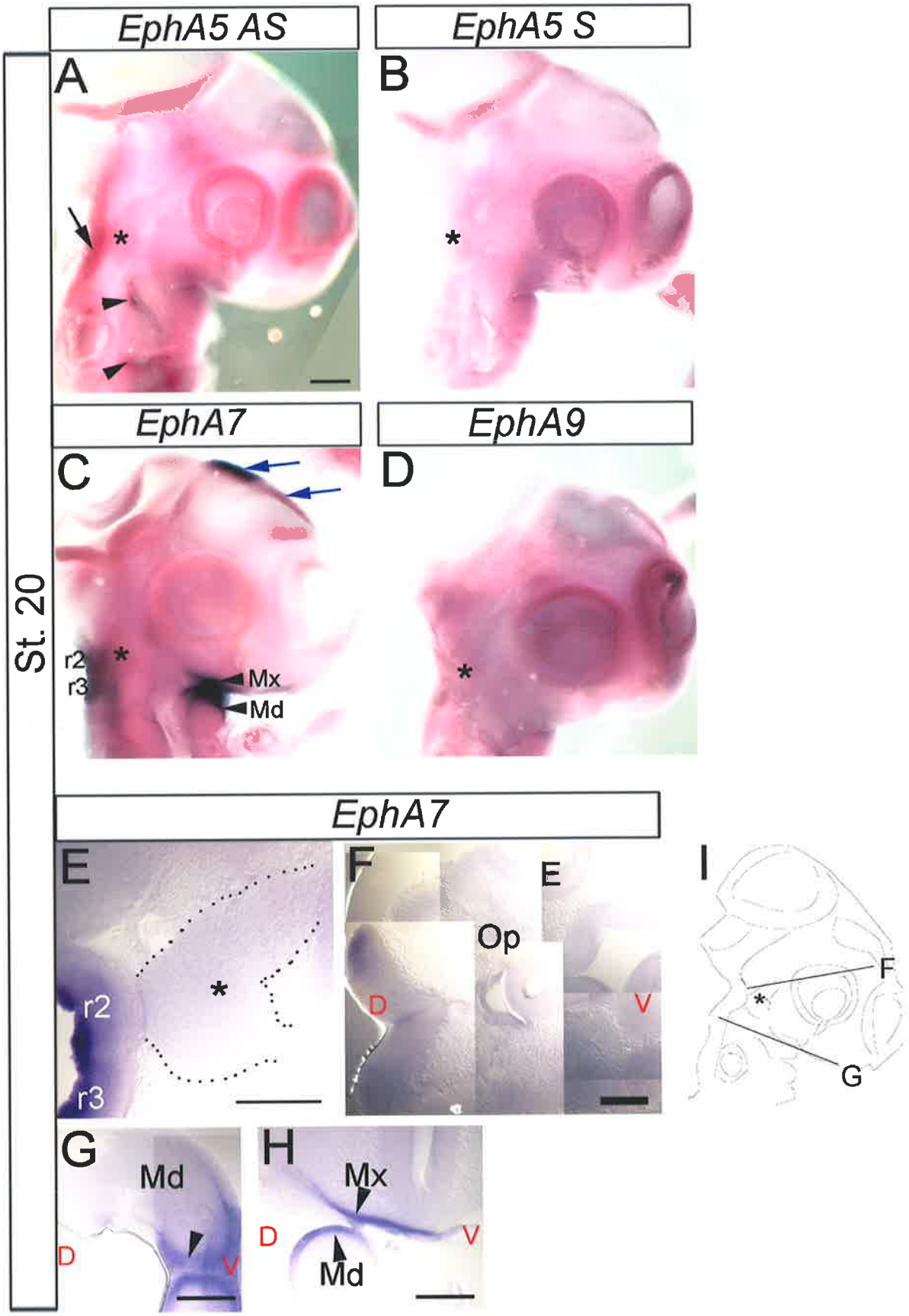
EphA5 AS
EphA5 S
A
B
St. 20
EphA7
EphA9
C
D
r2
r3
Mx
Md
EphA7
E
F
I
r2
r3
Op
D
V
F
G
G
H
Md
Mx
D
V
Md

In addition to *EphA5* and *EphA7*, analysis of *EphA9 in situ* hybridisation failed to reveal any staining in trigeminal ganglion peripheral targets or in the ganglion at stage 20 (asterisk; Figure 3.9D).

3.2.3 ephrin-A expression in the trigeminal ganglion peripheral target fields

Given the weak expression of EphA(s) in the ophthalmic lobe of the trigeminal ganglion as revealed with ephrin-A5-Fc (Figure 3.4A-B) and the observed EphA3 expression in the ganglion (asterisk; Figure 3.5G-G', 3.6B-B', 3.6E-E'), it was necessary to identify putative cognate interacting ephrin-A ligands in the target fields. The existence of ephrin-As in the trigeminal ganglion target fields was verified when whole-mount embryos were stained with EphA3- and A4-Fc proteins (Figure 3.3D-G). Three chick ephrin-A ligands are have been identified to date (ephrin-A2, -A5 and -A6) (Menzel *et al.,* 2001). Nevertheless, this study concentrated on the expression of ephrin-A2 and ephrin-A5 for the following reasons. Firstly, ephrin-A2 and -A5 are most closely related to each other than to ephrin-A6, and both ephrin-A2 and -A5 likely have overlapping and/ or redundant roles *in vivo* (Feldheim *et al.,* 1998; Menzel *et al.,* 2001). Secondly, ephrin-A5 was found to have a much higher affinity for EphA3 compared to ephrin-A6 (Menzel *et al.,* 2001), therefore the investigation of ephrin-A5 expression was justified given trigeminal ganglion EphA3 expression (Figure 3.5F-F', 3.6D-E). Thirdly, the highest affinity receptor for ephrin-A6, EphA4 (Menzel *et al.,* 2001), was not localised to the trigeminal ganglion in this study (asterisk; Figure 3.7C, 3.7E', 3.8B'), suggesting an unlikely role for this ligand as a putative guidance cue in the target fields to growing trigeminal ganglion axons. Therefore, the expression of *ephrin-A2* and *ephrin-A5* mRNA was analysed with anti-sense RNA probes directed against each ligand respectively (Figures 3.9-3.10). The negative sense controls for both probes did not reveal any specific staining (Figure 3.9N and 3.10M).

3.2.3.1 *ephrin-A2* is expressed in the maxillary and mandibular processes

Unlike EphA3 and EphA4, which were localised to the ophthalmic process at stages 13-15 (Figures 3.5, 3.7), *ephrin-A2* transcript was expressed in a complementary manner, being restricted to the mesenchyme that contributes to the formation of the mandibular and maxillary processes (Figures 3.10A-B). Sections of stained embryos revealed that in the mandibular process at stage 13 (arrow; Figure 3.10E) and 15 (Figure 3.10G), *ephrin-A2*

appeared to be uniformly distributed. This high *ephrin-A2* levels at stages 13 and 15, was maintained in the maxillary and mandibular processes at stage 20 (Figure 3.10C, 3.10K-L).

Sectioning *ephrin-A2 in situ* hybridised embryos clearly revealed that the ophthalmic process was not positive for *ephrin-A2* at stages 13 (Figure 3.10D) and 15 (arrowhead; Figure 3.10F). In comparison, *ephrin-A2* expression was observed in the eye at stage 15 (red arrowheads; Figure 3.10F). Further on during development, *ephrin-A2* transcripts continued to be absent from the ophthalmic process (Figure 3.10C, 3.10J), during the period when ophthalmic axons pathfinding through this region (arrowheads; Figure 3.10J').

Figure 3. 10 *ephrin-A2* mRNA is expressed in the first branchial arch at stages 13-20.

(A-C) Whole-mount *ephrin-A2* in situ hybridised embryos. (A) Dorsal, (A'-C) lateral view of the same embryo. (A) Arrowheads, mesenchymal staining adjacent rhombomeres 2 (r2) and 4 (r4). (A'-C) Black arrowheads: maxillary (Mx) and mandibular (Md) process expression. (B) White arrowhead: staining in the eye (E). Mb, midbrain.
(D-G) Cryostat sections highlight lack of *ephrin-A2* expression in the ophthalmic (Op) process (D, F) and the expression of the ligand in the Md process (E, G). (E) Arrow, Md staining. (F) Black arrowhead: Op process. Red arrowheads: staining in the eye.
(H-I) Schematics showing approximate plane of sections in (D-G).
(J-L) Stage 20 vibratome sections showing lack of *ephrin-A2* expression in the Op process (J-J') and expression of the ligand in the Mx (K-K') and Md (L-L') processes. (J-L) Bright-field images. (J'-L') Inverted images from (J-L), with any *ephrin-A2* staining appearing as white. These sections are merged with anti-neurofilament staining (NFM) in red. (J') Arrowhead: ophthalmic axons.
(M) Schematic showing approximate plane of sections in (J-L).
(N) Whole-mount embryo probed with *ephrin-A2* sense (S) riboprobes demonstrating non-specific staining.
Orientation shown in red lettering in (D) applies to images (D-G), and (J-L). D, dorsal; V, ventral.
Scale: 200 μm (A-C), (J-L); 100 μm (D-G); 250 μm (N).

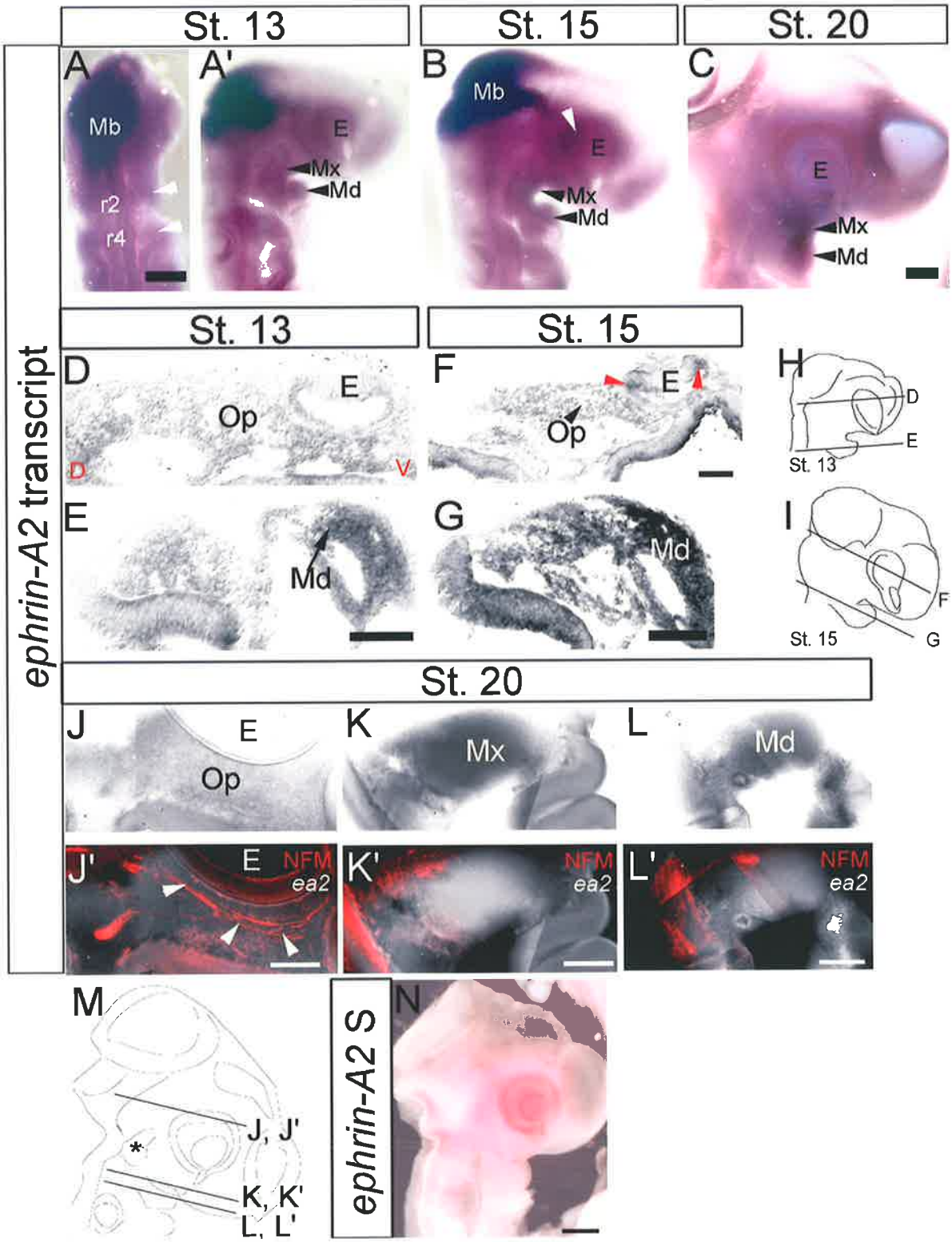
St. 13
St. 15
St. 20
ephrin-A2 transcript
A
A'
B
C
Mb
r2
r4
E
Mx
Md
D
Op
V
F
H
I
St. 13
St. 15
G
J
K
L
J'
K'
L'
NFM
ea2
M
J, J'
K, K'
L, L'
ephrin-A2 S
N

Collectively, the lack of *ephrin-A2* transcript localisation in the ophthalmic process, and yet expression in the first branchial arch components suggested that ephrin-A2 may function as a putative guidance cue to only a subset of trigeminal ganglion axons. Furthermore, the *ephrin-A2 in situ* hybridisation results verified the pattern of localisation observed for ephrin-A proteins when EphA3- and A4-Fc were utilised (Figure 3.3D-G). Notably in the maxillary process at stage 20 however, there was a disparity between the Fc-fusion (Figure 3.3F-G) and *ephrin-A2* transcript results (Figure 3.10C). While the Fc-fusion analysis revealed lack of ephrin-A(s) ligand localisation to the maxillary process, the *ephrin-A2* mRNA results suggested otherwise. This inconsistency may suggest that ephrin-As in the maxillary process are possibly involved in *cis/ trans-* interactions with endogenous EphA receptors expressed in that region (Figures 3.5C, 3.7A, 3.7C, 3.7D, 3.7E, 3.8B). Consistent with this notion, EphA3-Fc binding to the presumptive maxillary process at stages 13 and 15 (Figure 3.3D-E) revealed the expression of ephrin-As, and this coincided with the lack of EphA3/A4 localisation to this region at these stages (Figure 3.5A-B, 3.7F-F"). Alternatively, although highly unlikely, lack of EphA3- and A4-Fc fusion binding to the maxillary process may suggest disparities between ephrin-A2 mRNA and protein localisation in this tissue.

3.2.3.2 ephrin-A5 is expressed in the maxillary and mandibular processes and in the trigeminal ganglion

A comparison of *ephrin-A2* and *ephrin-A5* mRNA localisation in whole-mount embryos demonstrated similar patterns of expression for the two ligands in the trigeminal ganglion target fields from stage 13 to 20 (compare Figure 3.10A-C with Figure 3.11A-C). *Ephrin-A5* mRNA was observed in the developing first branchial arch components (black arrowheads; Figure 3.11A-C) and this was reminiscent of *ephrin-A2* expression pattern. Sectioning of stage 13 and 15 embryos verified *ephrin-A5* mRNA localisation to the mandibular process mesenchyme (Figures 3.11E, 3.11G). To examine if neural crest derived mesenchyme was ephrin-A5 positive, stained sections for *ephrin-A5* mRNA were immunostained with antibodies against the neural crest marker HNK-1, and this was found to be the case (Figure 3.11E-E'). Anti-ephrin-A5 staining further substantiated the ephrin-A5 localisation to the mandibular process mesenchyme (Figure 3.12B). Coherent with the pattern of expression for ephrin-A5 at stages 13 and 15, close inspection of stage 20 sectioned embryos demonstrated ephrin-A5 transcript and protein localisation to maxillary and mandibular process mesenchyme (Figure 3.11C, 3.11K, 3.12D-E). Conspicuously, the

distribution of *ephrin-A5* showed intense mesenchymal expression towards the middle of the mandibular process in sections from *in situ* hybridised embryos (arrowhead; Figure 3.11K), and this pattern was recapitulated using an ephrin-A5 antibody to detect protein (dotted outline and arrow: Figure 3.12E'). As noted with *ephrin-A2*, there was no ephrin-A5 mRNA or protein expression in the ophthalmic process during stages 13, 15, or 20 (arrowheads; Figure 3.11D, 3.11F, 3.11J, 3.12A). Collectively the data demonstrated that mesenchymal expression of ephrin-A5 in the maxillary and mandibular processes from stages 13-20 was consistent with a role for this ligand during trigeminal ganglion axon guidance.

Figure 3. 11 *ephrin-A5* transcripts are restricted to the first branchial arch at stages 13-20.

(A-C) Whole-mount *ephrin-A5* in situ hybridised embryos. (A) Dorsal, (A'-C) lateral view. (A) Arrowheads: mesenchymal staining adjacent rhombomeres 2 (r2) and 4 (r4). (A'-C) White arrowhead: ephrin-A5 positive condensing geniculate ganglion. Asterisk: ephrin-A5 positive trigeminal ganglion. Black arrowheads: staining in the maxillary (Mx) and mandibular (Md) processes. Mb, midbrain; E, eye. (A'-B) Red arrowhead: ephrin-A5 localisation to the frontonasal process.
(D-G) Cryostat sections from stage 13 and 15 embryos showing lack of expression in the ophthalmic (Op) process mesenchyme (black arrowhead; D, F), and expression of ephrin-A5 in the Md process (E, G). (E, G) White asterisk and/or outline: *ephrin-A5* positive trigeminal ganglion. (E-E') The mesenchyme stained for *ephrin-A5* is also HNK-1 positive. Red arrowhead: epithelium. Red outline: delineates mesenchyme from epithelium. (F) Red arrowhead: frontonasal staining.
(H-I) Schematics showing approximate plane of sections in (D-G).
(J-K) Stage 20 vibratome sections showing lack of *ephrin-A5* expression in the Op process (J-J') and expression of the ligand in the Mx and Md (K-K') processes. (J, K) Bright-field images. (J', K') Inverted images from (J, K), with any *ephrin-A5* staining appearing as white. These sections are merged with anti-neurofilament staining (NFM) in red. (J') Arrowhead, ophthalmic axons.
(K-K') Asterisk: trigeminal ganglion. White arrowhead: axons grow on *ephrin-A5*. Black arrow: diffuse transcript distribution in Md process. Arrowhead: intense transcript distribution in Md process.
(L) Schematic showing approximate plane of sections in (J-K).
(M) Whole-mount embryo demonstrating non-specific staining with *ephrin-A5* sense (S) riboprobes.
Orientation indicated in red lettering in (D) applies to images (D-G), (J-K). D, dorsal; V, ventral. Orientation in (D)
Scale: 200 μm (A-B), (C), (J, K); 100 μm (D-E), (F), (G); 200 μm (M).

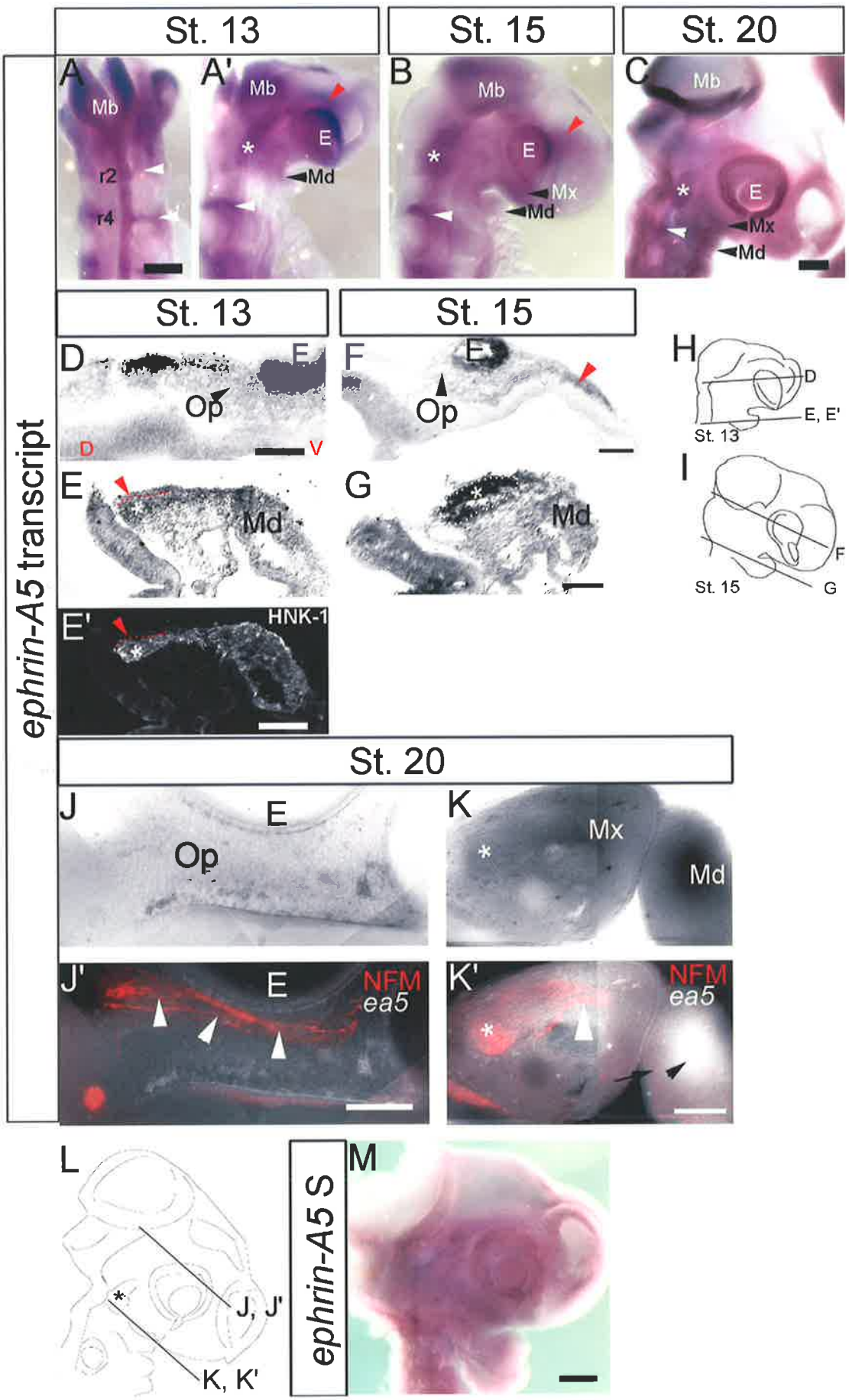
St. 13
St. 15
St. 20
ephrin-A5 transcript
A
A'
B
C
Mb
r2
r4
E
Md
Mx
St. 13
St. 15
D
F
Op
V
H
D
E, E'
St. 13
I
F
St. 15
G
E
G
E'
HNK-1
St. 20
J
K
J'
K'
NFM
ea5
L
J, J'
K, K'
ephrin-A5 S
M

Next, to clearly demonstrate that ephrin-A5 expression was consistent with a guidance role, it was necessary to understand where trigeminal ganglion axons were with respect to ephrin-A5 mesenchymal expression in the target fields. For this purpose, antibodies to the neuronal markers, neurofilament or β-tubulin, aided the visualisation of trigeminal ganglion axons. At stages 15 (asterisks; Figure 3.12A) and 20 during active axon pathfinding, ophthalmic axons were found to course through the ephrin-A5 negative ophthalmic process (arrowheads; Figure 3.11J-J', 3.12C-C'). This observation was reminiscent of what was demonstrated for *ephrin-A2* (Figure 3.10J-J'). Thus, it appeared that ophthalmic lobe axons were avoiding ephrin-A expressing mesenchyme. In contrast, at the level of the maxillary (arrowhead; Figure 3.11K' and 3.12D') and mandibular processes (arrowhead: Figure 3.12E') axons of the trigeminal ganglion were found to grow on ephrin-A5 positive mesenchyme.

In addition to exhibiting ephrin-A5 expression in two of the three target fields, the ligand also was found to localise to the developing trigeminal ganglion (asterisk; Figure 3.11A-B) and condensing sensory geniculate ganglion (white arrowheads; Figure 3.11A'-C). This localisation to the trigeminal ganglion was also confirmed when sectioned embryos were immunostained for ephrin-A5 protein and the neuronal marker β-tubulin (asterisk; Figure 3.12D'). Evidence to suggest that the ganglionic neural crest component was positive for ephrin-A5 came from staining for neural crest marker HNK-1, since the pattern of expression for ephrin-A5 was similar to what was observed with anti-HNK-1 staining (asterisk; Figure 3.11E-E'). Furthermore, ephrin-A5 was restricted to the epithelium at the level of the mandibular process, which possibly corresponded with the location of the trigeminal maxillomandibular placode, at stage 13 (red arrow; Figure 3.11E) and 15 (arrowhead; Figure 3.12B). Therefore, the evidence suggested that ephrin-A5 localised to the neural crest and placode components of the trigeminal ganglion. In contrast, no such staining of the sensory ganglia was apparent in *ephrin-A2 in situ* hybridised embryos.

Other regions that were ephrin-A5 positive were the frontonasal process (red arrowhead; Figure 3.11A-B), the developing eye, and the midbrain (Figure 3.11A'-B). A comparison of *ephrin-A2* and *ephrin-A5* mRNA expression revealed that the midbrain was strongly positive for ephrin-A2 (compare Figure 3.10A-B with Figure 3.11A-B). Furthermore, reminiscent of *ephrin-A2* expression (Figure 3.10A), *ephrin-A5* transcript expression was

observed in the mesenchyme adjacent to rhombomeres 2 and 4 at stage 13 when whole-mount embryos were viewed dorsally (white arrowheads; Figure 3.11A).

Collectively, *ephrin-A2* (Figure 3.10) and ephrin-A5 (Figures 3.11-3.12) showed similar expression patterns in the target fields of the trigeminal ganglion. This suggested that both ligands might have overlapping and redundant functions during trigeminal ganglion axon guidance. The results observed for ephrin-A5 were once again consistent with the results observed with EphA3- and A4-Fc proteins (Figure 3.3D-G). As previously suggested for *ephrin-A2*, the discrepancy exhibited between Fc-fusion protein and ephrin-A5 results in the maxillary process, may be due to cognate partner interactions between *ephrin-A5* expressed in this process (Figure 3.11K, 3.12D) and EphA receptors in that region (Figures 3.5C, 3.7A, 3.7C, 3.7D, 3.7E, 3.8B). Consistent with this notion, EphA3-Fc binding to the presumptive maxillary process at stages 13 and 15 (Figure 3.3D-E) revealed the expression of ephrin-As, and this coincided with the lack of EphA3/A4 localisation to this region at these stages (Figure 3.5A-B, 3.7F-F"). Any discrepancy in ephrin-A5 mRNA and protein tissue localisation is unlikely to account for the lack of EphA3- and A4-Fc-fusion binding to the maxillary process, since ephrin-A5 mRNA and protein were demonstrated to be expressed in the maxillary process.

Figure 3. 12 ephrin-A5 protein localises to the first branchial arch at stages 15 and 20.

(A-E) Transverse vibratome sections with anti-ephrin-A5 (green; A, B, C-D), and anti-β-tubulin (TuJ1) (red; A, B, C'-D') antibodies at stage 15 (A-B) and 20 (C-E). All images are confocal z-stacks. (A, B) Merged images demonstrating pattern of ephrin-A5 and β-tubulin expression. (C'-E') Merged images demonstrating ephrin-A5 (C-E) and -β-tubulin localisation. (A-B); (C-E) Brightness-contrast for adjusted identically.
(A, C) There is no ephrin-A5 expression at the level of the ophthalmic process (op). (A) Arrowheads: ophthalmic process mesenchyme. Asterisks: ephrin-A5 positive trigeminal ganglion axons (red) invading the ophthalmic process. Mb: midbrain. (C') Arrowheads: ophthalmic axons. E: eye.
(B, E) Ephrin-A5 is localised to the mandibular process (Md). (B) Dotted outline and arrowhead: epithelial ephrin-A5 staining. (E') Arrowhead: ephrin-A5 positive axons growing on ephrin-A5 mesenchyme. Arrow: intense ephrin-A5 staining in the Md process mesenchyme. Dotted outline delineates high ephrin-A5 expression from low ephrin-A5 expression.
(D-D') Ephrin-A5 positive trigeminal ganglion axons grow on ephrin-A5 positive maxillary process mesenchyme (Mx) (arrowhead). Asterisk: trigeminal ganglion.
(F) Schematics showing approximate plane of sections for (A-E).
Orientation indicated in red lettering in (A) and applies to all images. D, dorsal: V, ventral.
Scale: 100 μm.

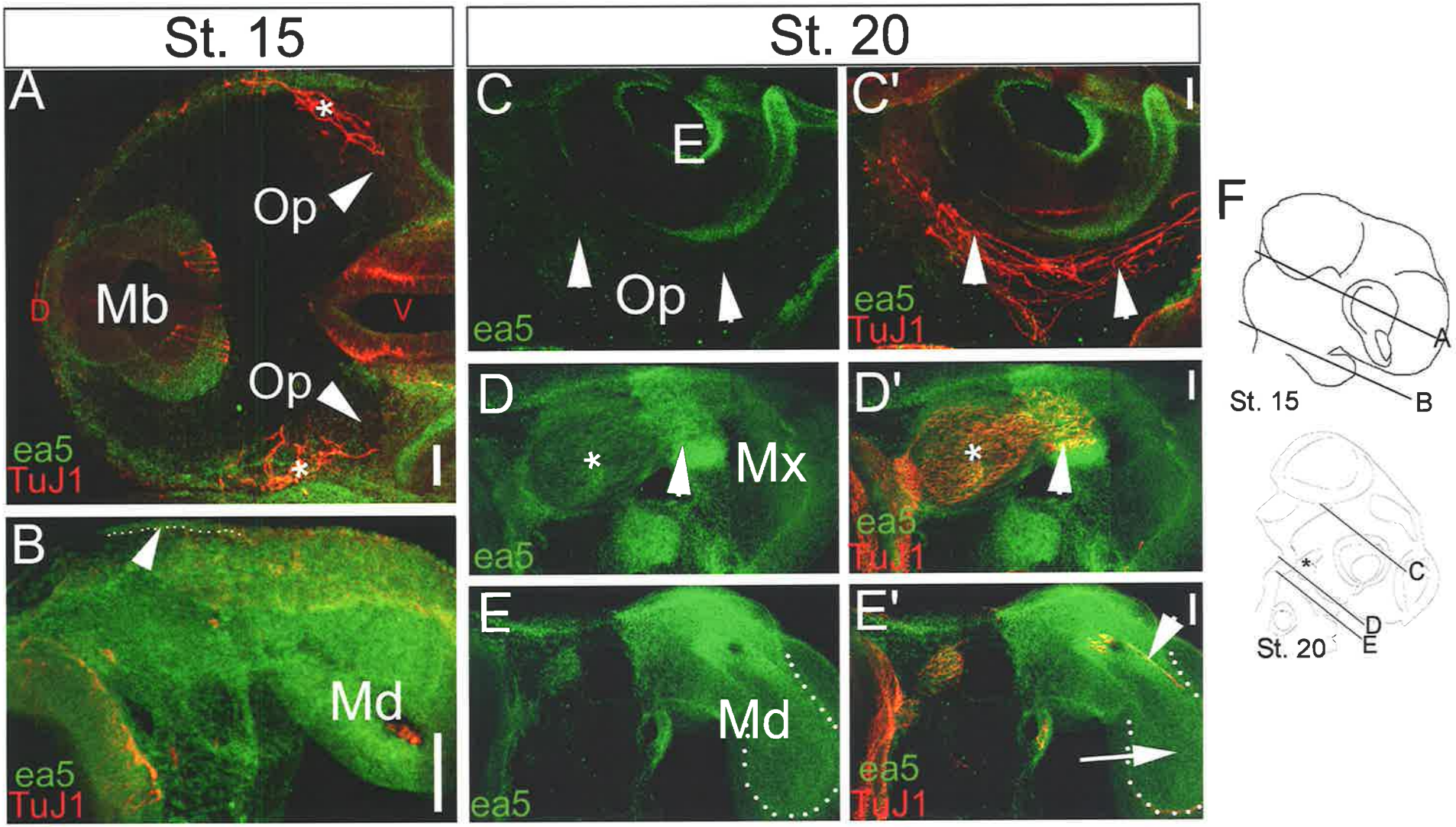
St. 15
St. 20
A
Op
Mb
D
V
Op
ea5
TuJ1
I
B
Md
ea5
TuJ1
C
E
Op
ea5
C'
I
ea5
TuJ1
D
Mx
ea5
D'
I
ea5
TuJ1
E
Md
ea5
E'
I
ea5
TuJ1
F
A
St. 15
B
C
D
E
St. 20

3.3 Summary and discussion

The results in this chapter illustrate that EphA3, EphA4, ephrin-A2 and ephrin-A5 transcripts and/or protein are expressed in a manner suggestive of a role for these as axon guidance cues to growing trigeminal ganglion axons. EphA receptors are expressed early at stages 13 and 15 in the ophthalmic process when ophthalmic axons are pathfinding (Figure 3.13). Strikingly, ephrin-A2 and -A5 were absent at stages 13, 15 and 20 in the ophthalmic process. Furthermore, ephrin-A ligands showed complementary pattern of expression to EphA receptors at stages 13 and 15, with these two ligands found to be localised to the maxillary and mandibular processes. These receptors and ligands are expressed during stages of trigeminal ganglion axon guidance in the mesenchyme of the trigeminal ganglion target fields.

3.3.1 Complementary expression of EphA3/A4 and ephrin-A2/A5 at stages 13 and 15 when trigeminal axons are pathfinding

Early during trigeminal ganglion development and pathfinding at stages 13 and 15, EphA3 and EphA4 receptors are expressed in the ophthalmic process (Figure 3.13). The roles of Ephs and ephrins as repulsive boundary/ axon guidance cues have well been documented during development (Birgbauer *et al.,* 2001; Donoghue *et al.,* 1996; Drescher *et al.,* 1995; Frisen *et al.,* 1998; Mellitzer *et al.,* 1999; Wang and Anderson, 1997). However, the observation that trigeminal ganglion axons grow on EphA3 and EphA4 mesenchyme, particularly in the ophthalmic process during outgrowth strongly suggest that these receptors do not act as repulsive cues to axons. This may also explain why EphA3/A4 are also expressed in the maxillary and mandibular processes at stage 20, when axons from the maxillomandibular lobe are extending into the target fields (Figure 3.13). Additionally, the similar pattern of EphA3 and A4 expression suggested that these two receptors might act in a redundant manner during trigeminal ganglion axon guidance.

The expression of EphA3 and EphA4 was complementary to the expression pattern of ephrin-A2 and -A5 mRNA and/or protein in the trigeminal ganglion target fields (Figure 3.13). Both ephrin-A ligands are expressed in the developing first branchial arch, and appear to be absent from the ophthalmic process. The complementary expression of EphAs and ephrin-As observed with Fc-fusion proteins is in agreement with these findings. Such

compartmentalised yet complementary expression of EphAs and ephrin-As, particularly during stages 13 and 15 may consequently influence trigeminal ganglion lobe specific axon guidance.

Thus the absence of EphA in the first branchial arch, or the absence of ephrin-A in the ophthalmic process was not due to a "masking effect" (Figure 3.1B). It is well documented that if endogenous receptors and ligands are interacting with their endogenous cognate binding partner(s), Fc-chimeric protein binding to their targets are interrupted (Cutforth *et al.,* 2003; Flenniken *et al.,* 1996; Hornberger *et al.,* 1999; Koblar *et al.,* 2000; Yin *et al.,* 2004).

3.3.2 Similar EphA/ ephrin-A expression patterns are observed for mouse and chick

The results from this chapter for the chick embryo are consistent with previous expression data obtained for Eph/ephrin-A during mouse embryogenesis (Flenniken *et al.,* 1996; Gale *et al.,* 1996). Therefore, this would suggest that the chick embryo was a suitable model system to study trigeminal ganglion axon guidance. During early mouse embryogenesis, EphA receptors are absent from the first branchial arch mesenchyme (Flenniken *et al.,* 1996), and this is consistent with EphA3 and EphA4 results at stages 13 and 15 in the chick embryo. Intriguingly, compared to chick embryonic stages 13 and 15, when *ephrin-A5* was localised to the mesenchyme and epithelium at the level of the first branchial arch (red arrow; Figure 3.11E), mouse *ephrin-A5* was only observed in the epithelium during equivalent stages of embryogenesis (Flenniken *et al.,* 1996). In contrast to the avian lineage, which has only three known members belonging to the ephrin-A subclass (Cheng *et al.,* 1995; Drescher *et al.,* 1995; Menzel *et al.,* 2001), five ephrin-A ligands have been identified in the mouse (Flenniken *et al.,* 1996; Gale *et al.,* 1996). Therefore, it remains to be elucidated whether another member of the ephrin-A family is expressed in the first branchial arch mesenchyme during murine embryogenesis (Flenniken *et al.,* 1996). Unlike the mouse developmental pattern, chick ephrin-A2 and -A5 were previously shown to localise to the branchial arch mesenchyme during early stages of chick development (Baker and Antin, 2003), and this was consistent with the findings from this study. *Ephrin-A5* positive regions also were HNK-1 positive, suggesting that cranial neural crest streams express *ephrin-A5*, and this has not been documented before. Interestingly, in the chick

embryo, condensing cranial sensory ganglia are also positive for *ephrin-A5*; this expression is similar to that observed in the developing trunk in the chick embryo. In the trunk, migrating neural crest and neural crest derived dorsal root ganglia express ephrin-A5 (McLennan and Krull, 2002); Edwina Ashby, personal communication).

3.3.3 Conclusion

To conclude, EphA3, EphA4, ephrin-A2 and ephrin-A5 transcripts and/or proteins are expressed in the target fields of the trigeminal ganglion, and the expressions of these molecules correspond with period during which trigeminal ganglion peripheral axons are pathfinding. Further to this, ephrin-A5 and EphA3 *in situ* hybridisation and immunofluorescent antibody staining alludes to the expression of EphA3 and ephrin-A5 in the trigeminal ganglion as cognate binding partners to these candidate guidance cues being expressed in the target fields.

Figure 3. 13 Summary schematic of EphA and ephrin-A expression in the trigeminal ganglion target fields at stage 13 and 20.

Various tones of colour represent different expression levels; for each schematic the light colour tones represent weak expression in comparison to strong expression (dark colour tones). Asterisk and dotted outline: location of future trigeminal ganglion (stage 13) or position of the maturing trigeminal ganglion (stage 20).

At stage 13: EphA3 and EphA4 appear to be localised to the ophthalmic (Op) process only. Ephrin-A2 and ephrin-A5 are expressed in a complementary manner to both EphA receptors, in the mesenchyme contributing to the maxillary (Mx) and mandibular (Md) processes. This expression pattern is also observed at stage 15 (not shown).
At stage 20: EphA3 and EphA4 expression domains have expanded from the ophthalmic process to include mesenchyme of the Mx and Md processes. However, ephrin-A2 and ephrin-A5 are still restricted to the Mx and Md processes as seen at stage 13.
Note: EphA3 and ephrin-A5 are expressed in the trigeminal ganglion at stage 20. Ephrin-A5 expression in the developing ganglion is also observed at stage 13.

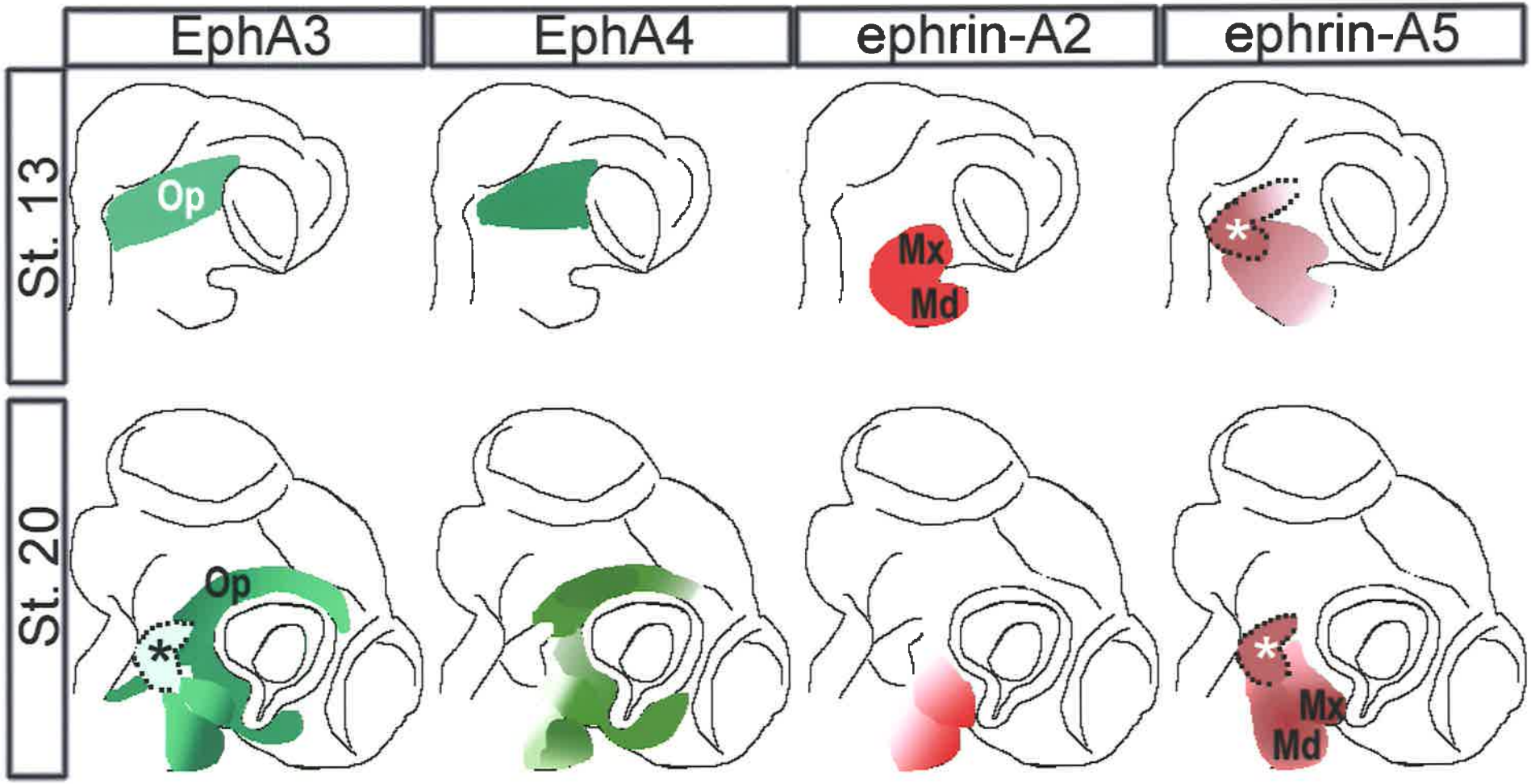
EphA3
EphA4
ephrin-A2
ephrin-A5
St. 13
St. 20
Op
Op
Mx
Md
Mx
Md
*
*
*

Chapter 4: EphA and ephrin-A expression in the trigeminal ganglion

"I never came upon any of my discoveries through the process of rational thinking".
--Albert Einstein

Chapter 4: EphA and ephrin-A expression analysis in the trigeminal ganglion

4.1 Introduction

Chapter 3 described the expression of EphA3, EphA4, ephrin-A2 and ephrin-A5 in the peripheral target fields of the trigeminal ganglion. Thus, did the trigeminal ganglion express cognate EphA(s) and ephrin-A(s) that would interact with these candidate guidance cues? Analysis of EphA3-Fc and ephrin-A5-Fc staining of the trigeminal ganglion revealed the presence of putative cognate guidance cue receptors. EphA3-Fc binding to the ganglion exhibited differential expression of ephrin-A(s) in the two lobes, while ephrin-A5-Fc binding demonstrated that receptor(s) localised to the ophthalmic lobe (Figure 3.3). Consequently, this led to a detailed interrogation of EphAs and ephrin-As that were expressed in the ganglion itself during trigeminal ganglion axon guidance. As previously described, stages 13, 15 and 20 of chick embryo development was appropriate to study trigeminal ganglion axon guidance because initial axon outgrowth (stage 13-13+; somite stage 19-21), primitive ganglion formation (stage 15), and axon pathfinding (stages 15-20) occurred at these stages (Figure 3.2) (Moody *et al.,* 1989).

Given the trigeminal ganglion is composed of a heterogeneous population of cells, it was necessary to determine which cell type expressed EphAs and/or ephrin-As. As has been demonstrated before, the ganglion has a dual embryonic origin. The two cell types that condense to form the trigeminal ganglion are the cranial neural crest and epidermal neurogenic placode cells (D'Amico-Martel and Noden, 1980; Hamburger, 1961). The neural crest derived component can be readily identified with an antibody against the cell marker HNK-1, a carbohydrate epitope localised to avian neural crest cells (Bronner-Fraser, 1986). Previously, Pax3 was shown to be a reliable marker for the trigeminal ophthalmic placode, and ophthalmic neurons (Baker and Bronner-Fraser, 2000; Baker *et al.,* 1999; Stark *et al.,* 1997). Therefore, Pax3 was utilized to distinguish between the two trigeminal placodes and lobes. To elucidate whether neurons are positive for Eph/ephrin-As, antibodies to two cell markers were utilized; anti-β-tubulin (TuJ1), which labels neuroblasts/ neurons (Memberg and Hall, 1995), or anti-neurofilament (NFM), a marker of neurons (Lee *et al.,* 1987).

4.2 Results

4.2.1 EphA4, A5, A7, A9 and ephrin-A2 are not expressed in the trigeminal ganglion

The previous chapter characterised the expression of EphA4, *EphA5, EphA7* and *EphA9* and showed that these receptors were not expressed in the trigeminal ganglion.

Further to this, detailed examination of *ephrin-A2* transcript revealed that this ligand did not co-localise with molecular markers of the ganglion at stages 13, 15 and 20 (Figure 4.1). Anti-HNK-1, -Pax3 and -TuJ1/ NFM fluorescence at no stage showed co-localisation with *ephrin-A2* transcript in the trigeminal ganglion anlagen or the maturing ganglion. Therefore, it appeared that *ephrin-A2* was not expressed in the trigeminal ganglion.

EphA3 and ephrin-A5 mRNA and protein showed localisation to the developing trigeminal ganglion (Chapter 3). Therefore, the expression of this receptor and ligand were further characterised using trigeminal ganglion markers.

4.2.2 EphA3 is differentially expressed in the trigeminal ganglion

4.2.2.1 EphA3 localises to the ophthalmic placode and trigeminal ganglion neurons at stages 13 and 15

The trigeminal ophthalmic placode is the first to generate neurons (Begbie *et al.,* 2002). Furthermore, neurons that invaginate from the ophthalmic placode to form the trigeminal ophthalmic lobe are likely to start axon pathfinding immediately following invagination (Begbie *et al.,* 2002; Covell and Noden, 1989; Moody *et al.,* 1989a). Hence, EphA3 protein localisation to the ophthalmic placode and neurons at stages 13 and 15 was examined.

During axon pathfinding at stage 13 (Moody *et al.,* 1989a), EphA3 was expressed in the ophthalmic placode, and by invaginating/ invaginated Pax3 positive cells (Figure 4.2A-C). Since Pax3 marked the ophthalmic placode (Baker *et al.,* 1999; Stark *et al.,* 1997), the caudal limit of Pax3 expression was used to delineate ophthalmic from maxillomandibular placodes. At the level of the Pax3 negative maxillomandibular placode, low levels of

EphA3 protein was localised to the epithelium (arrowheads; Figure 4.2D') in comparison to the ophthalmic placode. Some low EphA3 expressing cells were also detected in the mesenchyme, and presumably corresponded to invaginated cells from the maxillomandibular lobe (arrow; Figure 4.2D'). Since EphA3 receptor expression was localised to the ophthalmic placode, it was of interest to determine if EphA3 also co-localised with neuronal markers. As expected, neurons at the level of the ophthalmic lobe also showed expression for EphA3 at stage 13 (Figure 4.2E-F). Intriguingly, TuJ1 positive cells in the ophthalmic placode were positive for EphA3 at stage 13 (arrows: Figure 4.2F-F"), implying that differentiating neurons in the placode express EphA3 prior to invagination.

Figure 4. 1 *ephrin-A2* is not expressed in the trigeminal ganglion at stages 13, 15 and 20.

(A-B') The neural crest component (HNK-1 positive; A', B') of the trigeminal ganglion (asterisk) is negative for *ephrin-A2* (A, B) at stage 13 (A-A') and stage 15 (B-B'). (A, B) Bright field cryostat sections images. (A) Dotted outline delineates mesenchyme from epithelium. Arrowhead, the epithelium is *ephrin-A2* negative.
(C-C") The trigeminal ophthalmic placode marker, Pax3 and neuronal marker β-tubulin (TuJ1) do not co-localise with *ephrin-A2* at stage 13. (C) *ephrin-A2* bright field image, (C') Pax3/ TuJ1 positive, (C") merged image. (C-C") Blue arrow, Pax3 positive placode. Asterisk, Pax3 and/ or TuJ1 ophthalmic lobe of the trigeminal ganglion. Arrowhead, TuJ1 positive neuron.
(D-E) Schematic showing approximate plane of sections in (A-C).
(F-F') Stage 20 section from *ephrin-A2* in situ hybridised embryo. Bright field sagittal image (F), merged with anti-neurofilament (NFM) staining (red, F'). (F') Inverted image of (F), such that any *ephrin-A2* staining is in white. (F) Dotted outline highlights the trigeminal ganglion (TG). (F-F') Arrowhead, maxillary (Mx) process staining. E, eye.
Orientation indicated in red lettering in (A) and applies to images (A-C). D, dorsal; V, ventral.
Scale: 100 μm (A-B); 50 μm (C); 200 μm (F).

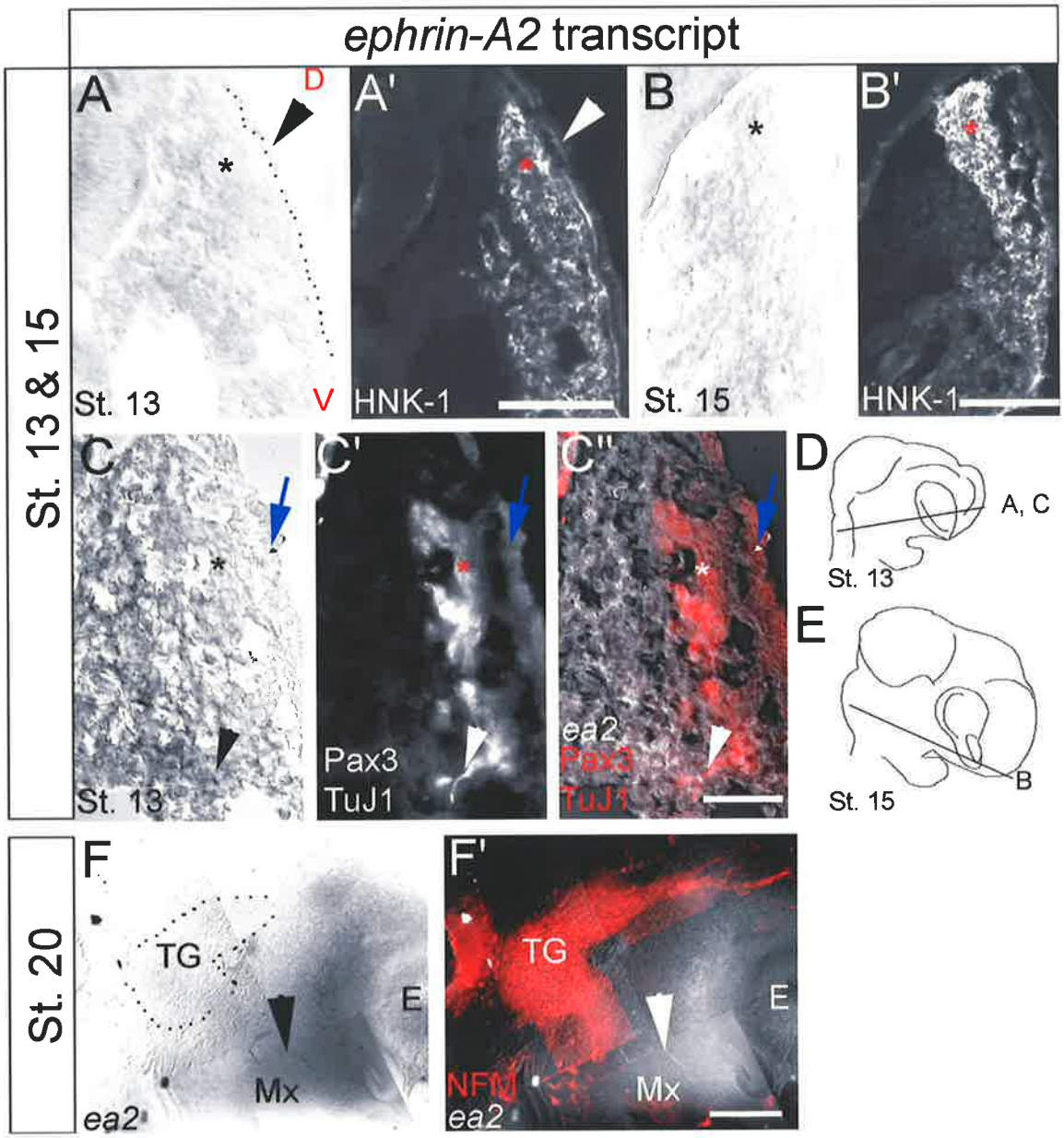
ephrin-A2 transcript
St. 13 & 15
A
D
St. 13
V
A'
HNK-1
B
St. 15
B'
HNK-1
C
St. 13
C'
Pax3
TuJ1
C''
ea2
Pax3
TuJ1
D
A, C
St. 13
E
B
St. 15
St. 20
F
TG
E
Mx
ea2
F'
TG
E
NFM
ea2
Mx

Having observed EphA3 expression in the ophthalmic placode and the forming ophthalmic lobe at stage 13, it was necessary to determine whether this expression of EphA3 continued into stage 15. During the period of gangliogenesis and axon pathfinding at stage 15 (Moody *et al.,* 1989a), Pax3 invaginated cells and placode cells expressed EphA3 (Figure 4.3A-B). As had been observed at stage 13, TuJ1 and EphA3 double positive cells were seen in the ophthalmic lobe in sagittal cryostat sections (Figure 4.3C-C' and 4.4A-B). The cell bodies of ophthalmic neurons showed high EphA3 expression (arrows) in contrast to weak EphA3 localisation to their axons (arrowheads: Figure 4.3C-C'). Furthermore, EphA3 was not exclusively expressed in ophthalmic neurons. When cryostat sections were viewed sagittally, EphA3 was present in both lobes of the ganglion (Figure 4.4). Interestingly, it appeared that high expressing EphA3 neurons were localised to the ophthalmic lobe (arrowheads; Figure 4.4A-B) compared to those neurons localised with EphA3 in the maxillomandibular lobe (arrowheads; Figure 4.4A, 4.4C).

Collectively, the results revealed that EphA3 was expressed during neurogenesis, gangliogenesis, and axon pathfinding. Therefore, EphA3 was an excellent candidate cognate partner for putative guidance cues (ephrin-As) being expressed in the target fields.

4.2.2.2 The ophthalmic lobe expresses high levels EphA3 transcript and protein at stage 20

To gain better insight into the pattern of EphA3 distribution within the maturing ganglion, sections from stage 20 embryos were immunostained for EphA3 and trigeminal ganglion markers. Inspection of high Pax3 expressing ophthalmic neurons within the trigeminal ganglion verified that EphA3 and Pax3 co-expression (Figure 4.5A, and arrowheads; Figure 4.5B). The maxillomandibular lobe placode derived neurons, which are Pax3 negative, also showed EphA3 expression (Figure 4.5A, and arrows; Figure 4.5C). However, EphA3 receptor staining of maxillomandibular neurons appeared to be weaker compared to ophthalmic lobe neurons (compare Figure 4.5B with Figure 4.5C). Analysis of the proximal neural crest region of the ganglion, which by now expresses low Pax3 levels (Baker *et al.,* 2002; Stark *et al.,* 1997), did not also exhibit high EphA3 expression (arrowheads; Figure 4.5D) compared to ganglionic neurons. The observed level of EphA3 in the proximal region of the ganglion was relatively low compared to the maxillomandibular lobe EphA3 expressing neurons (asterisk; Figure 4.5A, and compare Figure 4.5C with Figure 4.5D). Additionally, low Pax3 positive cells in the distal regions

of the maxillomandibular lobe were immunoreactive to EphA3 (arrowhead; Figure 4.5C), and these neural crest cells are believed to have a non-neural fate (Baker *et al.,* 2002). Therefore, the distal portions of the ganglion, where placode derived neurons reside, appeared to exhibit greater immunoreactivity to EphA3.

Figure 4. 2 EphA3 protein localises to the ophthalmic placode and developing trigeminal ganglion at stage 13.

(A-D) Vibratome confocal z-stack sections demonstrate EphA3 (A, A", B, C, C", D-D") and Pax3 (A'-A", B, C'-C", D-D') expression. Merged images shown in (A", B, C", D-D').
(A-A") At the level of the ophthalmic process and the ophthalmic placode. (A) Arrow: ophthalmic process mesenchyme expresses EphA3. (A-A') Arrowheads: ophthalmic placode. (A") Boxed region magnified in (B).
(B) Confocal section showing Pax3 (nuclear) positive cells that have invaginated are also positive for EphA3 (arrowheads).
(C-C") Vibratome confocal z-stack from another embryo. Pax3 positive ophthalmic placode (arrowhead) and invaginating cells (arrow) are EphA3 positive. (C', D) Dotted outline shows the Pax3 positive neural tube (nt). (C") Inset, high magnification of the region highlighted with the arrow.
(D) At the level of the maxillomandibular placode (demarcated by the absence of Pax3 in the epithelium). Arrow: Pax3 positive cells in the nt. The brightness-contrast adjusted identically as in (A, C). Arrowhead: zoomed region in (D'). (D') Brightness-contrast is not identical to (D), and has been modified to highlight the mentioned points. Arrowheads: weak EphA3 cells in the epithelium. Arrow: Pax3 negative low EphA3 expressing cells may correspond with invaginated maxillomandibular lobe neurons/ neuroblasts.
(E-F") Anti-EphA3 (E, F), and anti-β-tubulin (TuJ1) (E', F') at the level of the trigeminal ganglion ophthalmic lobe. (E", F") Merged image shows that EphA3 co-localises with TuJ1 positive cells. Both images are confocal z-stacks. (E-E") Asterisk: the ophthalmic lobe. (E") Boxed region, magnified in (F-F"). (F-F") TuJ1-EphA3 double positive cells in the ophthalmic lobe (arrowheads) and placode (arrows).
(G) Schematic showing approximate plane of sections in (A-F).
Orientation shown in red lettering in (A) and applies to all images. D, dorsal; V, ventral.
Scale: 100 μm (A, C, E, F); 50 μm (B); 25 μm (inset in C", D').

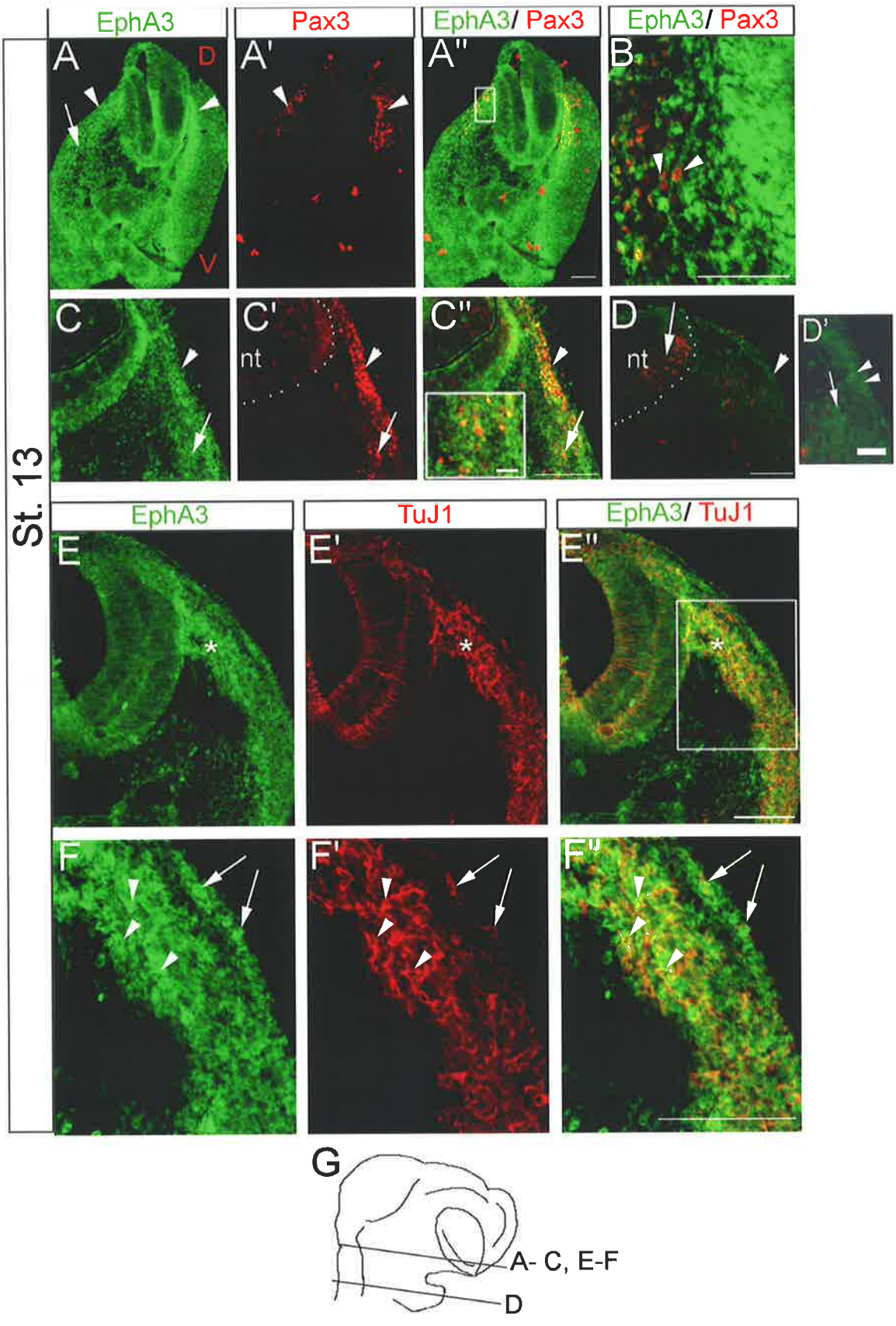
St. 13
EphA3
Pax3
EphA3/ Pax3
EphA3/ Pax3
A
D
V
A'
A''
B
C
C'
nt
C''
D
nt
D'
EphA3
TuJ1
EphA3/ TuJ1
E
E'
E''
F
F'
F''
G
A- C, E-F
D

Figure 4. 3 Ophthalmic placode and neurons express EphA3 at stage 15.

(A-A") Cryostat section demonstrates ophthalmic placode (p) and invaginated/ invaginating (arrow) Pax3 positive cells co-expressing EphA3. (B-B") Magnified view of boxed region in (A"). (A, B) Anti-EphA3, (A', B') anti-Pax3, (A", B") merged image. Both (A) and (B) are cryostat sections.

(C-C') Cryostat sagittal section showing ophthalmic neurons/ axons that are EphA3 positive. Arrows: intense cell body EphA3 expression. Arrowheads: EphA3 localisation to axons.

Orientation shown in red lettering in (A) and applies to all images. D, dorsal; V, ventral. Scale: 50 μm (A, C); 10 μm (B).

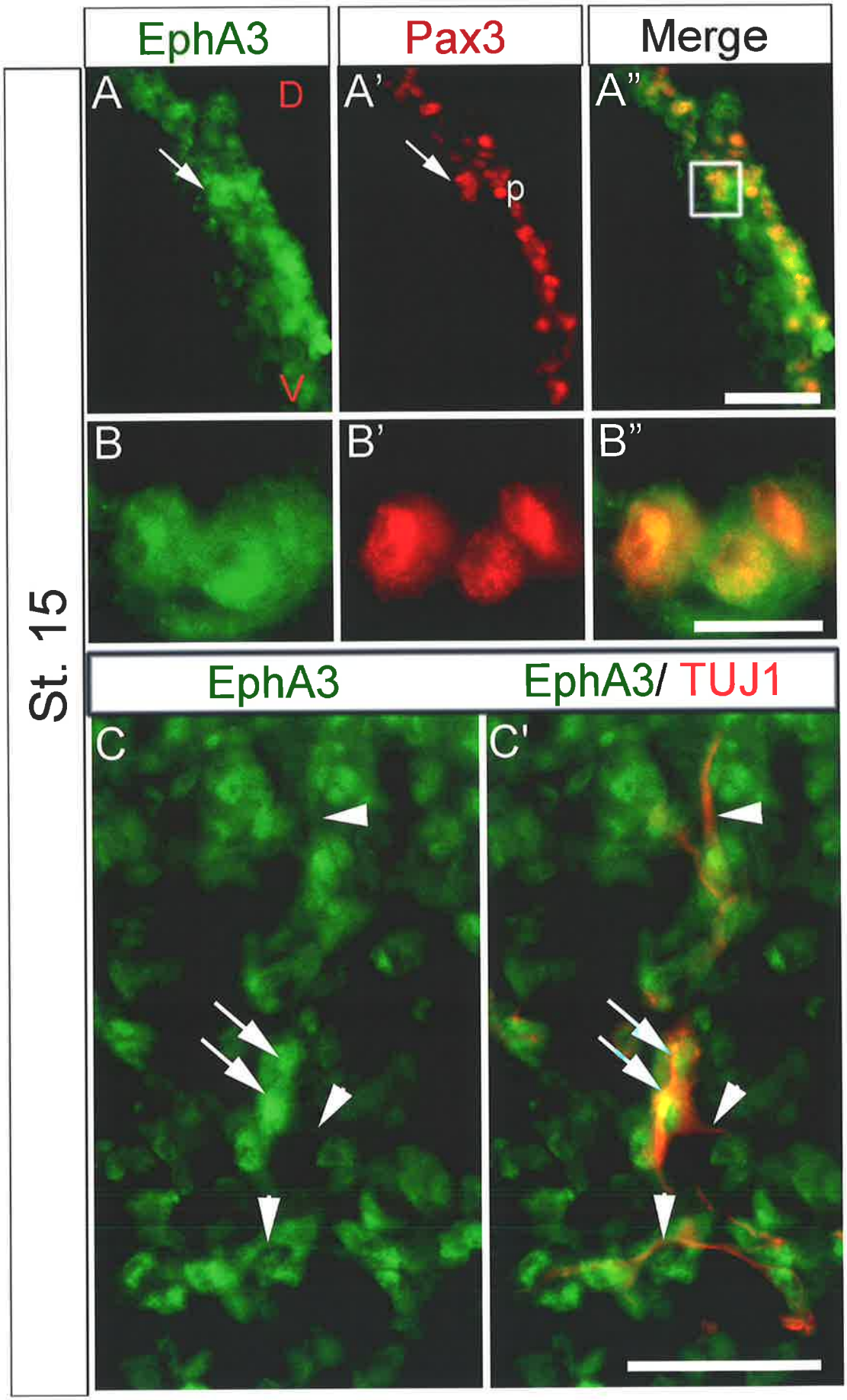
EphA3
Pax3
Merge
St. 15
A
D
V
A'
p
A''
B
B'
B''
EphA3
EphA3/ TUJ1
C
C'

Figure 4. 4 Ophthalmic and maxillomandibular neurons express EphA3 at stage 15.

(A-C) Sagittal oblique cryostat section stained with anti-EphA3 (A-C), and merged with anti-β-tubulin (TuJ1) staining (red; A, B', C'). (A) The ophthalmic (TGop) and maxillomandibular (TGmm) lobes are EphA3 and TuJ1 positive. (B) Magnified image of TGop from (A). (B-B') Arrowheads: high EphA3 TGop neurons. (C) Magnified image of TGmm from (A). (C-C') Arrowheads: low EphA3 TGmm neurons.
Orientation indicated in (A): D, dorsal; V, ventral.
Scale: 100 μm (A); 50 μm (B, C).

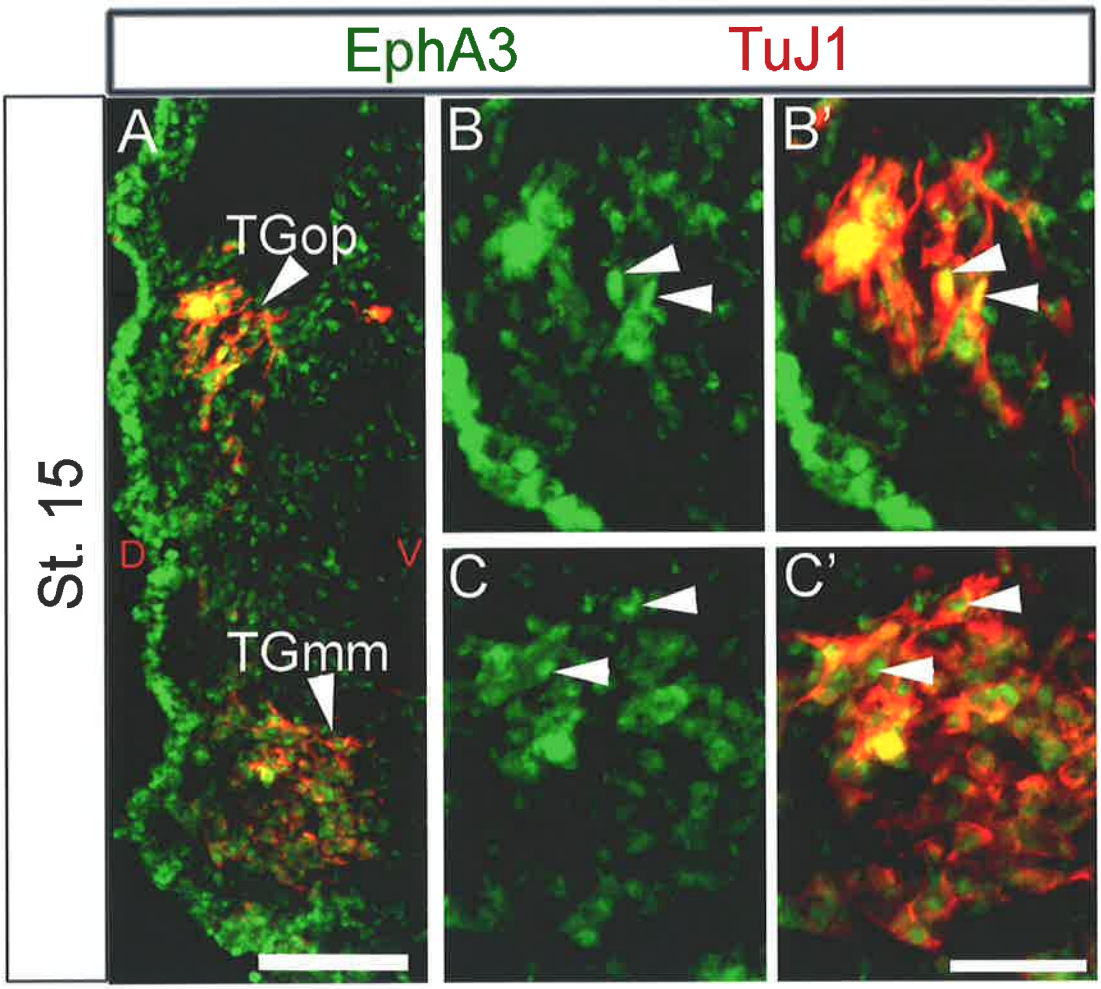
EphA3
TuJ1
St. 15
A
TGop
D
V
TGmm
B
B'
C
C'

Figure 4. 5 Differential EphA3 distribution within the stage 20 trigeminal ganglion.

(A-A") Sagittal cryostat view of the trigeminal ganglion (TG) stained with anti-EphA3 (A), and anti-Pax3 (A'). Merged image shown in (A"). The ophthalmic (op) lobe appears to express high levels of EphA3 and Pax3.

(B-D") Zoomed images of the ophthalmic (TGop) lobe (B-B"), maxillomandibular (TGmm) lobe (C-C"), and proximal neural crest region (D-D") from (A). Brightness-contrast adjusted equally. (B-D) Anti-EphA3 staining. (B'-D') Anti-Pax3 staining. (B"-D") Merged images.

(B-B") Arrowheads: high Pax3 and EphA3 positive TGop neurons.

(C-C") Arrowhead: low Pax3 and EphA3 positive neural crest cells. Arrows: Pax3 negative and EphA3 positive TGmm neurons.

(D-D") Arrowheads: low Pax3 and EphA3 positive neural crest cells.

(E) Schematic of a more mature trigeminal ganglion (stage 20+), showing relationships between the different types of cells within the ganglion. Mn, trigeminal motor nerve.

Orientation: dorsal to the left and ventral to the right; applies to all images.

Scale: 200 μm (A-A"); 25 μm (B-D).

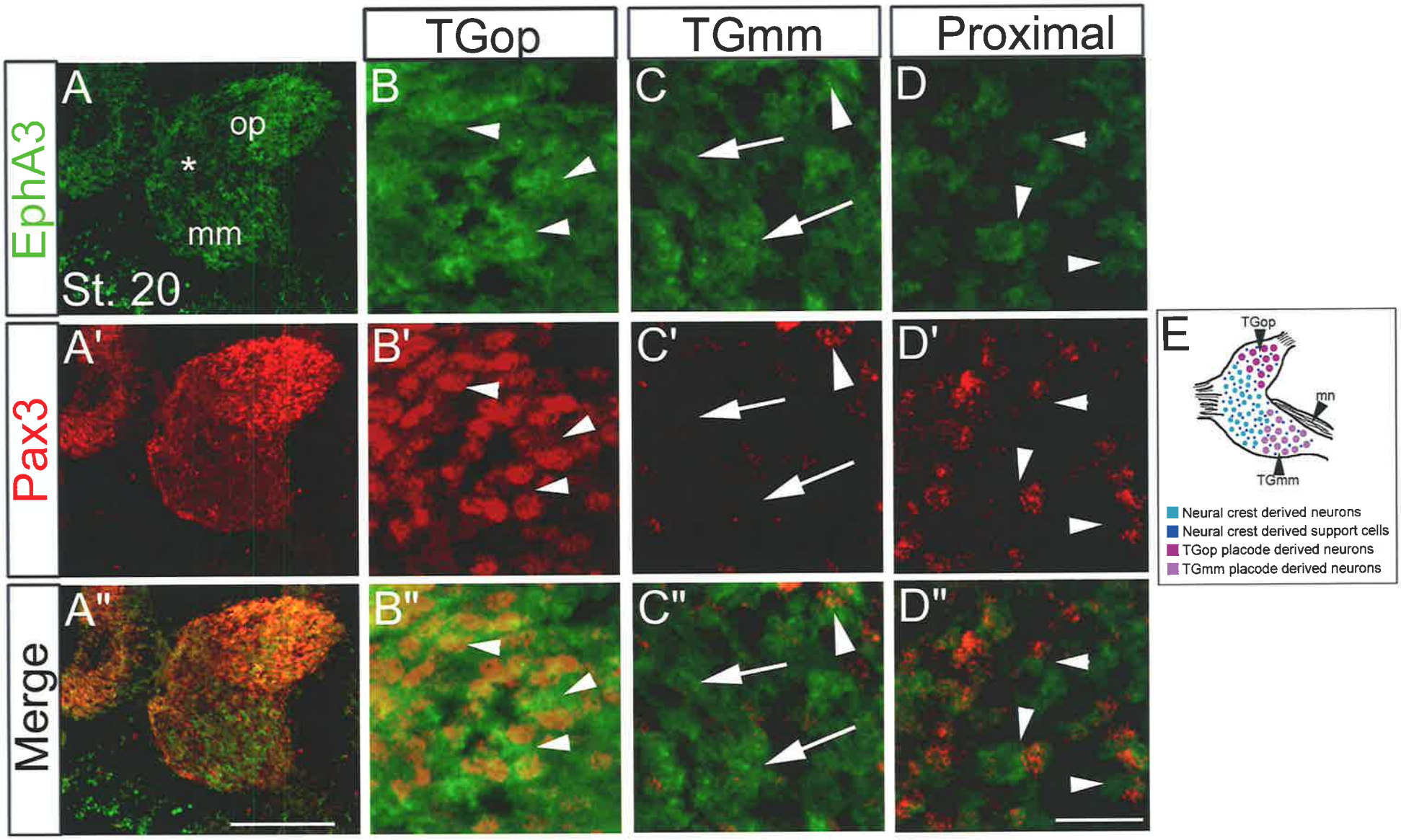
TGop
TGmm
Proximal
EphA3
Pax3
Merge
A
op
*
mm
St. 20
B
C
D
A'
B'
C'
D'
A"
B"
C"
D"
E
TGop
mn
TGmm
Neural crest derived neurons
Neural crest derived support cells
TGop placode derived neurons
TGmm placode derived neurons

In order to further substantiate EphA3 receptor localisation to ganglionic neurons at stage 20 (Figure 4.6), sections of the trigeminal ganglion were immunostained with an antibody against the neuronal marker, neurofilament (arrowheads; Figure 4.6A'-C"). In the ophthalmic lobe neurons/ axons, EphA3 immunoreactivity appeared to be slightly more intense compared with the maxillomandibular lobe neurons/ axons (Figure 4.6A). As mentioned earlier (Figure 4.5A), the proximal neural crest region was less intensely stained with the EphA3 antibody (asterisk; Figure 4.6A) compared to distal regions of both lobes. Therefore, EphA3 localisation to the trigeminal ganglion neurons was consistent with a role for this receptor as a cognate partner for ephrin-A ligands being expressed in the target fields.

The results for EphA3 from stage 15 (Figure 4.4) and stage 20 (Figure 4.5-4.6) implied that the two trigeminal ganglion lobes differentially expressed this receptor, with high expression observed in the ophthalmic lobe. Since this apparent differential EphA3 expression in the ganglion was not strikingly obvious in sectioned embryos, a number of other methods were used to confirm this observation. The fluorescence intensity of EphA3 immunoreactivity in whole-mount ganglia (n = whole ganglia from 3 embryos) was measured for the two trigeminal ganglion lobes at stage 20 (Figure 4.7A and Table 4.1). The analysis revealed that the ophthalmic lobe had a 1.69 ± 0.17 times greater fluorescence intensity compared with the maxillomandibular lobe. Differential EphA3 protein expression was further substantiated by the observation that the ophthalmic lobe was highly expressing *EphA3* following RNA *in situ* hybridisation (Figure 4.7B). The differential expression of *EphA3* by the trigeminal ganglion lobes was further supported with real-time PCR. From two separate pools of RNA (2 experiments), there was a reproducible increase in *EphA3* mRNA expression in the ophthalmic lobe compared to the maxillomandibular lobe (Figure 4.7C and Tables 4.2-4.3). The mean fold change in *EphA3* expression between the two lobes was found to be ~ 4-fold (Table 4.3), and indicated that there was differential expression of this receptor between the two lobes.

Figure 4. 6 Trigeminal ganglion neurons express EphA3 at stage 20.

(A-A") Sagittal confocal slice of the trigeminal ganglion, which with anti-EphA3 (A), and anti-neurofilament (NFM, A'). Merged image shown in (A"). The ophthalmic lobe (TGop) appears to express higher levels of EphA3 compared to the maxillomandibular lobe (TGmm). Asterisk: proximal region expresses low levels of EphA3 compared to the two lobes.

(B, C) Zoomed image of TGop lobe (B) and TGmm lobe (C) from (A). Brightness-contrast adjusted identically. Anti-EphA3 (B, C), anti-NFM (B', C') and merged image (B", C"). Arrowheads: EphA3 positive neurons.

Scale: 200 μm (A); 100 μm (B, C).

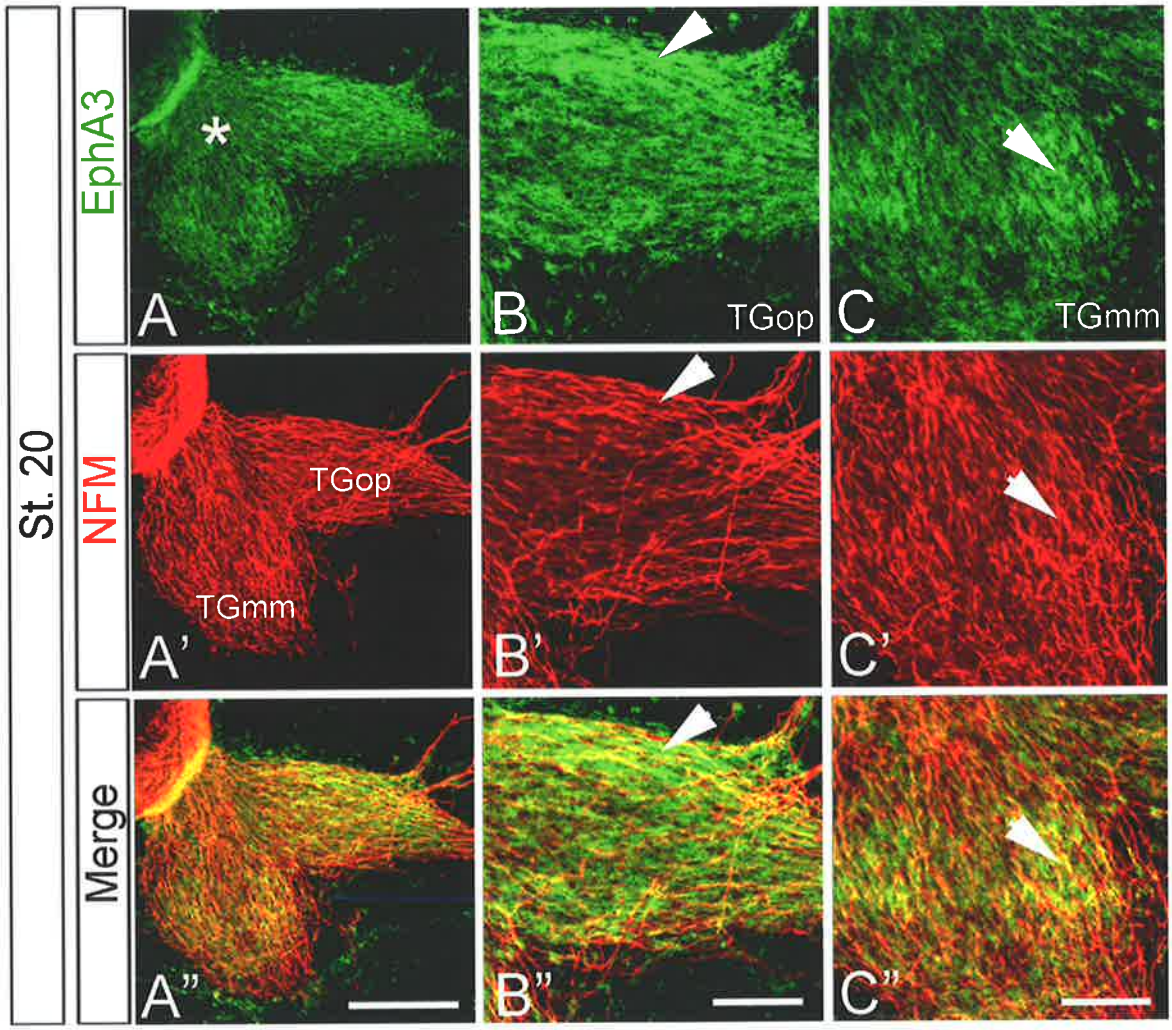
St. 20
EphA3
NFM
Merge
A
B
TGop
C
TGmm
TGop
TGmm
A'
B'
C'
A''
B''
C''

Figure 4. 7 The trigeminal ganglion lobes differentially express EphA3 mRNA and protein at stage 20.

(A-A") Example of whole-mount trigeminal ganglion stained for EphA3 and viewed with a confocal microscope. (A) Merged image of (A') and (A"). Anti-neurofilament (NFM) (A') and anti-EphA3 (A") staining. Note high expression of EphA3 in the ophthalmic lobe (op) compared to the maxillomandibular lobe (mm).

(B) Dissected whole trigeminal ganglion from an *EphA3 in situ* hybridised embryo. Note high staining for *EphA3* transcript in the ophthalmic lobe (op).

(C) Real-time PCR for *EphA3* shows differential expression between the two lobes of the trigeminal ganglion. Green horizontal line shows cycle threshold. *18s* ribosomal RNA (18s) was used as the internal reference because it is not differentially expressed between the two samples. TGop, ophthalmic lobe; TGmm, maxillomandibular lobe.

Scale: 200 μm (A, B).

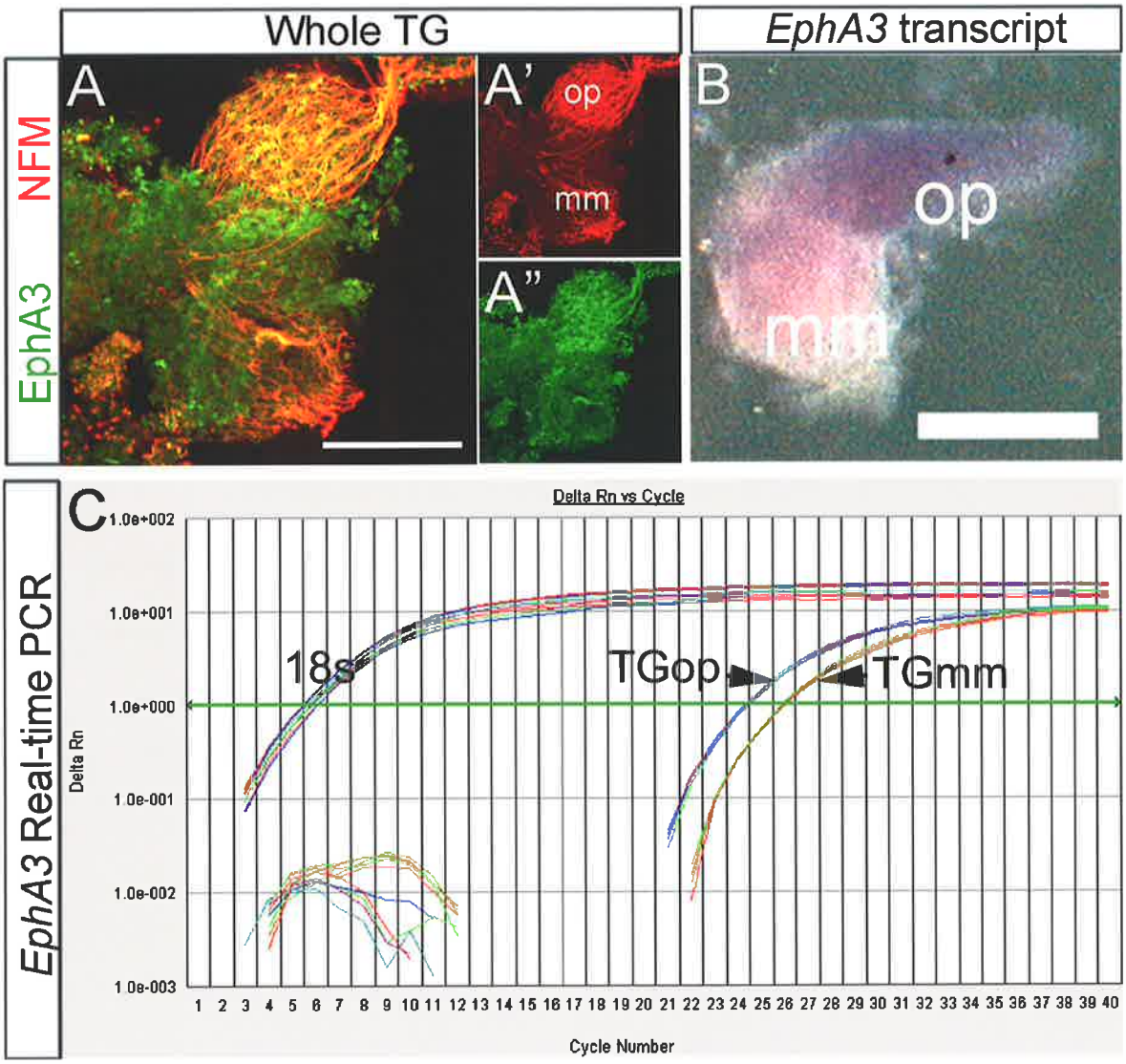
Whole TG
EphA3 transcript
EphA3
NFM
A
A'
op
mm
A"
B
op
mm
EphA3 Real-time PCR
C
Delta Rn vs Cycle
1.0e+002
1.0e+001
1.0e+000
1.0e-001
1.0e-002
1.0e-003
Delta Rn
18s
TGop
TGmm
1 2 3 4 5 6 7 8 9 10 11 12 13 14 15 16 17 18 19 20 21 22 23 24 25 26 27 28 29 30 31 32 33 34 35 36 37 38 39 40
Cycle Number

Table 4.1 EphA3 intensity measurements for ophthalmic (TGop) and maxillomandibular (TGmm) lobes.

TGop[a]	TGmm[a]	Intensity ratio (TGop/ TGmm)
85.18	59.03	1.44
127.08	77.88	1.63[c]
100.42	49.90	2.01
		1.69 ± 0.17[b]

[a] Measurements for each lobe are from 3 whole-mount TG and expressed as mean intensity per pixel (refer to chapter 2 for details). [b] Mean ± SEM. [c] Figure 4.6A is representative of the mean fluorescent intensity.

Table 4.2 Real-time PCR results for *EphA3* and *ephrin-A5* transcripts for the two trigeminal ganglion lobes.

	EphA3				*ephrin-A5*			
	Expt 1		Expt 2		Expt 1		Expt 2	
	TGop[a,c]	TGmm[a,c]	TGop[d,e]	TGmm[d,e]	TGop[b,c]	TGmm[b,c]	TGop[d,e]	TGmm[d,e]
Δ cycle threshold	18.23	20.46	15.99	18.21	16.69	16.52	15.83	15.84
	18.69	20.63	16.14	18.1	17.26	16.47	15.94	15.84
	18.37	20.6	16.27	18.04	17.57	16.44	15.89	15.9
	18.48	20.5	16.18	18.08	17.21	16.38	15.87	15.1
	18.49	20.51			17.15			
					17.03			
mean	**18.45**	**20.54**	**16.15**	**18.11**	**17.15**	**16.45**	**15.88**	**15.67**
SD	**0.17**	**0.07**	**0.12**	**0.07**	**0.29**	**0.06**	**0.03**	**0.38**

Δ cycle threshold is the cycle threshold normalised against *18s* ribosomal RNA (rRNA) internal reference.
[a] Data from Figure 4.6C. [b]Data from figure 4.11D. [c]Δ cycle threshold is shown for each reaction performed.
[d] EphA3 and ephrin-A5 were conducted in the same experiment to allow for comparisons between EphA3 and ephrin-A5 expression within each lobe. [e] Results shown in Figure 4.12.
Note: Any clear outliers for experiment 1 were omitted from further analysis.
Experiment 1 ($n \approx 60$ lobes from 30 embryos); Experiment 2 ($n \approx 80$ lobes from 40 embryos).
Abbreviations: Exp. Experiment; TGop, ophthalmic lobe; TGmm, maxillomandibular lobe; SD, standard deviation. Real-time PCR results were kindly generated by Dr. Warren Flood.

Table 4.3 Quantitation of *EphA3* and *ephrin-A5* mRNA levels in ophthalmic lobe relative to maxillomandibular lobe at stage 20.

	Fold change [a]	
	EphA3	*ephrin-A5*
Experiment 1	4.28	1.6
Experiment 2	3.89	1.15
Mean	**4.09**	**1.38**
SD	**0.28**	**0.32**

[a] Fold change refers to differences in transcript levels between ophthalmic lobe and maxillomandibular lobe. Fold change was derived from Table 4.2 results. Experiment 1 and 2 were generated from two different pools of RNA. Any fold changes greater than twofold were considered to be the result of differential expression between the two lobes.

4.2.3 ephrin-A5 is not differentially expressed in the trigeminal ganglion

4.2.3.1 ephrin-A5 localises to the ophthalmic placode and trigeminal ganglion neurons at stages 13 and 15

The previous chapter established that ephrin-A5 transcript and protein localised to the condensing trigeminal ganglion (Figure 3.11-3.12). This ephrin-A5 expression was further interrogated with trigeminal ganglion molecular markers to better understand the cell types expressing this ligand, and therefore the possible function of this ligand during trigeminal ganglion axon guidance.

As previously mentioned, of the trigeminal placodes, the ophthalmic placode cells are the first to undergo neurogenesis, and invaginating ophthalmic placode cells are likely to start axon pathfinding immediately following invagination (Begbie *et al.,* 2002; Covell and Noden, 1989; Moody *et al.,* 1989a). If ephrin-A5 functioned as a cognate partner for target field EphA receptors (Chapter 3), it was expected that ephrin-A5 would localise to ophthalmic placode cells and ophthalmic neurons. Inspection of Pax3 positive ophthalmic placode (arrow) and invaginating/ invaginated ophthalmic cells revealed that ephrin-A5 localised to these cells at stages 13 and 15 (arrowheads; Figure 4.8A-A" and 4.9A-B). To verify ephrin-A5 localisation to neurons of the trigeminal ganglion, TuJ1 antibody to the neuronal marker β-tubulin was used to label neurons/ axons in sections. As expected, staining of the primitive ophthalmic lobe with anti-ephrin-A5 antibody revealed coimmunoreactivity with anti-β-tubulin antibody at stage 13 (arrowheads and arrow; Figure 4.8B-C). The ephrin-A5 neuronal/ axonal expression at stage 13 (Figure 4.8C-C"), persisted at stage 15 in the ophthalmic lobe (Figure 4.10A-B). Furthermore, at the level of the ophthalmic process, ephrin-A5 puncta co-localised to ophthalmic axons (Figure 4.10A-B). Likewise, stage 15 maxillomandibular neurons were also observed to express ephrin-A5 (Figure 4.10C-D). Collectively, the results demonstrated that ephrin-A5 localised to ophthalmic placode cells and neurons of the primitive ganglion. Hence, these findings were coherent with a role for ephrin-A5 as a cognate interacting partner for EphA3/ A4 receptors being expressed in the trigeminal ganglion target fields.

To determine whether the neural crest component of the trigeminal ganglion was also positive for ephrin-A5, anti-HNK-1 antibody was utilized on sectioned embryos to label neural crest cells. Findings from the previous chapter (Figure 3.11) demonstrated co-that the primitive trigeminal ganglion at the level of the mandibular process was *ephrin-A5* mRNA positive and HNK-1 positive at stage 15 (Figure 4.11). To further verify these results, anti-ephrin-A5 antibody was used, and it was found that the neural crest component at the level of the ophthalmic (arrowheads; Figure 4.11A-B) and maxillomandibular (arrowheads; Figure 4.11C-D) lobes were ephrin-A5 positive. However, it was also noted that some ephrin-A5 positive cells within both lobes did not co-localise with HNK-1 (arrows; Figure 4.11B", 4.11D"). Such ephrin-A5 positive, yet HNK-1 negative cells are suspected to be of placode origin. Therefore, in addition to be expressed in the ophthalmic placode, ephrin-A5 localised to the neural crest component of the developing trigeminal ganglion.

Figure 4. 8 The ophthalmic placode and neurons express ephrin-A5 at stage 13.

(A-A") Transverse confocal z-stack images at the level of midbrain, showing anti-ephrin-A5 (green) (A-A") and anti-Pax3 (red; A, A") staining. (A) A low magnification image, and boxed region is magnified in (A'-A"). (A) Dotted outline: neural tube (nt). (A'-A") placode (arrow) and invaginated Pax3 cells (arrowheads) are ephrin-A5 positive.
(B-B") Confocal z-stack transverse image stained with anti-ephrin-A5 (B, B"), and anti-β-tubulin (TuJ1; B', B"). Arrow: ephrin-A5 and TuJ1 co-expression in the developing trigeminal ganglion. (C-C") Higher magnification view of (B-B"). Merged images shown in (B", C"). Arrow: TuJ1 positive processes in the epithelial layer are also ephrin-A5 positive. Arrowheads: ephrin-A5 positive trigeminal ganglion neurons.
Orientation highlighted in red lettering (A) and applies to all images. D, dorsal; V, ventral.
Scale: 100 μm (A, B); 25 μm (A'); 50 μm (C).

Pax3 ephrin-A5
A
A'
A''
nt
ephrin-A5
B
C
TuJ1
B'
C'
Merge
B''
C''

Figure 4. 9 Ophthalmic placode and ophthalmic neurons express ephrin-A5 at stages 15 and 20.

(A-A') Confocal z-stack stained with anti-ephrin-A5 (green; A, A') and anti-Pax3 (red) (A') at stage 15. Boxed region is magnified in (B-B').
(B) Anti-Pax3 and (B') merged image of ephrin-A5 (green) and Pax3. (B-B') Arrow: Pax3 cells in the placode are also stained for ephrin-A5. Arrowheads: invaginated Pax3 cells are ephrin-A5 positive.
(C-C') Confocal z-stack of the mature trigeminal ganglion at stage 20. The ophthalmic lobe (TGop) and the maxillomandibular lobe (TGmm) are positive for ephrin-A5 (green). (C') Image also shows Pax3 expression (red). The proximal region of the ganglion (asterisk) and peripheral axons tracts (arrowheads) are ephrin-A5 immunoreactive. Boxed region is magnified in (D-D').
(D-D') Anti-Pax3 (D), and merged with anti-ephrin-A5 (green, D'). Arrowheads: ephrin-A5 and Pax3 double positive TGop cells.
Orientation: shown in red lettering in (A) and (C). D, dorsal; V, ventral.
Scale: 100 μm (A); 50 μm (B, D); 200 μm (C).

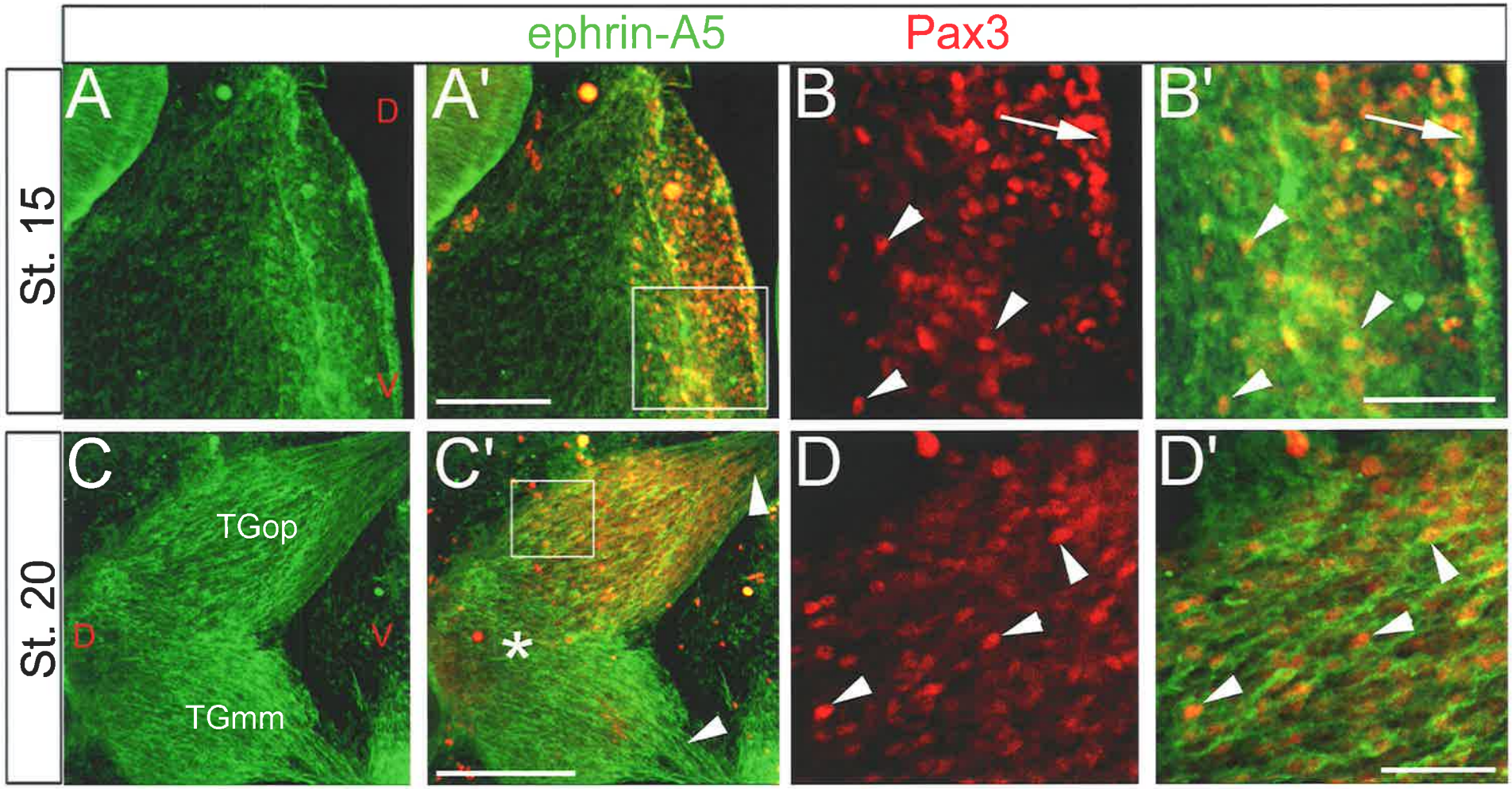
ephrin-A5
Pax3
St. 15
St. 20
A
A'
B
B'
C
C'
D
D'
D
V
TGop
TGmm
*

Figure 4. 10 Trigeminal sensory axons express ephrin-A5 at stage 15.

(A) Confocal z-stack at the level of the ophthalmic process showing trigeminal ganglion ophthalmic (TGop) axons stained with anti-ephrin-A5 (green) and anti-β-tubulin (TuJ1; red).

(B-B") Same image in (A) magnified. Anti-ephrin-A5 (B); anti-TuJ1 (B'), and merged image (B"). Arrowheads: ephrin-A5 puncta localise to TGop axons.

(C) Confocal z-stack at the level of the maxillomandibular (TGmm) lobe stained with anti-ephrin-A5 (green) and anti-β-tubulin (TuJ1; red). Same image magnified in (D-D"). Anti-ephrin-A5 (D); anti-TuJ1 (D'), and merged image (D"). Arrowheads: ephrin-A5 and TuJ1 positive cells/ axons.

(E) Schematic showing approximate plane of sections.

Orientation shown in red lettering in (A) applies to all images. D, Dorsal; V, ventral.

Scale: 100 μm (A, C); 50 μm (B, D).

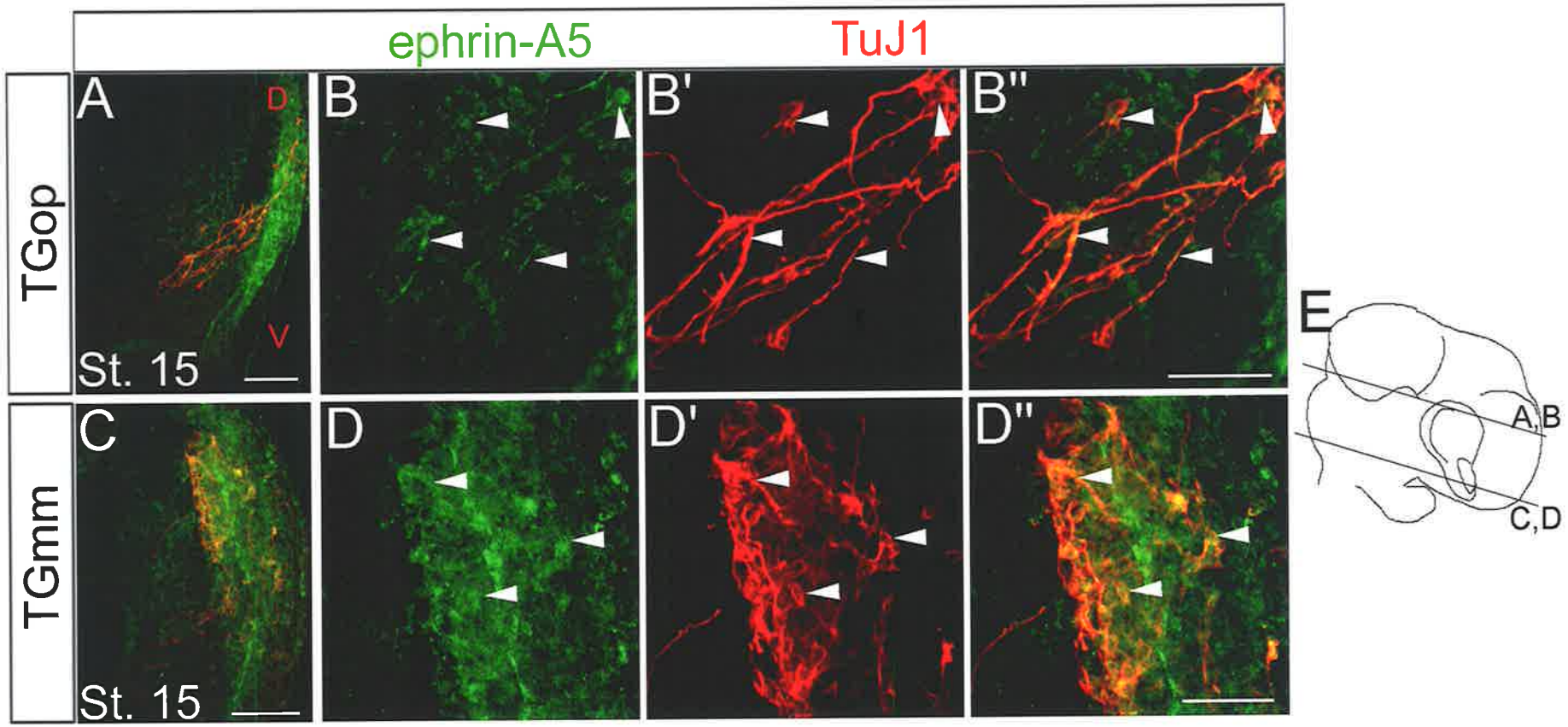
ephrin-A5
TuJ1
TGop
TGmm
A
B
B'
B''
C
D
D'
D''
D
V
St. 15
St. 15
E
A,B
C,D

Figure 4. 11 Trigeminal ganglion neural crest cells express ephrin-A5 at stage 15.

(A-A') Confocal z-stack at the level of the ophthalmic (TGop) lobes (asterisks). E, eye. Boxed region in (A') has been magnified in (B-B"). Anti-ephrin-A5 (A- A', B, B"); anti-HNK-1 (A', B'-B"). (B-B") Arrowheads: ephrin-A5 and HNK-1 positive cells. Arrow: some ephrin-A5 expressing cells do not co-localise with HNK-1.

(C-C') Confocal z-stack at the level of the maxillomandibular lobe (asterisk) and boxed region is magnified in (D-D"). (C) Mx, Maxillary process. Anti-ephrin-A5 (C-C', D, D") and anti-HNK-1 (C', D'-D"). Arrowheads: HNK-1 and ephrin-A5 positive cells. Arrows: some cells do not show co-localisation between ephrin-A5 and HNK-1.

(E) Schematic shows approximate plane of sections.

Orientation is indicated in red lettering in (A) and applies to all images. D, dorsal; V, ventral.

Scale: 200 μm (A, C); 100 μm (B, D).

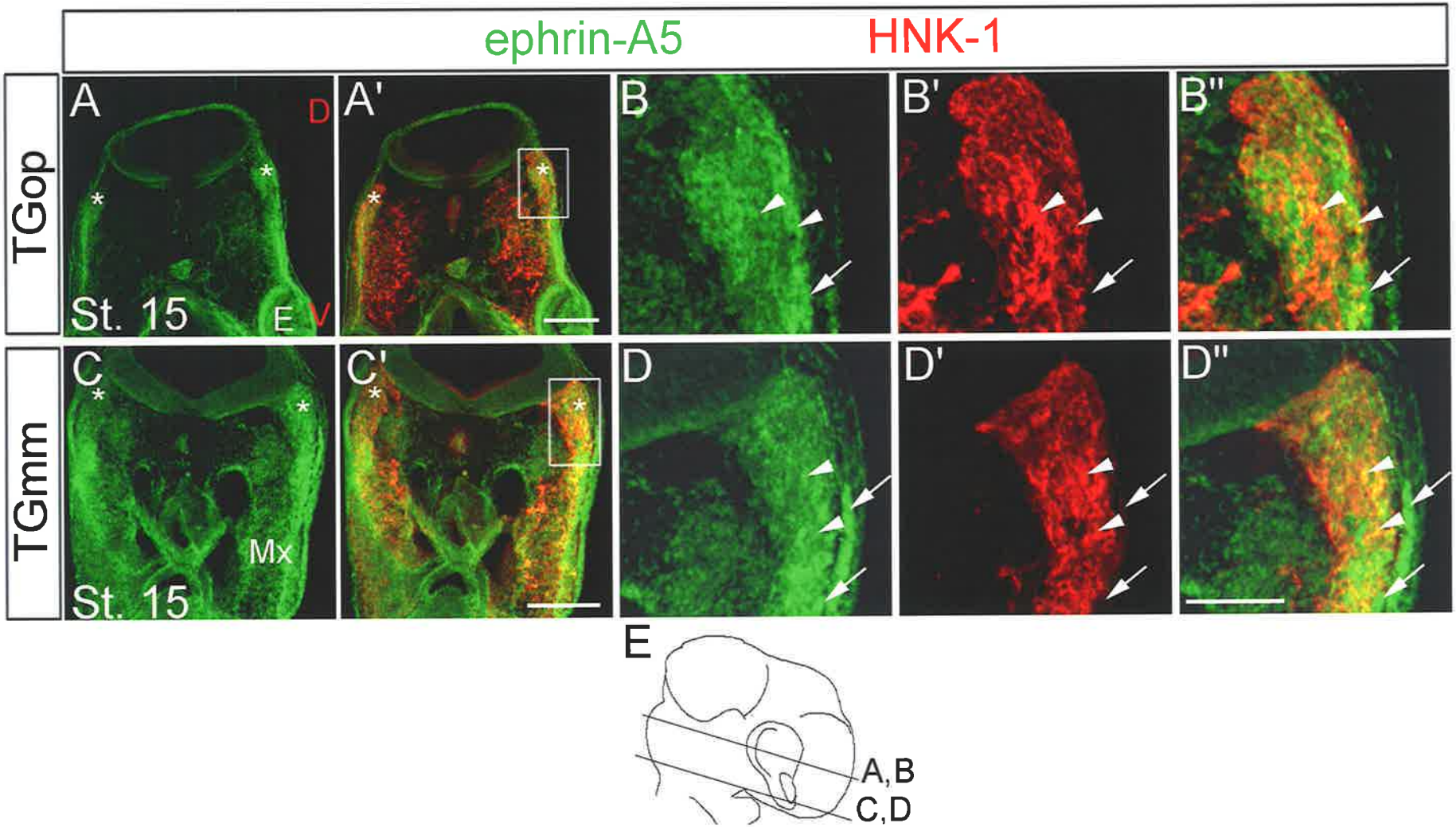
ephrin-A5
HNK-1
TGop
TGmm
A
A'
B
B'
B''
C
C'
D
D'
D''
D
V
E
Mx
St. 15
St. 15
A,B
C,D

4.2.3.2 The trigeminal ganglion at stage 20 non-differentially expresses ephrin-A5

In order to gain insight into the expression pattern of ephrin-A5 in the maturing trigeminal ganglion at stage 20, sections were co-immunoreacted with anti-ephrin-A5 and various other antibodies directed against ganglionic cell markers. To verify that ophthalmic neurons in the ophthalmic lobe continued to express ephrin-A5, anti-Pax3 antibody was utilized. Indeed, it was found that high Pax3 positive ophthalmic neurons were also ephrin-A5 positive at stage 20 (Figure 4.9C, and arrowheads; Figure 4.9D). Neuronal ephrin-A5 expression within the ganglion was additionally substantiated since some cells exhibited co-localisation with TuJ1 (Figure 4.12A-C). Other cells within the two lobes did not exhibit co-immunoreactivity to TuJ1 and ephrin-A5 antibodies (Figure 4.12B-C), and are likely to be neural crest derived support cells. The proximal region of the ganglion that is neural crest derived, also immunoreacted with anti-ephrin-A5 antibody (asterisk; Figure 4.9C). Within the trigeminal ganglion the peripheral axon tracts were ephrin-A5 positive (arrowhead; Figure 4.9C). Hence, ephrin-A5 localisation to neurons/ axons of the ganglion was further consistent with a role for ephrin-A5 as a cognate binding partner for EphA receptors being expressed in the trigeminal ganglion target fields.

In contrast to trigeminal ganglion EphA3 expression (Figure 4.7), the two lobes did not exhibit differential ephrin-A5 expression when stained with antibodies (Figure 4.9C, 4.12A). This notion was further strengthened by the real-time PCR results, which indicated a mean fold change of 1.38 ± 0.32 (Figure 4.12D and Tables 4.2-4.3).

The data jointly demonstrated that ephrin-A5 expression observed at stages 13 and 15 in the trigeminal ganglion persisted into stage 20. In addition, ephrin-A5 was expressed at similar levels in the two lobes at stage 20.

4.2.4 Differential co-expression of EphA3 and ephrin-A5 in the maxillomandibular lobe

In vivo cis-interactions between co-expressed EphAs and ephrin-As can occur and these interactions are dependent on receptor/ ligand abundance. Furthermore, such interactions can also have consequences for EphA receptor sensitivity to ligands expressed in the environment and may play a role during axon guidance (Flenniken *et al.*, 1996; Hornberger

et al., 1999; Yin *et al.,* 2004). Some insight into intra-ganglionic EphA3/ ephrin-A5 interactions was gained when Fc-fusion chimeras were used on whole embryos to detect EphAs and ephrin-As (Figure 3.3) because there was disparity between the Fc-fusion results and antibody data from this chapter (see discussion section 4.3). To assess the abundance of EphA3 with that of ephrin-A5 within each of the trigeminal ganglion lobes, the real-time PCR approach was used (Table 4.2 and Table 4.4, Figure 4.13); antibodies against EphA3 and ephrin-A5 could not be used for this purpose because both antibodies were raised in goat and were polyclonal.

The results showed that within the ophthalmic lobe, *EphA3* and *ephrin-A5* mRNA were expressed at similar levels (~1 fold change) following normalisation against the 18s ribosomal RNA (rRNA) internal reference (Table 4.4 and Figure 4.13A). In comparison, *ephrin-A5* expression was ~5.4 fold greater than that of *EphA3* in the maxillomandibular lobe (Table 4.4 and Figure 4.13B), suggesting differential expression of these two genes within this lobe.

Table 4.4 Fold-change comparison of *ephrin-A5* relative to *EphA3* expression within each trigeminal ganglion lobe.

	Fold change[a]	
	TGop	**TGmm**
EphA3 v. ephrin-A5	1.21	5.41

[a]Fold change for each lobe between *EphA3* and *ephrin-A5* expression was calculated from experiment 2 data shown in Table 4.2. Any fold changes greater than twofold were considered to be the result of differential expression between the two genes.

Figure 4. 12 Ephrin-A5 is non-differentially expressed in the stage 20 trigeminal ganglion.
(A-A') Confocal z-stack low magnification sagittal view of the trigeminal ganglion stained with anti-ephrin-A5 (A-A') and merged with anti-β-tubulin (TuJ1; red) staining (A'). Arrowhead: proximal region of the trigeminal ganglion is ephrin-A5 positive and note majority of cells are not TuJ1 positive.
(B-B') Magnified image of the ophthalmic (TGop) lobe from (A). Anti-ephrin-A5 (B) and merged with anti-β-tubulin (TuJ1; B'). Arrowheads: ephrin-A5 neurons.
(C-C') Magnified image of the maxillomandibular (TGmm) lobe from (A). Anti-ephrin-A5 (C) and merged anti-β-tubulin (TuJ1; C'). Arrowheads: ephrin-A5 neurons.
(D) Real-time PCR for *ephrin-A5* shows no differential expression between the TGop (5 reactions) and TGmm lobes (5 reactions) when compared to internal reference *18s* ribosomal RNA. Green horizontal line: cycle threshold.
Orientation shown in red lettering in (A) and applies to images (A-C). D, dorsal: V, ventral.
Scale: 100 μm (A-C).

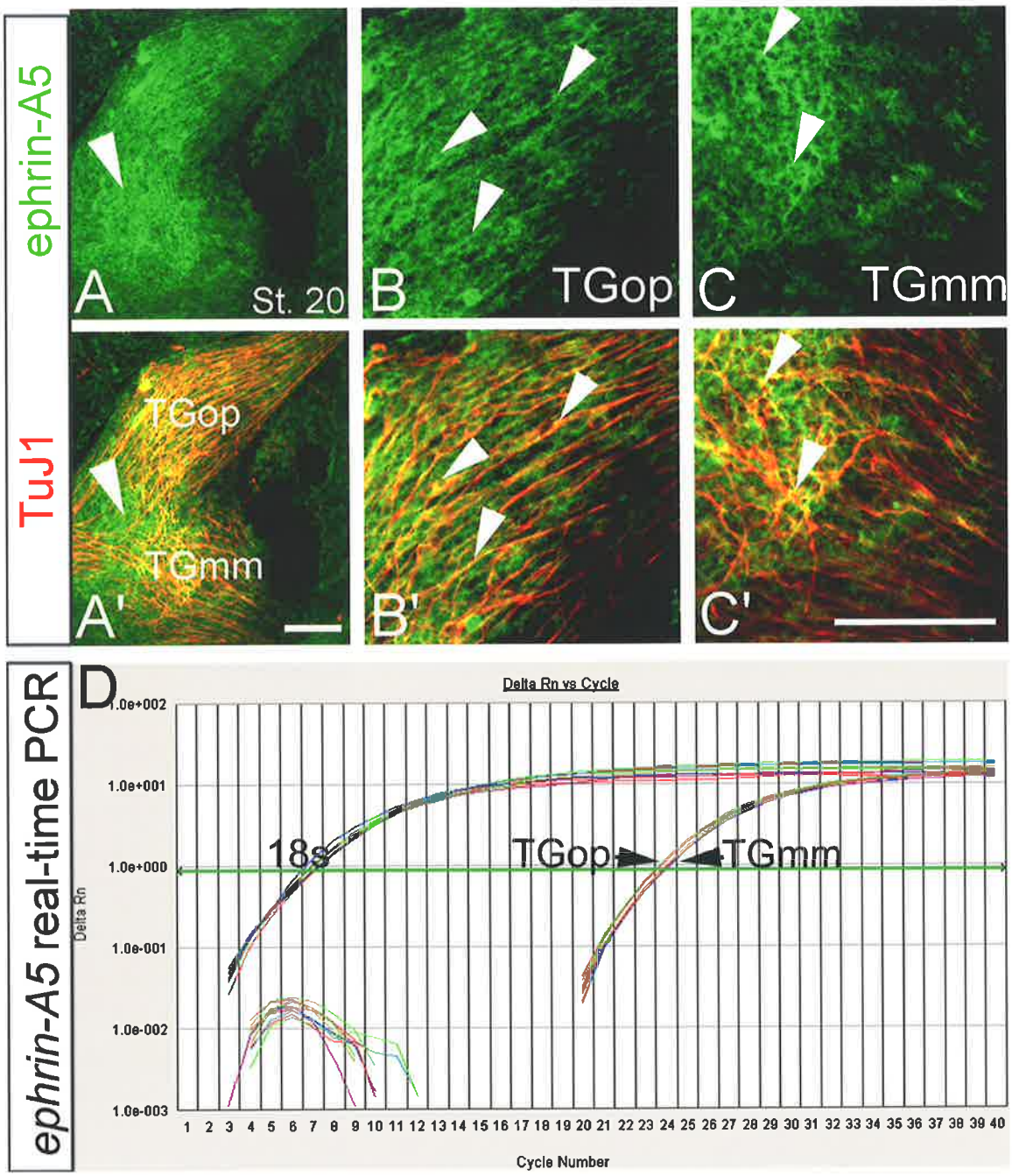
ephrin-A5
TuJ1
A
St. 20
B
TGop
C
TGmm
TGop
TGmm
A'
B'
C'
ephrin-A5 real-time PCR
D
Delta Rn vs Cycle
1.0e+002
1.0e+001
1.0e+000
1.0e-001
1.0e-002
1.0e-003
Delta Rn
18s
TGop
TGmm
1 2 3 4 5 6 7 8 9 10 11 12 13 14 15 16 17 18 19 20 21 22 23 24 25 26 27 28 29 30 31 32 33 34 35 36 37 38 39 40
Cycle Number

Figure 4. 13 Comparison of *EphA3* and *ephrin-A5* transcript expression within ophthalmic and maxillomandibular lobes.

(A) Real-time PCR showing *EphA3* and *ephrin-A5* are expressed at similar levels within the ophthalmic (TGop) lobe.

(B) Real-time PCR showing *EphA3* and *ephrin-A5* are differentially expressed in the maxillomandibular (TGmm) lobe.

(A-B) Comparisons between *EphA3* and *ephrin-A5* were made relative to *18s* ribosomal RNA (18s). Results shown are from experiment 2 shown in Table 4.2.

Green horizontal line: cycle threshold.

Real-time PCR TGop

Real-time PCR TGmm

4.3 Summary and discussion

The results from this chapter clearly showed that trigeminal ganglion neurons and axons that course through the target fields localise with EphA3 and ephrin-A5 (Figure 4.14). Additionally, the two lobes of the trigeminal ganglion exhibited differential EphA3 expression, whilst ephrin-A5 showed similar levels of expression. Recently, consistent with the findings from this study, mouse *ephrin-A2, -A4* and *-A5* transcripts were found to localise to the trigeminal ganglion around E12.5-13.5 (Luukko *et al.,* 2004). In this study, *ephrin-A2* transcripts did not appear to localise to the ganglion in this study, suggesting it was not expressed. Alternatively, *ephrin-A2* transcripts may be present in the ganglion, but at negligible levels, lending support to the idea that any putative guidance role may be performed dominantly by ganglionic ephrin-A5. The possibility remains that the RNA *in situ* hybridisation method used was not sensitive enough to detect *ephrin-A2* ligand transcripts in the ganglion. The presence/ absence of ephrin-A2 remains to be further validated with anti-ephrin-A2 antibodies.

4.3.1 Insights into intra-ganglionic EphA3/ ephrin-A5 interactions

Ephrin-A5-Fc expression *in vivo* provided evidence for EphA receptor(s) expression in the ophthalmic lobe (Figure 3.4). Subsequent immunofluorescent staining and RNA *in situ* hybridisation revealed that the candidate EphA was EphA3. Although both lobes were EphA3 positive, the ophthalmic lobe expressed *EphA3* mRNA and protein at a higher level in comparison to the maxillomandibular lobe. Thus there are inconsistencies between ephrin-A5-Fc data and EphA3 RNA *in situ*/ antibody staining of the trigeminal ganglion. Intra-ganglionic interactions between EphA3/ ephrin-A5 are likely to provide an explanation for this. Additional evidence for possible EphA3/ ephrin-A5 interactions within the trigeminal ganglion came from *in situ* EphA3-Fc and A4-Fc (Figure 3.4) binding. Contrary to *ephrin-A5 in situ* hybridisation, real-time PCR and immunofluorescent antibody staining results, all of which indicated a lack of differential ephrin-A5 expression in the trigeminal ganglion, EphA3/ A4-Fc binding indicated otherwise. As mentioned in the previous chapter, endogenous interactions between co-expressed Ephs/ ephrins can block Fc-fusion chimera binding (Flenniken *et al.,* 1996; Hornberger *et al.,* 1999; Yin *et al.,* 2004). The inability to detect EphA3 with ephrin-A5-Fc or conversely, the intense binding seen with EphA3/ A4-Fc in the maxillomandibular lobe

is accounted for by the observation that *EphA3* transcripts are less abundantly expressed compared to *ephrin-A5* in this lobe (Figure 4.13). Jointly therefore, the Fc-fusion chimera analysis and the real-time PCR results imply that most, if not all receptors in the maxillomandibular lobe are probably involved in intra-ganglionic EphA3/ ephrin-A5 interactions. Based on previous studies (Hornberger *et al.,* 1999; Yin *et al.,* 2004), these ganglionic interactions will presumably have consequences during trigeminal ganglion axon guidance.

4.3.2 EphA3 is differentially expressed within the ganglion

Levels of EphA3 receptor within different sub-populations of ganglionic cells at stage 20 appeared to vary (Figure 4.14A). The proximal neural crest portion, as identified by low Pax3 expression and location within the ganglion, expressed low levels of EphA3 compared to Pax3 negative neurons within the distal regions of maxillomandibular lobe. Additionally, neuronal expression of EphA3 in the ophthalmic lobe was found to be greater than that compared to neuronal expression in the maxillomandibular lobe. Since the trigeminal ganglion also expressed ephrin-A5, EphA3 activity in various populations of cells could be modified through *cis*-interactions (Yin *et al.,* 2004). Once again, there was no evidence to suggest that there was differential expression of ephrin-A5 in various sub-populations of cells (Figure 4.14B). The significance of intra-ganglionic EphA3/ ephrin-A5 interactions during integration of placode and neural crest components, and during trigeminal ganglion axon guidance remains to be elucidated.

4.3.3 Significance of EphA3 and ephrin-A5 expression in the placode during axon guidance

Ophthalmic placode and invaginated placode cell expression of EphA3 and ephrin-A5 is likely to be significant during trigeminal ganglion axon guidance, especially during ophthalmic axon guidance (Figure 4.14). In support of this, ophthalmic axons were positive for EphA3 and ephrin-A5, and neurons invaginating from the placode are positive for this receptor-ligand pair. Stage 13 cells from the ophthalmic placode invaginating to form the ganglion are reported to be postmitotic (Begbie *et al.,* 2002), and likely start axon pathfinding immediately following invagination (Covell and Noden, 1989). The first axons to pioneer from the trigeminal ganglion to the targets are those derived from the placode component of the ganglion (Lwigale, 2001; Moody *et al.,* 1989a), and this component of

the ganglion is the first to initiate neurogenesis (Begbie *et al.,* 2002; D'Amico-Martel and Noden, 1983; Moody *et al.,* 1989a; Stark *et al.,* 1997). In this study, TuJ1 reactive cells were seen in the ophthalmic placode and would corroborate with such a notion. The evidence also suggest that the proximal neural crest component of the ganglion does not appear to produce axons till at least stage 15 (Moody *et al.,* 1989a), and a large majority do not appear to adopt a neural fate till well after stage 20, when axon pathfinding has occurred (Baker *et al.,* 2002; Covell and Noden, 1989; D'Amico-Martel and Noden, 1980; Moody *et al.,* 1989a). The possibility cannot be excluded however, that EphA3 and ephrin-A5 expression in the placode has a role during placode development as well.

In comparison to the ophthalmic placode, the epithelium adjacent to the maxillomandibular lobe expressed low levels of EphA3 (Figure 4.14A), and this epithelium was suspected to correspond to the maxillomandibular placode. However at stage 15, *EphA3* transcript did not appear to be restricted to epithelium at the level of the maxillomandibular lobe (Figure 3.5F). This discrepancy could be explained by the insensitivity of *in situ* hybridisation technique used. Ephrin-A5 visualisation in the epithelium at the level of the maxillomandibular lobe indicated that this placode was perhaps also positive for this ligand (Figure 4.14B). The caudal limit of Pax3 expression in the epithelium was used as a guide to distinguish expression in the ophthalmic versus maxillomandibular placodes in this study. However in hindsight, this was not a good approach to characterise the expression of EphA3 and ephrin-A5 in the maxillomandibular placode. One marker that is specific to the maxillomandibular placode has recently been identified, and this is *neurogenin-1* (Begbie *et al.,* 2002). Therefore, the expression of EphA3 and ephrin-A5 needs to be further validated by studying the co-localisation of this receptor-ligand pair with that of *neurogenin-1*.

4.3.4 Conclusion

Overall, the localisation of both EphA3 and ephrin-A5 to trigeminal ganglion neurons/ axons and the ophthalmic placode are consistent with a role for this pair during trigeminal ganglion axon guidance.

Figure 4. 14 (part A) A Schematic summary of EphA3 expression during trigeminal ganglion development at stages 13 and 20.

(A) At stage 13-15, the brown numbers highlights the sequence of events that leads to the formation of the trigeminal ganglion. (1) Placode cells, (2) invaginating neurons/ neuroblasts; and (3) invaginated trigeminal ganglion lobe cells. EphA3 is depicted with varying shades of green and nuclear Pax3 expression with dark/light red.

Different cell types of the trigeminal ganglion differentially express EphA3. The expression results suggest that the ophthalmic placode and lobe cells (stage 13-20) express EphA3 at a higher level compared to maxillomandibular lobe cells (stage 15-20). The low expression of EphA3 in the maxillomandibular placode remains to be verified (indicated with a ?). At stage 20 in the ganglion, proximal neural crest cells (depicted by their comparatively low Pax3 expression than the ophthalmic lobe neurons) appeared to express even lower levels of EphA3 compared to maxillomandibular lobe neurons.

Hb, hindbrain; nt, neural tube; TGop, trigeminal ganglion ophthalmic; TGmm, trigeminal ganglion maxillomandibular.

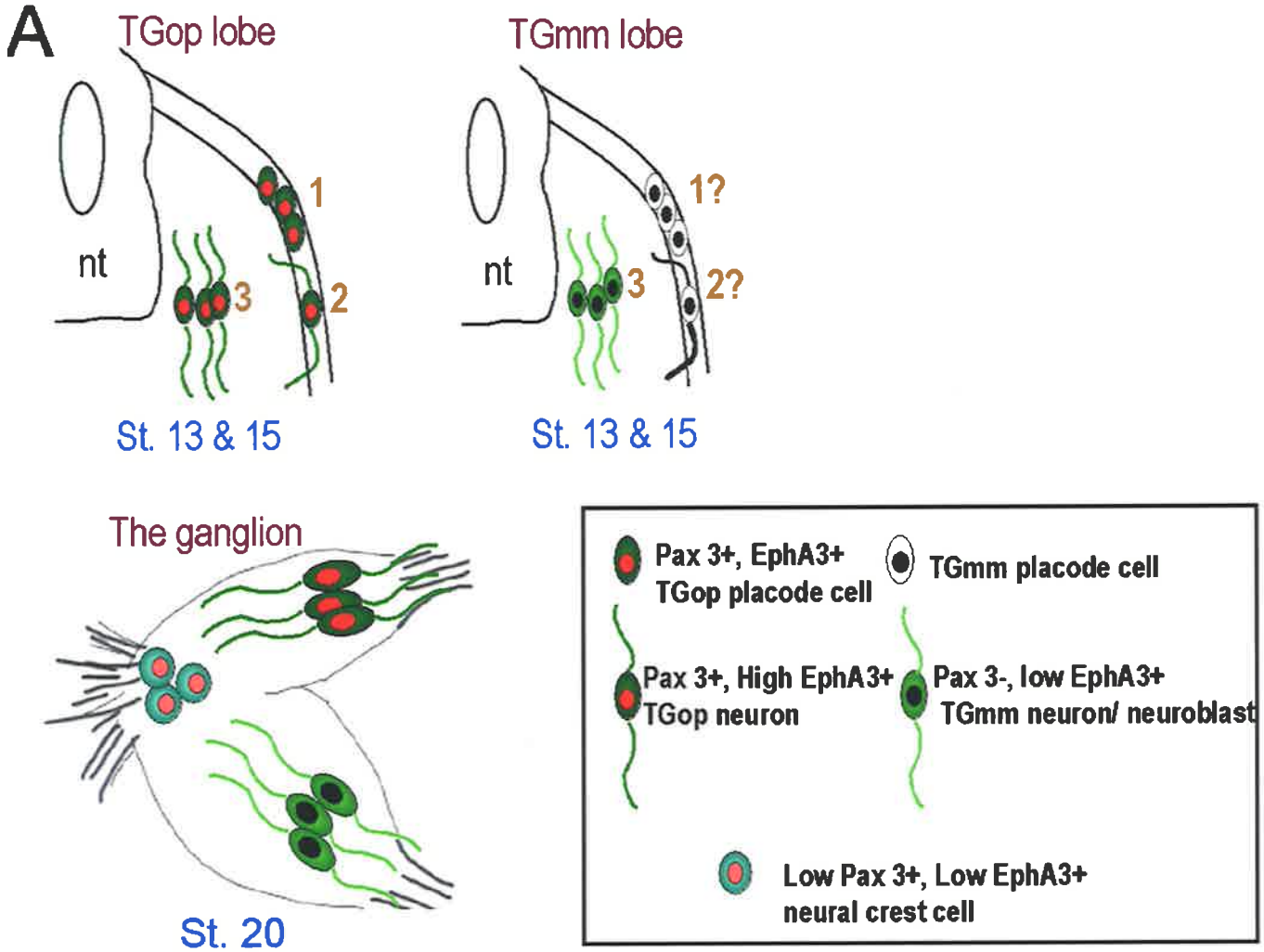

Figure continued next page.

Figure 4. 14 (part B) A Schematic summary of ephrin-A5 expression during trigeminal ganglion development at stages 13 and 20.

(B) At stage 13-15, the brown numbers highlights the sequence of events that leads to the formation of the trigeminal ganglion. (1) Placode cells, (2) invaginating neurons/ neuroblasts; and (3) invaginated trigeminal ganglion lobe cells. Ephrin-A5 is depicted with blue; HNK-1 with orange, and nuclear Pax3 expression with dark/light red.

There does not appear to be differential expression of ephrin-A5 by sub-populations of trigeminal ganglion cells. The expression results suggest that ophthalmic placode (stage 13-20) and lobe cells express ephrin-A5 at similar levels to maxillomandibular lobe neurons (stage 15-20). The expression of ephrin-A5 in the maxillomandibular placode remains to be verified (indicated with a ?). The neural crest cells of the ganglion as indicated by either anti-HNK-1 staining (orange; stage 13-15) or location within the ganglion (light grey; stage 20) also appeared to express ephrin-A5 at similar levels to trigeminal ganglion neurons in both lobes.

Hb, hindbrain; nt, neural tube; TGop, trigeminal ganglion ophthalmic; TGmm, trigeminal ganglion maxillomandibular

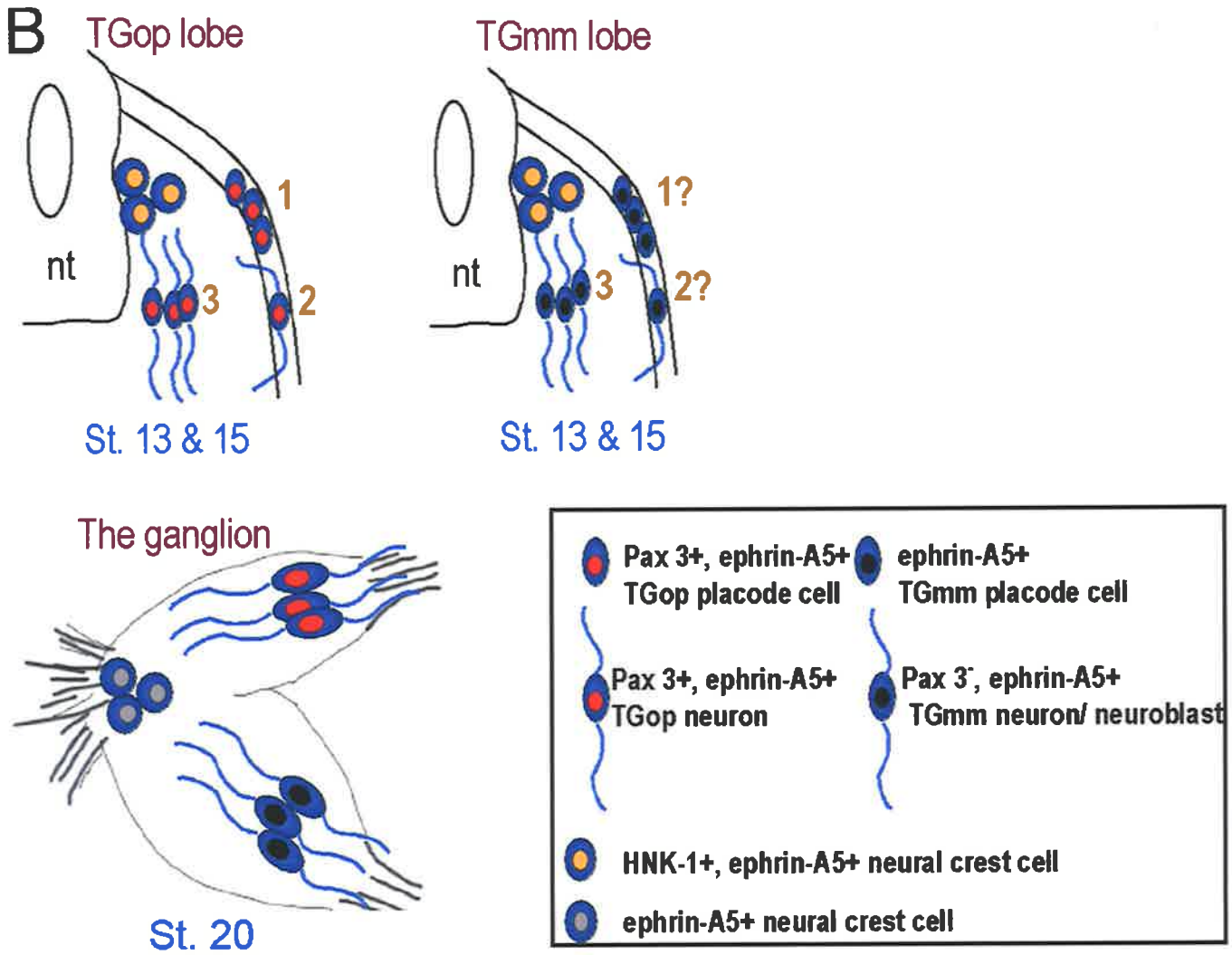
B
TGop lobe
TGmm lobe
nt
nt
1
2
3
1?
2?
3
St. 13 & 15
St. 13 & 15
The ganglion
St. 20
Pax 3+, ephrin-A5+
TGop placode cell
ephrin-A5+
TGmm placode cell
Pax 3+, ephrin-A5+
TGop neuron
Pax 3-, ephrin-A5+
TGmm neuron/ neuroblast
HNK-1+, ephrin-A5+ neural crest cell
ephrin-A5+ neural crest cell

Chapter 5: *In vitro* analysis of trigeminal ganglion EphA3 forward signalling

"There's two possible outcomes: if the result confirms the hypothesis, then you've made a discovery. If the result is contrary to the hypothesis, then you've made a discovery."
--Enrico Fermi

Chapter 5: *In vitro* analysis of trigeminal ganglion EphA3 forward signalling

5.1 Introduction

In different developmental contexts ephrins may also act as "receptors" (Birgbauer *et al.,* 2000; Birgbauer *et al.,* 2001; Knoll and Drescher, 2002) and ephrin bearing cells can transmit signals intracellularly (reviewed by Gauthier and Robbins, 2003; Klein, 1999). Therefore, at any one time there can be Eph forward signalling (Drescher *et al.,* 1995; Krull *et al.,* 1997; Wang and Anderson, 1997), ephrin reverse signalling (Birgbauer *et al.,* 2000; Knoll *et al.,* 2001), and bi-directional signalling into receptor and ligand bearing cells (Mellitzer *et al.,* 1999) (Figure 5.1A). This makes *in vivo* analysis of Eph-ephrin signalling somewhat complicated, especially when there is co-expression of Ephs and ephrins. Although one approach to address Eph/ ephrin signalling mechanisms is through genetic manipulations, it can be time consuming. *In vitro* analysis is another approach to tackling issues of Eph/ ephrin interactions since Eph forward signalling can often be readily uncoupled from ephrin reverse signalling. This separation of forward from reverse signalling is achieved by using cognate Fc-chimeric binding partners, which are only capable of transmitting unidirectional signals into the Eph or ephrin bearing cell (Figure 5.1B). In order to develop clear hypotheses prior to undertaking genetic *in vivo* electroporation manipulations, an *in vitro* approach was taken in this study.

Since ephrin-As and EphA receptors are membranous proteins *in vivo*, it was important that the *in vitro* assay mimicked this. The substratum choice assay (Birgbauer *et al.,* 2001) is a modification of the commonly used stripe assay (Figure 5.2), and is useful for determining whether interactions between candidate EphAs and ephrin-As are repulsive. For those reasons, this assay was utilized to elucidate the roles of EphA3 forward (Chapter 5) and ephrin-A5 reverse (Chapter 6) signalling in trigeminal ganglion neurons. Chapter 4 showed that the trigeminal ganglion during the period of gangliogenesis and axon pathfinding at stages 13, 15 and 20 (Moody *et al.,* 1989a) expressed EphA3. Furthermore, Pax3 positive ophthalmic lobe neuronal precursors in the placode were EphA3 positive, also implying a possible guidance role for this receptor during axon guidance/ pathfinding.

Figure 5.1 Eph/ ephrin interactions and the use of Fc-fusion chimeras to elucidate Eph forward and ephrin reverse signalling.

(A) A simplistic schematic showing the consequences of EphA (green)/ ephrin-A (yellow) interactions.
Top schematic: two cells are shown; one is expressing an ephrin-A (left) and the other expressing EphA (right). Double headed maroon arrow indicates the ephrin-A and EphA are about to interact.
Second schematic from top schematic: EphA/ ephrin-A interactions can lead to forward signalling into the EphA bearing cell.
Third schematic from top schematic: EphA/ ephrin-A interactions can lead to reverse signalling into the ephrin-A bearing cell.
Last schematic: EphA/ ephrin-A interactions can lead to bi-directional signalling into the EphA and ephrin-A bearing cells respectively. Although the schematics concentrate on EphA/ ephrin-A interactions, these schematics can also be applied to the B-subclass Eph/ ephrins.

(B) Fc-fusions chimeras can be used to elucidate EphA forward and ephrin-A reverse signalling *in vitro*.
Left schematics: the structure of EphA (green-red; top) and ephrin-A (yellow-red; bottom) Fc fusion proteins.
Right schematics: illustrates tissue ephrin-A/ substrate-EphA-Fc interactions (top; pink unidirectional arrow) and tissue EphA/ substrate-ephrin-A-Fc interactions (right; pink unidirectional arrow). Note interactions with either tissue expressed EphA or ephrin-A and substratum bound Fc-fusion proteins only result in unidirectional signalling (maroon arrows into EphA or ephrin-A bearing cells).

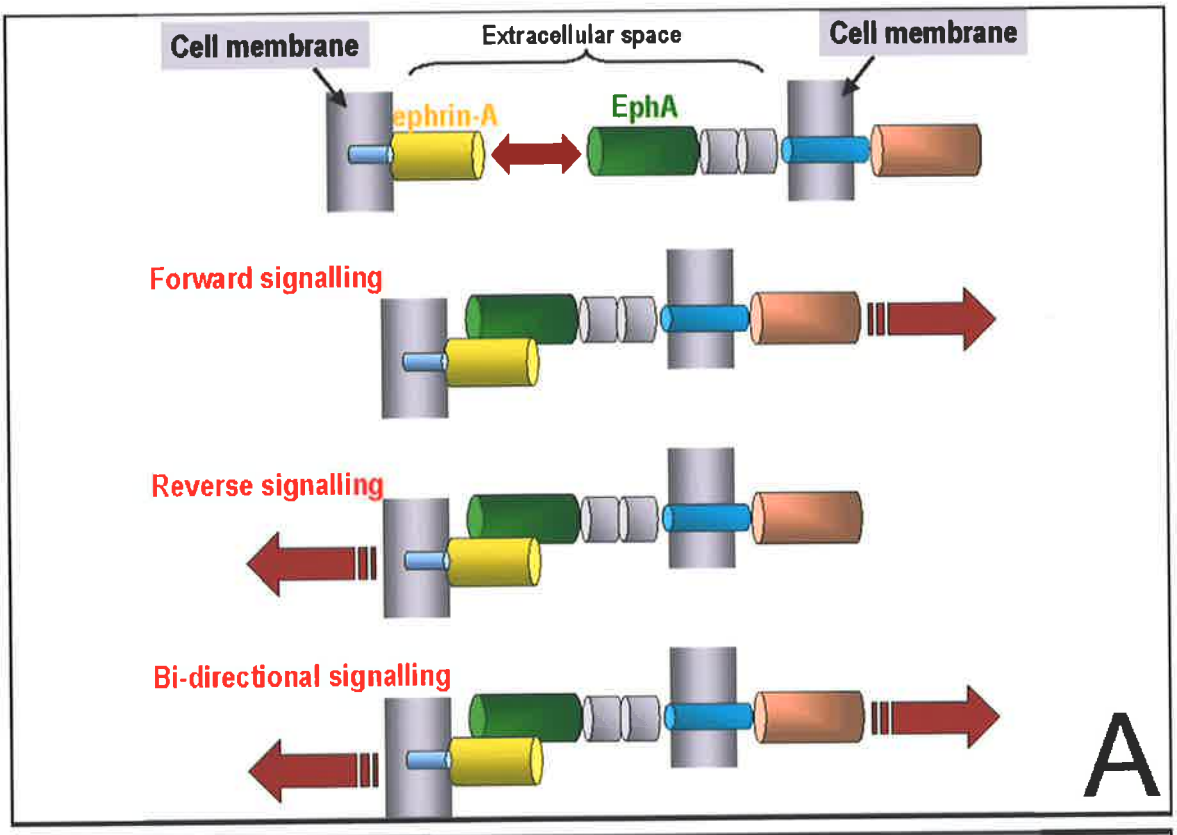
Cell membrane
Extracellular space
Cell membrane
ephrin-A
EphA
Forward signalling
Reverse signalling
Bi-directional signalling
A

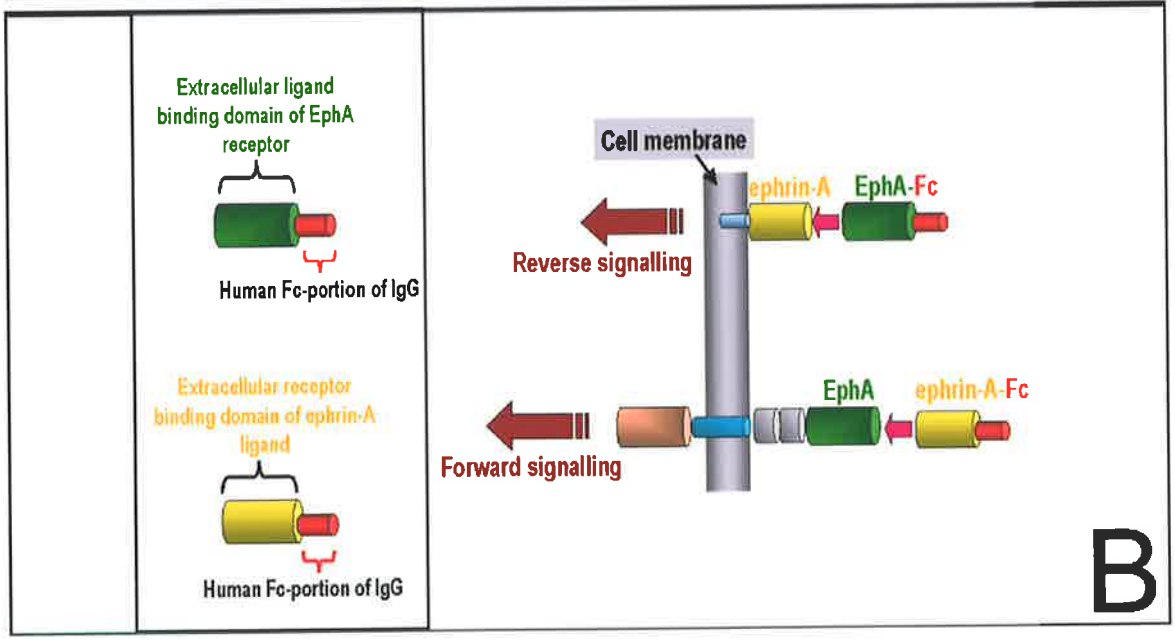
Extracellular ligand binding domain of EphA receptor
Human Fc-portion of IgG
Extracellular receptor binding domain of ephrin-A ligand
Human Fc-portion of IgG
Cell membrane
ephrin-A
EphA-Fc
Reverse signalling
EphA
ephrin-A-Fc
Forward signalling
B

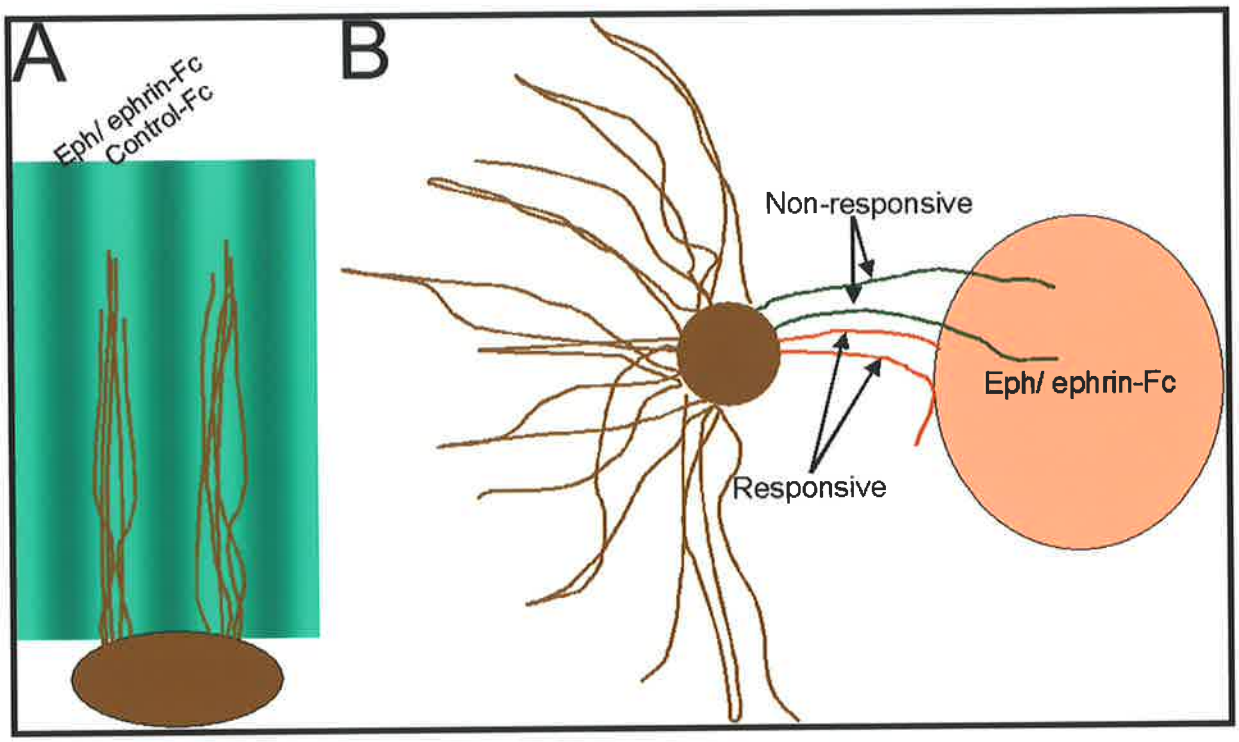

Figure 5. 2 A Schematic demonstrating the layout of a stripe and substratum choice assay.

(A) A schematic of a stripe assay with alternating stripes of Eph or ephrin-Fc (dark green stripes). If there are repulsive Eph/ ephrin interactions, axons from the explant (brown) avoid growing into the dark green stripes.

(B) Schematic of a substratum choice assay. After 24 hours, axon behaviour from the explant (brown) at the Eph/ ephrin-Fc substrate border is quantitated. Non-responsive axons (green) show growth into the Eph or ephrin (orange). Meanwhile, responsive axons (red) stop/ turn at the border presumably due to repulsive interactions with the substrate of interest.

5.2 Results

5.2.1 Trigeminal ganglion explant axons express EphA(s)

Prior to using 24 hour trigeminal ganglion explants in the substratum choice assay it was important to verify the maintenance of any EphA(s) receptor expression. For this purpose, ephrin-A5-Fc was utilised. As previously mentioned, ephrin-A5-Fc will non-discriminately bind to all EphA receptors because of the promiscuous interactions which exist between Ephs and ephrins. Importantly, since the previous chapter described the localisation of EphA3 to the trigeminal ganglion, ephrin-A5-Fc was an appropriate Fc-fusion protein to use given its high affinity interactions with this receptor (Gale *et al.,* 1996; Lackmann *et al.,* 1997).

To confirm that the Fc-portion of the human immunoglobulin protein (control-Fc) did not bind specifically to explant axons, the control-Fc was used to stain 24 hour trigeminal ganglion axons (Figure 5.3A-A"). As expected, little background staining was exhibited when control-Fc was used to stain explants (Figure 5.3A-A") and the result suggested that using control-Fc as a negative control was valid. Localisation of EphA(s) to axons was substantiated by dual immunofluorescent staining with 5 μg/ml of ephrin-A5-Fc and the antibody directed against the neuron/ axon marker, neurofilament (Figure 5.3B-B"). Notably, ephrin-A5-Fc appeared to localise to all axons from whole trigeminal ganglion explants (Figure 5.3A-A'), and this was consistent with the expression of EphA3 in the ganglion (chapter 4). Even so, given the demonstrated differential expression of EphA3 by the two lobes of the trigeminal ganglion (Chapter 4), it was difficult to distinguish whether there was a population of axons that were highly stained for ephrin-A5-Fc compared with another. Additionally, EphA3 localisation to explant axons was demonstrated (section 5.2.4), suggesting that ephrin-A5-Fc was possibly detecting axonal-EphA3.

5.2.2 A sub-population of trigeminal ganglion axons are sensitive to substratum bound ephrin-A5

Chapter 3 demonstrated similar expression patterns for *ephrin-A2* and *-A5* in the target regions, implying similar and/ or redundant biological roles for these two ligands *in vivo* (Klein, 1999). Biochemically, both ephrin-A2 and -A5 have similar binding affinities for EphA3 (Flanagan and Vanderhaeghen, 1998; Lackmann *et al.,* 1997; Wimmer-Kleikamp

et al., 2004), thereby extenuating the use of ephrin-A5-Fc to mimic target ephrin-A interactions with trigeminal ganglion expressed EphA3 *in vitro*.

The behaviour of axons from stage 20 ganglionic explants to ephrin-A5-Fc was assayed using the substratum choice assay. Previously, axon behaviour at the substratum border was categorised as being "non-responsive" (i.e. growing into the substrate) or "responsive" (i.e. axons stopping or turning at the border) (Birgbauer *et al.,* 2001). Axons were demonstrated to be responsive to the substrate if there were repulsive Eph/ ephrin interactions. Therefore, the same criteria were used in this study (Figure 5.2).

The importance of cell-cell contact for Eph receptor activation is highlighted by the requirement for interactions with oligomeric membrane-attached ligands *in vivo* (Davis *et al.,* 1994). *In vitro*, *in vivo* conditions can be mimicked by artificially oligomerising (clustering) soluble dimeric Fc-fusion ligands with an anti-Fc fusion antibody (Davis *et al.,* 1994) (Figure 5.4). It has been demonstrated that artificially clustering Fc-fusion proteins in this manner can activate Eph receptors (Davis *et al.,* 1994), and can exert biologically relevant effects (Wang and Anderson, 1997). Clustering of the dimeric Fc-fusion ligand protein is proposed to lead to tetramer ligand formation, and facilitate higher order oligomerisation, thereby leading to enhanced receptor activation (Davis *et al.,* 1994; Himanen and Nikolov, 2002; Lackmann *et al.,* 1998; Smith *et al.,* 2004; Wimmer-Kleikamp *et al.,* 2004) (Figure 5.4). For these reasons, 5 μg/ml ephrin-A5-Fc was pre-clustered prior to use in the assay with an anti-Fc antibody. Additionally, 5 μg/ml pre-clustered ephrin-A5-Fc has been shown to exert a biological effect on growing axons (Weinl *et al.,* 2003; Wimmer-Kleikamp *et al.,* 2004).

Figure 5. 3 EphA receptor expression is maintained by cultured whole trigeminal ganglia.
(A-B) Stage 20 explants grown for 24 hours with Control-Fc (A), and ephrin-A5-Fc (B). (A'-B') Images (A-B) merged with anti-neurofilament (NFM) staining (red). (A"-B") Higher magnification images from (A'-B'). (B") Arrowheads: ephrin-A5-Fc binding to axons (orange-yellow).
Scale: 100 μm (A-B); 50 μm (A'-B').

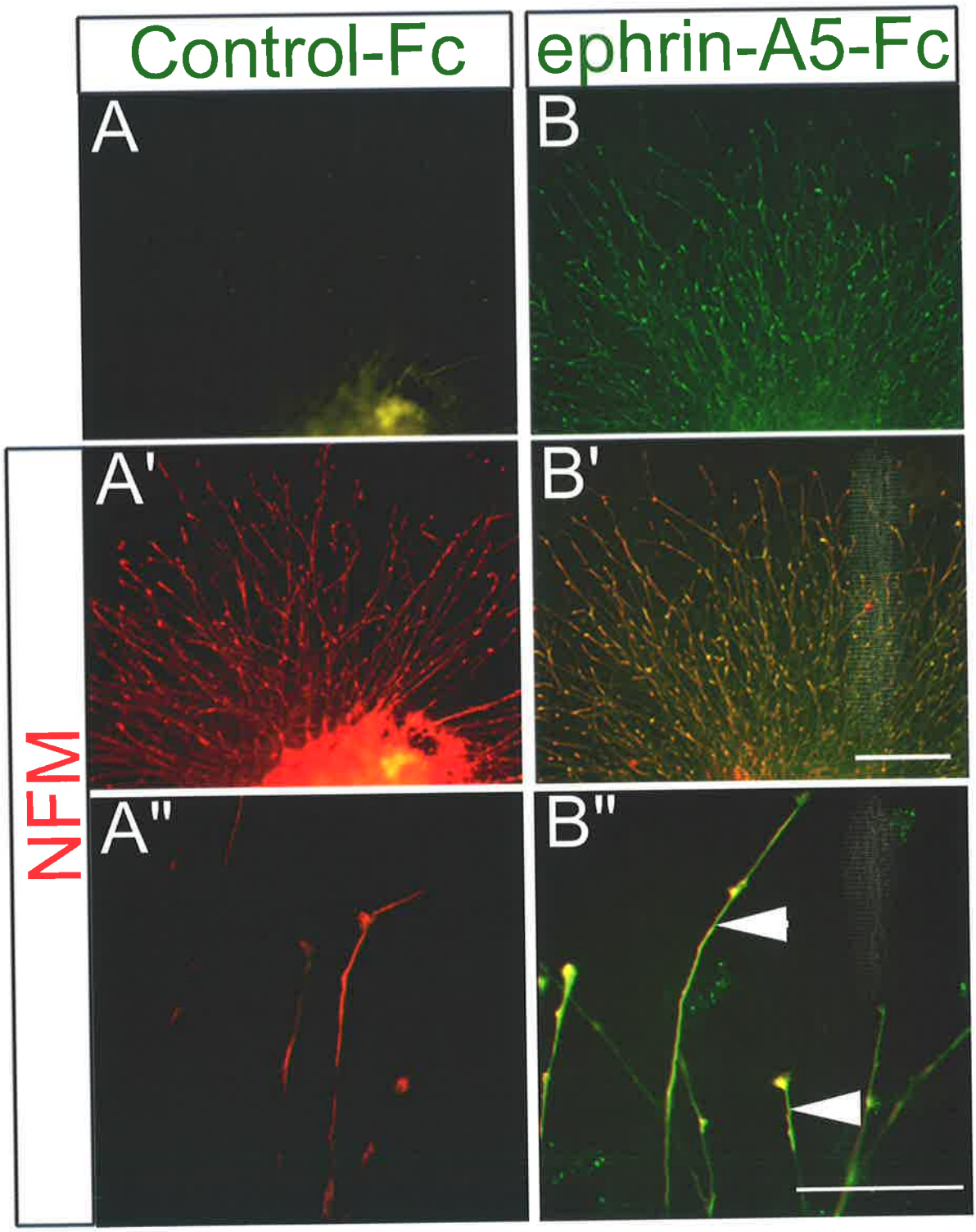
Control-Fc
ephrin-A5-Fc
A
B
A'
B'
A"
B"
NFM

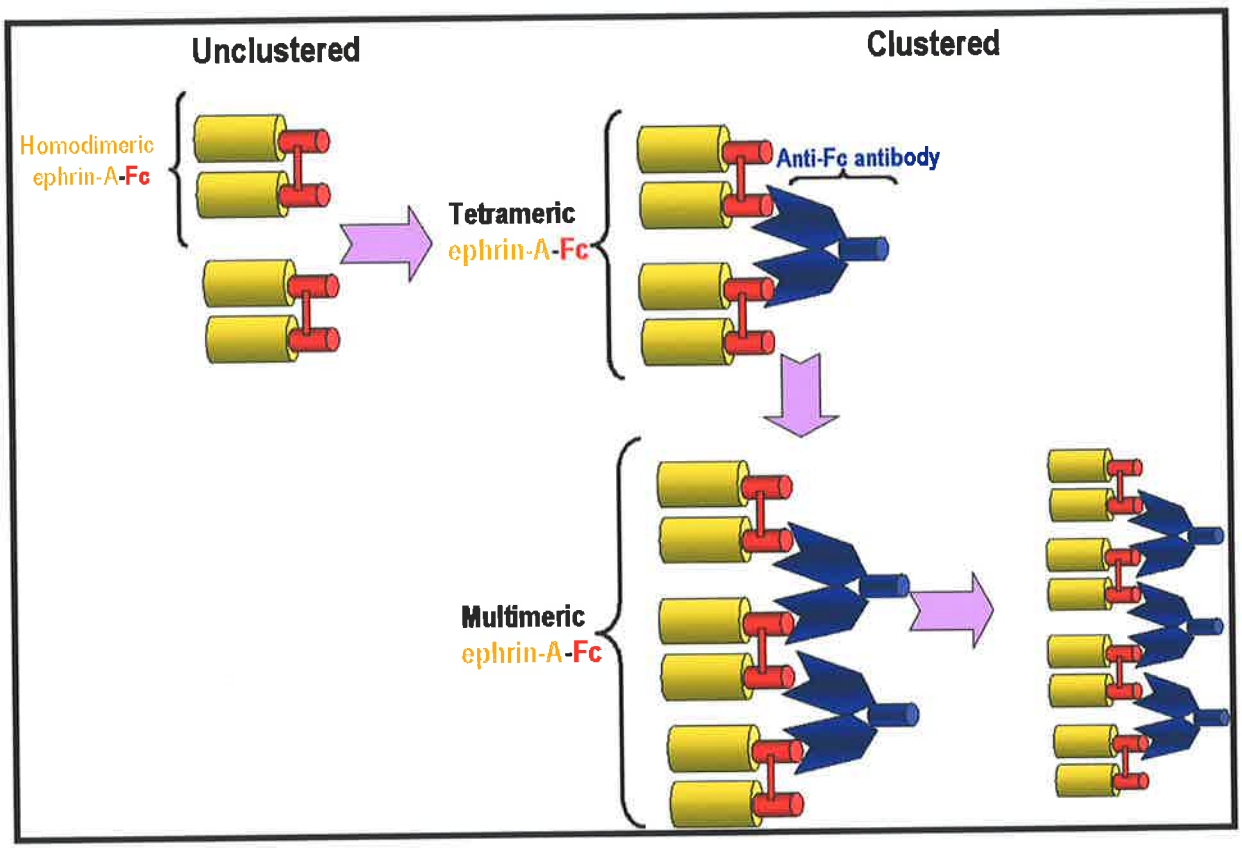

Figure 5.4 A schematic illustrating Fc-fusion clustering.

The schematic focuses on ephrin-A-Fc clustering, although the same principles apply for EphA-Fc clustering. The mature ephrin-A-Fc (yellow-red) chimera is a homodimeric protein, consisting of two fusion proteins linked by a disulphide bond. Clustering of ephrin-A-Fc with an anti-Fc antibody (blue) results in tetrameric and multimeric forms, which cause strong activation of receptors.

To demonstrate specificity of ephrin-A5-Fc in the assay, the behaviour of axons to control-Fc substrate was firstly analysed. Trigeminal ganglion axons that encountered a pre-clustered control-Fc (5 μg/ml) substrate, showed uninhibited growth into the region (Figure 5.5A-A'). Only 52/ 325 axons were found to stop or turn away at the control-Fc border. The total mean axon response and the % mean axon response/ explant were found to be 15.54% and 22 ± 5% for control-Fc. In contrast, ephrin-A5-Fc elicited a stop or turn response on trigeminal ganglion axons (112/ 240 axons) (Figure 5.5B-B'). The total axon response, and mean axon response/ explant were 46.67% and 49 ± 4% respectively, and reached statistical significance when compared with control-Fc ($p < 0.001$; Mann-Whitney U test) (Figure 5.5). These data suggested that a population of axons from whole trigeminal ganglion explants were sensitive to ephrin-A5-Fc.

5.2.3 Trigeminal ganglion ophthalmic lobe axons are sensitive to substratum-bound ephrin-A5

In an attempt to identify the sub-population of ephrin-A5-Fc sensitive axons from whole trigeminal ganglion explants (Figures 5.5), the response of ophthalmic and maxillomandibular lobe explants to pre-clustered ephrin-A5-Fc (5 μg/ml) was quantitated using the substratum choice assay (Figure 5.6). The *in vivo* expression results from chapter 3 revealed that *ephrin-A2* and *-A5* were not expressed in the ophthalmic process (Chapter 3). Furthermore, the ophthalmic lobe was previously demonstrated to express higher levels of EphA3 receptor compared to the maxillomandibular lobe (Chapter 4). This hinted that ephrin-A5 responsive axons were of ophthalmic lobe origin.

Axons from ophthalmic and maxillomandibular explants that encountered 5 μg/ml control-Fc borders grew uninhibited into the substrate (Figures 5.6A and 5.6B). The number of axons that responded was 77 axons ($n = 645$ axons) for ophthalmic lobe explants, and 71 axons ($n = 477$ axons) for maxillomandibular lobe explants. The total mean axon response for ophthalmic and maxillomandibular axons avoiding control-Fc was 11.94% and 14.88% respectively; the mean axon response/ explant was 13 ± 3% for ophthalmic lobe explants and 16 ± 3% for maxillomandibular lobe explants. There were no significant differences between the controls for the two trigeminal ganglion lobes ($p > 0.05$; student t-test) (Figure 5.7).

Figure 5. 5 A population of trigeminal ganglion axons respond to ephrin-A5-Fc.

(A-B) Substratum choice assay with control-Fc (A), and ephrin-A5-Fc (B). (A'-B') High magnification images from (A-B). Asterisk: substratum. (B-B') Dotted line: ephrin-A5 substrate border. All explants were stained with anti-neurofilament (NFM) and images shown are of representative explants.
(C) Quantitation of % mean axon (stop/ run) response/ explant to either control-Fc or ephrin-A5-Fc conditions. n = number of explants which are indicated in brackets. $^{*} = p < 0.001$ (Mann-Whitney U-test). All values are mean ± SEM.
Scale: 200 μm (A-B); 50 μm (A'-B').

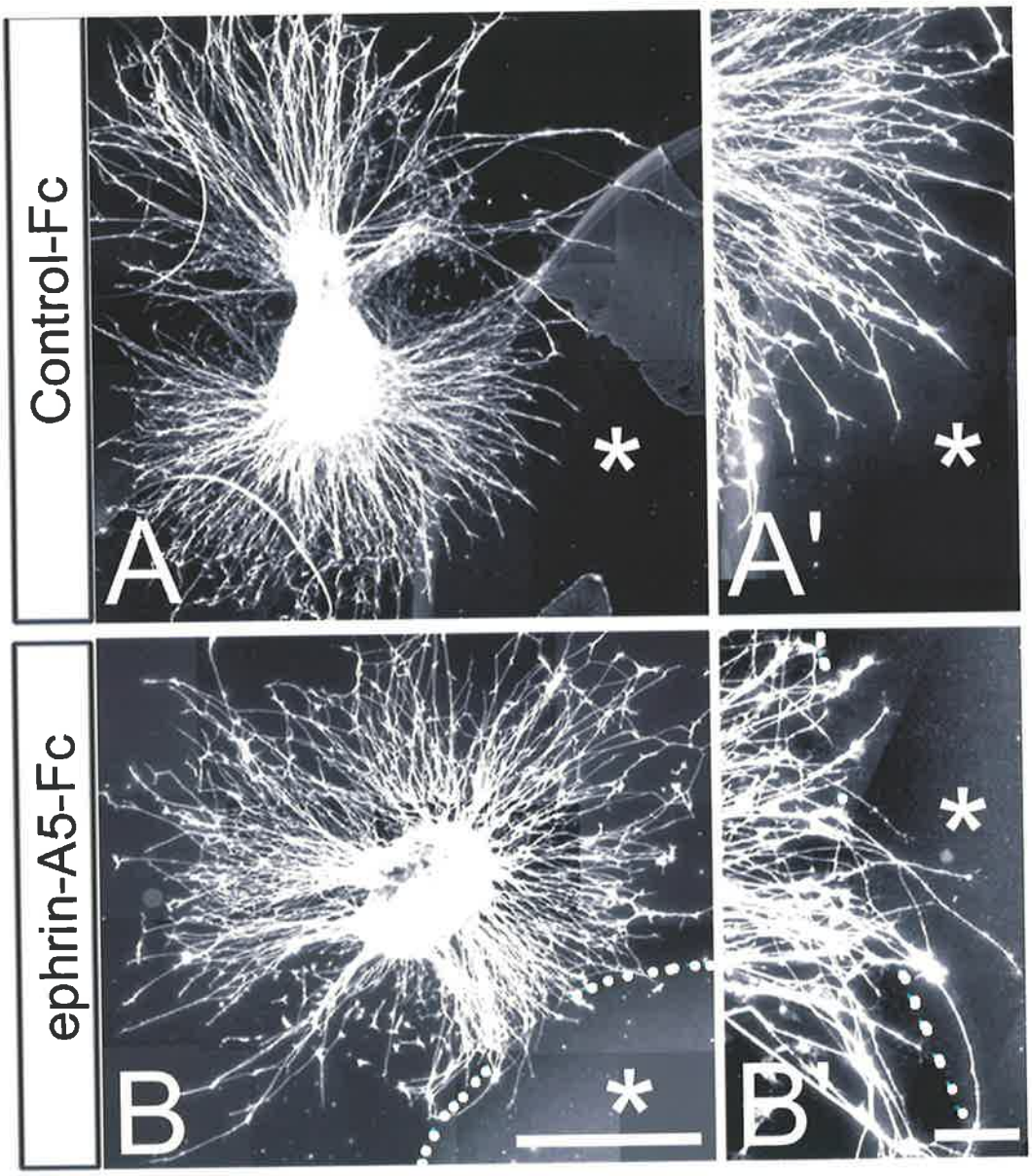
Control-Fc
A
A'
*
*
ephrin-A5-Fc
B
B'
*
*

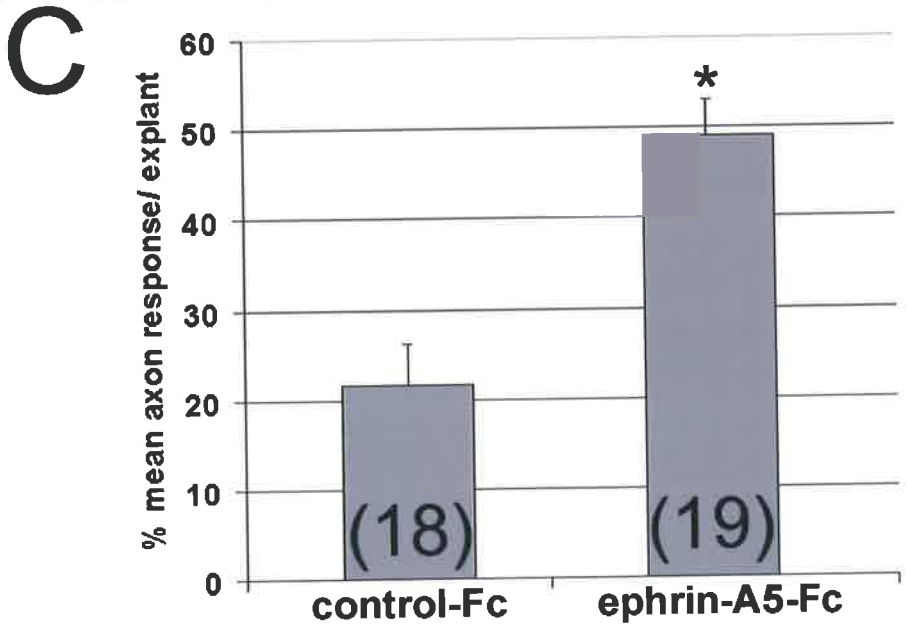
C
% mean axon response/ explant
60
50
40
30
20
10
0
*
(18)
(19)
control-Fc
ephrin-A5-Fc

However, the majority of ophthalmic axons avoided ephrin-A5-Fc substrate (332 responsive axons of 550 axons; Figure 5.6C-C'), with a total mean axon response of 60.38% and a mean axon response/ explant of 69 ± 5% ($p < 0.0001$ compared to control; student t-test) (Figure 5.7). In contrast, maxillomandibular axons grew uninhibited into ephrin-A5-Fc (138 responsive axons of 766 axons; Figure 5.6D-D'), with a total mean axon response of 18.02% and a mean axon response/ explant of 21 ± 2%. The total mean axon response and mean axon response/ explant for maxillomandibular axons encountering ephrin-A5-Fc was not significantly different from those axons encountering control-Fc ($p > 0.05$; student t-test) (Figure 5.7).

Ephrin-A5-Fc was found to significantly prevent the growth of ophthalmic axons into the substrate compared with maxillomandibular axons ($p < 0.0001$; student t-test) (Figure 5.7). This raised the possibility that the majority of ephrin-A5 sensitive axons from whole trigeminal ganglion explants might have been of ophthalmic lobe origin. It is noteworthy that the average of the combined % mean axon response/ explant for the two trigeminal ganglion lobes (~ 45 %; Figure 5.7) is similar to the % mean axon response/ explant observed with whole trigeminal ganglion explants (~ 49 %) to ephrin-A5-Fc (Figure 5.5). In summary, ophthalmic lobe explant axons are sensitive to ephrin-A5-Fc compared to maxillomandibular lobe explant axons.

Figure 5. 6 Substratum bound ephrin-A5-Fc exerts differential effects on growing axons from ophthalmic (TGop) versus maxillomandibular (TGmm) lobe explants.

(A-D) Substratum choice assay with control-Fc (A, B) and ephrin-A5-Fc (C, D) performed for TGop (A, C) or TGmm (B, D) lobe explants. Images are of representative explants. Asterisk: substratum. Dotted outline: substratum border. Explants are stained with anti-neurofilament (NFM).

(C'-D') Higher magnification view of images in (C) and (D) respectively. (C') Arrowheads: axons that appear to turn. Arrows: axon that appears to have stopped.

Scale: 100 μm (A- D).

TGop
TGmm
Control-Fc
ephrin-A5-Fc
A
B
C
D
TGop
TGmm
C'
D'

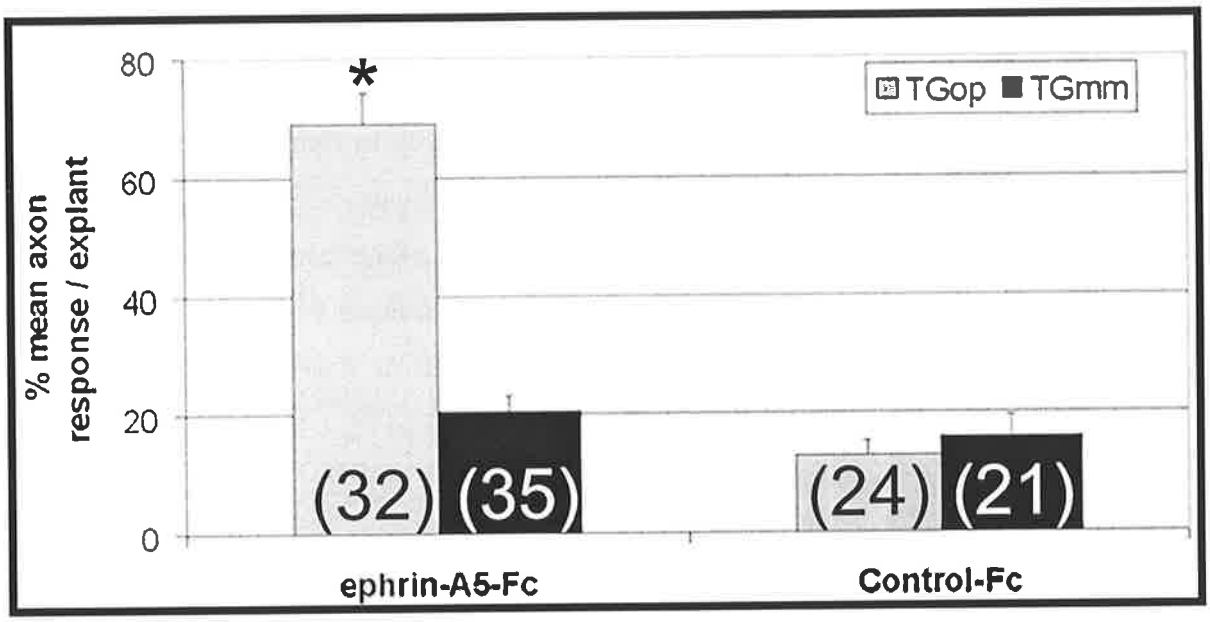

Figure 5. 7 Quantitation of % mean axon (stop/ turn) response/ explant for separated trigeminal ganglion lobe explants on ephrin-A5-Fc or control-Fc.

TGmm, maxillomandibular lobe; TGop, ophthalmic lobe. n = number of explants (indicated in brackets). * = $p < 0.0001$ (significance compared to TGmm ephrin-A5-Fc and TGop control-Fc; Student t-test). All values are mean ± SEM.

5.2.4 Axons and growth cones from Ophthalmic and maxillomandibular lobe explants express EphA3

Chapter 4 suggested that the trigeminal ganglion expressed EphA3. To verify this, the expression of the receptor was confirmed in separated ganglionic explant cultures (Figures 5.8 and 5.9). As a negative control, explants were stained without anti-EphA3 antibody, and very little background staining due to the secondary anti-goat antibody was demonstrated (Figure 5.8A-A'). Neuronal immunoreactivity to EphA3 was demonstrated when explants were stained with anti-β-tubulin (TuJ1) (Figure 5.8B, 5.8C'-D') and anti-EphA3 (Figure 5.8B', 5.8C-D') antibodies. Importantly, axons from ophthalmic explants appeared to express higher levels of EphA3 compared to those from maxillomandibular explants (Figure 5.8C-D), which was in agreement with *in vivo* evidence for the two trigeminal ganglion lobes (Chapter 4).

Finally, closer inspection of ophthalmic growth cones appeared to show more EphA3 protein localisation compared to maxillomandibular growth cones (compare Figure 5.9A-B with Figure 5.9C-D). Preliminary analysis of anti-EphA3 growth cone intensity revealed that ophthalmic growth cones had a significantly greater mean intensity (0.62 ± 0.07) compared with maxillomandibular growth cones (0.24 ± 0.03) ($p < 0.001$; Mann-Whitney U test; Figure 5.10). Also, EphA3 puncta could be visualised on filopodia of growth cones (Figure 5.9), consistent with a role for this receptor during axon guidance. Together, all results point to the possibility that differential lobe sensitivity to ephrin-A5-Fc *in vitro* (Figure 5.5 and 5.6) is likely due to the differential expression of EphA3 at the level of the growth cone.

Figure 5. 8 EphA3 expression is maintained in trigeminal ganglion lobe explants after 24 hours *in vitro*.
(A-B') Explants stained without primary anti-EphA3 (A-A') or with anti-EphA3 (B'). (A-A') Bright field (A) and fluorescent image (A') of no primary control indicate little background staining. (B-B') Ophthalmic (TGop) explant stained with anti-TuJ1 (B) and anti-EphA3 (B'). Arrows: axonal staining (B-B').
(C-D) Axons from TGop (C) and maxillomandibular (TGmm) (D) explants express EphA3. (C'-D') Images (C-D) merged with anti-TuJ1 staining (red) pattern. Arrowheads: axonal EphA3 expression. Note that EphA3 staining of TGop axons appear to be more intense compared to TGmm axons. Brightness-contrast adjusted equally.
Scale: 100 μm (A- B); 50 μm (C-D).

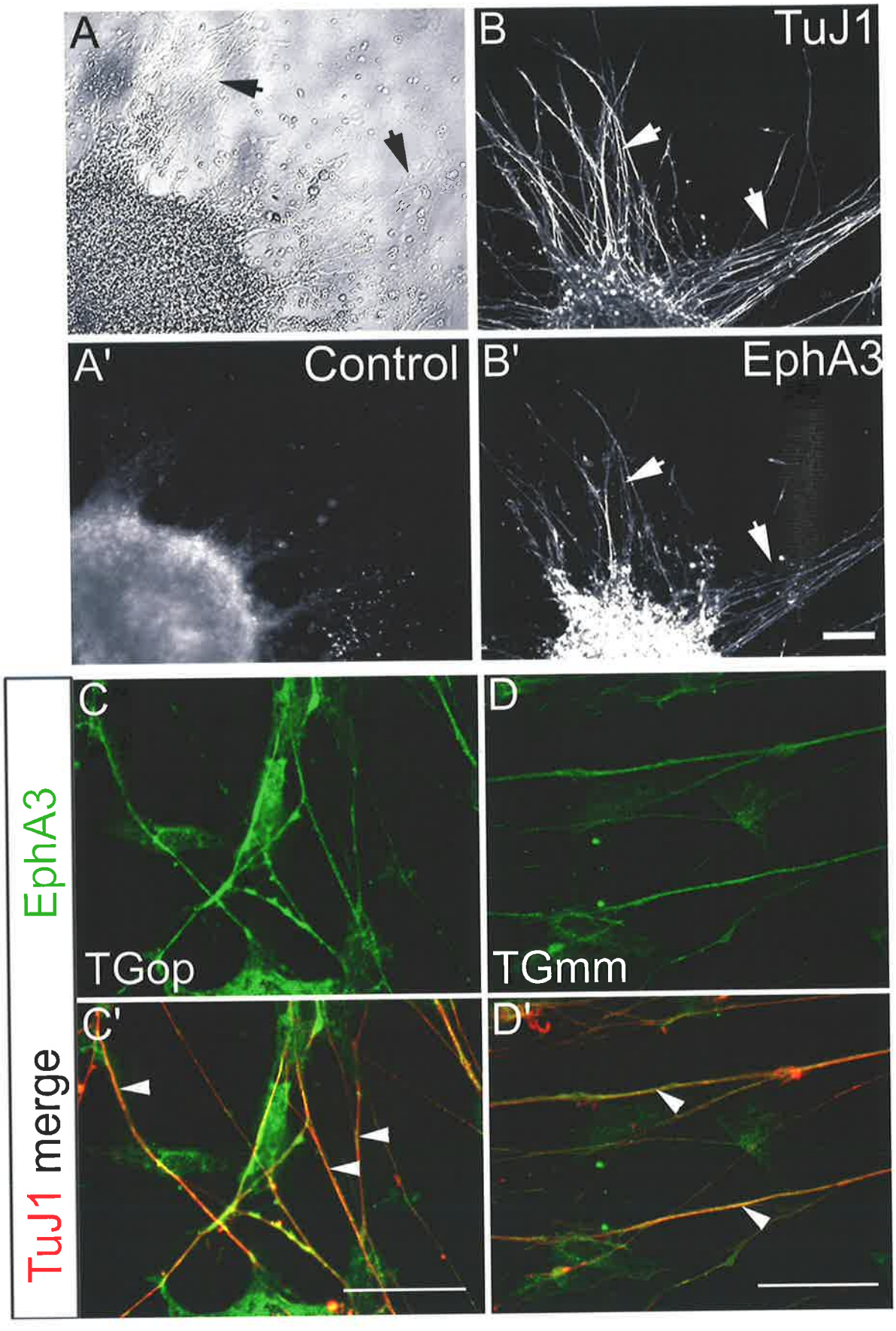
A
B
TuJ1
A'
Control
B'
EphA3
C
D
EphA3
TGop
TGmm
C'
D'
TuJ1 merge

Figure 5. 9 Trigeminal ganglion lobe growth cones in culture appear to differentially express EphA3.

(A-D) Ophthalmic (TGop) (A-B), and maxillomandibular (TGmm) (C-D) growth cones stained with anti-EphA3. (A'-D') Images (A-D) merged with anti-TuJ1 staining (red) pattern. EphA3 and TuJ1 co-localisation is in yellow-orange. Images are representative, taken at the same exposure time, and brightness-contrast adjusted identically. Arrowheads: EphA3 puncta are distributed along the filopodia.
Scale: 10 μm (A- D).

TGop
TGmm
A
EphA3
A'
EphA3
TuJ1
B
EphA3
B'
EphA3
TuJ1
C
EphA3
C'
EphA3
TuJ1
D
EphA3
D'
EphA3
TuJ1

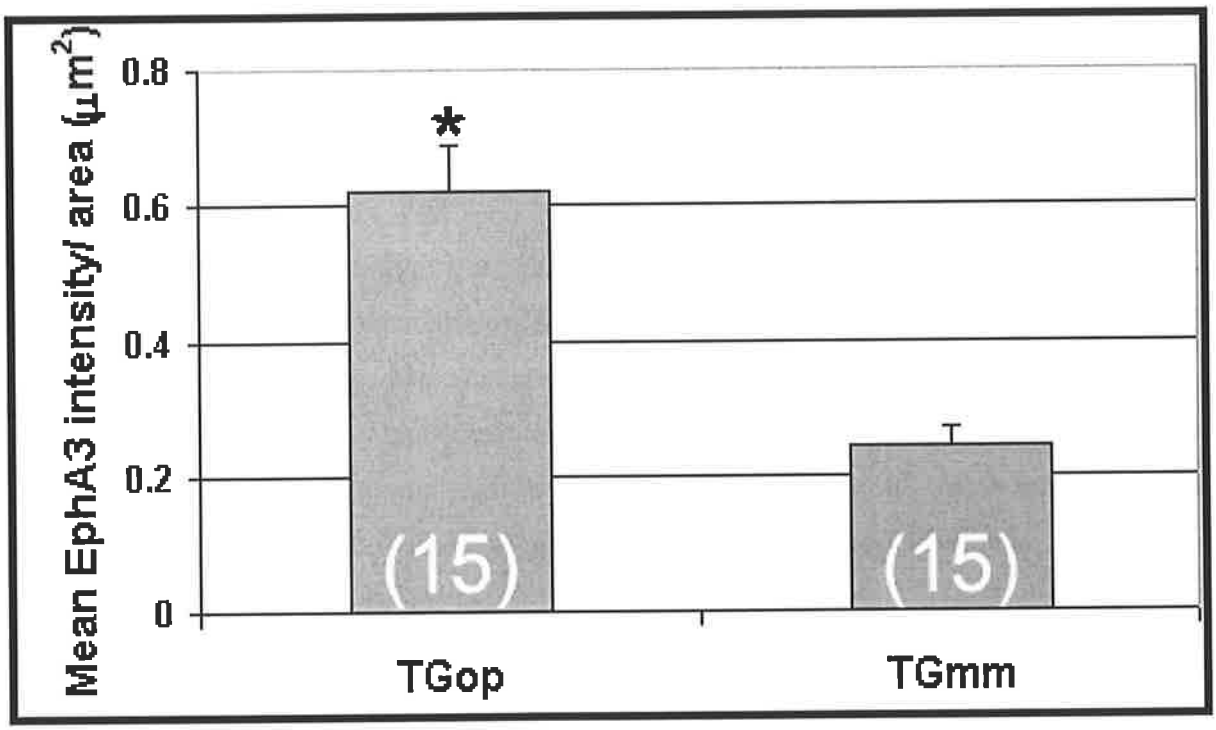

Figure 5.10 Preliminary comparison of EphA3 growth cone intensity between ophthalmic (TGop) and maxillomandibular (TGmm) explants.

Results were derived from 2 experiments. n = number of growth cones analysed (shown in brackets). * = $p < 0.001$ (Mann-Whitney U-test). All values are mean ± SEM.

5.3 Summary and discussion

The previous chapter (Chapter 4) established that EphA3 and ephrin-A5 were expressed during trigeminal ganglion development. The functional significance of these two proteins during trigeminal ganglion axon guidance was assessed in a substratum choice *in vitro* assay. The results from this chapter implicate EphA3 forward signalling in mediating ophthalmic axon sensitivity to substratum bound ephrin-A5. In contrast, EphA3 forward signalling in maxillomandibular axons did not appear to exert a response upon contact with ephrin-A5-Fc.

5.3.1 Ephrin-A5 as a guidance cue

Some ophthalmic growth cones of axons encountering ephrin-A5-Fc appeared to show turning, demonstrating that ephrin-A5 could cause growth cone/ axon turning, and possibly act as a guidance cue. Previously, elegant experiments with ephrin-A5-Fc coated beads demonstrated that ephrin-A5 could act as a guidance cue and cause the turning of growth cones (Weinl *et al.,* 2003). Also it was shown that this "smooth" turning effect of retinal ganglion axons away from ephrin-A5-Fc was due to partial collapse of the growth cone (Weinl *et al.,* 2003). Therefore, the *in vitro* results from this study, although not observed with time-lapse video-microscopy, would be consistent with the findings from Weinl *et al.,* (2003). It will be interesting to determine whether ophthalmic growth cones undergo partial growth cone collapse when interacting with ephrin-A5. Furthermore, since some ophthalmic axons appeared to stop at the ephrin-A5-Fc border, this would indicate that ephrin-A5 could act as a "stop" signal. In support of this, presenting ephrin-A5-Fc coated beads to retinal ganglion growth cones causes some to undergo full growth cone collapse (Weinl *et al.,* 2003). Therefore, further elucidation of ophthalmic growth cone behaviour at the ephrin-A5-Fc border in conjunction with time-lapse video microscopy is required. *In vivo*, it is likely that ephrin-A5 function as both a guidance cue (i.e. cause partial growth cone collapse and turning) and a stop signal (i.e. cause full growth cone collapse and retraction) to ophthalmic axons, thereby preventing ophthalmic axons from invading non-target tissue regions.

5.3.2 Ephrin-A5-Fc and the differential guidance of ophthalmic versus maxillomandibular lobe axons

The target region for the ophthalmic lobe axons, the ophthalmic process, was not positive for *ephrin-As* from stage 13 through to 20 (Chapter 3); however, expression was observed in the maxillomandibular lobe targets (the maxillary and mandibular processes). This hinted that ephrin-As may differentially guide trigeminal ganglion axon projections from the two lobes during chick embryo development. In other words, mesenchymal ephrin-A2/-A5 in the first branchial arch was repulsive to ophthalmic axons, whilst supporting the growth of maxillomandibular axons. Consistent with this idea, a differential sensitivity to substratum-bound ephrin-A5-Fc was demonstrated with ophthalmic and maxillomandibular lobe axons (Figure 5.11).

When whole trigeminal ganglia were explanted near ephrin-A5-Fc substrate, only a sub-population of axons (about 50%) showed sensitivity to ephrin-A5. This would be consistent with the separated trigeminal ganglion lobe explant analysis, if the population of axons responding to ephrin-A5-Fc were of ophthalmic lobe origin. To further substantiate that this is the case, it may be necessary to retrograde label the ophthalmic lobe axon population *in vivo* with a lipophilic dye prior to harvesting whole explants at stage 20 and performing the ephrin-A5-Fc substratum assay.

Concerning the differential sensitivity of ophthalmic axons to ephrin-A5-Fc compared with maxillomandibular lobe axons, differential trigeminal ganglion lobe EphA3 expression is likely to be the explanation. A number of lines of evidence point to this notion. Firstly, real-time PCR showed an approximate 4-fold differential expression of *EphA3* between the two lobes at stage 20 (Chapter 4). Secondly, there was greater expression of protein and transcript in the ophthalmic lobe (Chapter 4). Finally, consistent with this idea, EphA3 immunostained ophthalmic growth cones appeared to express the receptor at a higher level compared to maxillomandibular growth cones. Therefore, the sensitivity of ophthalmic axons to substratum ephrin-A5-Fc *in vitro* could be explained by the higher expression of EphA3 on these axons. Collectively, the *in vitro* and *in vivo* results provide evidence for EphA3 forward signalling in mediating ophthalmic axon responsiveness to ephrin-A5-Fc (Figure 5.11).

If EphA3 forward signalling is responsible for mediating ophthalmic axon responsiveness to ephrin-A5-Fc, then comparing the phosphorylation states and levels of ophthalmic and maxillomandibular-EphA3 following ephrin-A5-Fc stimulation *in vitro* may be insightful. In expressing higher levels of EphA3, a greater level of receptors on ophthalmic neurons may become strongly tyrosine phosphorylated following ephrin-A5-Fc binding; this may also correlate with increased EphA3 forward signalling and ephrin-A5-Fc avoidance. Previous studies have revealed induced tyrosine phosphorylation of Eph receptors following cognate ligand binding (Brambilla *et al.,* 1996; Davis *et al.,* 1994; Gale *et al.,* 1996; Huynh-Do *et al.,* 1999). Furthermore, the tyrosine phosphorylated receptor sites facilitate docking of adapter proteins that relay signals intracellularly (Hock *et al.,* 1998; Holland *et al.,* 1997). Thus, increased tyrosine phosphorylation of ophthalmic growth cone EphA3 may lead to greater recruitment of adaptor proteins, and therefore increased intracellular signalling to the growth cone cytoskeleton.

In vivo examination of EphA3 activation may also provide a better understanding of the differential responses of these trigeminal ganglion axon populations to ephrin-A ligands. For this purpose, an anti-phosphorylated Eph antibody (Shamah *et al.,* 2001) could be used to immunofluorescently detect phosphorylated EphA3 receptors localised to ophthalmic and maxillomandibular axons at stages 15 and 20 during axon pathfinding. If high EphA3 activation leads to ophthalmic axon repulsion from non-target ephrin-As, then this anti-phosphorylated Eph antibody should bind predominantly to ophthalmic axons.

Despite the *in vitro* data presented here, strong evidence for the importance of putative repulsive interactions between ophthalmic axon-EphA3 and non-target field first branchial arch ephrin-A ligands in the in directing ophthalmic axons into the ophthalmic process requires elucidation *in vivo* (refer to section 7.3 of chapter 7).

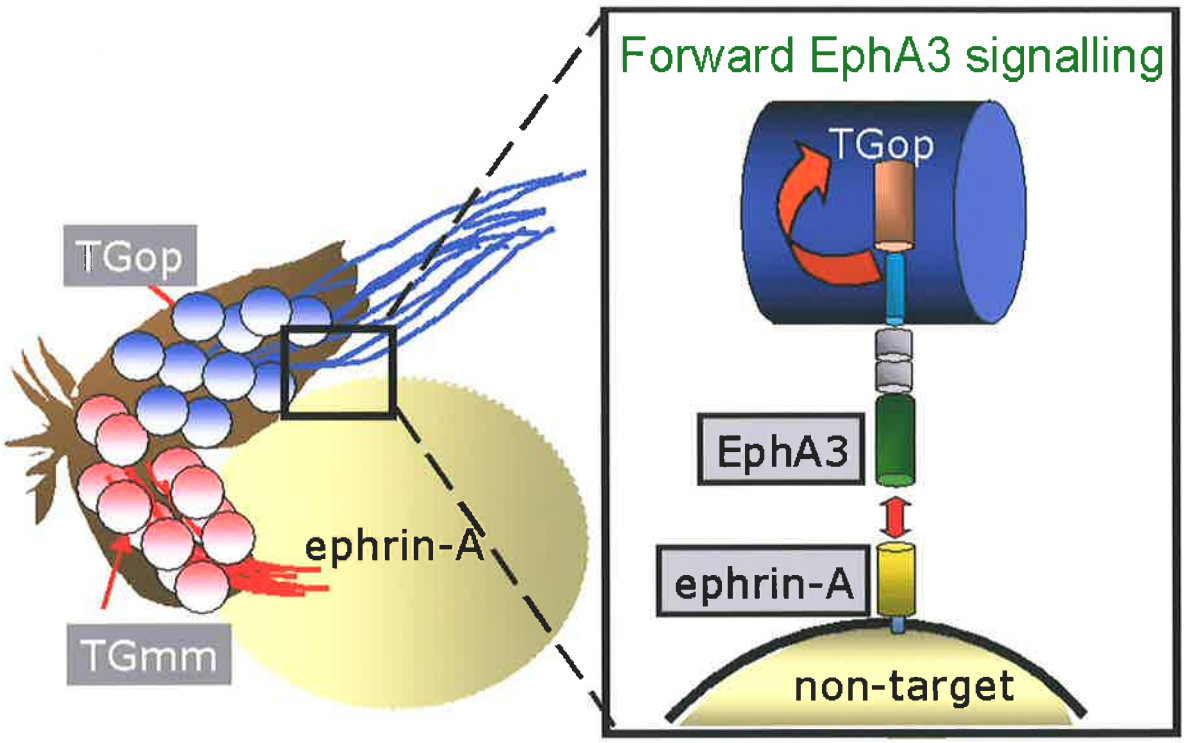

Figure 5. 11 A schematic model showing how ophthalmic (TGop; blue) versus maxillomandibular (TGmm; red) axon branches may be guided during development. There is differential expression of ephrin-As in the trigeminal ganglion target fields, with ephrin-As being exclusively expressed in the first branchial arch. During axon pathfinding, TGop axons and growth cones express higher levels of EphA3 compared to TGmm axons/ growth cones. This leads to TGop axons becoming repelled from ephrin-As being expressed in the non-target. Boxed region demonstrates the interaction between EphA3 on the TGop axon (blue) and ephrin-As in the non-target (double headed red arrow). Upon engagement with ephrin-As, TGop expressed EphA3 may transmit a repulsive signal (red arrow) intracellularly. The resulting signal in these axons/ growth cones may cause either in full growth cone collapse and retraction, or partial growth cone collapse and steering of axons away from the non-target.

5.3.3 EphA3 expressing maxillomandibular axons are not responsive to ephrin-A5-Fc

How could a lack of sensitivity of maxillomandibular axons to ephrin-A5-Fc be reconciled with the observed expression of EphA3 (shown both *in vitro* and *in vivo*) by maxillomandibular axons? Also *in vivo*, EphA3 positive maxillomandibular axons grow into ephrin-A2/ -A5 mesenchyme in the first branchial arch. These observations could be explained if EphA3 receptors on these axons had become desensitised.

The first line of evidence is provided by ephrin-A5-Fc *in situ* staining of whole embryos (Chapter 3). As previously mentioned, fusion protein binding to endogenous EphAs could be compromised if these receptors are already involved in interactions with endogenous ligands (Flenniken *et al.,* 1996; Hornberger *et al.,* 1999; Yin *et al.,* 2004). Since, trigeminal ganglion axons co-express ephrin-A5 as well (Chapter 4), evidence for ganglionic EphA3/ephrin-A5 interactions is supported by the inability of ephrin-A5-Fc to stain maxillomandibular lobe EphA3 in whole-mount embryos. *Cis*-interactions, which occur between receptors and ligands co-expressed on the same cell, were found recently to reduce EphA activation by *trans*-expressed ligands (Yin *et al.,* 2004). Furthermore, in the visual system, *cis*-interactions between co-expressed ephrin-As and EphAs are predicted to make EphA expressing nasal retinal ganglion cell (RGC) axons insensitive to high ephrin-A expression in their target, the posterior tectum (Hornberger *et al.,* 1999; Yin *et al.,* 2004).

Another factor for maxillomandibular axon insensitivity could be related to the level of axonal EphA3 expression (Chapter 4 and 5) and thus the level of EphA3 recruitment into signalling clusters. This is implied by the observation that nasal RGCs in the visual system express very low levels of EphA receptors compared to temporal RGCs, whilst co-expressing high levels of ephrin-As (Cheng *et al.,* 1995; Feldheim *et al.,* 1998). Analysis of EphA3/ephrin-A5 interactions using a functional mutagenesis screen has provided substantial evidence for sites on EphA3 that facilitate Eph/ephrin dimerisation, hetero-tetramerisation and "cluster polymerisation" (Smith *et al.,* 2004). As a consequence, the size of clusters would depend on the local Eph and ephrin density and the strength of Eph signalling would be proportional to the level of Eph/ephrin clustering (Hansen *et al.,* 2004;

Holmberg *et al.,* 2000; Klein, 1999; Smith *et al.,* 2004). Furthermore, high order clustering is often correlated with repulsive signalling (Hansen *et al.,* 2004; Holmberg *et al.,* 2000). Therefore one can envisage that maxillomandibular axons may behave in a similar manner to nasal RGC axons in their respective target fields. The low expression of EphA3, together with *cis*-interactions of these receptors with co-expressed ephrin-A5 on maxillomandibular axons may not lead to the efficient recruitment of these receptors into higher order clusters upon *trans*-interactions with ephrin-A5-Fc. A comparison of *EphA3* and *ephrin-A5* transcript levels within the maxillomandibular lobe further substantiates this view because real-time PCR revealed that *ephrin-A5* was expressed at a greater level compared to *EphA3* (1: 5 *EphA3: ephrin-A5* ratio). To elucidate whether EphA3/ ephrin-A5 *cis*-interactions contribute to maxillomandibular axons insensitivity to ephrin-A5-Fc substrate, EphA3/ ephrin-A5 *cis*-interactions may need to be blocked. One approach would be to enzymatically treat maxillomandibular axons during the course of the substratum assay with PI-PLC, which enzymatically sheds cells membranes of GPI-linked proteins, including ephrin-A ligands. In removing ephrin-A5 with PI-PLC, the number of maxillomandibular EphA3 receptors able to part-take in *trans*-interactions with ephrin-A5-Fc are predicted to increase, rendering maxillomandibular axons sensitive to ephrin-A5-Fc.

An alternative explanation as to why EphA3 positive maxillomandibular axons do not respond to ephrin-A5-Fc could be attributed to differences in downstream EphA3 signalling components in maxillomandibular axons compared to ophthalmic axons. Perhaps, neuronal EphA3 signalling could selectively promote maxillomandibular axon adhesion/ neurite extension and this is not without precedent. Tiam1, a guanine-nucleotide exchange factor of Rac1, can interact with EphA2 and promotes EphA2 forward signalling induced neurite extension *in vitro* (Tanaka *et al.,* 2004). Hence it maybe necessary to determine if Tiam1 is a downstream EphA3 signalling effector in maxillomandibular axons *in vivo*, and using pharmacological inhibitors to Rac1 may prevent maxillomandibular axon growth on ephrin-A5-Fc *in vitro*. Although EphA3 induced neurite extension cannot be excluded, the parallels between maxillomandibular axons and nasal RGC axons strongly suggest ganglionic *cis*-interactions as a likely reason for the observed maxillomandibular axon insensitivity to ephrin-A5-Fc.

The likely significance of EphA3 signalling *in vivo* in maxillomandibular axons could be in mediating axon fasciculation rather than during axon pathfinding (Figure 5.12). In support of this, EphAs and ephrin-As play a role during motor axon fasciculation (Eberhart *et al.*, 2000) and *in vitro* induces cortical neurite fasciculation through repulsive EphA/ephrin-A interactions (Caras, 1997). It may be that other families of guidance cues play a major role in guiding maxillomandibular axons to their target fields (refer to section 7.2 of Chapter 7).

5.3.4 Conclusion

The differential expression of EphA3 in the trigeminal ganglion lobes (Chapter 4), together with the observed differential response to ephrin-A5-Fc by ophthalmic and maxillomandibular lobe explant axons suggest that EphA3/ ephrin-A5 interactions may play a role during trigeminal ganglion lobe specific guidance.

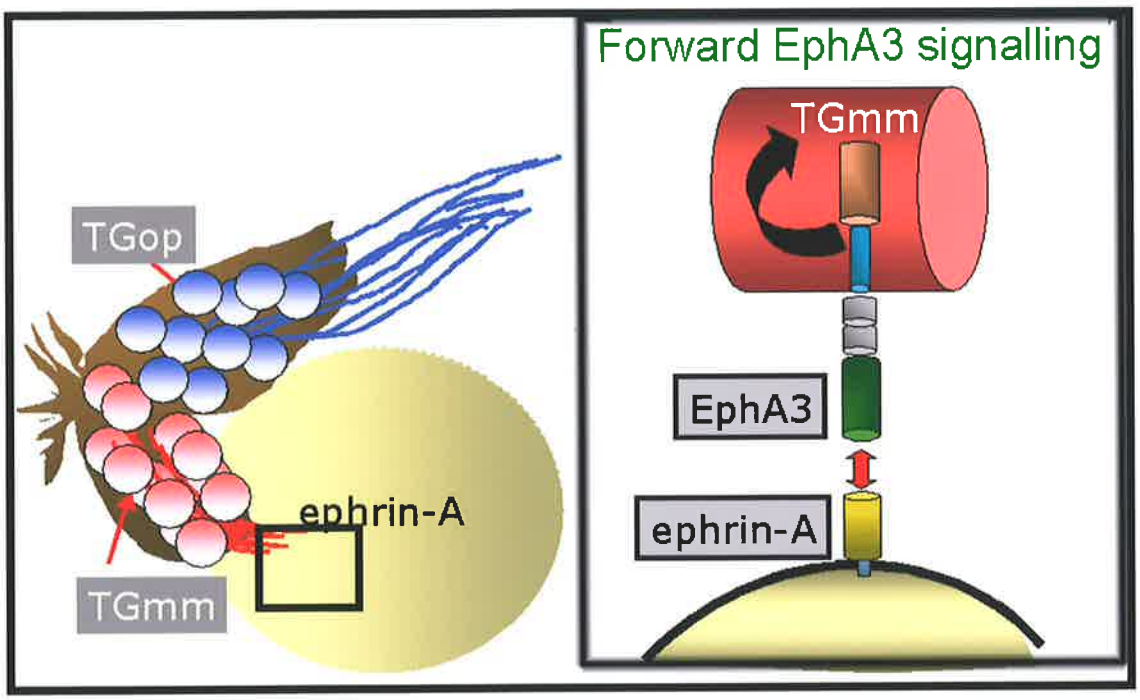

Figure 5.12 A schematic model showing the role of EphA3 forward signalling during maxillomandibular (TGmm; red) axon fasciculation during development.
Ephrin-As are expressed exclusively in the first branchial arch (yellow oval). During axon pathfinding, TGmm axons and growth cones express low levels of EphA3 compared to ophthalmic (TGop) axons/ growth cones. Therefore, TGmm axons do not become repelled from ephrin-As being expressed in the target. Boxed region demonstrates the interaction between EphA3 on the TGmm axon (red) and ephrin-As in the target (red double headed arrow). Upon engagement with ephrin-As (double headed red arrow), TGmm expressed EphA3 transmits a weak signal sufficient to cause axon fasciculation (black arrow).

Chapter 6: *In vitro* analysis of trigeminal ganglion ephrin reverse signalling

"I fully realize that I have not succeeded in answering all of your questions. Indeed, I feel I have not answered any of them completely. The answers I have found only serve to raise a whole new set of questions, which only lead to more problems, some of which we weren't even aware were problems. To sum it all up . . . In some ways I feel we are confused as ever, but I believe we are confused on a higher level, and about more important things".

--Unknown

Chapter 6: *In vitro* analysis of trigeminal ganglion ephrin reverse signalling

6.1 Introduction

As mentioned earlier, GPI-anchored ephrin ligands can participate in Eph kinase independent signalling and have the capacity to transduce intracellular signals through the Src kinase family into the ephrin bearing cells (Chin-Sang *et al.,* 1999; Davy *et al.,* 1999; Davy and Robbins, 2000; George *et al.,* 1998; Huai and Drescher, 2001; Knoll *et al.,* 2001). The downstream consequence of ephrin-A ligand activation was the modulation of integrin function, resulting in changes to cell adhesion and morphology (Davy *et al.,* 1999; Davy and Robbins, 2000; Huai and Drescher, 2001) (Figure 1.10). The trigeminal ganglion was demonstrated to be ephrin-A5 positive for both mRNA and protein in chapters 3 and 4. Hence, it was of interest to determine the functional significance of trigeminal ganglion ephrin-A5 expression. Given the expression of EphA3/ A4 receptors in the trigeminal ganglion target fields (chapter 3), could ephrin-A5 act as a cognate partner to these receptors? To gain an insight into the significance of ganglionic ephrin-A5 expression an *in vitro* approach was taken. This was in the hope that clear hypotheses may be developed prior to *in ovo* electroporation to analyse ephrin-A5 function *in vivo*.

Firstly, to determine whether trigeminal ganglion axonal-ephrin-A5 and EphA receptor interactions were repulsive, the substratum choice assay was utilised (Figure 5.2). Based on the previous data (Chin-Sang *et al.,* 1999; Davy *et al.,* 1999; Davy and Robbins, 2000; George *et al.,* 1998; Huai and Drescher, 2001; Knoll *et al.,* 2001), it was hypothesised that ephrin-A5 would have a role during neurite outgrowth and/ or growth cone morphology. Therefore, another *in vitro* assay was used to determine whether ephrin-A5 had an effect on growth cone morphology and length of trigeminal ganglion axons; for this purpose, explants were grown on a uniform EphA-Fc surface for 24 hours.

6.2 Results

6.2.1 Trigeminal ganglion explants express ephrin-A5

An identical pattern of expression to EphA3-Fc (Figure 3.3) was also visualised with EphA4-Fc (Figure 3.3) in the trigeminal ganglion in whole-mount embryos, implying that both receptors were interacting with ganglionic ephrin-A5 in a similar manner. Since *ephrin-A2* mRNA did not show any apparent localisation to the ganglion, it was highly unlikely that EphA3- and -A4-Fc chimeras were binding to ephrin-A2. Expression analysis demonstrated a wider expression pattern for EphA4 in all three targets fields (Figure 3.6) compared to EphA3 (Figure 3.5) at stage 20, suggesting a more prevalent role for EphA4 during trigeminal ganglion axon guidance. Subsequently therefore, EphA4-Fc was used to analyse potential ephrin-A5 reverse signalling.

Since EphA4-Fc was demonstrated to bind to trigeminal ganglia in whole-mount embryos, the binding of EphA4-Fc to the trigeminal ganglion was further confirmed *in vitro*. As mentioned earlier (section 5.2.1), little background staining of 24 hour whole trigeminal ganglion explants was observed with the negative control, which was the human Fc portion of the immunoglobulin protein (Figure 6.1A-A"). Analysis of whole trigeminal ganglion explants revealed binding of EphA4-Fc to most if not all axons (Figure 6.1B-B"), suggesting cognate interacting ephrin partner(s) for EphA4 were expressed on these axons.

In order to verify axonal ephrin-A5 expression, anti-ephrin-A5 immunofluorescence was performed on 24 hour trigeminal ganglion explants. Due to an inability to identify axons from the two lobes when whole ganglia are cultured, stains were performed on separated lobe cultures. As anticipated, ephrin-A5 was restricted to ophthalmic and maxillomandibular axon shafts, as well as growth cones (Figure 6.2). As observed with EphA3, ephrin-A5 staining was punctate, and this was most conspicuous on the filopodia of growth cones (arrowheads: Figure 6.2F-G). In ophthalmic and maxillomandibular axons/ growth cones, ephrin-A5 levels appeared to be similar (compare Figure 6.2F with Figure 6.2G) as shown in chapter 4.

6.2.2 Trigeminal ganglion axons are not responsive to EphA4-Fc

The relevance of trigeminal ganglion ephrin-A5 reverse signalling was firstly investigated using the substratum choice assay. For this purpose, substratum bound pre-clustered EphA4-Fc (5 μg/ml) was utilized to mimic *in vivo* target EphA interactions with ganglionic-ephrin-A5 *in vitro*. Since ephrin-A5 appeared to localise to the whole ganglion *in vivo* (chapter 4), whole trigeminal ganglion explants were used in this assay.

In the previous chapter, the results for pre-clustered 5 μg/ml control-Fc were described (Section 5.2.2 and Figure 6.3A-A'). Axons from whole trigeminal ganglion explants freely crossed the EphA4-Fc border (Figure 6.3B-B') in a similar manner to what is observed for control-Fc, and only a few were found to be stop/ turn at the substrate border (40/ 412 axons). The total axon response (9.71%) and the mean axon response/ explant (12 ± 3%) for EphA4-Fc was less compared to control-Fc, although this was not significant ($p > 0.05$, Mann-Whitney U-test; Figure 6.3). Also of note, the mean axon response/ explant observed for EphA4-Fc was approximately half of what was observed with control-Fc (22 ± 5%). In summary, the substratum choice assay data suggested that ephrin-A5 positive trigeminal ganglion axons were not responsive to EphA4-Fc.

Figure 6.1 Trigeminal ganglion explant axons express cognate interacting partners to EphA4-Fc.

(A-B) Stage 20 explants grown for 24 hours with Control-Fc (A), and EphA4-Fc (B). (A'-B') Images (A-B) merged with neurofilament (NFM) staining pattern (red). (A"-B") Higher magnification images from (A'-B'). Arrowheads: EphA4-Fc binding to axons (orange-yellow) (B").
Scale: 100 μm (A-B); 50 μm (A'-B').

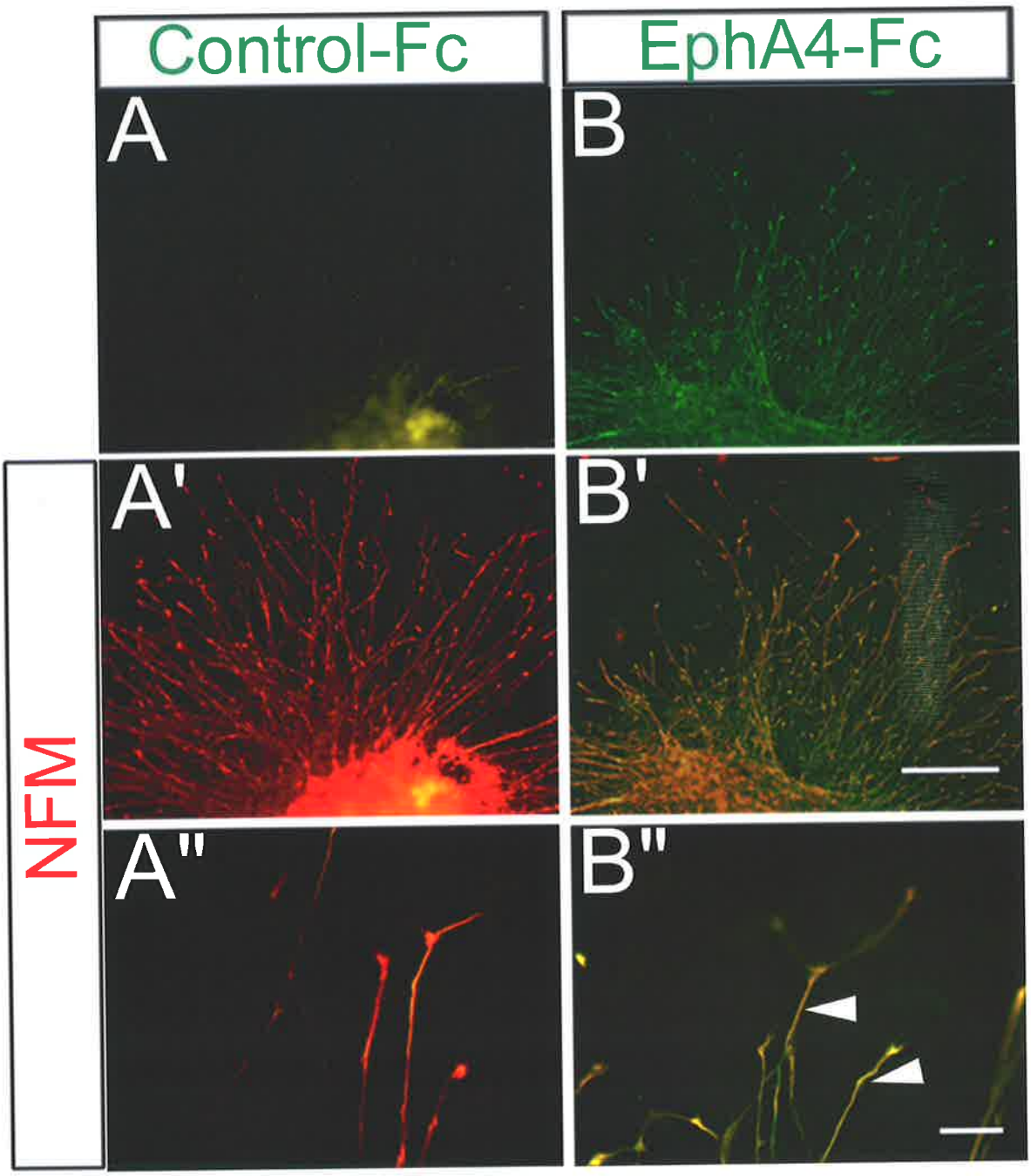
Control-Fc
EphA4-Fc
A
B
A'
B'
A"
B"
NFM

Figure 6.2 Ephrin-A5 expression in stage 20 trigeminal ganglion cultures.

(A) Control explant with no primary antibody shows little background. (B-C) Ephrin-A5 expression in ophthalmic (TGop) (B) and maxillomandibular (TGmm) (C) lobe explants. Brightness-contrast for all images is identical.

(D-E) High magnification view showing axonal ephrin-A5 expression (green) for TGop (D) and TGmm (E) explants. Images have been merged with staining pattern for anti-β-tubulin (TuJ1) antibody (red). Arrowheads: ephrin-A5 localisation to axons. Arrows: non-neural migrating cells are ephrin-A5 positive. Brightness-contrast for all images is identical.

(F-G) TGop (F) and TGmm (G) growth cones are ephrin-A5 (green) and TuJ1 positive (red). Arrowheads: ephrin-A5 puncta localisation to filopodia. Brightness-contrast adjusted identically for both images.

Scale: 100 μm (A-C); 50 μm (D, E); 10 μm (F, G).

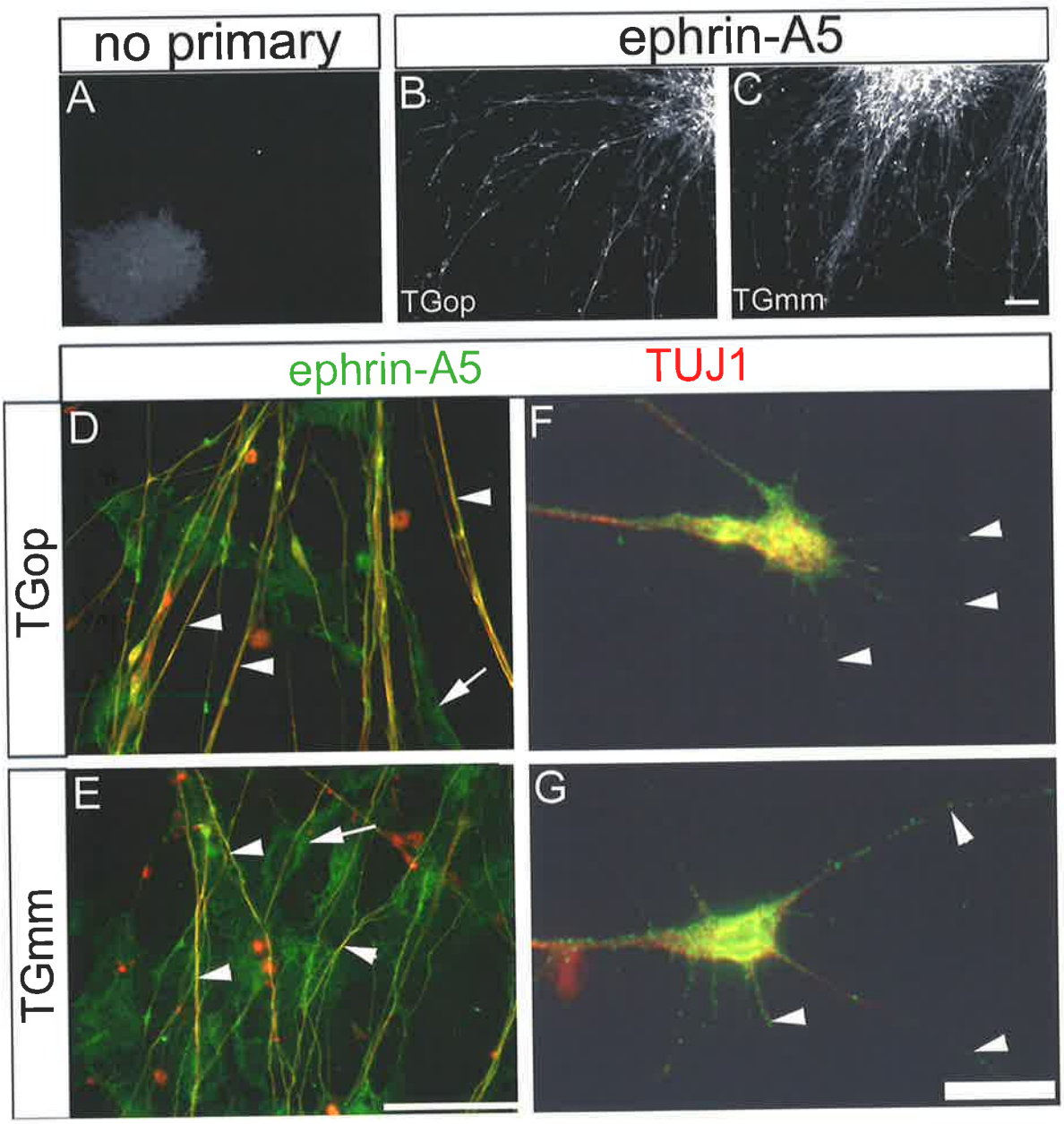
no primary
ephrin-A5
A
B
C
TGop
TGmm
ephrin-A5
TUJ1
TGop
D
F
TGmm
E
G

6.2.3 EphA4-Fc does not promote neurite growth

The mesenchyme proximal to the ophthalmic lobe appeared to express EphA4 at a greater level compared to the mesenchyme proximal to the maxillomandibular lobe (Figure 3.6E-E'). Therefore, mesenchymal expressed EphA4 may exert differential effects on the two lobes. The observed lack of response to EphA4-Fc in the substratum choice assay (Figure 6.3) correlated well with the expression data (Chapter 3). Nevertheless, the role of target EphA4 was further elucidated *in vitro* by culturing separated trigeminal ganglion lobes on a uniform substrate of 5 μg/ml EphA4-Fc or control-Fc for 24 hours (Figure 6.4). The mitogen-activate protein kinase (MAPK) is a known mediator of neurite/ axon extension and was found to be activated by ephrin-A reverse signalling (Davy and Robbins, 2000; Huai and Drescher, 2001). Additionally, ephrin-A5 induced neurite growth of retinal axons has been demonstrated on a uniform EphA5-Fc substrate after 16 hours (Davy and Robbins, 2000). Correspondingly, it was believed that if ephrin-A5 were indeed the cognate interacting partner for EphA4, ephrin-A5 induced trigeminal ganglion neurite extension would be revealed on a uniform EphA4-Fc substrate.

Nevertheless, analysis of neurite length and number of neurites/ explant (Figure 6.4A-D) revealed no significant difference between EphA4-Fc and control-Fc ($p > 0.05$; student t-test) (Table 6.1). Furthermore, it was noted that ophthalmic axons displayed longer axons compared to maxillomandibular axons, regardless of the substratum condition. This may reflect the distance axons from each lobe have to travel to innervate their respective target fields *in vivo*. These *in vitro* results confirmed that EphA4-Fc was permissive to trigeminal ganglion lobe axon growth as seen with the substratum choice assay (Figure 6.3B-C). However, EphA4-Fc did not appear to be growth stimulating to trigeminal ganglion lobe axons.

Figure 6.3 Whole trigeminal ganglion explants are not responsive to EphA4-Fc in the substratum choice assay.

(A-B) Substratum choice assay with control-Fc (A), and EphA4-Fc (B). (A'-B') High magnification images from (A-B). Asterisk: substratum. (B-B') All explants were stained with anti-neurofilament (NFM) antibody and images are of representative explants.

(C) Quantitation of % mean axon (stop/ run) response/ explant to either control-Fc or EphA4-Fc conditions. *n* = number of explants which are indicated in brackets. All values are mean ± SEM. There is no significance difference between % mean axon response/ explant between control-Fc and Eph4-Fc.

Scale: 200 μm (A-B); 50 μm (A'-B').

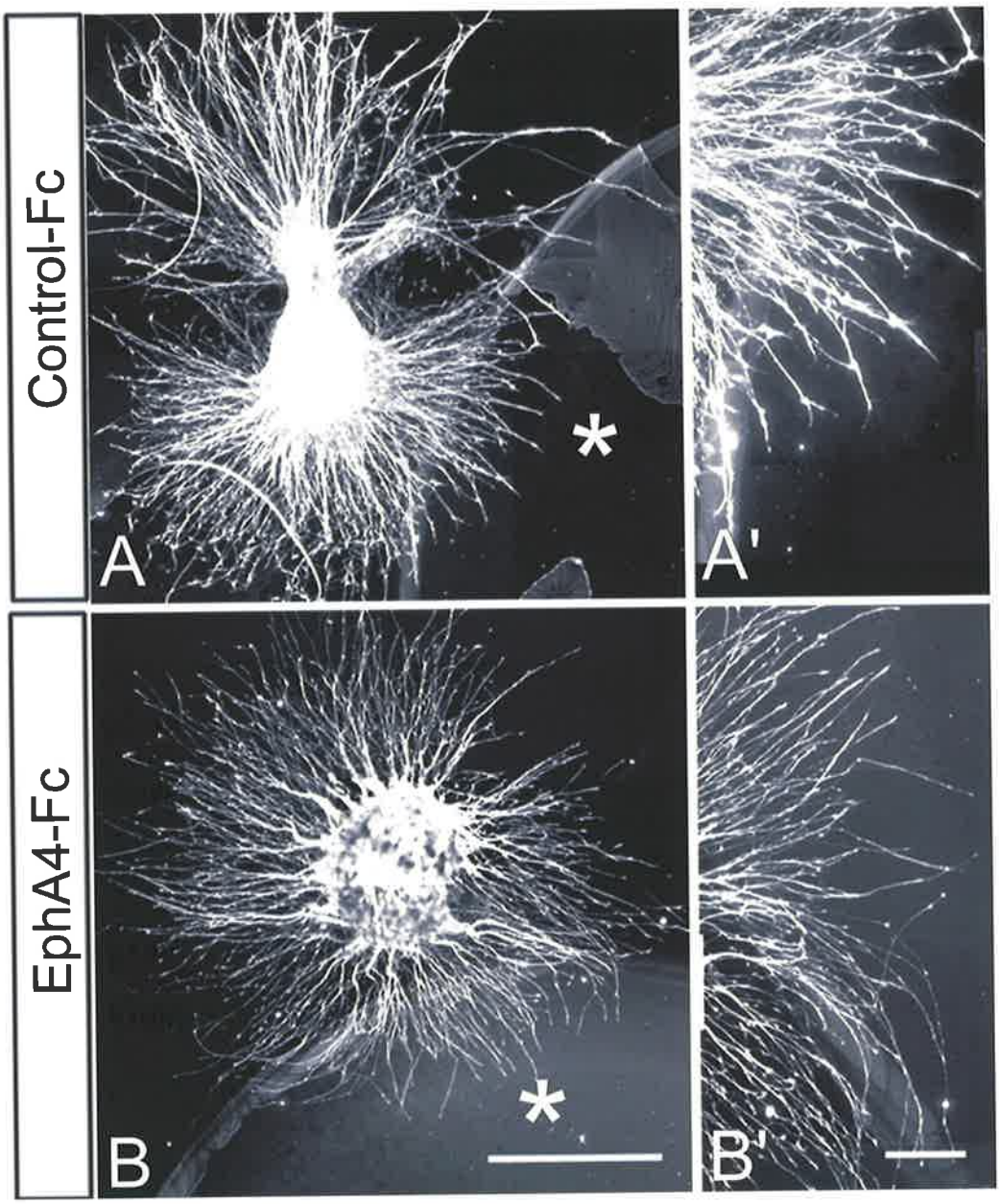
Control-Fc
EphA4-Fc
A
A'
B
B'
*
*

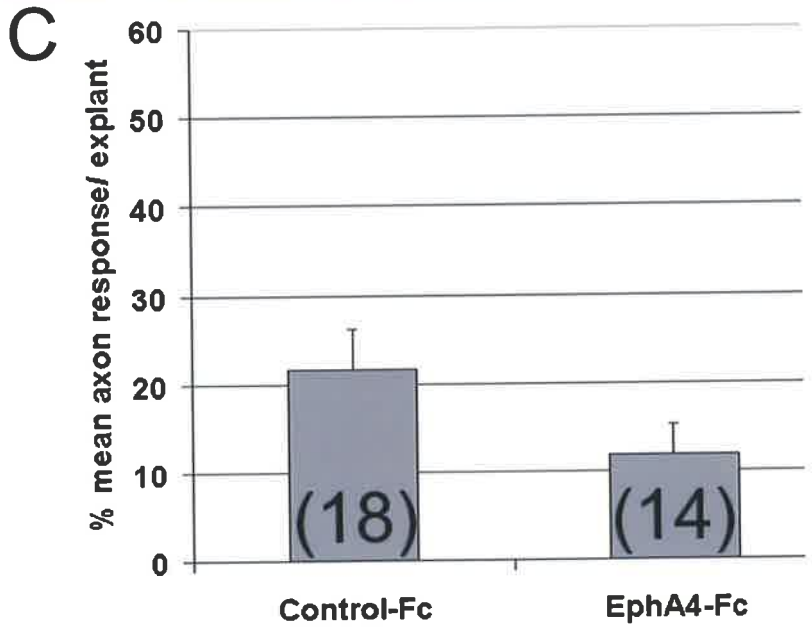
C
% mean axon response/ explant
60
50
40
30
20
10
0
(18)
(14)
Control-Fc
EphA4-Fc

Figure 6.4 Uniform EphA4-Fc substrate influences stage 20 ophthalmic (TGop) and maxillomandibular (TGmm) explant growth cone morphology.

(A-D) TGop (A-B) and TGmm (C-D) lobe explants grown on uniform control-Fc (A, C) or EphA4-Fc (B, D) substrate for 24 hours. Images are of representative explants, and were stained with anti-neurofilament (NFM).

(E-H) TGop (E, G) and TGmm (F, H) lobe growth cones have smaller surface area on uniform control-Fc (E, F) compared on EphA4-Fc (G, H). Growth cones are stained with phalloidin. Images are of representative growth cones.

(I) Quantification of mean growth cone area on EphA4-Fc versus control-Fc. n = growth cones, shown in brackets. $^{*} = p < 0.0001$ (student t-test).

Scale: 200 μm (A-D); 10 μm (E-H).

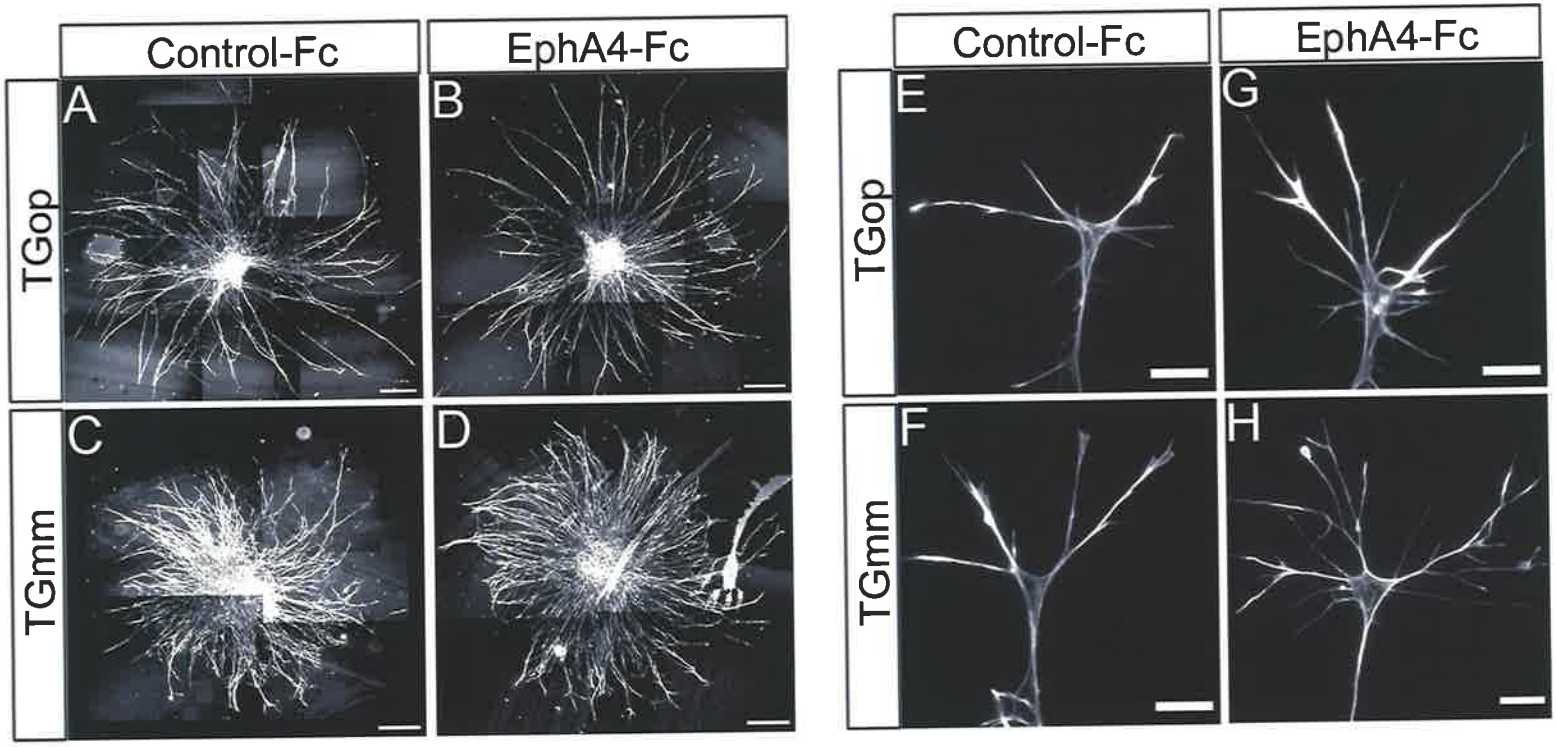
Control-Fc
EphA4-Fc
Control-Fc
EphA4-Fc
TGop
TGmm
TGop
TGmm
A
B
C
D
E
G
F
H

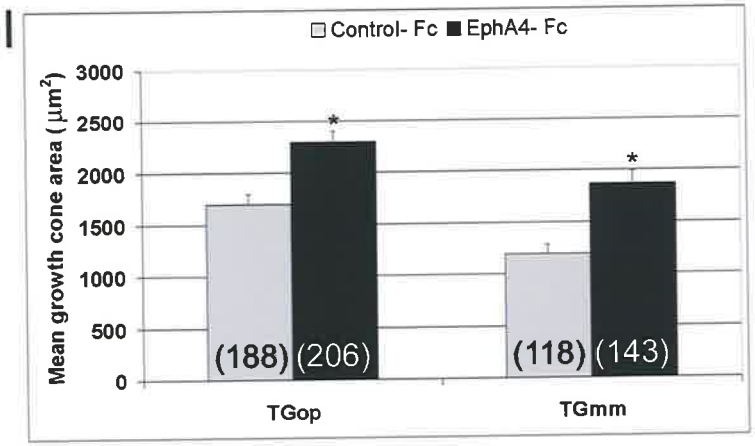
I
Control- Fc
EphA4- Fc
Mean growth cone area (μm²)
3000
2500
2000
1500
1000
500
0
(188)
(206)
(118)
(143)
*
*
TGop
TGmm

Table 6.1 Neurite and growth cone parameters on EphA4-Fc versus Control-Fc for ophthalmic (TGop) and maxillomandibular (TGmm) explants.

	TGop[a]		TGmm[a]	
Parameters	**Control-Fc**	**EphA4-Fc**	**Control-Fc**	**EphA4-Fc**
Neurite length (μm)	906 ± 26 *(100)*[b]	884 ± 19 *(130)*[b]	776 ±18 *(85)*[b]	742 ± 24 *(95)*[b]
# neurites/ explant	74 ± 6 *(24)*[c]	71 ± 6 *(25)*[c]	74 ± 6 *(25)*[c]	88 ± 7 *(24)*[c]
Filopodial stalk length (μm)	19.7 ± 0.5 *(592)*[d]	21.4 ± 0.4[†] *(724)*[d]	16 ± 0.4 *(517)*[d]	17.7 ± 0.4[†] *(603)*[d]
# long filopodial stalks	258 *(592)*[d]	366[**] *(724)*[d]	221 *(517)*[d]	274[**] *(603)*[d]
% long filopodial stalks/ growth cone	46 ± 2 *(104)*[e]	54 ± 2[*] *(114)*[e]	40 ± 2 *(104)*[e]	48 ± 3[*] *(106)*[e]

[a] Mean ± SEM except for # long filopodial stalks. *n* values shown in brackets. [b] Number of neurites; [c] number of explants; [d] number filopodial stalks, [e] number of growth cones analysed. [*] $p < 0.05$ (student t-test); [**] $p < 0.05$ (χ^2 test); [†] $p < 0.01$ (student t-test).

6.2.4 EphA4-Fc influences growth cone morphology

A lack of effect on neurite length and number prompted the investigation of growth cone F-actin morphology on uniform EphA4-Fc substrate (Figure 6.4E-H). Since ephrin-A5 reverse signalling induces changes in cell adhesion and morphology in a β1-integrin dependent manner (Davy *et al.,* 1999; Davy and Robbins, 2000; Huai and Drescher, 2001), it was hypothesised that changes in trigeminal ganglion growth cone morphology would be observed. As opposed to ophthalmic and maxillomandibular growth cones grown on control-Fc (Figure 6.4E-F), those on EphA4-Fc (Figure 6.4G-H) exhibited a greater mean surface area (Figure 6.4I). Ophthalmic growth cones on control-Fc had a mean surface area of 1695 ± 99 μm^2, compared with 2294 ± 108 μm^2 growth cones grown on EphA4-Fc ($p < 0.0001$; student t-test; Figure 6.4I). Likewise, maxillomandibular growth cones grown on control-Fc had a mean surface area of 1192 ± 91 μm^2, as opposed to 1869 ± 111 μm^2 for growth cones grown on EphA4-Fc ($p < 0.0001$; student t-test) (Figure 6.4E-I). Following standardisation against their respective controls, EphA4-Fc appeared to exert a greater effect (~ 10%) on

maxillomandibular growth cone surface area relative to ophthalmic growth cones (Figure 6.4I). In summary, an increase in growth cone surface area on EphA4-Fc would be consistent with increased adhesion, and this is likely to be mediated through ephrin-A5 reverse signalling.

As mentioned earlier, engagement of ephrin-A5 with EphA5-Fc can promote neurite outgrowth of cultured ephrin-A5 expressing retinal ganglion cells (Davy and Robbins, 2000). Although an effect on trigeminal ganglion neurite length was not shown here, it was plausible that on EphA4-Fc, ephrin-A5 expressing trigeminal ganglion growth cones exhibited increased filopodial lengths. This notion would be consistent with reported long filopodial like protrusions for cells expressing ephrin-A5 grown on substrate consisting of EphA5-Fc and fibronectin (Davy and Robbins, 2000). To assess if this was the case, the mean length of growth cone filopodial stalks on uniform EphA4-Fc was compared with those grown on control-Fc for 24 hours (Table 6.1). Assessment of mean filopodial stalk lengths for ophthalmic and maxillomandibular growth cones revealed a greater mean length on EphA4-Fc compared to control-Fc ($p < 0.01$; student t-test) (Table 6.1). There was a negligible difference (~ 1%) in mean filopodial stalk lengths between ophthalmic and maxillomandibular lobes on EphA4-Fc following standardisation with their respective controls. Also, a strong association was found between the number of long filopodial stalks and substratum type, with EphA4-Fc promoting longer filopodial stalks ($p < 0.05$; χ^2 test) (Table 6.1). Analysis of growth cones on EphA4-Fc for both lobes revealed that the % of long filopodial stalks/ growth cone was increased on EphA4-Fc compared to controls ($p < 0.05$; student t-test) (Table 6.1). The relative difference between ophthalmic and maxillomandibular for filopodial stalk length was ~ 3% on EphA4-Fc following standardisation with their respective controls. These data would be consistent with an ephrin-A5 signalling mediated increase in filopodial stalk length following interactions with substrate EphA4-Fc.

6.2.5 Trigeminal ganglion explants express ephrin-B2

Since EphA4 is a low affinity receptor for ephrin-B2 (Gale *et al.,* 1996), the presence of ephrin-B2 on trigeminal ganglion explants was also investigated. Antibody staining displayed the expression of ephrin-B2 on ophthalmic and maxillomandibular axons and growth cones (Figure 6.5). As for ephrin-A5, punctate staining was visualised on filopodia (Figure 6.5C-D). Hence, in addition to trigeminal ganglion axon-ephrin-A5 interactions with EphA4-Fc, there may be axon-ephrin-B2 interactions with substrate-EphA4-Fc.

Figure 6.5 Ephrin-B2 expression in stage 20 trigeminal ganglion cultures.

(A-B) Ophthalmic (TGop) (A) and maxillomandibular (TGmm) (B) lobe axons are ephrin-B2 (green) positive (arrowheads). The images have been merged with staining pattern from anti-TuJ1 antibody (red).

Brightness-contrast has been adjusted equally for both images.

(C-D) TGop (C) and TGmm (D) growth cones express ephrin-B2. Arrowheads: ephrin-B2 puncta localise to filopodia. Brightness-contrast adjusted identically for all images.

Scale: 50 μm (A-B); 10 μm (C-F).

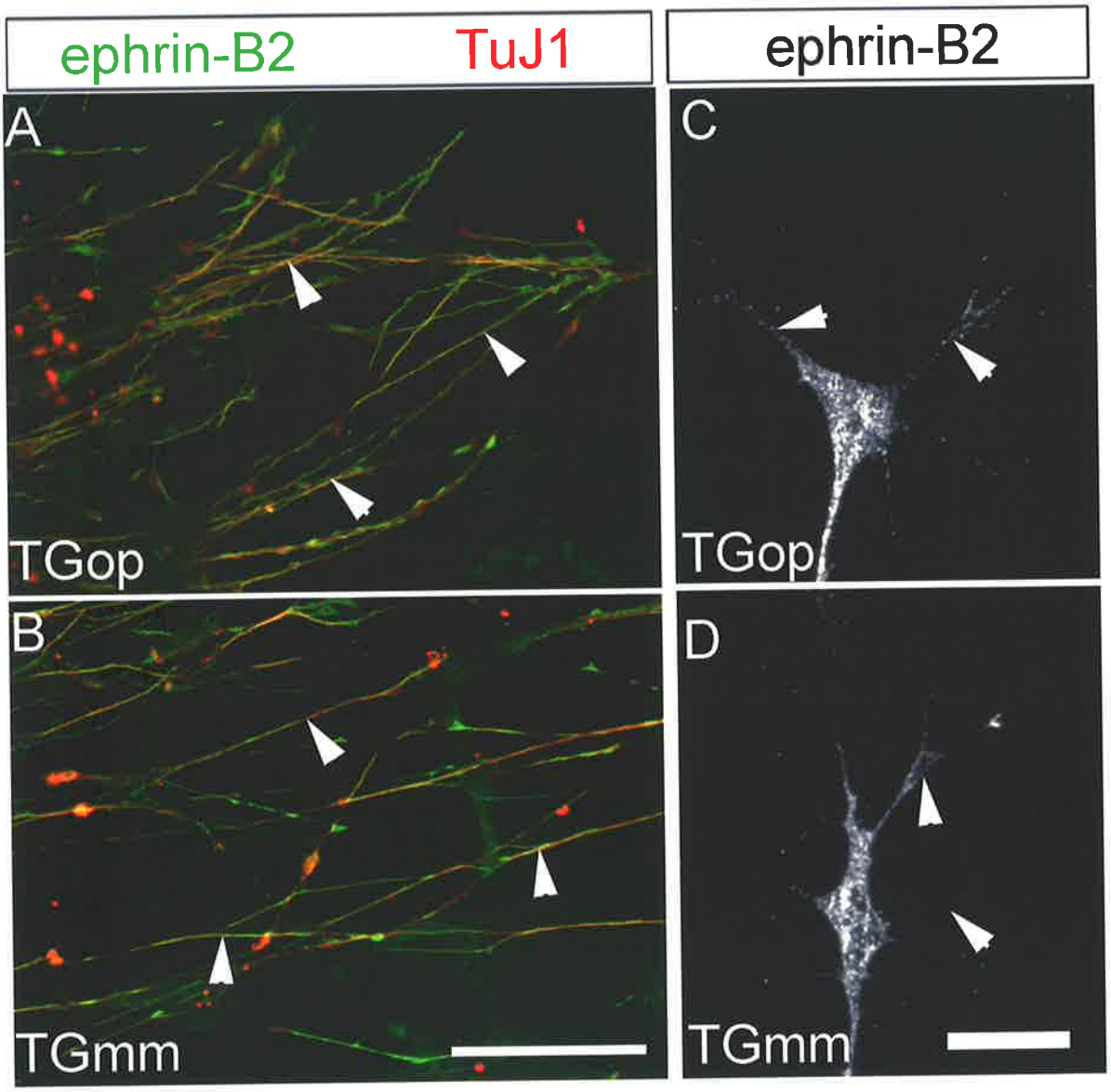
ephrin-B2
TuJ1
ephrin-B2
A
C
TGop
TGop
B
D
TGmm
TGmm

6.3 Summary and discussion

The results showed that ephrin-A5 positive trigeminal ganglion axons were not responsive to substratum bound EphA4. Additionally, growth cones from ophthalmic and maxillomandibular grown on EphA4-Fc have a greater surface area, and longer filopodia compared to their respective controls.

6.3.1 *In vivo* EphA3/ A4 expression patterns correlate with *in vitro* substratum choice assay results

A lack of response to EphA4-Fc for trigeminal ganglion axons correlated well with the *in vivo* expression data. During trigeminal ganglion axon guidance from stage 13-20, EphA3 and EphA4 are expressed in all the target tissues, in a similar pattern, implying similar/ redundant functions for these two receptors (Chapter 3). The exhibited growth of axons into or through EphA3 and EphA4 mesenchyme also suggested that target EphAs were not repulsive (Chapter 3). Preliminary data suggested that whole trigeminal ganglion explants (n = 3 explants) were not responsive to EphA3-Fc, however due to time constraints these experiments were not pursued. Thus, based on the preliminary EphA3-Fc data, trigeminal ganglion explant axons appear behave in the similar manner to both EphA3 and EphA4 *in vitro*. Nevertheless in future, it will be necessary further validate and extend the EphA3-Fc results.

The observed lack of trigeminal ganglion axon response to EphA4-Fc in the substratum choice assay had two possible explanations. The first was that trigeminal ganglion explants did not express a cognate interacting partner for EphA4-Fc. This possibility was excluded on account that EphA4-Fc was observed to bind to trigeminal ganglion axons *in vitro*, suggesting that these axons expressed a cognate interacting partner(s) for this receptor. The second alternative explanation was that trigeminal ganglion axons extended onto EphA4-Fc substrate through active engagement of axonal expressed cognate ephrins, rather than the passive growth seen into control-Fc. This notion was favoured because ephrin-A5 was found to localise to the trigeminal ganglion *in vivo* (Chapter 3 and 4) and *in vitro* (Chapter 6). Further to this, the expression of ephrin-B2 by trigeminal ganglion explants was seen, raising the possibility that this ligand, which has a lower affinity to EphA4 compared to ephrin-A5 (Brambilla *et al.,* 1996; Gale *et al.,* 1996), was also interacting with EphA4-Fc. The cognate trigeminal ganglion

interacting partners to EphA4 will need to be assessed by performing co-immunoprecipitation using anti-ephrin-A5, anti-ephrin-B2 and EphA4-Fc. Of course, the selective contribution of axonal-ephrin-A5 signalling to trigeminal ganglion could be assessed with EphA3-Fc *in vitro*, since EphA3 does not interact with ephrin-B2 (Gale *et al.*, 1996).

6.3.2 ephrin-A5 reverse signalling and the growth cone

Given that ephrin-A5 was expressed by trigeminal ganglion neurons and axons of both lobes (chapter 4, 6), the observed lack of response to substratum bound EphA4-Fc raised the possibility that growth into EphA4-Fc was promoted through active axonal-ephrin-A5 signalling in contrast to the passive growth on control-Fc. This reasoning was based on previous *in vitro* (Davy *et al.*, 1999; Davy and Robbins, 2000; Huai and Drescher, 2001) and *in vivo* (Knoll *et al.*, 2001) evidence, which suggested that activated ephrin-A5 mediated reverse signalling could lead to adhesion and possibly attraction. Additionally, ephrin-A5 induced changes to adhesion and cell morphology were dependent on β1-integrin and MAPK signalling (Davy and Robbins, 2000; Huai and Drescher, 2001). It is reported that the activation of β1-integrin signalling causes an increase in adhesion between the cell and the substrate, whilst MAPK signalling promotes neurite outgrowth and changes to the cytoskeleton (Nakamoto *et al.*, 2004). Based on this collective evidence, a role for ephrin-A5 reverse signalling during trigeminal ganglion axon guidance/ outgrowth was implied. Nevertheless, in contrast to ephrin-A5 positive primary retinal neurons, which showed a dependence on EphA5-Fc substrate for axon growth (Davy and Robbins, 2000), this study did not demonstrate a neurite growth-promoting role for EphA4-Fc. Despite this, at the level of the growth cone, EphA4-Fc was found to promote greater growth cone surface areas and longer filopodia in culture, possibly consistent with ephrin-A5 reverse signalling.

Why did uniform EphA4-Fc not promote longer neurites or increase the mean number of neurites/ explant of stage 20 trigeminal ganglia *in vitro*? In hindsight, analysis of neurite growth could have been performed using dissociated trigeminal ganglion neurons. The reasoning for this is two fold. Firstly, Davy and Robbins (2000) who demonstrated a growth-promoting role for ephrin-A5 positive retinal cells on EphA5-Fc, substrate did so with dissociated retinal ganglion neurons. Secondly, it is conceivable that axon fasciculation or axon bundling may account for the lack of neurite

growth promotion on EphA4-Fc. *In vitro*, trigeminal ganglion explant axons often exhibit highly fasciculated (bundled) growth, consequently an EphA4-Fc effect on neurite growth may be difficult to observe because axons are not always relying on interactions with the substrate for growth. Another issue future experiments on uniform EphA4-Fc may need to confront is the stage of the embryo trigeminal ganglion neurons are taken from. In a previous report, EphA/ ephrin-A interactions were demonstrated to promote neurite outgrowth of dissociated cortical neuronal precursors in a developmental stage manner (Zhou *et al.*, 2001). Likewise, it will be of interest to determine whether EphA4-Fc promotes neurite outgrowth of dissociated trigeminal ganglion neurons from embryos younger than stage 20.

While a lack of effect on neurite growth parameters was not seen, a growth-promoting role for EphA4-Fc (albeit a minor one) cannot be excluded since the assay used in this study may not have been sensitive enough to detect such an effect. *In vivo*, the apparent graded expression of EphA3 and EphA4 in the trigeminal ganglion target fields, particularly evident in the ophthalmic process, may still be coherent with a growth-promoting role for these receptors. Since this graded *in vivo* expression was not mimicked in the current study, some caution should be exerted when extrapolating data from uniform EphA4-Fc substrate.

The mesenchyme proximal to the ophthalmic lobe appeared to express EphA4 at a greater level compared to the mesenchyme proximal to the maxillomandibular lobe. Therefore, a differential effect of EphA4 on the two lobes was predicted. Interestingly, EphA4-Fc exerted a modest 10% greater response on maxillomandibular growth cone area compared to ophthalmic growth cones. Why might this be, and how might this be related to the level of EphA3 and ephrin-A5 growth cone expression? Even though both lobes expressed similar levels of ephrin-A5 (Chapters 4 and 6), the greater expression of EphA3 in the ophthalmic lobe may compete with substratum bound EphA4-Fc for ephrin-A5 in the ophthalmic growth cones. The predicted outcome is a reduction in the pool of unoccupied ephrin-A5 in these growth cones compared to maxillomandibular growth cones. Furthermore, due to high expression of EphA3 on the ophthalmic axons, the target tissue may need to express a higher level of EphA receptors to competitively displace axonal-EphA3 from axonal-ephrin-A5. This view is further substantiated by the high expression of EphA receptors in the ophthalmic process compared to the

maxillomandibular process (Chapter 3). Other than a weak difference between the two lobes at the level of the gross growth cone morphology, the other differences for the measured growth cone parameters were negligible.

6.3.3 Is there convergence of ephrin-A5 and ephrin-B2 reverse signalling?

Contrary to EphB2-Fc whole-mount staining (Chapter 3) and a previous study (Braisted *et al.,* 1997) which did not show ephrin-B2 localisation to the stage 20 trigeminal ganglion, immunofluorescent ephrin-B2 staining of cultured trigeminal ganglia suggested otherwise. The reasons for this inconsistency may have been that ganglionic EphB(s) were masking the detection of ephrin-B2, and/ or that the levels of ephrin-B2 protein were lowly abundant. As a result, the interpretation of the uniform EphA4-Fc *in vitro* results is somewhat complicated. EphA4 is known to interact with both A and B classes of ephrins (Gale *et al.,* 1996; Mellitzer *et al.,* 1999). Therefore the contribution of axonal-ephrin-B2 reverse signalling on EphA4-Fc uniform substrate cannot be excluded. Ephrin-Bs can also mediate adhesive/ attractive reverse signalling in a number of systems (Kullander *et al.,* 2001; Mann *et al.,* 2002; Santiago and Erickson, 2002), and also have the ability to modulate β1-integrin signalling (Huynh-Do *et al.,* 2002). Nonetheless, growth cone ephrin-A5 reverse signalling may dominate because of its high affinity interactions with EphA4 (Gale *et al.,* 1996) and any axonal-ephrin-B2/ target-EphA4 interactions may act to modulate the strength of axonal ephrin-A5 reverse signalling *in vivo* and *in vitro*. To fully understand the contributions of ephrin-B2 signalling during trigeminal ganglion axon guidance *in vitro*, ephrin-A5 could be stripped off these axons by treatment with PI-PLC, which sheds GPI-anchored proteins including ephrin-As (Hornberger *et al.,* 1999). Alternatively, a function blocking antibody to either ephrin-A5 or ephrin-B2 may reveal the signalling contribution each ligand makes during aspects of trigeminal ganglion axon guidance *in vitro*.

The expression of ephrin-B2 in the trigeminal ganglion demonstrated in this study is not surprising given the reported expression of EphB receptors in the chick at stages 13-20 in the target fields (Baker *et al.,* 2001; Santiago and Erickson, 2002). Therefore, in addition to EphB/ephrin-B interactions, cross talk between the A and B subclass of Eph/ephrins is likely to add another level of complexity.

6.3.4 Is EphA4-Fc permissive or adhesive to trigeminal ganglion growth cones/ axons?

The increase in growth cone area and long filopodia observed on uniform EphA4-Fc *in vitro* could be due to increased permissiveness or increased adhesion. If the growth cone morphological changes are due to activation of ephrin reverse signalling, in a β1-intergrin dependent manner leading to increased adhesion (Davy *et al.,* 1999; Davy and Robbins, 2000; Huai and Drescher, 2001; Huynh-Do *et al.,* 2002), then the addition of a β1-intergrin function blocking antibody would neutralise these effects seen on EphA4-Fc. It is conceivable that the changes observed in the growth cone morphology require prolonged activation of the MAPK pathway when ephrin-A5 signalling is activated, as has been previously shown by Davy and Robbins (2000), then it is speculated there would be an increase in phosphorylation of MAPKs extracellular regulated kinases (ERK) 1 and 2 in the growth cone. This view is based on the evidence that there is minimal activation of MAPKs, when NIH-3T3 cells expressing ephrin-A5 are cultured on only the extracellular matrix, fibronectin (Davy and Robbins, 2000). The phosphorylation status of ERK1/2 relative to the pool of total MAPK can also be determined by subjecting trigeminal ganglion explants grown on EphA4-Fc for 24 hours to immunofluorescence staining with antibodies directed against phosphorylated and total MAPK, and compared to those explants grown on control-Fc.

6.4.5 EphAs are pathfinding cues to trigeminal ganglion growth cones?

A prior study showed that an increase in growth cone area correlated with grasshopper growth cone pathfinding activity *in vivo* (O'Connor *et al.,* 1990) and this may signify a role for mesenchymal EphAs as guidance cues during pathfinding of trigeminal ganglion growth cones (Figure 6.6). Axon pathfinding appears to involve both instructive and permissive cues. The importance of laminin, a permissive cue, during neuronal pathfinding in the grasshopper limb bud was demonstrated with functional blocking reagents against the nidogen-binding site on laminin important for axonal-β1-integrin binding (Bonner and O'Connor, 2001). Based on the fore mentioned observations *in vivo* in the grasshopper limb for laminin (Bonner and O'Connor, 2001), and *in vitro*, where neurons appear to regulate integrin receptor levels based on the

concentrations of laminin, (Condic and Letourneau, 1997), the function of laminin may be to make pathfinding growth cones responsive to instructive cues in the environment. Laminin may function by balancing growth cone adhesion to the substrate and growth cone motility (Bonner and O'Connor, 2001). Indeed, the observed *in vitro* trigeminal ganglion growth cone morphological changes in this study were in the presence of both laminin and EphA4-Fc substrate. Furthermore, the use of laminin as a substrate to grow trigeminal ganglion explants in this study was justified because of the reported expression of laminin in the pathways of trigeminal ganglion axons (Moody *et al.*, 1989b; Riggott and Moody, 1987). Despite the reported expression of laminin in the mesenchyme of the mandibular process (Riggott and Moody, 1987), laminin distribution in the ophthalmic process mesenchyme remains to be analysed with anti-laminin antibodies.

Generally, instructive cues are expressed in a restricted graded manner (Bonner and O'Connor, 2001) and this criterion would corroborate with the observed *in vivo* expression patterns for EphA3/ A4 in the target fields of the trigeminal ganglion (Chapter 3). Indeed, both EphA receptors displayed a graded expression pattern *in vivo*, suggesting that axons grow from regions of low (proximal mesenchyme to the ganglion) to high EphA receptor expression (distal mesenchyme to the ganglion). This may imply that EphAs increasingly promote axon pathfinding activity of pioneers as axons invade their respective target fields (Figure 6.6). Given the co-expression of EphA3 and EphA4 in the trigeminal ganglion target fields, the combined effect of the two receptors on ephrin-A5 positive axons/ growth cones is speculated to be synergistic. To test this possibility, trigeminal ganglion growth cone morphology on a substrate consisting of both EphA3- and EphA4-Fc could be analysed. Also, the function of EphA3 and EphA4 may to be redundant or overlapping based on their similar distribution in the trigeminal ganglion target fields. For this reason, a role for EphAs as trigeminal ganglion pathfinding cues may be revealed when *EphA3*$^{-/-}$ (Vaidya *et al.*, 2003), *EphA4*$^{-/-}$ (Dottori *et al.*, 1998) and *EphA3*$^{-/-}$; *EphA4*$^{-/-}$ null mice are compared. However, it cannot be excluded that EphA3 and EphA4 expression may not have a role during trigeminal ganglion axon guidance. Rather, the possibility exists that the expression of EphAs in the trigeminal ganglion targets may play a role during craniofacial morphological development.

It is noteworthy that only a modest increase in the length of filopodia was observed with EphA4-Fc *in vitro* and as to whether such an increase is physiologically relevant during axon pathfinding needs further investigation. In zebrafish and grasshopper embryos, analysis of *in vivo* pathfinding growth cone kinetics has provided enormous insight and has revealed an increase in growth cone width to length ratio (Bak and Fraser, 2003; O'Connor *et al.,* 1990), which was not determined in this study due to time constraints. Therefore, length of filopodia and the area of filopodial sampling appear to play a crucial role, especially in light of the finding that a single filopodial contact with high-affinity substrates can lead to growth cone steering (O'Connor *et al.,* 1990). To fully comprehend the role of EphA/ephrin-A interactions during trigeminal ganglion axon pathfinding at stages 13-20, it may be necessary to study the kinetics of pathfinding axons in the chick embryo.

6.3.6 Conclusion

The observed lack of stop/ turn response to EphA4-Fc indicate that EphA4, and perhaps EphA3 are not repulsive to growing trigeminal ganglion axons. Furthermore, the observed changes to growth cone morphology *in vitro* in response to EphA4-Fc suggest that EphA4 may act as a pathfinding cue, possibly involving ephrin-A5/ EphA4 interactions. In addition, the expression of ephrin-B2 on trigeminal ganglion axons implies that there may be cross talk between the A and the B subclasses during trigeminal axon guidance.

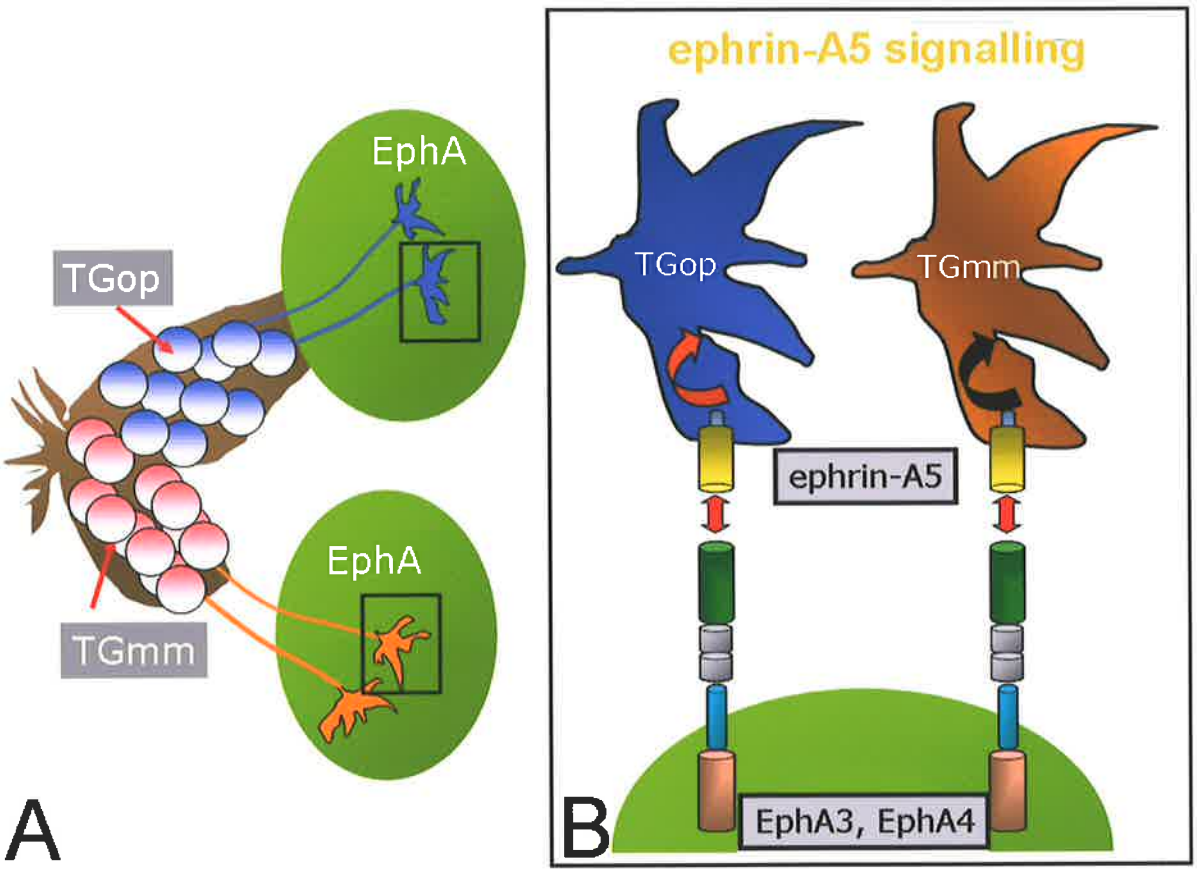

Figure 6.6 A schematic model showing the role of ephrin-A5 reverse signalling during trigeminal ganglion axon guidance.
(A) Pathfinding axons/ growth cones from the ophthalmic (TGop, blue) and maxillomandibular (TGmm, red) neurons encounter EphA expressing mesenchyme (green). The boxed regions illustrate pathfinding ophthalmic (blue) and maxillomandibular (red) growth cones.
(B) Close up of boxed regions indicated in (A) shows ephrin-A5 expressing growth cones from the two lobes interacting with EphA3/ A4 expressing mesenchyme (double-headed red arrow) and transmitting a signal into the growth cone (arrows). Reverse signalling through ephrin-A5 would encourage pathfinding growth cones to sample the environment. This could be achieved through increased growth cone surface area due to increased adhesion between the growth cone and the EphA3/ A4 expressing mesenchyme.

Chapter 7: General discussion and future directions

"To find the point where hypothesis and fact meet; the delicate equilibrium between dream and reality; the place where fantasy and earthly things are metamorphosed into a work of art; the hour when faith in the future becomes knowledge of the past; to lay down one's power for others in need; to shake off the old ordeal and get ready for the new; to question, knowing that never can the full answer be found; to accept uncertainties quietly, even our incomplete knowledge of God; this is what man's journey is about, I think."
--Lillian Smith

Chapter 7: General discussion and future directions

The trigeminal ganglion, which provides cutaneous sensory innervation to the vertebrate face, has been studied extensively. However, the basic fundamental question of how lobe specific axon peripheral projections are guided has not been addressed. In the peripheral nervous system, dorsal versus ventral motor axon projections into the hindlimb are dictated by an EphA-ephrin-A code (Eberhart *et al.,* 2004; Eberhart *et al.,* 2000; Eberhart *et al.,* 2002; Helmbacher *et al.,* 2000; Kania and Jessell, 2003). In the hindlimb, EphA4 positive lateral motor axons are repelled from ephrin-A expressing ventral limb bud, ensuring that these axons innervate the dorsal limb bud (Eberhart *et al.,* 2004; Eberhart *et al.,* 2000; Eberhart *et al.,* 2002; Helmbacher *et al.,* 2000; Kania and Jessell, 2003). Akin to this, it was hypothesised that EphA/ephrin-A interactions would guide ophthalmic versus maxillomandibular lobe projections of the trigeminal ganglion in the chick embryo. More specifically, it was speculated that repulsive Eph/ ephrin-A interactions would ensure ophthalmic lobe projections innervated the ophthalmic process.

The findings from this study have demonstrated that the A-subclass of Eph receptors and ephrins are expressed during trigeminal ganglion sensory innervation of the chick embryonic face (Figure 7.1). The *in vitro* data supports the contention that during facial development there may be trigeminal ganglion lobe specific guidance of ophthalmic in comparison to maxillomandibular peripheral sensory axonal projections to target fields coordinated through EphA3 and ephrin-A2/A5 repulsive interactions. Furthermore, this study provided *in vitro* evidence that trigeminal ganglion axons were not responsive to EphA4-Fc, possibly implying that EphAs expressed in the target fields were not repulsive to ganglionic axons during pathfinding.

Figure 7.1 Summary of EphA and ephrin-A expression during trigeminal ganglion axon guidance at stages 13 and 20.

Various tones of colour represent different expression levels; for each schematic the light colour tones represent weak expression in comparison to strong expression (dark colour tones). Asterisk indicates location of future trigeminal ganglion (TG) (stage 13) or position of the maturing TG (stage 20).
Target expression at stage 13: EphA3 and EphA4 appear to be localised to the ophthalmic (Op) process only. Ephrin-A2 and ephrin-A5 are expressed in a complementary manner to both EphA receptors, in the mesenchyme contributing to the maxillary (Mx) and mandibular (Md) processes. This expression pattern is also observed at stage 15 (not shown).
Target expression at stage 20: EphA3 and EphA4 expression domains have expanded from the ophthalmic process to include mesenchyme of the Mx and Md processes. However, ephrin-A2 and ephrin-A5 are still restricted to the Mx and Md processes as seen at stage 13.

Expression in the trigeminal ganglion: EphA3 and ephrin-A5 are expressed in the trigeminal ganglion at stage 13 and 20. The ophthalmic lobe of the ganglion localised with EphA3 at stage 13. EphA3 localisation to the maxillomandibular lobe neurons at stage 13 remains to be elucidated, although expression is observed at stage 15. At stage 20, EphA3 is differentially expressed, with high expression observed in the ophthalmic lobe.

Figure 7.2 A schematic demonstrating lateral motor column (LMC) axon outgrowth into the hindlimb.

(A) LMC axons originating from the neural tube (NT) sort at the crural plexus. Lateral LMC (LMC[l]; orange) axons innervate the dorsal hindlimb and medial LMC (LMC[m]; green) innervate the ventral hindlimb.
(B) Expression profile of EphA and ephrin-A during LMC axon sorting into dorsal and ventral trajectories (stage 23) and during innervation of the hindlimb (stage 28). During sorting, high EphA4 positive LMC[l] axons become segregated from those expressing low EphA4. At both stages, EphA4 and possibly other receptors are expressed in the dorsal hindlimb mesenchyme (light green), which ephrin-A ligands are expressed in the ventral mesenchyme. The stages described correspond to chick embryo stages.
(C) Active EphA4-LMC[l] axon (orange arrows) and ephrin-A-ventral mesenchyme repulsive interactions play a dominant during lateral axon innervation of dorsal hindlimb. Another putative second repulsive guidance mechanism (yellow-red), independent of EphA/ ephrin-A interactions may guarantee LMC[m] axon innervation of the ventral hindlimb. The repellent (yellow) is speculated to be expressed in the dorsal hindlimb mesenchyme, and the receptor (red arrows) expressed by all LMC axons. In the absence of dominant EphA4 signalling in lateral axons in *EphA4* deficient mutants, LMC[l] axons become sensitive to dorsal hindlimb putative repellent activity and become directed into the ventral mesenchyme.
(D) LIM homeodomain transcription factors control LMC neuron identity and guidance of their projections into the hindlimb. Lim1 is expressed by LMC[l] neurons, and induces high EphA4 receptor expression. Islet1 is expressed by LMC[m] neurons and induces low EphA4 receptor expression. EphA4 is a downstream effector of LIM transcription factors.

Images adapted from Eberhart *et al.,* (2000, 2002, 2004), and Kania and Jessell (2003).

Figure 7.1 Summary of EphA and ephrin-A expression during trigeminal ganglion axon guidance at stages 13 and 20.

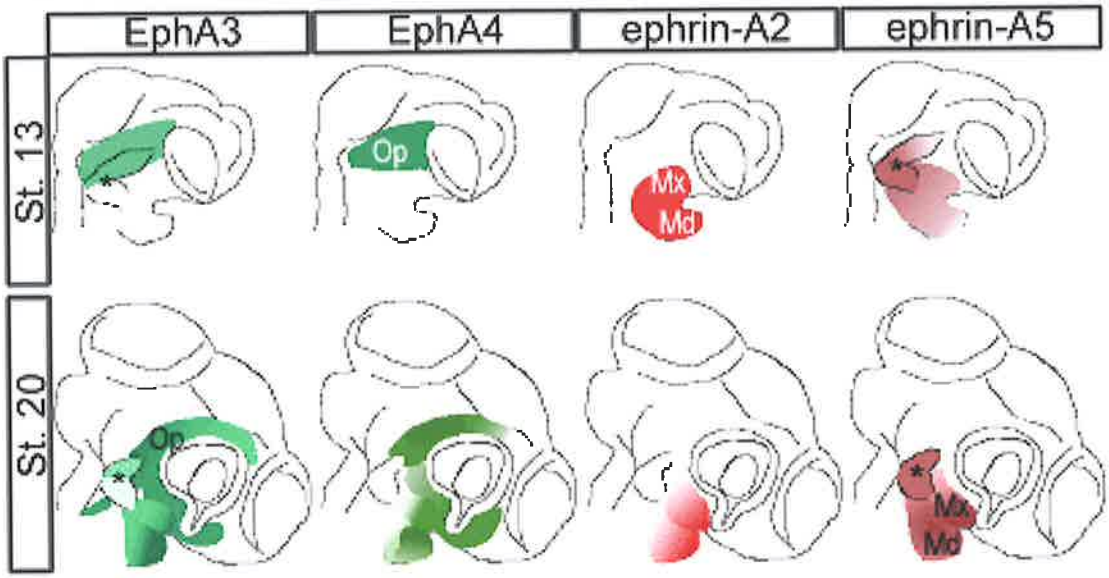

Figure 7.2 A schematic demonstrating lateral motor column (LMC) axon outgrowth into the hindlimb.

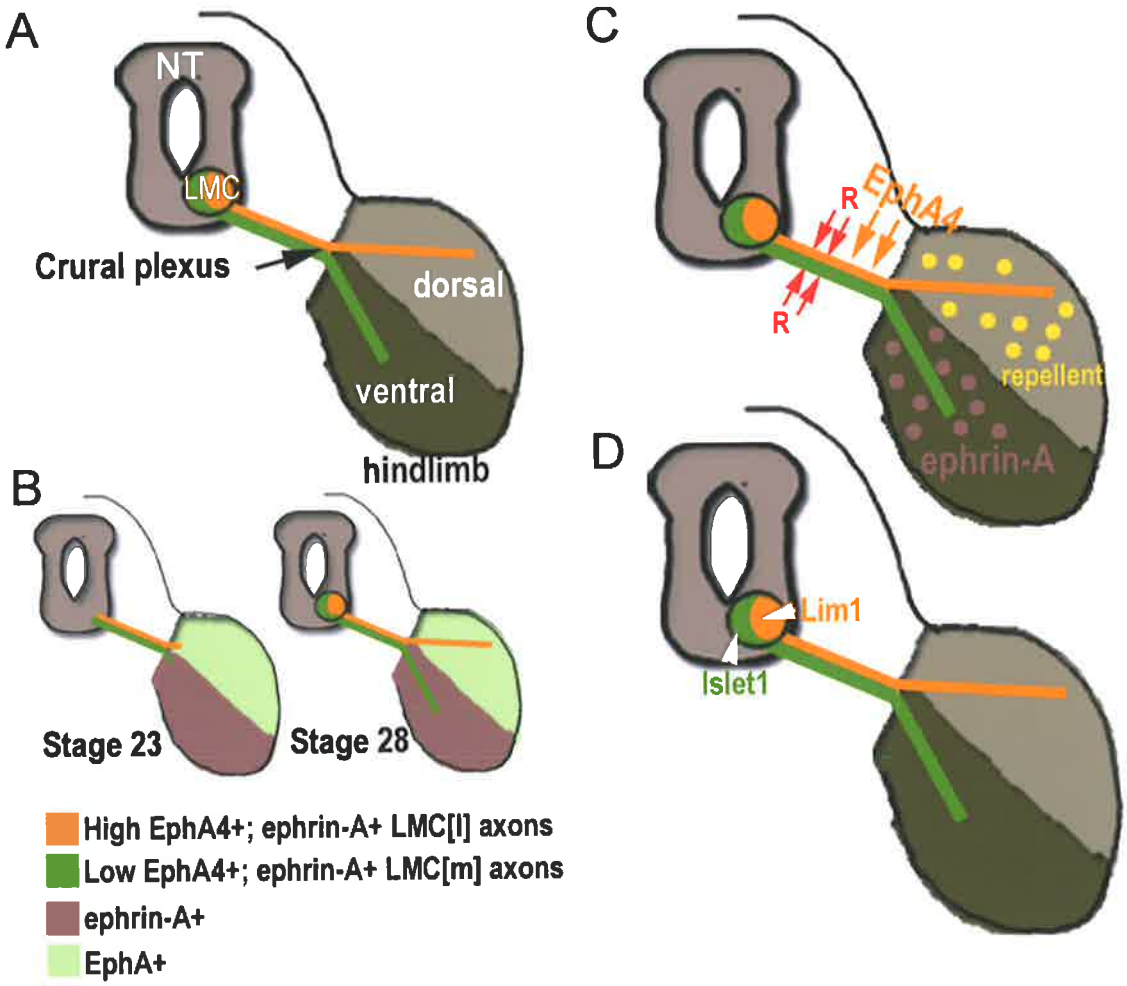

7.1 Similarities and differences between trigeminal ganglion lobe guidance and motor axon hindlimb innervation

Is the projection of lateral motor column (LMC) axons into the hindlimb a good paradigm for understanding EphA/ ephrin-A interactions during trigeminal ganglion sensory lobe specific axon guidance? From the data presented in this project, LMC innervation of the hind limb shares many parallels with trigeminal ganglion sensory system, and thus the former (Figure 7.2) appears to be a good paradigm in providing insights into the latter (Figure 7.1).

In both systems, there is differential expression of ephrin-A and EphAs in the target fields. More specifically, there is restricted ephrin-A ligand expression to the ventral hindlimb (Eberhart *et al.,* 2004; Eberhart *et al.,* 2000; Eberhart *et al.,* 2002; Kania and Jessell, 2003) (Figure 7.2B), and similarly, ephrin-A ligands are restricted to the maxillary and mandibular processes (Figure 7.1). There is high EphA4 expression in the lateral LMC axons, which innervate the ephrin-A negative dorsal limb bud (Eberhart *et al.,* 2004; Eberhart *et al.,* 2000; Eberhart *et al.,* 2002; Kania and Jessell, 2003), and similarly, there is high EphA3 expression in the ophthalmic lobe neurons/axons, which innervate the ephrin-A ligand negative ophthalmic process (Figure 7.1). Also, there is low EphA3 expression in the maxillomandibular lobe and similarly medial LMC neurons that innervate the ventral limb bud are reported to express low levels of EphA4 (Helmbacher *et al.,* 2000; Kania and Jessell, 2003) (Figure 7.2B). The dorsal limb bud is EphA4 positive (Helmbacher *et al.,* 2000; Kania and Jessell, 2003) (Figure 7.2B), similarly EphA3/A4 receptor expression is initially restricted to the ophthalmic process at stages 13 and 15 (Figure 7.1). Ephrin-A5 ligands were demonstrated in this study to localise to all neurons of the trigeminal ganglion, similarly all LMC neurons express ephrin-A2/ A5 ligands (Eberhart *et al.,* 2000) (Figure 7.2B).

The high EphA4 localisation to the lateral LMC axons appears to be important during selection of dorsal hindlimb trajectory. When EphA4 is ectopically expressed in the medial LMC neurons, these axons are now deflected away from their ephrin-A expressing target

field to the dorsal limb bud (Eberhart *et al.,* 2002). Conversely, loss of EphA4 expression in this population of neurons in *EphA4* mutant mice leads to the misrouting of lateral LMC axons into the ventral limb bud (Helmbacher *et al.,* 2000). This suggests that the high EphA4 expression in the lateral LMC neurons is responsible for their axons being deflected from ephrin-A expressing ventral limb bud. Further evidence for this came from Eberhart *et al.,* (2004), who demonstrated inhibition of EphA4 positive LMC[l] axon growth into ephrin-A5 positive mesenchyme, if ephrin-A5 is expressed broadly in the chick hindlimb. Consistent with these findings, this study has demonstrated that high EphA3 expressing ophthalmic axons are deflected from ephrin-A5-Fc substrate *in vitro*, If as in the LMC-hindlimb system where the strength of EphA4 signalling is important for selection of dorsal versus ventral projections, then the strength of EphA3 signalling is also predicted to be important for selection of ophthalmic versus maxillomandibular axon projections (Figure 7.2C and refer to section 7.3).

Although EphA signalling appears to be a major determinant of dorsal trajectory of LMC axons, two lines of evidence suggest that a distinct guidance mechanism directs the ventral trajectory of medial LMC axons (Helmbacher *et al.,* 2000; Kania and Jessell, 2003). Firstly, although medial LMC axons express low levels of EphA4, they faithfully select a ventral trajectory into ephrin-A positive ventral hindlimb. Secondly, in the absence of EphA4 function in *EphA4* mutant mice, lateral LMC axon projections into the dorsal limb bud are prevented although there is no randomisation of the dorsoventral axon trajectories (Helmbacher *et al.,* 2000). These observations are apparently best accounted for if there is another repulsive guidance mechanism, which promotes the ventral trajectory of all LMC axons. If so, the repellent may be expressed in the dorsal limb mesenchyme with all LMC axons expressing a receptor. In the presence of EphA4 signalling however, this second signalling system is speculated to be subordinate, leading to the selection of a dorsal trajectory by high EphA4 expressing lateral LMC axons (Helmbacher *et al.,* 2000; Kania and Jessell, 2003). (Figure 7.2C)

Consistent with a second signalling mechanism speculated for the LMC-hindlimb system (Figure 7.2C), low EphA3 expressing maxillomandibular axons are observed to growth on ephrin-A5 positive mesenchyme of the maxillary and mandibular processes *in vivo*. In addition, maxillomandibular axons exhibit growth into ephrin-A5-Fc substrate *in vitro*. So

what keeps these maxillomandibular axon projections restricted to the first branchial arch mesenchyme? If the second guidance system prevents medial LMC axons from innervating non-target dorsal limb mesenchyme (Helmbacher *et al.,* 2000; Kania and Jessell, 2003), then similarly such a second signalling mechanism may be responsible for preventing maxillomandibular lobe projections from innervating the ophthalmic process. Although this second signalling system could be accounted for by the initial restricted expression of EphA3/ A4 in the ophthalmic process mesenchyme (stages 13, 15) and reverse signalling into ephrin-A5 expressing maxillomandibular axons, this is highly unlikely for three reasons. Firstly, ephrin-A5 reverse signalling has been reported to result in adhesive interactions rather than repulsive interactions (Davy *et al.,* 1999; Davy and Robbins, 2000). Secondly, later on during development at stage 20, EphA receptors are expressed in the maxillary and mandibular processes, and axons from the maxillomandibular process are observed to extend into these EphA positive regions (Figure 7.1). This is in stark contrast to what is observed in the LMC-hindlimb system, where EphA4 expression remains restricted to the dorsal limb bud (Figure 7.2B). Thirdly, repulsive interactions for a subpopulation of axons could not be demonstrated from whole stage 20 trigeminal ganglion explants in the substratum choice assay using EphA4-Fc. The existence of a subordinate secondary signalling mechanism that is EphA/ ephrin-A independent for guiding maxillomandibular lobe projections early in development in the trigeminal ganglion system could be revealed in the absence of EphA3 function in the ganglion and mesenchymal EphA3/A4 function in the target fields (refer to section 7.3.2).

In contrast to LMC axon guidance, ophthalmic and maxillomandibular axons do not start highly fasciculated (bundled) to each other, defasciculate and sort into ophthalmic and maxillomandibular lobe trajectories prior to innervation of the ophthalmic process and the first branchial arch respectively. Therefore, guidance of motor axons into the hindlimb appears to share parallels with the trigeminal ganglion system at the point when there is innervation of axons into the hindlimb following sorting of lateral from medial LMC axons at the crural plexus (Figure 7.2B, stages 23-28).

7.2 Suggested model of trigeminal ganglion axon guidance

It is becoming evident that guidance of trigeminal ganglion axons into the respective target regions is a complex process, involving multiple guidance cues acting in concert (O'Connor and Tessier-Lavigne, 1999). The following model of trigeminal ganglion axon guidance is suggested based on the results from this study and those of others (Figure 7.3).

The expression of ephrin-A in the first branchial arch would act as a barrier and prevent pathfinding of EphA3 positive ophthalmic pioneer axons in non-target regions around stages 13-15 in the chick embryo (Figure 7.3). This maybe mediated through trigeminal ganglion axon EphA3 forward signalling. Axons pathfinding from the maxillomandibular lobe would not be repelled by ephrin-A in the first branchial arch because of their low EphA3 expression compared to ophthalmic lobe neurons. This early barrier function of ephrin-A in the first branchial arch to ophthalmic axons will be further reinforced by repellent cues such as Sema3A later during development, helping to maintain separate trigeminal ganglion axon projcctions from the two lobes. Given that the *in vitro* results from this study did not indicate a major role for EphA/ ephrin-A interactions during guidance of maxillomandibular lobe projection, it is likely that another family of guidance cues specifically act on maxillomandibular axons to repel them from the ophthalmic process (not shown in Figure 7.3), similarly to what is speculated for LMC[m] axons during hindlimb innervation (Helmbacher *et al.,* 2000; Kania and Jessell, 2003).

During early development stages 13-18 in the chick, target mesenchymal expression of EphAs is likely to encourage pathfinding activity of growth cones (Figure 7.3). This activity may be mediated though trigeminal ganglion ephrin-A5 reverse signalling, and possibly involve axonal-ephrin-B2 signalling as well. In addition, from stage 18 onwards in the chick embryo (E10 in mouse), neurotrophins such as BDNF and NT-3 secreted by targets (O'Connor and Tessier-Lavigne, 1999) are speculated to be permissive to axons. Furthermore BDNF may act in concert with target field EphAs to further encourage axon pathfinding because BDNF was recently shown to not only encourage axon growth but also act as a long-range attractive guidance cue (Guirland *et al.,* 2004).

From stage 18 onwards in chick (E10-10.5 in the mouse) Sema3A and Sema3F (Chen *et al.,* 1997; Chilton and Guthrie, 2003; Giger *et al.,* 2000; Kitsukawa *et al.,* 1997; Kobayashi *et al.,* 1997; Taniguchi *et al.,* 1997) expression in non-target regions will cause axon fasciculation (Figure 7.3). Sema3A is required for fasciculation of trigeminal ganglion axon projections at E10.5 in the mouse during axon growth, and not during E9.5, presumably when axons are pathfinding (Kitsukawa *et al.,* 1997; Taniguchi *et al.,* 1997). Furthermore, it is likely maxillomandibular-EphA3 interactions with target ephrin-A2/A5 also function during axon fasciculation.

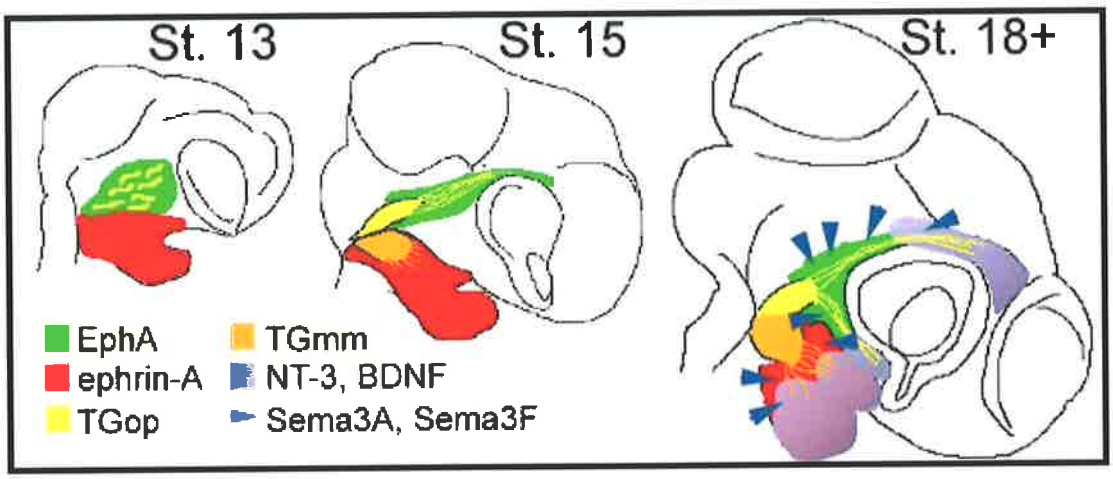

Figure 7.3 A schematic model of trigeminal ganglion axon guidance.
For details refer to text. For simplicity, EphA expression in the first branchial arch at stage 18+ has been omitted, and differing levels of EphA and ephrin-A expression are not shown. Gradients of BDNF and/ or NT-3 have been superimposed on EphA and ephrin-A expression; dark tones represent high expression and light tones represent low expression of neurotrophins. BDNF, brain derived neurotrophic factor; NT-3, neurotrophin-3; TGmm, maxillomandibular lobe; TGop, ophthalmic lobe; Sema, semaphorin.

7.3 In vivo examination of EphA/ ephrin-A interactions during trigeminal ganglion axon guidance

Although, some insight into the role of EphA3/ephrin-A5 interactions during lobe-specific axon guidance of the trigeminal ganglion has been gained through *in vitro* examination, *in vivo* this remains to be elucidated.

7.3.1 Elucidating *in vivo* trigeminal axonal-EphA3 and first branchial arch-ephrin-A2/A5 interactions in the chick embryo

In terms of genetic manipulations, the chick embryo is an excellent model system to address this issue. Micro *in ovo* electroporation enables the expression of transgenes in a spatially restricted manner in the tissues of interest (Momose *et al.,* 1999) and hence would be an excellent tool to address *in vivo* EphA3/ephrin-As interactions. Based on the *in vitro* results from this study, misexpression of ephrin-As in the ophthalmic process mesenchyme early during embryogenesis around stage 10-12 is predicted to inhibit ophthalmic axon growth. This speculated outcome would be similar to what is observed in the LMC-hindlimb system in chick, where ectopic expression of ephrin-A5 in the dorsal hindlimb mesenchyme inhibits EphA4 positive lateral axons from entering their target tissue (Eberhart *et al.,* 2004).

The strength of EphA3 signalling during trigeminal ganglion axon guidance could be addressed with the expression of an EphA3 kinase inactive mutant under ophthalmic lobe/ placode specific promoters, such as the Pax3 promoter. Pax3 is an excellent marker of ophthalmic placode cells and neurons (Baker *et al.,* 2002; Baker *et al.,* 1999; Stark *et al.,* 1997), although given its importance during neural crest development (Serbedzija and McMahon, 1997; Stark *et al.,* 1997), it may be necessary to identify ophthalmic lobe specific enhancers in the Pax3 promoter thereby ensuring restricted transgene expression to the ophthalmic placode. In such experiments, a decrease in EphA3 signalling may cause aberrant misrouting of ophthalmic axons into ephrin-A2/-A5 non-target mesenchyme in the first branchial arch. In performing lipophilic dye injections in the maxillary and mandibular processes, those ophthalmic axons that have been diverted into these processes due to decreased EphA3 signalling can be traced retrogradely to the ophthalmic lobe. In the converse experiment, an overexpression of full-length EphA3 under maxillomandibular

lobe/ placode specific promoters is predicted to deflect these axons from their ephrin-A expressing target fields; although specific genes expressed in both the maxillomandibular placode and lobe have yet to be identified.

7.3.2 Elucidating *in vivo* EphA/ ephrin-A interactions in the mouse embryo

There is remarkable conservation in expression of EphAs and ephrin-As during retinal axon topographic mapping between chick (Drescher *et al.,* 1995) and mouse (Cheng and Flanagan, 1994; Cheng *et al.,* 1995), and during motor axon pathfinding into the hindlimb (Eberhart *et al.,* 2004; Eberhart *et al.,* 2000; Eberhart *et al.,* 2002; Kania and Jessell, 2003). For that reason, EphA and ephrin-A expressions are envisaged to be conserved or similar during trigeminal ganglion axon guidance between these two species.

Indeed, the overall expressions of EphAs and ephrin-As during mouse embryogenesis (Flenniken *et al.,* 1996; Gale *et al.,* 1996) are similar to that observed in this study during an equivalent chick embryonic stage. Furthermore, *ephrin-A5* has been recently reported to localise to the ganglion (Luukko *et al.,* 2004), consistent with the findings from this study in chick. On the other hand, redundancy may prove to be a problem when investigating the role of *ephrin-A5* in the mouse trigeminal ganglion, since the murine ganglion also appears to express *ephrin-A2* and *ephrin-A4* transcripts (Luukko *et al.,* 2004). The chick trigeminal ganglion in contrast did not appear to localise with *ephrin-A2* transcript. Nonetheless, examination of available *ephrin-A2* (Feldheim *et al.,* 2000), *ephrin-A5* (Frisen *et al.,* 1998; Prakash *et al.,* 2000) and *ephrin-A2; ephrin-A5* (Feldheim *et al.,* 2000) knockout mutants for trigeminal ganglion axon guidance defects may be insightful. *Ephrin-A2* and ephrin-A5 are visualised in the maxillary and mandibular processes and exhibit similar expression patterns (Figure 7.1), hence these ligands are predicted to be functionally redundant to some extent. If the same ligands function during trigeminal ganglion axon guidance in the murine embryo then *ephrin-A2*$^{-/-}$; *ephrin-A5*$^{-/-}$ viable mutants are likely to be informative (Feldheim *et al.,* 2000).

Assuming that EphA3 receptor also localises to the murine trigeminal ganglion and demonstrates high expression in the ophthalmic lobe, as observed in the chick embryo, then analysis of *EphA3* null mice is justified (Vaidya *et al.,* 2003), As discussed in section

7.1, the speculated second EphA-ephrin-A independent signalling system that specifically guides maxillomandibular projections early in development, may only be revealed in these *EphA3* mutants, assuming there are no other murine receptors being expressed in the ganglion. In the LMC-hindlimb system (Figure 7.2C), the existence of a subordinate secondary guidance mechanism which may guide ventral projections supported in the absence of EphA4 function in the LMC axons and in the dorsal limb bud (Helmbacher *et al.,* 2000). Therefore, clear evidence for the existence of the secondary guidance system in the trigeminal ganglion system, may only be revealed in mice deficient for both *EphA3* and *EphA4*. The rational being that EphA3 and EphA4 are both observed in the chick trigeminal ganglion target fields in a similar manner, suggesting redundant or overlapping function during axon guidance.

7.4 In vivo elucidation of guidance cue interactions during trigeminal ganglion axon guidance

To fully understand the intricate interplay between different types of guidance cues during trigeminal ganglion axon guidance (Figure 7.3), genetic manipulations in the mouse may be very insightful. To validate the above model (Figure 7.3), it will be necessary to systematically mate existing mutant lines in all possible combinations to generate double or even triple homozygotes deficient for two or three guidance cues.

An important aspect of the model is the targeting of ophthalmic lobe projections and the assumption that high levels of EphA3 restrict these axons to the ophthalmic process. Therefore, the initial creation of a transgenic line with restricted Cre-recombinase activity under the Pax3 promoter in the ophthalmic placode would be essential. Pax3 is an excellent marker of ophthalmic placode cells and neurons (Baker *et al.,* 2002; Baker *et al.,* 1999; Stark *et al.,* 1997), although it is important for neural crest development (Serbedzija and McMahon, 1997; Stark *et al.,* 1997). Therefore to cause minimal disruption to neural crest migration in the embryo, it will be necessary to drive Cre-recombinase expression under a Pax3 promoter containing ophthalmic placode/lobe specific enhancer elements. The resultant *Pax3-Cre* animals could be used to specifically inactivate *EphA3* in ophthalmic lobe placode derived neurons by crossing with mutant line carrying a Cre-responsive conditional *EphA3* null allele. Once generated, the *Pax3-Cre; EphA3*$^{-/-}$ mice may be crossed with different mutants lacking a particular guidance cue such as *Sema3A*

(Taniguchi *et al.,* 1997). In the *Sema3A* mutant background (Taniguchi *et al.,* 1997), *EphA3* deficiency in ophthalmic axons is expected to lead to aberrant axon misrouting to the first branchial arch early during development around E9-9.5. This would be in stark contrast to the *Sema3A* mutant phenotype, which showed defasciculation of trigeminal axons en route to the target fields around E10-11 and yet still correctly innervated the target fields (Taniguchi *et al.,* 1997). Therefore, not only would the *Pax3-Cre; EphA3*$^{-/-}$ animals in the *Sema3A*$^{-/-}$ background exhibit an early phenotype, ophthalmic lobe projections would be severely compromised by E10-11, due to an inability to respond to repulsive ephrin-As in the first branchial arch during pathfinding with the combined loss of repulsive Sema3A activity. One caveat however, is that the differential lobe expression of EphA3 in the mouse trigeminal ganglion remains to be verified.

The *BDNF*$^{-/-}$*; NT-3*$^{-/-}$ double homozygotes did not exhibit aberrant trigeminal axon guidance (O'Connor and Tessier-Lavigne, 1999). Therefore, to examine the combined roles of EphA3/ EphA4 and neurotrophins during trigeminal axon pathfinding, *EphA3*$^{-/-}$*; EphA4*$^{-/-}$ mice could be mated with existing *BDNF*$^{-/-}$*; NT-3*$^{-/-}$ animals (O'Connor and Tessier-Lavigne, 1999).

7.5 What signals lie downstream of EphA3 activation in trigeminal ganglion axons/ growth cones?

The avoidance of ephrin-A5-Fc substrate by ophthalmic axons visualised after 24 hours in culture points to the classic EphA/ephrin-A repulsive interactions. What down stream effectors mediate this repulsive interaction between axonal-EphA3 and substratum ephrin-A5-Fc that leads to cytoskeletal changes? Previously, addition of ephrin-A5-Fc to cultured cortical neurons was found to cause a net loss of F-actin from the neuron by perturbing polymerisation of F-actin (Meima *et al.,* 1997). In the collapsing growth cone, F-actin depolymerisation in response to ephrin-A5 is mediated through the activation of RhoA and RhoA kinase (Wahl *et al.,* 2000). Thus, in the presence of RhoA or RhoA kinase inhibitors, high EphA3 positive ophthalmic axons may not exhibit sensitivity to ephrin-A5-Fc in the substratum choice assay.

Links between ephrin-A mediated signalling and F-actin cytoskeleton is further signified by the requirement for Rac1 during ephrin-A2 mediated growth cone collapse. During growth cone extension, the small GTPase Rac1 promotes F-actin polymerisation and drives lamellapodial extensions. However, following treatment with ephrin-A2, Rac1 activity is initially lost leading to the cessation of growth cone extension. Subsequently, Rac1 activity is required for endocytosis of the plasma membrane and F-actin reorganisation, suggesting an altered function for Rac1 during growth cone collapse (Jurney *et al.*, 2002). Consistent with the actions of ephrin-As on F-actin, EphA3 receptor puncta were observed scattered along F-actin filopodia of cultured growth cones from both ophthalmic and maxillomandibular explant cultures in this study.

Another downstream mediator of EphA repulsive signalling in vitro is Src family tyrosine kinases (SFKs) (Knoll and Drescher, 2004). Inhibiting SFKs, either enzymatically or pharmacologically, reduced EphA mediated repulsion of chick embryonic retinal ganglion cell (RGC) axons. Also, co-expression of SFKs and EphAs on RGC axons facilitated the recruitment of SFKs to EphAs following ephrin-A stimulation. Cortactin (a protein required for *de novo* actin polymerisation), ephexin (a RhoGEF) and EphA receptors themselves are targets of SFKs, and this may provide a mechanism for localised breakdown of cytoskeleton in the growth cone. Tyrosine phosphorylation of EphAs by SFKs was predicted to further recruit signalling molecules (Knoll and Drescher, 2004). It will be interesting to determine whether there is recruitment of SFKs not only in ophthalmic axons/ growth cones but also in maxillomandibular neurons. In future experiments, pharmacological and enzymatic inhibitors could be used to address the roles of small GTPases and SFKs during trigeminal ganglion axon guidance *in vitro*.

7.6 Other roles for ganglionic EphA3/ ephrin-A5 interactions during trigeminal ganglion development?

The trigeminal ganglion is composed of a heterogeneous population of cells (D'Amico-Martel and Noden, 1980; D'Amico-Martel and Noden, 1983; Hamburger, 1961). A further function for EphA3/ephrin-A5 ganglionic interactions could be therefore during assimilation of these various cell populations into the ganglion during gangliogenesis. No attention has been devoted to elucidating the function of cell adhesion molecules during the process of gangliogenesis. It is likely that complex repulsive and/ or attractive

signalling mediated by EphA3/ephrin-A5 interactions play a pivotal role during this process. Evidence presented in this study denote that ophthalmic neurons, maxillomandibular neurons and proximal region neural crest express varying levels of EphA3, although ephrin-A5 levels appear to be similar at stage 20.

Cells of placode origin are found to settle in the distal portions of the trigeminal ganglion (D'Amico-Martel and Noden, 1983) and derivatives from the two placodes (ophthalmic and maxillomandibular) do not appear to mingle. This was particularly clear since at no stage were high Pax3 expressing cells observed in the distal portions of the maxillomandibular lobe in this study. Therefore, the settling pattern of placode derivatives from the two placodes may confer trigeminal ganglion lobe identity and induce somatotopy[1]. Indeed in the mouse embryo (E10-11), target tissue epithelium does not induce somatotopy of the maxillomandibular components of the ganglion, implying that an intrinsic code confers lobe identity (Scott and Atkinson, 1999). Additionally, evidence in the field suggests that molecules in the developing head ectomesenchyme, may promote axon fasciculation and guide axons, and in doing so induce gross somatotopy in the trigeminal ganglion (Riggott and Moody, 1987; Scott and Atkinson, 1999). In other words, it is believed that neuronal sub-type identity and axon guidance are tightly coupled (Blagburn and Bacon, 2004; Kania and Jessell, 2003).

In the vertebrate trunk, Ephs and ephrins are downstream effectors of LIM homeodomain transcription factors, which determine motor neuron sub-type identity in the LMC and influence dorsal versus ventral trajectories into the hindlimb (Kania and Jessell, 2003). In much the same way, Ephs and ephrins may be effectors of transcription factors (e.g. the Pax genes), and provide the intrinsic code necessary to establish somatotopy in the trigeminal ganglion early during development. If so, the expression of EphA3 and ephrin-A5 in the trigeminal ganglion shown here signifies that these are likely effector candidates for this process. Additionally, the restricted expression of transcription factors Islet1, in the medial LMC and Lim1, in the lateral LMC neurons appear to participate in controlling the expression levels of EphA4 in LMC neurons; Islet 1 expression reduces EphA4 levels, while Lim1 were shown to increase EphA4 expression (Kania and Jessell, 2003) (Figure

[1] Somatotopy is the mapping of neurons to discrete regions of a ganglion, nucleus or higher centre, which depicts axon projections to specific topographies in the embryo.

7.2C-D). Hence, it is likely that high EphA3 expression exhibited in the ophthalmic lobe neurons may be under the direct control of the transcription factor Pax3, which is specifically expressed by ophthalmic neurons and required for their specification (Baker *et al.,* 2002; Baker *et al.,* 1999; Stark *et al.,* 1997). To directly test this hypothesis, ectopic Pax3 could be expressed using *in ovo* electroporation in the chick maxillomandibular neurons around stages 13. The predicted outcome is an elevation of EphA3 expression in these ectopic Pax3 expressing maxillomandibular neurons compared to those neurons on the unelectroporated side.

One implication for the variation in EphA3 expression and yet the non-differential ephrin-A5 expression within ophthalmic versus maxillomandibular neurons, could be in mediating repulsive signalling between ophthalmic and maxillomandibular placode derivatives within the ganglion itself. This repulsive signalling would ensure that ophthalmic neuron populations do not mingle with maxillomandibular neurons within the ganglion. The possibility also remains that EphA3/ephrin-A5 interactions may play a role during trigeminal placode development.

7.7 Conclusion

From the data presented in this study it is suggested that EphA/ephrin-A interactions may present a lobe specific directionality to trigeminal ganglion axon projections during development, previously not evident from the investigation of other molecular guidance cues.

"One does not discover new lands without consenting to lose sight of the shore for a very long time."--André Gide

References

Adams, R. H., Diella, F., Hennig, S., Helmbacher, F., Deutsch, U., and Klein, R. (2001). The cytoplasmic domain of the ligand ephrinB2 is required for vascular morphogenesis but not cranial neural crest migration. *Cell* **104,** 57-69.

Araujo, M., and Nieto, M. A. (1997). The expression of chick EphA7 during segmentation of the central and peripheral nervous system. *Mech Dev* **68,** 173-7.

Bak, M., and Fraser, S. E. (2003). Axon fasciculation and differences in midline kinetics between pioneer and follower axons within commissural fascicles. *Development* **130,** 4999-5008.

Baker, C. V., and Bronner-Fraser, M. (2000). Establishing neuronal identity in vertebrate neurogenic placodes. *Development* **127,** 3045-56.

Baker, C. V., and Bronner-Fraser, M. (2001). Vertebrate cranial placodes I. Embryonic induction. *Dev Biol* **232,** 1-61.

Baker, C. V., Bronner-Fraser, M., Le Douarin, N. M., and Teillet, M. A. (1997). Early- and late-migrating cranial neural crest cell populations have equivalent developmental potential in vivo. *Development* **124,** 3077-87.

Baker, C. V., Stark, M. R., and Bronner-Fraser, M. (2002). Pax3-expressing trigeminal placode cells can localize to trunk neural crest sites but are committed to a cutaneous sensory neuron fate. *Dev Biol* **249,** 219-36.

Baker, C. V., Stark, M. R., Marcelle, C., and Bronner-Fraser, M. (1999). Competence, specification and induction of Pax-3 in the trigeminal placode. *Development* **126,** 147-56.

Baker, R. K., and Antin, P. B. (2003). Ephs and ephrins during early stages of chick embryogenesis. *Dev Dyn* **228,** 128-42.

Baker, R. K., Vanderboom, A. K., Bell, G. W., and Antin, P. B. (2001). Expression of the receptor tyrosine kinase gene EphB3 during early stages of chick embryo development. *Mech Dev* **104,** 129-32.

Bastiani, M. J., Raper, J. A., and Goodman, C. S. (1984). Pathfinding by neuronal growth cones in grasshopper embryos. III. Selective affinity of the G growth cone for the P cells within the A/P fascicle. *J Neurosci* **4,** 2311-28.

Bate, C. M. (1976). Pioneer neurones in an insect embryo. *Nature* **260,** 54-6.

Becker, E., Huynh-Do, U., Holland, S., Pawson, T., Daniel, T. O., and Skolnik, E. Y. (2000). Nck-interacting Ste20 kinase couples Eph receptors to c-Jun N-terminal kinase and integrin activation. *Mol Cell Biol* **20,** 1537-45.

Begbie, J., Ballivet, M., and Graham, A. (2002). Early steps in the production of sensory neurons by the neurogenic placodes. *Mol Cell Neurosci* **21,** 502-11.

Birgbauer, E., Cowan, C. A., Sretavan, D. W., and Henkemeyer, M. (2000). Kinase independent function of EphB receptors in retinal axon pathfinding to the optic disc from dorsal but not ventral retina. *Development* **127,** 1231-41.

Birgbauer, E., Oster, S. F., Severin, C. G., and Sretavan, D. W. (2001). Retinal axon growth cones respond to EphB extracellular domains as inhibitory axon guidance cues. *Development* **128,** 3041-8.

Blagburn, J. M., and Bacon, J. P. (2004). Control of central synaptic specificity in insect sensory neurons. *Annu Rev Neurosci* **27,** 29-51.

Blanco, M. J., Pena-Melian, A., and Nieto, M. A. (2002). Expression of EphA receptors and ligands during chick cerebellar development. *Mech Dev* **114,** 225-9.

Bonner, J., and O'Connor, T. P. (2001). The permissive cue laminin is essential for growth cone turning in vivo. *J Neurosci* **21,** 9782-91.

Braisted, J. E., McLaughlin, T., Wang, H. U., Friedman, G. C., Anderson, D. J., and O'Leary D, D. (1997). Graded and lamina-specific distributions of ligands of EphB receptor tyrosine kinases in the developing retinotectal system. *Dev Biol* **191,** 14-28.

Brambilla, R., Br, uuml, ckner, K., Orioli, D., Bergemann, A. D., Flanagan, J. G., and Klein, R. (1996). Similarities and Differences in the Way Transmembrane-Type Ligands Interact with the Elk Subclass of Eph Receptors. *Mol Cell Neurosci* **8,** 199-209.

Bronner-Fraser, M. (1986). Analysis of the early stages of trunk neural crest migration in avian embryos using monoclonal antibody HNK-1. *Dev Biol* **115,** 44-55.

Brown, A., Yates, P. A., Burrola, P., Ortuno, D., Vaidya, A., Jessell, T. M., Pfaff, S. L., O'Leary, D. D., and Lemke, G. (2000). Topographic mapping from the retina to the midbrain is controlled by relative but not absolute levels of EphA receptor signaling. *Cell* **102,** 77-88.

Brown, D. A., and London, E. (1998). Functions of lipid rafts in biological membranes. *Annu Rev Cell Dev Biol* **14,** 111-36.

Bruckner, K., Pablo Labrador, J., Scheiffele, P., Herb, A., Seeburg, P. H., and Klein, R. (1999). EphrinB ligands recruit GRIP family PDZ adaptor proteins into raft membrane microdomains. *Neuron* **22,** 511-24.

Caras, I. W. (1997). A link between axon guidance and axon fasciculation suggested by studies of the tyrosine kinase receptor EphA5/REK7 and its ligand ephrin-A5/AL-1. *Cell Tissue Res* **290,** 261-4.

Chan, W. Y., and Tam, P. P. (1988). A morphological and experimental study of the mesencephalic neural crest cells in the mouse embryo using wheat germ agglutinin-gold conjugate as the cell marker. *Development* **102,** 427-42.

Chen, H., Bagri, A., Zupicich, J. A., Zou, Y., Stoeckli, E., Pleasure, S. J., Lowenstein, D. H., Skarnes, W. C., Chedotal, A., and Tessier-Lavigne, M. (2000). Neuropilin-2 regulates the development of selective cranial and sensory nerves and hippocampal mossy fiber projections. *Neuron* **25,** 43-56.

Chen, H., Chedotal, A., He, Z., Goodman, C. S., and Tessier-Lavigne, M. (1997). Neuropilin-2, a novel member of the neuropilin family, is a high affinity receptor for the semaphorins Sema E and Sema IV but not Sema III. *Neuron* **19,** 547-59.

Cheng, H. J., Bagri, A., Yaron, A., Stein, E., Pleasure, S. J., and Tessier-Lavigne, M. (2001). Plexin-A3 mediates semaphorin signaling and regulates the development of hippocampal axonal projections. *Neuron* **32,** 249-63.

Cheng, H. J., and Flanagan, J. G. (1994). Identification and cloning of ELF-1, a developmentally expressed ligand for the Mek4 and Sek receptor tyrosine kinases. *Cell* **79,** 157-68.

Cheng, H. J., Nakamoto, M., Bergemann, A. D., and Flanagan, J. G. (1995). Complementary gradients in expression and binding of ELF-1 and Mek4 in development of the topographic retinotectal projection map. *Cell* **82,** 371-81.

Chilton, J. K., and Guthrie, S. (2003). Cranial expression of class 3 secreted semaphorins and their neuropilin receptors. *Dev Dyn* **228,** 726-33.

Chin-Sang, I. D., George, S. E., Ding, M., Moseley, S. L., Lynch, A. S., and Chisholm, A. D. (1999). The ephrin VAB-2/EFN-1 functions in neuronal signaling to regulate epidermal morphogenesis in C. elegans. *Cell* **99,** 781-90.

Condic, M. L., and Letourneau, P. C. (1997). Ligand-induced changes in integrin expression regulate neuronal adhesion and neurite outgrowth. *Nature* **389,** 852-6.

Connor, R. J., Menzel, P., and Pasquale, E. B. (1998). Expression and tyrosine phosphorylation of Eph receptors suggest multiple mechanisms in patterning of the visual system. *Dev Biol* **193,** 21-35.

Covell, D. A., Jr., and Noden, D. M. (1989). Embryonic development of the chick primary trigeminal sensory-motor complex. *J Comp Neurol* **286,** 488-503.

Cowan, C. A., and Henkemeyer, M. (2002). Ephrins in reverse, park and drive. *Trends Cell Biol* **12,** 339-46.

Cowan, C. A., Yokoyama, N., Saxena, A., Chumley, M. J., Silvany, R. E., Baker, L. A., Srivastava, D., and Henkemeyer, M. (2004). Ephrin-B2 reverse signaling is required for axon pathfinding and cardiac valve formation but not early vascular development. *Dev Biol* **271,** 263-71.

Cutforth, T., Moring, L., Mendelsohn, M., Nemes, A., Shah, N. M., Kim, M. M., Frisen, J., and Axel, R. (2003). Axonal ephrin-As and odorant receptors: coordinate determination of the olfactory sensory map. *Cell* **114,** 311-22.

D'Amico-Martel, A., and Noden, D. M. (1980). An autoradiographic analysis of the development of the chick trigeminal ganglion. *J Embryol Exp Morphol* **55,** 167-82.

D'Amico-Martel, A., and Noden, D. M. (1983). Contributions of placodal and neural crest cells to avian cranial peripheral ganglia. *Am J Anat* **166,** 445-68.

Davies, A. M. (1988). The trigeminal system: an advantageous experimental model for studying neuronal development. *Development* **103,** 175-83.

Davis, S., Gale, N. W., Aldrich, T. H., Maisonpierre, P. C., Lhotak, V., Pawson, T., Goldfarb, M., and Yancopoulos, G. D. (1994). Ligands for EPH-related receptor tyrosine kinases that require membrane attachment or clustering for activity. *Science* **266,** 816-9.

Davy, A., Gale, N. W., Murray, E. W., Klinghoffer, R. A., Soriano, P., Feuerstein, C., and Robbins, S. M. (1999). Compartmentalized signaling by GPI-anchored ephrin-A5 requires the Fyn tyrosine kinase to regulate cellular adhesion. *Genes Dev* **13,** 3125-35.

Davy, A., and Robbins, S. M. (2000). Ephrin-A5 modulates cell adhesion and morphology in an integrin- dependent manner. *Embo J* **19,** 5396-405.

Dent, E. W., and Gertler, F. B. (2003). Cytoskeletal dynamics and transport in growth cone motility and axon guidance. *Neuron* **40,** 209-27.

Donoghue, M. J., Merlie, J. P., and Sanes, J. R. (1996). The Eph Kinase Ligand AL-1 Is Expressed by Rostral Muscles and Inhibits Outgrowth from Caudal Neurons. *Mol Cell Neurosci* **8,** 185-98.

Dottori, M., Hartley, L., Galea, M., Paxinos, G., Polizzotto, M., Kilpatrick, T., Bartlett, P. F., Murphy, M., Kontgen, F., and Boyd, A. W. (1998). EphA4 (Sek1) receptor tyrosine kinase is required for the development of the corticospinal tract. *Proc Natl Acad Sci U S A* **95,** 13248-53.

Drescher, U. (1997). The Eph family in the patterning of neural development. *Curr Biol* **7,** R799-807.

Drescher, U., Kremoser, C., Handwerker, C., Loschinger, J., Noda, M., and Bonhoeffer, F. (1995). In vitro guidance of retinal ganglion cell axons by RAGS, a 25 kDa tectal protein related to ligands for Eph receptor tyrosine kinases. *Cell* **82,** 359-70.

Easter, S. S., Jr., Ross, L. S., and Frankfurter, A. (1993). Initial tract formation in the mouse brain. *J Neurosci* **13,** 285-99.

Eberhart, J., Barr, J., O'Connell, S., Flagg, A., Swartz, M. E., Cramer, K. S., Tosney, K. W., Pasquale, E. B., and Krull, C. E. (2004). Ephrin-A5 exerts positive or inhibitory effects on distinct subsets of EphA4-positive motor neurons. *J Neurosci* **24,** 1070-8.

Eberhart, J., Swartz, M., Koblar, S. A., Pasquale, E. B., Tanaka, H., and Krull, C. E. (2000). Expression of EphA4, ephrin-A2 and ephrin-A5 during axon outgrowth to the hindlimb indicates potential roles in pathfinding. *Dev Neurosci* **22,** 237-50.

Eberhart, J., Swartz, M. E., Koblar, S. A., Pasquale, E. B., and Krull, C. E. (2002). EphA4 constitutes a population-specific guidance cue for motor neurons. *Dev Biol* **247,** 89-101.

Elowe, S., Holland, S. J., Kulkarni, S., and Pawson, T. (2001). Downregulation of the Ras-mitogen-activated protein kinase pathway by the EphB2 receptor tyrosine kinase is required for ephrin-induced neurite retraction. *Mol Cell Biol* **21,** 7429-41.

Epstein, D. J., Vekemans, M., and Gros, P. (1991). Splotch (Sp2H), a mutation affecting development of the mouse neural tube, shows a deletion within the paired homeodomain of Pax-3. *Cell* **67,** 767-74.

Feldheim, D. A., Kim, Y. I., Bergemann, A. D., Frisen, J., Barbacid, M., and Flanagan, J. G. (2000). Genetic analysis of ephrin-A2 and ephrin-A5 shows their requirement in multiple aspects of retinocollicular mapping. *Neuron* **25,** 563-74.

Feldheim, D. A., Vanderhaeghen, P., Hansen, M. J., Frisen, J., Lu, Q., Barbacid, M., and Flanagan, J. G. (1998). Topographic guidance labels in a sensory projection to the forebrain. *Neuron* **21,** 1303-13.

Flanagan, J. G., and Vanderhaeghen, P. (1998). The ephrins and Eph receptors in neural development. *Annu Rev Neurosci* **21,** 309-45.

Flenniken, A. M., Gale, N. W., Yancopoulos, G. D., and Wilkinson, D. G. (1996). Distinct and overlapping expression patterns of ligands for Eph-related receptor tyrosine kinases during mouse embryogenesis. *Dev Biol* **179,** 382-401.

Friedrichson, T., and Kurzchalia, T. V. (1998). Microdomains of GPI-anchored proteins in living cells revealed by crosslinking. *Nature* **394,** 802-5.

Frisen, J., Yates, P. A., McLaughlin, T., Friedman, G. C., O'Leary, D. D., and Barbacid, M. (1998). Ephrin-A5 (AL-1/RAGS) is essential for proper retinal axon guidance and topographic mapping in the mammalian visual system. *Neuron* **20,** 235-43.

Gale, N. W., Holland, S. J., Valenzuela, D. M., Flenniken, A., Pan, L., Ryan, T. E., Henkemeyer, M., Strebhardt, K., Hirai, H., Wilkinson, D. G., Pawson, T., Davis, S., and Yancopoulos, G. D. (1996). Eph receptors and ligands comprise two major specificity subclasses and are reciprocally compartmentalized during embryogenesis. *Neuron* **17,** 9-19.

Gauthier, L. R., and Robbins, S. M. (2003). Ephrin signaling: One raft to rule them all? One raft to sort them? One raft to spread their call and in signaling bind them? *Life Sci* **74,** 207-16.

George, S. E., Simokat, K., Hardin, J., and Chisholm, A. D. (1998). The VAB-1 Eph receptor tyrosine kinase functions in neural and epithelial morphogenesis in C. elegans. *Cell* **92,** 633-43.

Giger, R. J., Cloutier, J. F., Sahay, A., Prinjha, R. K., Levengood, D. V., Moore, S. E., Pickering, S., Simmons, D., Rastan, S., Walsh, F. S., Kolodkin, A. L., Ginty, D. D., and Geppert, M. (2000). Neuropilin-2 is required in vivo for selective axon guidance responses to secreted semaphorins. *Neuron* **25,** 29-41.

Giniger, E. (2002). How do Rho family GTPases direct axon growth and guidance? A proposal relating signaling pathways to growth cone mechanics. *Differentiation* **70,** 385-96.

Graham, A., and Begbie, J. (2000). Neurogenic placodes: a common front. *Trends Neurosci* **23,** 313-6.

Guirland, C., Suzuki, S., Kojima, M., Lu, B., and Zheng, J. Q. (2004). Lipid rafts mediate chemotropic guidance of nerve growth cones. *Neuron* **42,** 51-62.

Hamburger, V. (1961). Experimental analysis of the dual origin of the trigeminal ganglion in the chick embryo. *J Exp Zool* **148,** 91-123.

Hamburger, V., and Hamilton, H. L. (1951). A series of normal stages in the development of the chick embryo. *J Embryol Exp Morphol* **88,** 49-92.

Hansen, M. J., Dallal, G. E., and Flanagan, J. G. (2004). Retinal axon response to ephrin-as shows a graded, concentration-dependent transition from growth promotion to inhibition. *Neuron* **42,** 717-30.

Hattori, M., Osterfield, M., and Flanagan, J. G. (2000). Regulated cleavage of a contact-mediated axon repellent. *Science* **289,** 1360-5.

Helmbacher, F., Schneider-Maunoury, S., Topilko, P., Tiret, L., and Charnay, P. (2000). Targeting of the EphA4 tyrosine kinase receptor affects dorsal/ventral pathfinding of limb motor axons. *Development* **127,** 3313-24.

Henkemeyer, M., Marengere, L. E., McGlade, J., Olivier, J. P., Conlon, R. A., Holmyard, D. P., Letwin, K., and Pawson, T. (1994). Immunolocalization of the Nuk receptor tyrosine kinase suggests roles in segmental patterning of the brain and axonogenesis. *Oncogene* **9,** 1001-14.

Henkemeyer, M., Orioli, D., Henderson, J. T., Saxton, T. M., Roder, J., Pawson, T., and Klein, R. (1996). Nuk controls pathfinding of commissural axons in the mammalian central nervous system. *Cell* **86,** 35-46.

Henrique, D., Adam, J., Myat, A., Chitnis, A., Lewis, J., and Ish-Horowicz, D. (1995). Expression of a Delta homologue in prospective neurons in the chick. *Nature* **375,** 787-90.

Himanen, J. P., Chumley, M. J., Lackmann, M., Li, C., Barton, W. A., Jeffrey, P. D., Vearing, C., Geleick, D., Feldheim, D. A., Boyd, A. W., Henkemeyer, M., and Nikolov, D. B. (2004). Repelling class discrimination: ephrin-A5 binds to and activates EphB2 receptor signaling. *Nat Neurosci* **7,** 501-9.

Himanen, J. P., and Nikolov, D. B. (2002). Purification, crystallization and preliminary characterization of an Eph-B2/ephrin-B2 complex. *Acta Crystallogr D Biol Crystallogr* **58,** 533-5.

Hock, B., Bohme, B., Karn, T., Feller, S., Rubsamen-Waigmann, H., and Strebhardt, K. (1998). Tyrosine-614, the major autophosphorylation site of the receptor tyrosine kinase HEK2, functions as multi-docking site for SH2-domain mediated interactions. *Oncogene* **17,** 255-60.

Holland, S. J., Gale, N. W., Gish, G. D., Roth, R. A., Songyang, Z., Cantley, L. C., Henkemeyer, M., Yancopoulos, G. D., and Pawson, T. (1997). Juxtamembrane tyrosine residues couple the Eph family receptor EphB2/Nuk to specific SH2 domain proteins in neuronal cells. *Embo J* **16,** 3877-88.

Holmberg, J., Clarke, D. L., and Frisen, J. (2000). Regulation of repulsion versus adhesion by different splice forms of an Eph receptor. *Nature* **408,** 203-6.

Holmberg, J., and Frisen, J. (2002). Ephrins are not only unattractive. *Trends Neurosci* **25,** 239-43.

Hornberger, M. R., Dutting, D., Ciossek, T., Yamada, T., Handwerker, C., Lang, S., Weth, F., Huf, J., Wessel, R., Logan, C., Tanaka, H., and Drescher, U. (1999). Modulation of EphA receptor function by coexpressed ephrinA ligands on retinal ganglion cell axons. *Neuron* **22,** 731-42.

Huai, J., and Drescher, U. (2001). An ephrin-A-dependent signaling pathway controls integrin function and is linked to the tyrosine phosphorylation of a 120-kDa protein. *J Biol Chem* **276,** 6689-94.

Huber, A. B., Kolodkin, A. L., Ginty, D. D., and Cloutier, J. F. (2003). Signaling at the growth cone: ligand-receptor complexes and the control of axon growth and guidance. *Annu Rev Neurosci* **26,** 509-63.

Huynh-Do, U., Stein, E., Lane, A. A., Liu, H., Cerretti, D. P., and Daniel, T. O. (1999). Surface densities of ephrin-B1 determine EphB1-coupled activation of cell attachment through alphavbeta3 and alpha5beta1 integrins. *Embo J* **18,** 2165-73.

Huynh-Do, U., Vindis, C., Liu, H., Cerretti, D. P., McGrew, J. T., Enriquez, M., Chen, J., and Daniel, T. O. (2002). Ephrin-B1 transduces signals to activate integrin-mediated migration, attachment and angiogenesis. *J Cell Sci* **115,** 3073-81.

Isbister, C. M., and O'Connor, T. P. (2000). Mechanisms of growth cone guidance and motility in the developing grasshopper embryo. *J Neurobiol* **44,** 271-80.

Iwamasa, H., Ohta, K., Yamada, T., Ushijima, K., Terasaki, H., and Tanaka, H. (1999). Expression of Eph receptor tyrosine kinases and their ligands in chick embryonic motor neurons and hindlimb muscles. *Dev Growth Differ* **41,** 685-98.

Jurney, W. M., Gallo, G., Letourneau, P. C., and McLoon, S. C. (2002). Rac1-mediated endocytosis during ephrin-A2- and semaphorin 3A-induced growth cone collapse. *J Neurosci* **22,** 6019-28.

Kania, A., and Jessell, T. M. (2003). Topographic Motor Projections in the Limb Imposed by LIM Homeodomain Protein Regulation of Ephrin-A:EphA Interactions. *Neuron* **38,** 581-96.

Kitsukawa, T., Shimizu, M., Sanbo, M., Hirata, T., Taniguchi, M., Bekku, Y., Yagi, T., and Fujisawa, H. (1997). Neuropilin-semaphorin III/D-mediated chemorepulsive signals play a crucial role in peripheral nerve projection in mice. *Neuron* **19,** 995-1005.

Klein, R. (1999). Bidirectional signals establish boundaries. *Curr Biol* **9,** R691-4.

Knoll, B., and Drescher, U. (2002). Ephrin-As as receptors in topographic projections. *Trends Neurosci* **25,** 145-9.

Knoll, B., and Drescher, U. (2004). Src family kinases are involved in EphA receptor-mediated retinal axon guidance. *J Neurosci* **24,** 6248-57.

Knoll, B., Zarbalis, K., Wurst, W., and Drescher, U. (2001). A role for the EphA family in the topographic targeting of vomeronasal axons. *Development* **128,** 895-906.

Kobayashi, H., Koppel, A. M., Luo, Y., and Raper, J. A. (1997). A role for collapsin-1 in olfactory and cranial sensory axon guidance. *J Neurosci* **17,** 8339-52.

Koblar, S. A., Krull, C. E., Pasquale, E. B., McLennan, R., Peale, F. D., Cerretti, D. P., and Bothwell, M. (2000). Spinal motor axons and neural crest cells use different molecular guides for segmental migration through the rostral half-somite. *J Neurobiol* **42,** 437-47.

Koeberle, P. D., and Bahr, M. (2004). Growth and guidance cues for regenerating axons: where have they gone? *J Neurobiol* **59,** 162-80.

Krull, C. E., Lansford, R., Gale, N. W., Collazo, A., Marcelle, C., Yancopoulos, G. D., Fraser, S. E., and Bronner-Fraser, M. (1997). Interactions of Eph-related receptors and ligands confer rostrocaudal pattern to trunk neural crest migration. *Curr Biol* **7,** 571-80.

Kullander, K., and Klein, R. (2002). Mechanisms and functions of Eph and ephrin signalling. *Nat Rev Mol Cell Biol* **3,** 475-86.

Kullander, K., Mather, N. K., Diella, F., Dottori, M., Boyd, A. W., and Klein, R. (2001). Kinase-dependent and kinase-independent functions of EphA4 receptors in major axon tract formation in vivo. *Neuron* **29,** 73-84.

Kury, P., Gale, N., Connor, R., Pasquale, E., and Guthrie, S. (2000). Eph receptors and ephrin expression in cranial motor neurons and the branchial arches of the chick embryo. *Mol Cell Neurosci* **15,** 123-40.

Lackmann, M., Mann, R. J., Kravets, L., Smith, F. M., Bucci, T. A., Maxwell, K. F., Howlett, G. J., Olsson, J. E., Vanden Bos, T., Cerretti, D. P., and Boyd, A. W. (1997). Ligand for EPH-related kinase (LERK) 7 is the preferred high affinity ligand for the HEK receptor. *J Biol Chem* **272,** 16521-30.

Lackmann, M., Oates, A. C., Dottori, M., Smith, F. M., Do, C., Power, M., Kravets, L., and Boyd, A. W. (1998). Distinct subdomains of the EphA3 receptor mediate ligand binding and receptor dimerization. *J Biol Chem* **273,** 20228-37.

Landmesser, L. (1978). The development of motor projection patterns in the chick hind limb. *J Physiol* **284,** 391-414.

Le Douarin, N. M., and Kalcheim, C. (1999). From Neural Crest to the ganglia of the peripheral nervous system: the sensory ganglia. *In* "The Neural Crest", pp. 153-196. Cambridge University Press.

Lee, V. M., Carden, M. J., Schlaepfer, W. W., and Trojanowski, J. Q. (1987). Monoclonal antibodies distinguish several differentially phosphorylated states of the two largest rat neurofilament subunits (NF-H and NF-M) and demonstrate their existence in the normal nervous system of adult rats. *J Neurosci* **7,** 3474-88.

Lopresti, V., Macagno, E. R., and Levinthal, C. (1973). Structure and development of neuronal connections in isogenic organisms: cellular interactions in the development of the optic lamina of Daphnia. *Proc Natl Acad Sci U S A* **70,** 433-7.

Lumsden, A. G. (1988). Spatial organization of the epithelium and the role of neural crest cells in the initiation of the mammalian tooth germ. *Development* **103 Suppl,** 155-69.

Lumsden, A. G., and Davies, A. M. (1983). Earliest sensory nerve fibres are guided to peripheral targets by attractants other than nerve growth factor. *Nature* **306,** 786-8.

Lumsden, A. G., and Davies, A. M. (1986). Chemotropic effect of specific target epithelium in the developing mammalian nervous system. *Nature* **323,** 538-9.

Luukko, K., Loes, S., Kvinnsland, I. H., and Kettunen, P. (2004). Expression of ephrin-A ligands and EphA receptors in the developing mouse tooth and its supporting tissues. *Cell Tissue Res.*

Lwigale, P. Y. (2001). Embryonic origin of avian corneal sensory nerves. *Dev Biol* **239,** 323-37.

Ma, Q., Chen, Z., del Barco Barrantes, I., de la Pompa, J. L., and Anderson, D. J. (1998). neurogenin1 is essential for the determination of neuronal precursors for proximal cranial sensory ganglia. *Neuron* **20,** 469-82.

Mann, F., Miranda, E., Weinl, C., Harmer, E., and Holt, C. E. (2003). B-type Eph receptors and ephrins induce growth cone collapse through distinct intracellular pathways. *J Neurobiol* **57,** 323-36.

Mann, F., Ray, S., Harris, W., and Holt, C. (2002). Topographic mapping in dorsoventral axis of the Xenopus retinotectal system depends on signaling through ephrin-B ligands. *Neuron* **35,** 461-73.

Marcus, R. C., Gale, N. W., Morrison, M. E., Mason, C. A., and Yancopoulos, G. D. (1996). Eph family receptors and their ligands distribute in opposing gradients in the developing mouse retina. *Dev Biol* **180,** 786-9.

Marin, O., Blanco, M. J., and Nieto, M. A. (2001). Differential expression of Eph receptors and ephrins correlates with the formation of topographic projections in primary and secondary visual circuits of the embryonic chick forebrain. *Dev Biol* **234,** 289-303.

Marston, D. J., Dickinson, S., and Nobes, C. D. (2003). Rac-dependent trans-endocytosis of ephrinBs regulates Eph-ephrin contact repulsion. *Nat Cell Biol.*

McLennan, R., and Krull, C. E. (2002). Ephrin-as cooperate with EphA4 to promote trunk neural crest migration. *Gene Expr* **10,** 295-305.

Meima, L., Moran, P., Matthews, W., and Caras, I. W. (1997). Lerk2 (ephrin-B1) is a collapsing factor for a subset of cortical growth cones and acts by a mechanism different from AL-1 (ephrin-A5). *Mol Cell Neurosci* **9,** 314-28.

Mellitzer, G., Xu, Q., and Wilkinson, D. G. (1999). Eph receptors and ephrins restrict cell intermingling and communication. *Nature* **400,** 77-81.

Memberg, S. P., and Hall, A. K. (1995). Dividing neuron precursors express neuron-specific tubulin. *J Neurobiol* **27,** 26-43.

Menzel, P., Valencia, F., Godement, P., Dodelet, V. C., and Pasquale, E. B. (2001). Ephrin-A6, a new ligand for EphA receptors in the developing visual system. *Dev Biol* **230,** 74-88.

Miao, H., Burnett, E., Kinch, M., Simon, E., and Wang, B. (2000). Activation of EphA2 kinase suppresses integrin function and causes focal-adhesion-kinase dephosphorylation. *Nat Cell Biol* **2,** 62-9.

Momose, T., Tonegawa, A., Takeuchi, J., Ogawa, H., Umesono, K., and Yasuda, K. (1999). Efficient targeting of gene expression in chick embryos by microelectroporation. *Dev Growth Differ* **41,** 335-44.

Monschau, B., Kremoser, C., Ohta, K., Tanaka, H., Kaneko, T., Yamada, T., Handwerker, C., Hornberger, M. R., Loschinger, J., Pasquale, E. B., Siever, D. A., Verderame, M. F., Muller, B. K., Bonhoeffer, F., and Drescher, U. (1997). Shared and distinct functions of RAGS and ELF-1 in guiding retinal axons. *Embo J* **16,** 1258-67.

Moody, S. A., Quigg, M. S., and Frankfurter, A. (1989a). Development of the peripheral trigeminal system in the chick revealed by an isotype-specific anti-beta-tubulin monoclonal antibody. *J Comp Neurol* **279,** 567-580.

Moody, S. A., Quigg, M. S., and Little, C. D. (1989b). Extracellular matrix components of the peripheral pathway of chick trigeminal axons. *J Comp Neurol* **283,** 38-53.

Nakamoto, M., Cheng, H. J., Friedman, G. C., McLaughlin, T., Hansen, M. J., Yoon, C., O'Leary, D. D. M., and Flanagan, J. G. (1996). Topographically specific effects of ELF-1 on retinal axon guidance in vitro and retinal axon mapping in vivo. *Cell* **86,** 755-766.

Nakamoto, T., Kain, K. H., and Ginsberg, M. H. (2004). Neurobiology: New connections between integrins and axon guidance. *Curr Biol* **14,** R121-3.

Noden, D. M. (1978). The control of avian cephalic neural crest cytodifferentiation. II. Neural tissues. *Dev Biol* **67,** 313-29.

O'Connor, R., and Tessier-Lavigne, M. (1999). Identification of maxillary factor, a maxillary process-derived chemoattractant for developing trigeminal sensory axons. *Neuron* **24,** 165-78.

O'Connor, T. P., Duerr, J. S., and Bentley, D. (1990). Pioneer growth cone steering decisions mediated by single filopodial contacts in situ. *J Neurosci* **10,** 3935-46.

Orioli, D., Henkemeyer, M., Lemke, G., Klein, R., and Pawson, T. (1996). Sek4 and Nuk receptors cooperate in guidance of commissural axons and in palate formation. *Embo J* **15,** 6035-49.

Pietri, T., Eder, O., Breau, M. A., Topilko, P., Blanche, M., Brakebusch, C., Fassler, R., Thiery, J.-P., and Dufour, S. (2004). Conditional {beta}1-integrin gene deletion in neural crest cells causes severe developmental alterations of the peripheral nervous system. *Development* **131,** 3871-3883.

Prakash, N., Vanderhaeghen, P., Cohen-Cory, S., Frisen, J., Flanagan, J. G., and Frostig, R. D. (2000). Malformation of the functional organization of somatosensory cortex in adult ephrin-A5 knock-out mice revealed by in vivo functional imaging. *J Neurosci* **20,** 5841-7.

Riggott, M. J., and Moody, S. A. (1987). Distribution of laminin and fibronectin along peripheral trigeminal axon pathways in the developing chick. *J Comp Neurol* **258,** 580-96.

Santiago, A., and Erickson, C. A. (2002). Ephrin-B ligands play a dual role in the control of neural crest cell migration. *Development* **129,** 3621-32.

Scott, L., and Atkinson, M. E. (1999). Compartmentalisation of the developing trigeminal ganglion into maxillary and mandibular divisions does not depend on target contact. *J Anat* **195,** 137-45.

Seaman, C., Anderson, R., Emery, B., and Cooper, H. M. (2001). Localization of the netrin guidance receptor, DCC, in the developing peripheral and enteric nervous systems. *Mech Dev* **103,** 173-5.

Seaman, C., and Cooper, H. M. (2001). Netrin-3 protein is localized to the axons of motor, sensory, and sympathetic neurons. *Mech Dev* **101,** 245-8.

Serbedzija, G. N., and McMahon, A. P. (1997). Analysis of neural crest cell migration in Splotch mice using a neural crest-specific LacZ reporter. *Dev Biol* **185,** 139-47.

Shamah, S. M., Lin, M. Z., Goldberg, J. L., Estrach, S., Sahin, M., Hu, L., Bazalakova, M., Neve, R. L., Corfas, G., Debant, A., and Greenberg, M. E. (2001). EphA receptors regulate growth cone dynamics through the novel guanine nucleotide exchange factor ephexin. *Cell* **105,** 233-44.

Shenoy-Scaria, A. M., Dietzen, D. J., Kwong, J., Link, D. C., and Lublin, D. M. (1994). Cysteine3 of Src family protein tyrosine kinase determines palmitoylation and localization in caveolae. *J Cell Biol* **126,** 353-63.

Silver, J. (1993). Glia-neuron interactions at the midline of the developing mammalian brain and spinal cord. *Perspect Dev Neurobiol* **1,** 227-36.

Simons, K., and Toomre, D. (2000). Lipid rafts and signal transduction. *Nat Rev Mol Cell Biol* **1,** 31-9.

Smith, F. M., Vearing, C., Lackmann, M., Treutlein, H., Himanen, J., Chen, K., Saul, A., Nikolov, D., and Boyd, A. W. (2004). Dissecting the EphA3/Ephrin-A5 interactions using a novel functional mutagenesis screen. *J Biol Chem* **279,** 9522-31. Epub 2003 Dec 2.

Sperry, R. W. (1951). Regulative factors in the orderly growth of neural circuits. *Growth* **15,** 63-87.

Sperry, R. W. (1963). Chemoaffinity in the Orderly Growth of Nerve Fiber Patterns and Connections. *Proc Natl Acad Sci U S A* **50,** 703-10.

Stainier, D. Y., and Gilbert, W. (1990). Pioneer neurons in the mouse trigeminal sensory system. *Proc Natl Acad Sci U S A* **87,** 923-7.

Stainier, D. Y., and Gilbert, W. (1991). Neuronal differentiation and maturation in the mouse trigeminal sensory system, in vivo and in vitro. *J Comp Neurol* **311,** 300-12.

Stark, M. R., Sechrist, J., Bronner-Fraser, M., and Marcelle, C. (1997). Neural tube-ectoderm interactions are required for trigeminal placode formation. *Development* **124,** 4287-95.

Stein, E., Lane, A. A., Cerretti, D. P., Schoecklmann, H. O., Schroff, A. D., Van Etten, R. L., and Daniel, T. O. (1998). Eph receptors discriminate specific ligand oligomers to determine alternative signaling complexes, attachment, and assembly responses. *Genes Dev* **12,** 667-78.

Swartz, M. E., Eberhart, J., Pasquale, E. B., and Krull, C. E. (2001). EphA4/ephrin-A5 interactions in muscle precursor cell migration in the avian forelimb. *Development* **128,** 4669-80.

Tanaka, M., Ohashi, R., Nakamura, R., Shinmura, K., Kamo, T., Sakai, R., and Sugimura, H. (2004). Tiam1 mediates neurite outgrowth induced by ephrin-B1 and EphA2. *Embo J* **23,** 1075-88.

Taniguchi, M., Yuasa, S., Fujisawa, H., Naruse, I., Saga, S., Mishina, M., and Yagi, T. (1997). Disruption of semaphorin III/D gene causes severe abnormality in peripheral nerve projection. *Neuron* **19,** 519-30.

Tessier-Lavigne, M., and Goodman, C. S. (1996). The molecular biology of axon guidance. *Science* **274,** 1123-33.

Tosney, K. W., and Landmesser, L. T. (1985). Specificity of early motoneuron growth cone outgrowth in the chick embryo. *J Neurosci* **5,** 2336-44.

Tremblay, P., Kessel, M., and Gruss, P. (1995). A transgenic neuroanatomical marker identifies cranial neural crest deficiencies associated with the Pax3 mutant Splotch. *Dev Biol* **171,** 317-29.

Ulupinar, E., Datwani, A., Behar, O., Fujisawa, H., and Erzurumlu, R. (1999). Role of semaphorin III in the developing rodent trigeminal system. *Mol Cell Neurosci* **13,** 281-92.

Vaidya, A., Pniak, A., Lemke, G., and Brown, A. (2003). EphA3 null mutants do not demonstrate motor axon guidance defects. *Mol Cell Biol* **23,** 8092-8.

Varma, R., and Mayor, S. (1998). GPI-anchored proteins are organized in submicron domains at the cell surface. *Nature* **394,** 798-801.

Verwoerd, C. D., and van Oostrom, C. G. (1979). Cephalic neural crest and placodes. *Adv Anat Embryol Cell Biol* **58,** 1-75.

Wahl, S., Barth, H., Ciossek, T., Aktories, K., and Mueller, B. K. (2000). Ephrin-A5 induces collapse of growth cones by activating Rho and Rho kinase. *J Cell Biol* **149,** 263-70.

Wang, H. U., and Anderson, D. J. (1997). Eph family transmembrane ligands can mediate repulsive guidance of trunk neural crest migration and motor axon outgrowth. *Neuron* **18,** 383-96.

Wang, X., Roy, P. J., Holland, S. J., Zhang, L. W., Culotti, J. G., and Pawson, T. (1999). Multiple ephrins control cell organization in C. elegans using kinase-dependent and -independent functions of the VAB-1 Eph receptor. *Mol Cell* **4,** 903-13.

Weinl, C., Drescher, U., Lang, S., Bonhoeffer, F., and Loschinger, J. (2003). On the turning of Xenopus retinal axons induced by ephrin-A5. *Development* **130,** 1635-43.

Wimmer-Kleikamp, S. H., Janes, P. W., Squire, A., Bastiaens, P. I., and Lackmann, M. (2004). Recruitment of Eph receptors into signaling clusters does not require ephrin contact. *J Cell Biol* **164,** 661-6.

Winslow, J. W., Moran, P., Valverde, J., Shih, A., Yuan, J. Q., Wong, S. C., Tsai, S. P., Goddard, A., Henzel, W. J., Hefti, F., and et al. (1995). Cloning of AL-1, a ligand for an Eph-related tyrosine kinase receptor involved in axon bundle formation. *Neuron* **14,** 973-81.

Wybenga-Groot, L. E., Baskin, B., Ong, S. H., Tong, J., Pawson, T., and Sicheri, F. (2001). Structural basis for autoinhibition of the Ephb2 receptor tyrosine kinase by the unphosphorylated juxtamembrane region. *Cell* **106,** 745-57.

Yin, Y., Yamashita, Y., Noda, H., Okafuji, T., Go, M. J., and Tanaka, H. (2004). EphA receptor tyrosine kinases interact with co-expressed ephrin-A ligands in *cis*. *Neurosci Res* **48,** 285-296.

Zhou, X., Suh, J., Cerretti, D. P., Zhou, R., and DiCicco-Bloom, E. (2001). Ephrins stimulate neurite outgrowth during early cortical neurogenesis. *J Neurosci Res* **66,** 1054-63.

Zimmer, M., Palmer, A., Kohler, J., and Klein, R. (2003). EphB-ephrinB bi-directional endocytosis terminates adhesion allowing contact mediated repulsion. *Nat Cell Biol.* **5**, 869-78.

Zisch, A. H., Stallcup, W. B., Chong, L. D., Dahlin-Huppe, K., Voshol, J., Schachner, M., and Pasquale, E. B. (1997). Tyrosine phosphorylation of L1 family adhesion molecules: implication of the Eph kinase Cek5. *J Neurosci Res* **47,** 655-65.

Zou, J. X., Wang, B., Kalo, M. S., Zisch, A. H., Pasquale, E. B., and Ruoslahti, E. (1999). An Eph receptor regulates integrin activity through R-Ras. *Proc Natl Acad Sci U S A* **96,** 13813-8.

Addendum

Page XV:

Chathurani S. Jayasena[1], Warren D. Flood[1, 2] and Simon A. Koblar[1] **(2004). *In vitro* EphA-ephrin-A interactions during lobe specific guidance of trigeminal ganglion axons. (Submitted to Journal of Neurobiology).** *was corrected to read*:

Chathurani S. Jayasena[1], Warren D. Flood[1, 2] and Simon A. Koblar[1] **(2005). High EphA3 expressing ophthalmic trigeminal sensory axons are sensitive to ephrin-A5-Fc: implications for lobe specific axon guidance. *Neuroscience* (accepted).**

Page 8, line 11, section 1.1.2.3:

(reviewed by Giniger, 2002; Huber *et al.*, 2003)) *was corrected to* (reviewed by Giniger, 2002; Huber *et al.*, 2003).

Page 17, paragraph 2, line 10, *the following was added*:

More specifically, Pax3 function has been suggested to be required for cardiac neural crest stem cell expansion (Conway *et al.,* 2000), and cell autonomously control cell surface properties in the somites and the neural tube (Mansouri *et al.,* 2001). Based on this evidence, loss of *Pax3* in *Splotch* mutants may lead to defects in ophthalmic placode cell expansion and/ or altered cell surface properties which may interfere with placode cell invagination and/or migration thus contributing to a reduction in ophthalmic lobe neurons and projections.

Page 66, first paragraph was replaced with the following:

As demonstrated in the trunk peripheral nervous system, Eph/ ephrins are expressed in the developing vertebrate face during trigeminal ganglion axon guidance. A number of studies have demonstrated that EphBs and ephrin-Bs localise to the target fields of the trigeminal ganglion in mouse embryonic day (E) 9-11 (Adams *et al.,* 2001; Henkemeyer *et al.,* 1996) and chick embryo stages 13-20 (Baker *et al.,* 2001; Santiago and Erickson, 2002). In addition, EphB2 and EphB3 localise to the murine trigeminal ganglion at E9-10.5 (Adams *et al.,* 2001; Henkemeyer *et al.,* 1996) during trigeminal ganglion axon pathfinding. Consistent with the notion of possible EphA/ ephrin-A interactions during

trigeminal ganglion guidance, prior studies in both chick and mouse have reported expression of EphAs and ephrin-As in the developing head (Araujo and Nieto, 1997; Baker and Antin, 2003; Flenniken *et al.,* 1996; Gale *et al.,* 1996; Kury *et al.,* 2000; Santiago and Erickson, 2002). In the trigeminal ganglion target fields in the mouse, EphAs and ephrin-As are differentially expressed during trigeminal ganglion axon pathfinding at E9-10.5; ephrin-A ligands show restricted localisation to the first branchial arch components while EphA receptors show restricted localisation to the ophthalmic process (Flenniken *et al.,* 1996; Gale *et al.,* 1996). However, trigeminal ganglion EphA/ ephrin-A expression during E9-10.5 remain to be elucidated. Although, EphAs and ephrin-As are expressed in the early chick embryonic face (stages 8-12) prior to trigeminal ganglion axon pathfinding (Baker and Antin, 2003), analysis of Eph/ ephrin-A subclass expression and the requirement for EphA/ ephrin-A signalling during trigeminal ganglion axon pathfinding/ guidance during chick stages 13-20 remains to be elucidated.

Page 73, section 2.1:
EDTA is the abbreviation for **'ethylenediaminetetraacetic acid'** *and not* **'disodium salt'**.

Page 80, section 2.3.3.7, line 7:
"The primers assayed were similar in reaction efficiency to the *18srRNA* internal **reference.**" *was corrected to* "The primers assayed were similar in reaction efficiency to the *18srRNA* internal reference, **as determined by the slopes of the curves**.

Page 81, line 5:
"…to determine any differences between the ophthalmic and maxillomandibular lobes." *was corrected to read as* "…to determine any differences **in gene expression** between the ophthalmic and maxillomandibular lobes

Page 89, section 2.3.10., lines 12-13:

"Axons were visualized anti-neurofilament in 2% BSA plus PBST as states above for sections" was corrected to read as "Axons were visualized **with** anti-neurofilament in 2% BSA plus PBST as states above for sections".

Page 97, section 3.2.1.1, paragraph 2, line 15-16:

"In addition, other regions of the embryo that were positive for EphAs (for example, the **eye** and otic placodes) ..." *was corrected to* "In addition, other regions of the embryo that were positive for EphAs (for example, the **optic** and otic placodes)..."

Page 105, paragraph 3, line 24:

"In summary at stage 20, in addition to **be** expressed..." *was corrected to* "In summary at stage 20, in addition to **being** expressed..."

Page 111, line 15, section 3.2.2.2: "Other regions that were noted to be positive for EphA4 were a group cells..." *was corrected to* "Other regions that were noted to be positive for EphA4 were a **of** group cells..."

Page 117, section 3.2.3, line 6:

"Three chick ephrin-A ligands **are** have..." *was corrected to read* "Three chick ephrin-A ligands have..."

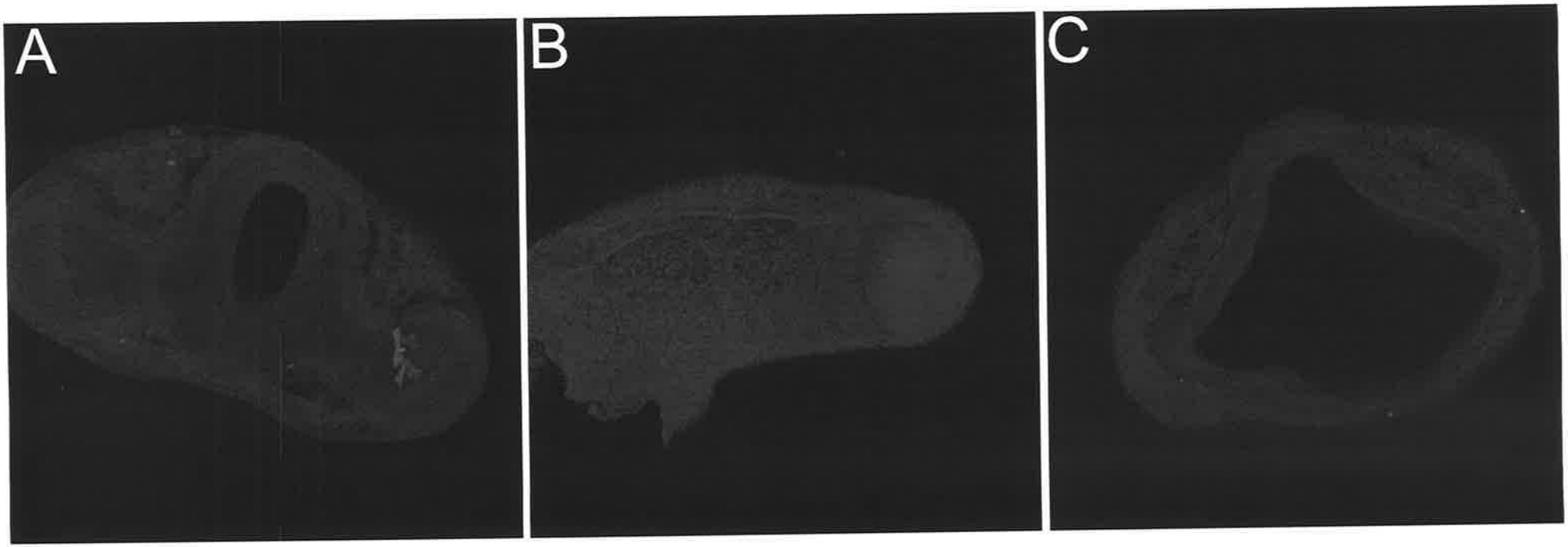

Insert figure panel following Figure 3.12, page 124:

Figure 3. 12B. No primary control figures for (A) anti-EphA3, (B) anti-EphA4 and (C) anti- ephrin-A5 demonstrates no significant background staining.

Page 127, section 3.3.3, line 7, *the following sentence was added*:
Alternatively, the expression of EphA3, EphA4, ephrin-A2 and ephrin-A5 in the targets, and the expression of EphA3 and ephrin-A5 in the trigeminal ganglion may participate in cell sorting and migration of trigeminal ganglion neural crest and placode cells.

Page 150, line 3:
"Findings from the previous chapter (Figure 3.11) demonstrated **co**-that..." *was corrected to read* "Findings from the previous chapter (Figure 3.11) demonstrated that..."

Page 190, paragraph 3, line 3:
"...arch ephrin-A ligands **in the** in directing..." *was corrected to* "...arch ephrin-A ligands in directing..."

Page 216, paragraph 2, line 12-13:
"Also the function of EphA3 and EphA4 may **to** be redundant..." *was corrected to* "Also the function of EphA3 and EphA4 may be redundant..."

Page 217, line 3, insert sentence following "...axon pathfinding needs further investigation.":
Rather than calculating the mean growth cone area and the mean length of filopodia, it may be more useful to bin the sizes of growth cones. Recently, application of pre-clustered EphA7-Fc to motor column explants positive for ephrin-As demonstrated a shift in distribution of growth cone sizes towards larger sizes; this was demonstrated by binning the sizes of growth cone areas (Marquardt *et al.*, 2005). Additionally, motor column explants were maintained for 36 hours prior to addition of EphA7-Fc. Therefore, it may be necessary to determine whether culturing trigeminal ganglion explants in the presence of neurotrophins for 36 hours will also result in growth cones that are larger in size in the presence of EphA4-Fc.

Page 221, paragraph 2, line 3, insert sentence following "...embryonic face (Figure 7.1).":

The expression data revealed complex patterns of graded Eph/ ephrin-A expression in the target fields of the trigeminal ganglion. As to whether this graded expression of Eph/ ephrin-As are relevant to trigeminal ganglion axon guidance requires further investigation *in vivo*.

Page 227, paragraph 2, line 2:

"More specifically, there is restricted ephrin-A ligand expression to the ventral hindlimb (Eberhart *et al.*, 2004; Eberhart *et al.*, 2000; Eberhart *et al.*, 2002; Kania and Jessell, 2003) (Figure 7.2B)..." *was corrected to* "More specifically, there is restricted ephrin-A ligand expression to the ventral hindlimb in **chick and mouse** (Eberhart *et al.*, 2004; Eberhart *et al.*, 2000; Eberhart *et al.*, 2002; Kania and Jessell, 2003) (Figure 7.2B)..."

Page 228, paragraph 2, lines 1-2:

"Although EphA signalling appears to be a major determinant of dorsal trajectory of LMC axons, two lines of evidence suggest that a distinct guidance mechanism directs..." *was corrected to* "EphA signalling appears to be a major determinant of dorsal trajectory of LMC axons. Two lines of evidence **from studies in the murine model system** suggest that a distinct guidance mechanism directs..."

Page 228, paragraph 3, line 2:

"...low EphA3 expressing maxillomandibular axons were observed to **growth** on..." *was corrected to* "...low EphA3 expressing maxillomandibular axons were observed to **grow** on..."

Page 234, line 3, paragraph 4:

"...the analysis of EphA3 null mice is justified (Vaidya et al., 2003)**. As** discussed..." *was corrected to* "...the analysis of EphA3 null mice is justified (Vaidya et al., 2003)**. As** discussed..."

Page 242, following reference was inserted following Conwan *et al.*, (2004):

Conway, S. J., Bundy, J., Chen, J., Dickman, E., Rogers, R. and Will, B. M. (2000). Decreased neural crest stem cell expansion is responsible for the conotruncal heart defects within the splotch (Sp(2H))/Pax3 mouse mutant. *Cardiovasc Res* **47**, 314-28.

Page 246, following reference was inserted after Mann et al., (2002):

Mansouri, A., Pla, P., Larue, L. and Gruss, P. (2001). Pax3 acts cell autonomously in the neural tube and somites by controlling cell surface properties. *Development* **128**, 1995-2005.

Page 246, following reference was inserted after Marin et al., (2001):

Marquardt, T., Shirasaki, R., Ghosh, S., Andrews, S. E., Carter, N., Hunter, T. and Pfaff, S. L. (2005). Coexpressed EphA receptors and ephrin-A ligands mediate opposing actions on growth cone navigation from distinct membrane domains. Cell 121, 127-39.